The Abdus Salam
International Centre for Theoretical Physics

United Nations
Educational, Scientific and
Cultural Organization

IAEA
International Atomic Energy Agency

2167-16

Advanced School on Direct and Inverse Problems of Seismology

27 September - 8 October, 2010

SURFACE WAVES

Jean-Paul Montagner

Dept. Seismology
I.P.G.
Paris
France

SURFACE WAVES and UPPER MANTLE ANISOTROPY

Jean-Paul Montagner

Dept. Seismology, I.P.G., Paris; France

Overview
Large scale Seismology: an observational field

- Data (Seismic source) + Instrument (Seismometer) -> Observations (seismograms)
- Historical evolution: Ray theory, Normal mode theory, Numerical techniques (SEM, NM-SEM)
- Scientific Issues: Earthquakes (Sumatra-Andaman 04, Haiti 10),

  Anisotropic structure of the Earth
- Tomographic Technique
- Geodynamic Applications: continental deformation

  Seismic Experiment: Plume detection
- Adjoint and time reversal methods

Haiti earthquake, Jan. 12, 2010

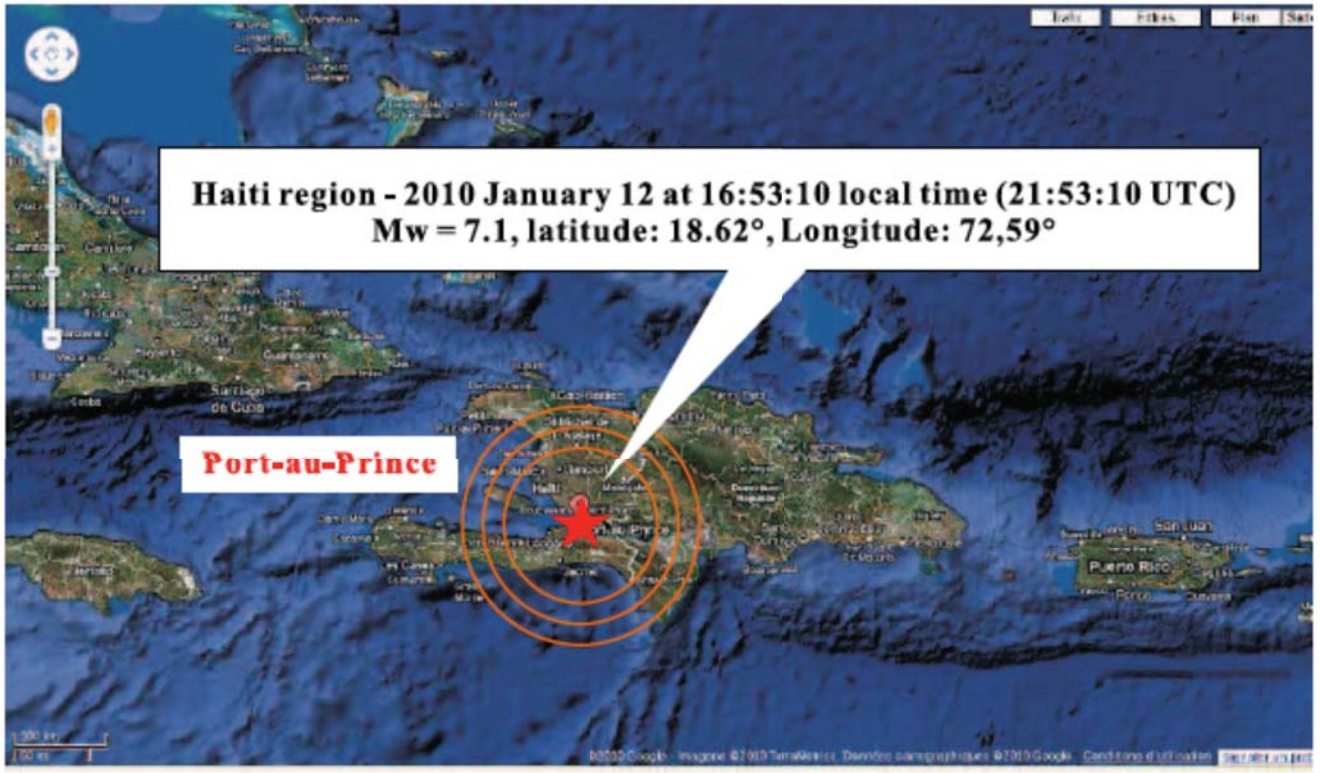

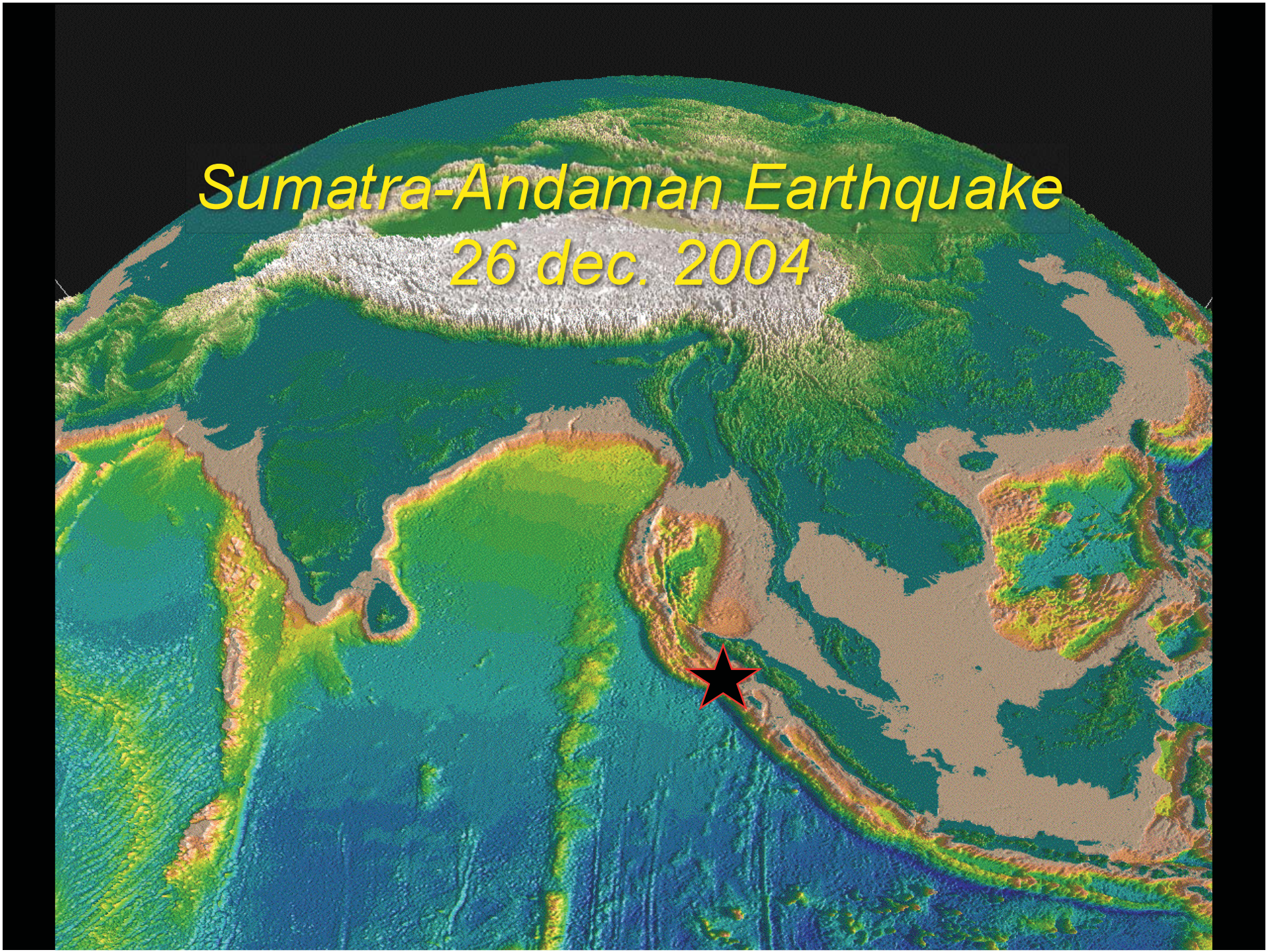
Sumatra-Andaman Earthquake
26 dec. 2004


Sumatra-Andaman Earthquake
26 dec. 2004
HIMALAYA
20°N
INDE
Andaman
10°N
Nicobar
Sri Lanka
Maldives
Thailand
26-12-2004 M ≥ 9
epicenter NEIC
CMT Harvard
28-3-2005 M 8.7
epicenter NEIC
CMT Harvard
1861
M8.5
1833
M9.0
Sumatra
0°
Epicenters
80°E
90°E
100°E
110°E

Sumatra - Andaman Islands Earthquake (M_w=9.0)

Global Displacement Wavefield from the Global Seismographic Network

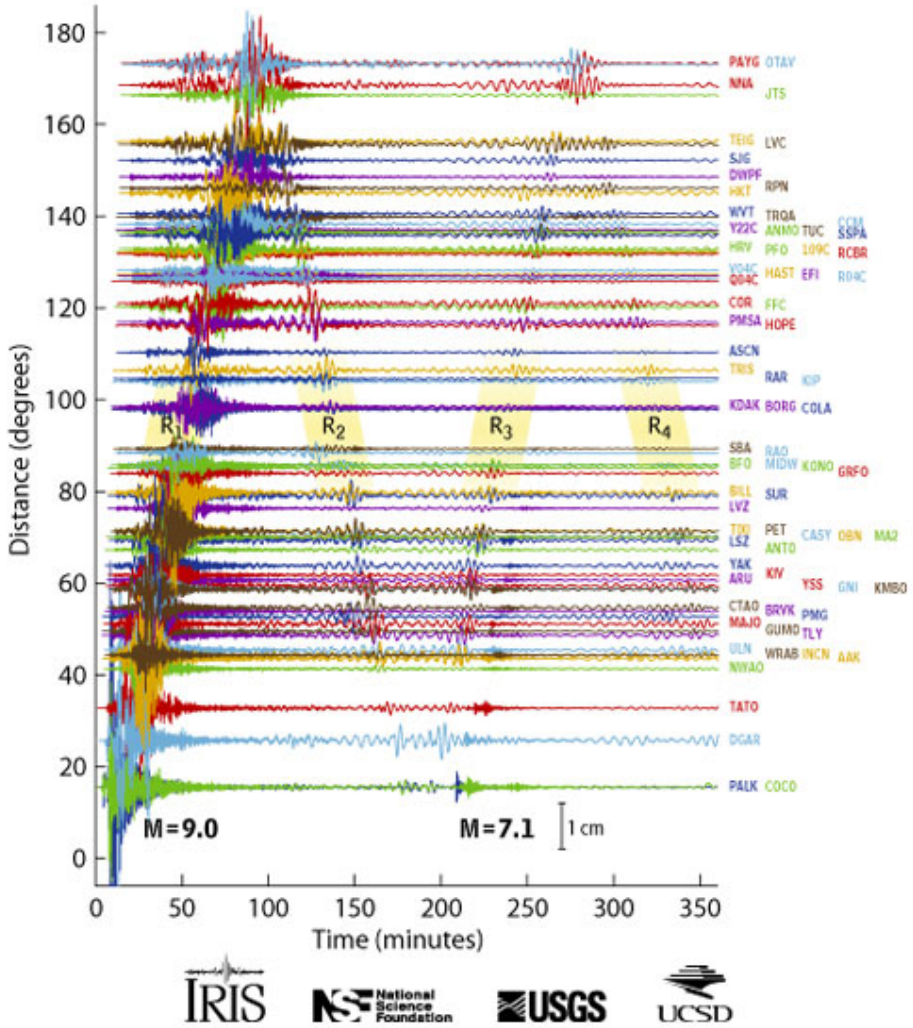

IRIS · National Science Foundation · USGS · UCSD

Sumatra - Andaman Islands Earthquake

Global Seismographic Network Stations

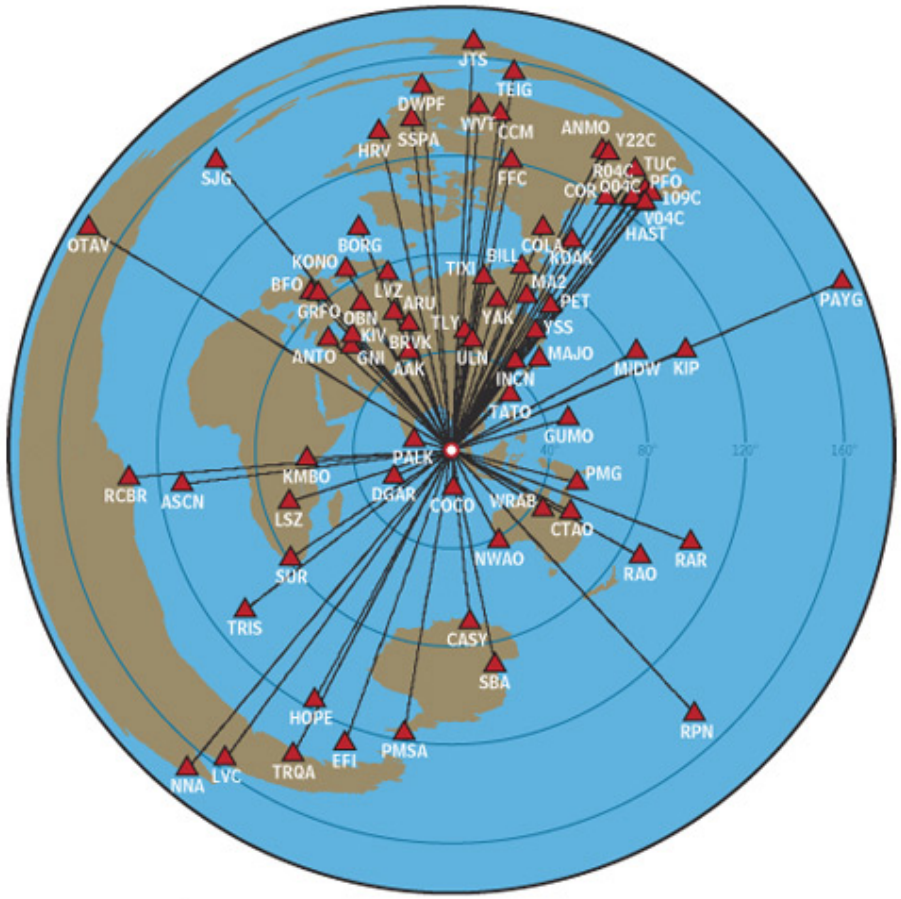

IRIS · National Science Foundation · USGS · UCSD

Seismic Instruments

- Seismoscope

(China -100BC)

Broadband Seismometer (1mHz-20Hz) (Cacho, 1998)

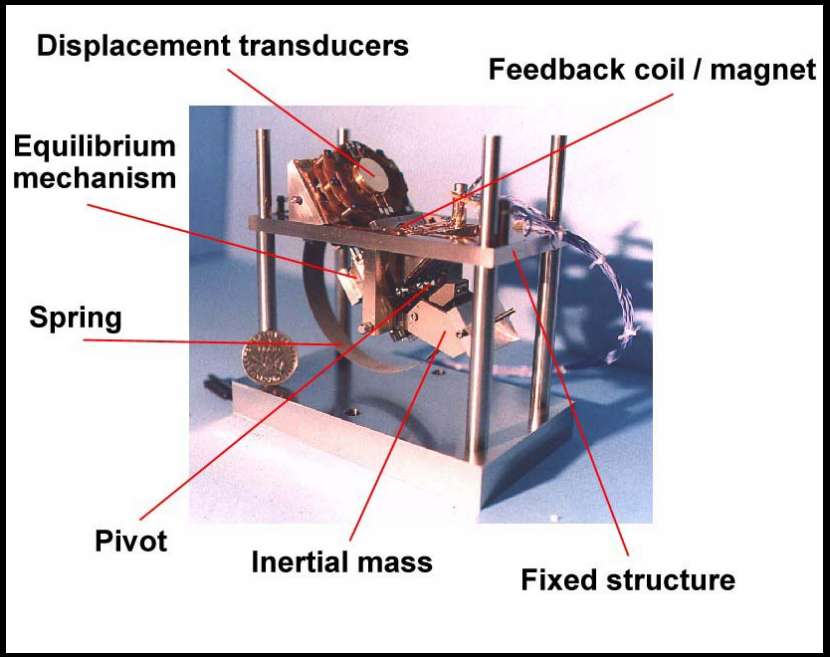

Principle of a Seismometer

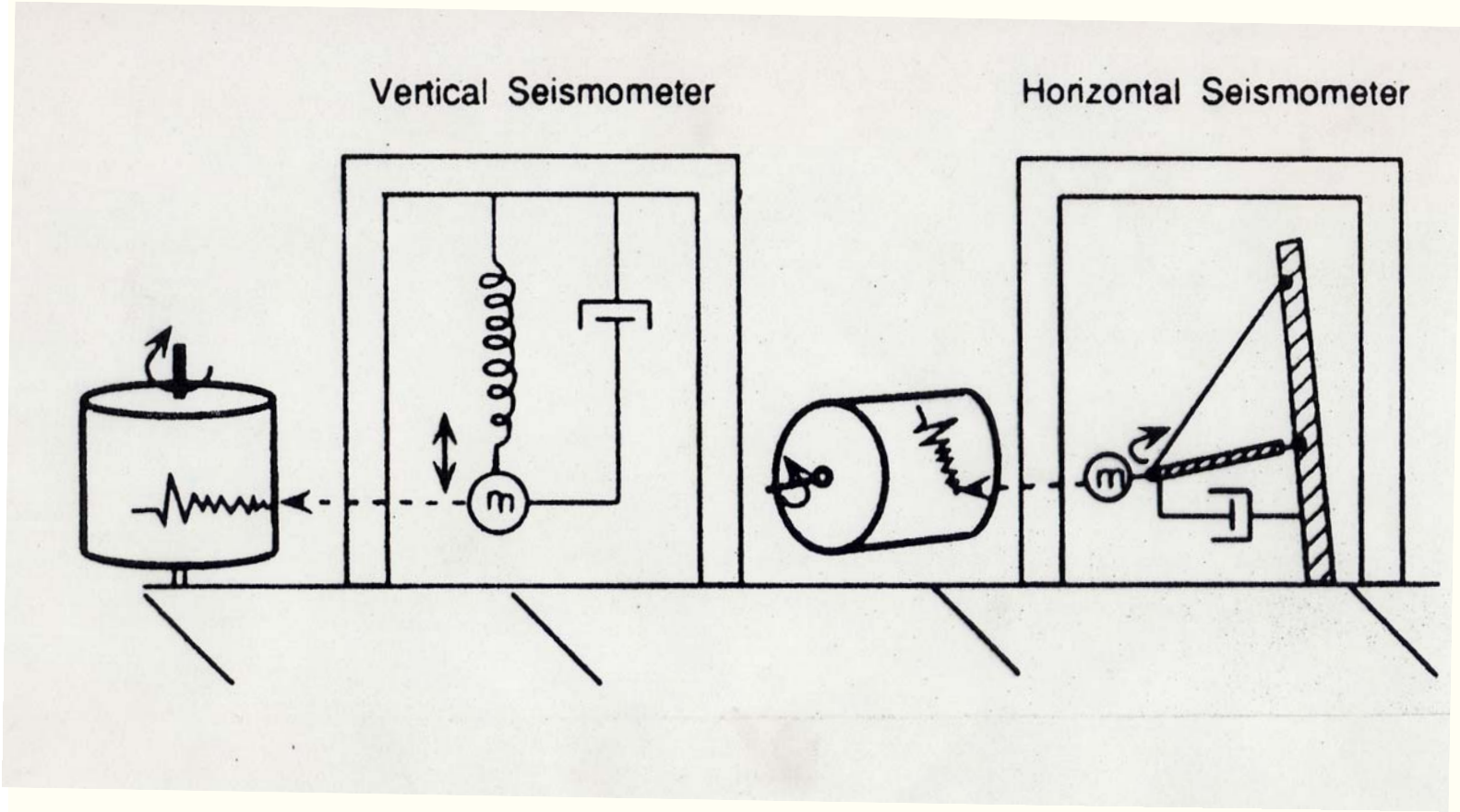

Tiltmeter (1960)

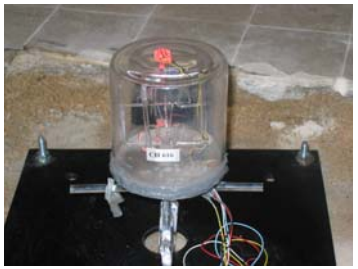

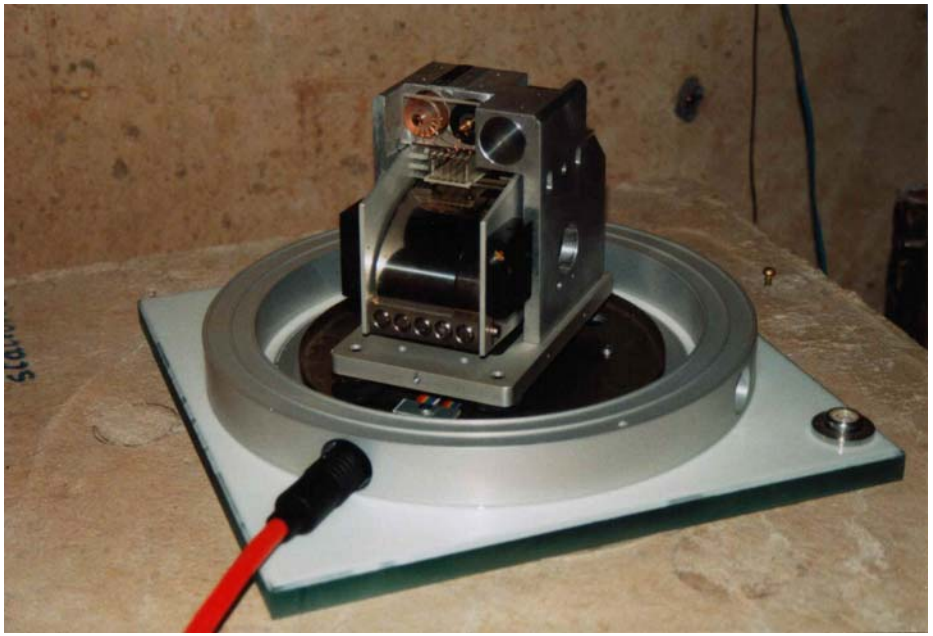

Broadband Seismometer (1982)
Streckeisen STS1: 0.05s< T< 5000s

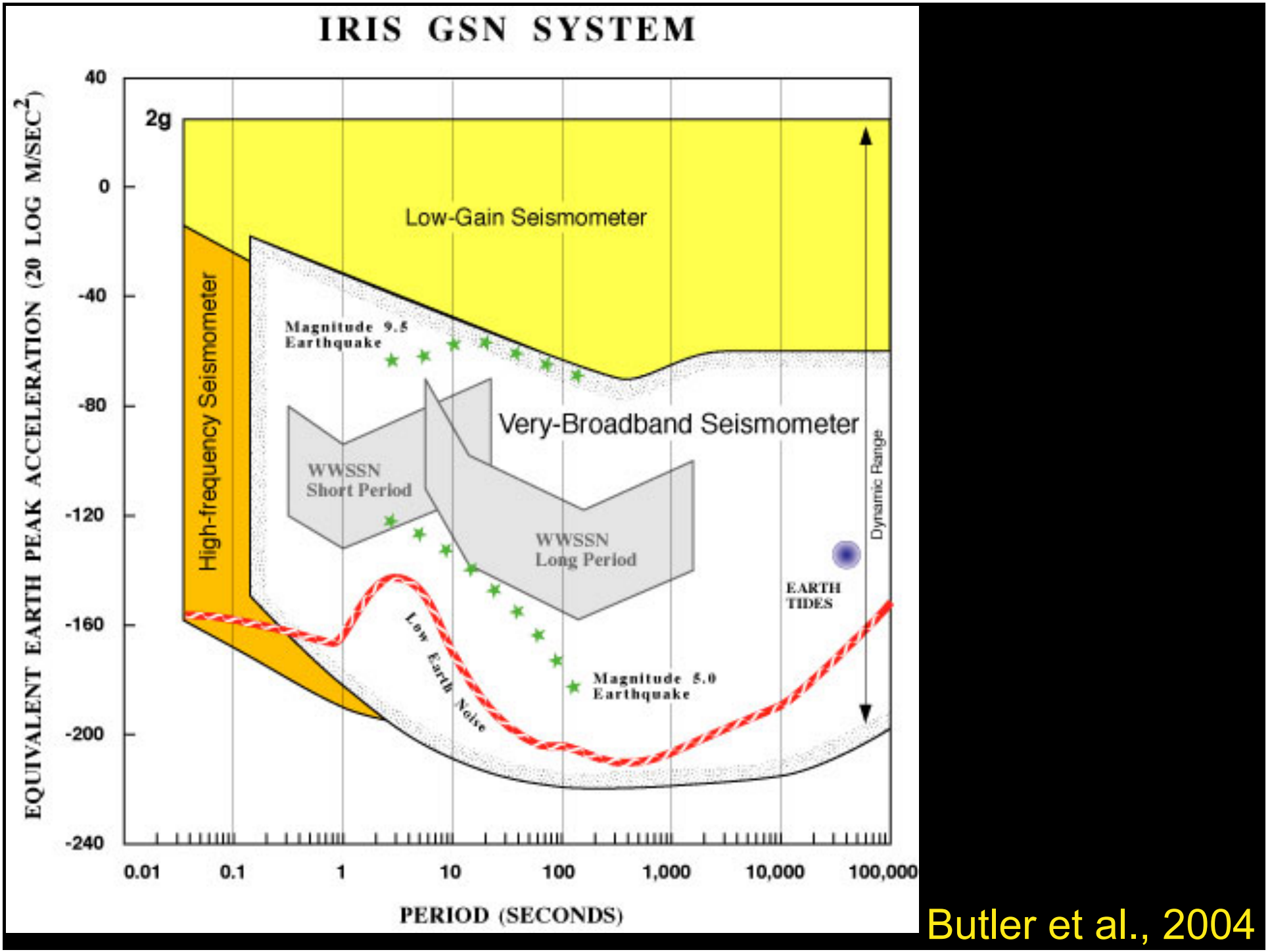

Butler et al., 2004

3 components
frequency range: 1mHz-20Hz
Period range: 0.05-1000s

Chile July 30, 1995, Ms=7.3

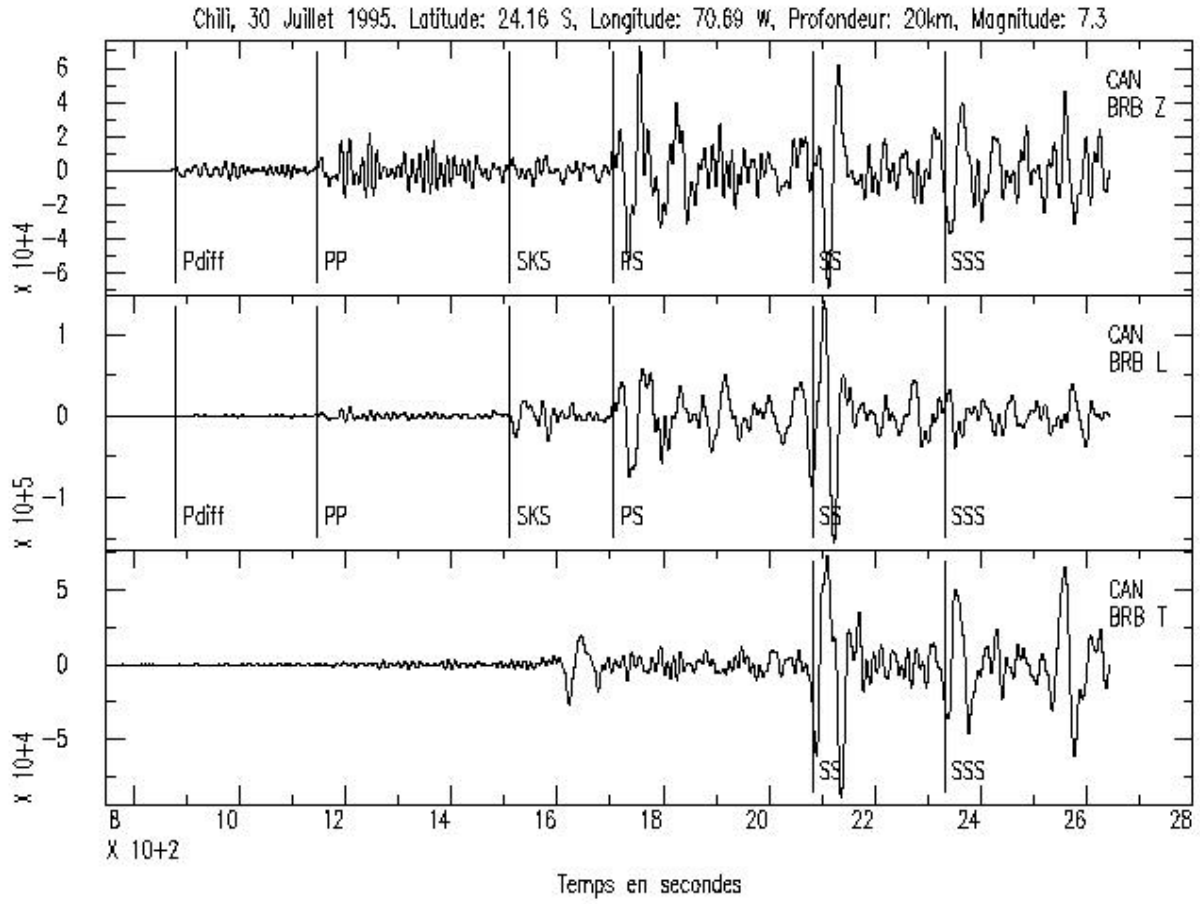

Chile earthquake magnitude= 7.3
Epicentral distance = 12,300km-depth 20km

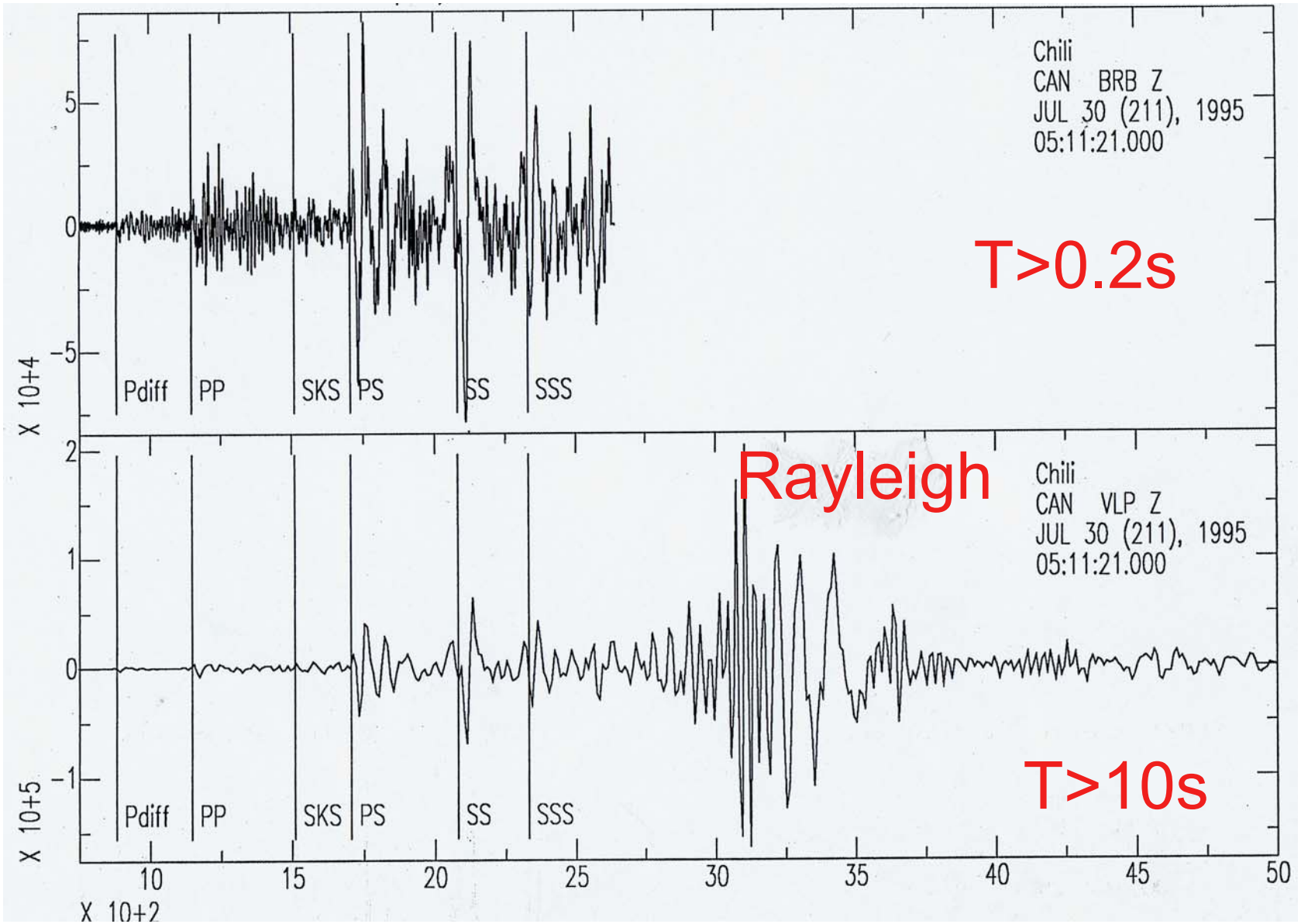

Chile Earthquake Jul. 1995

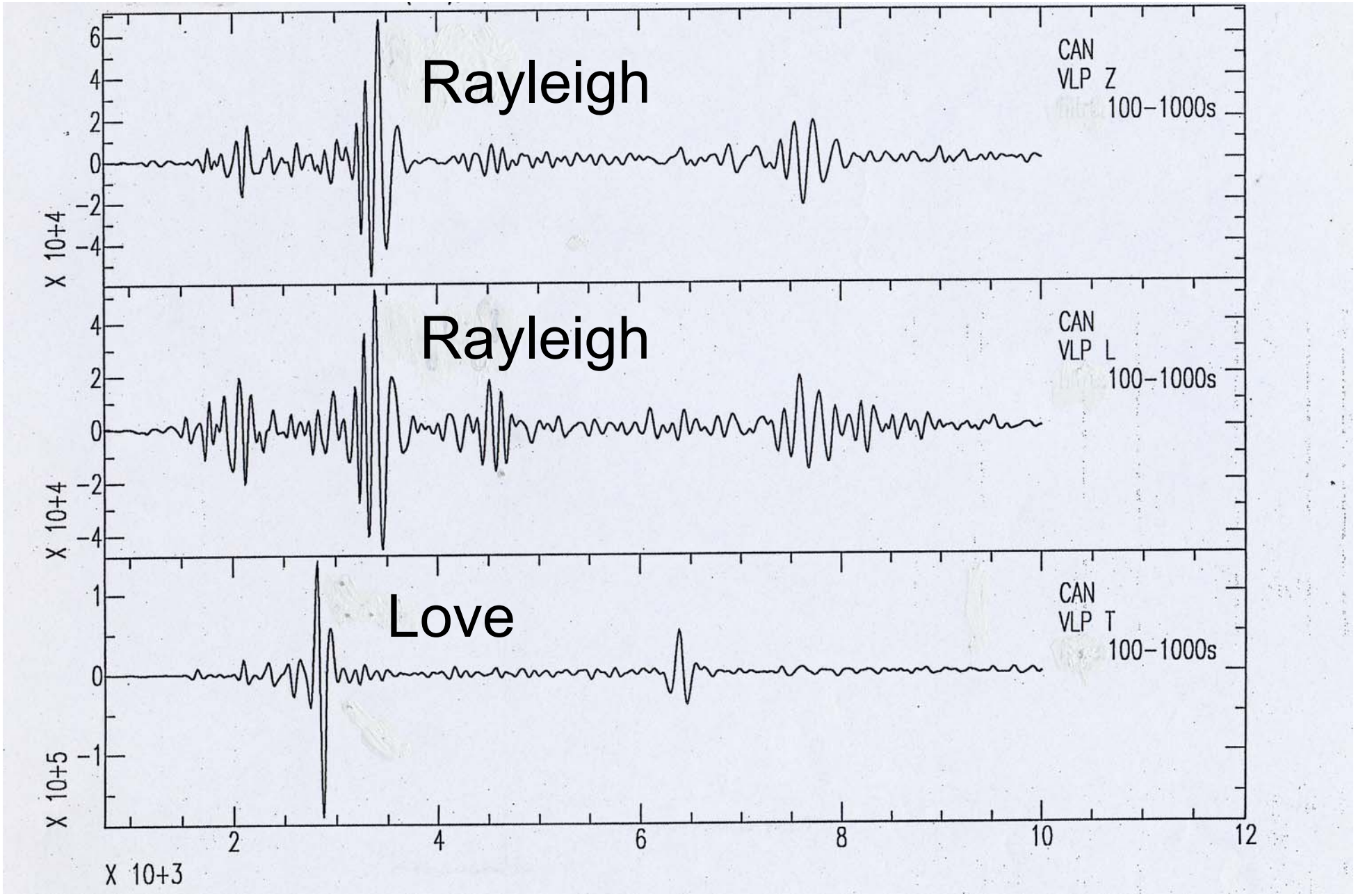

- Dispersive waves,
- Good global coverage,
- Large scale heterogeneities (min. 600 km).

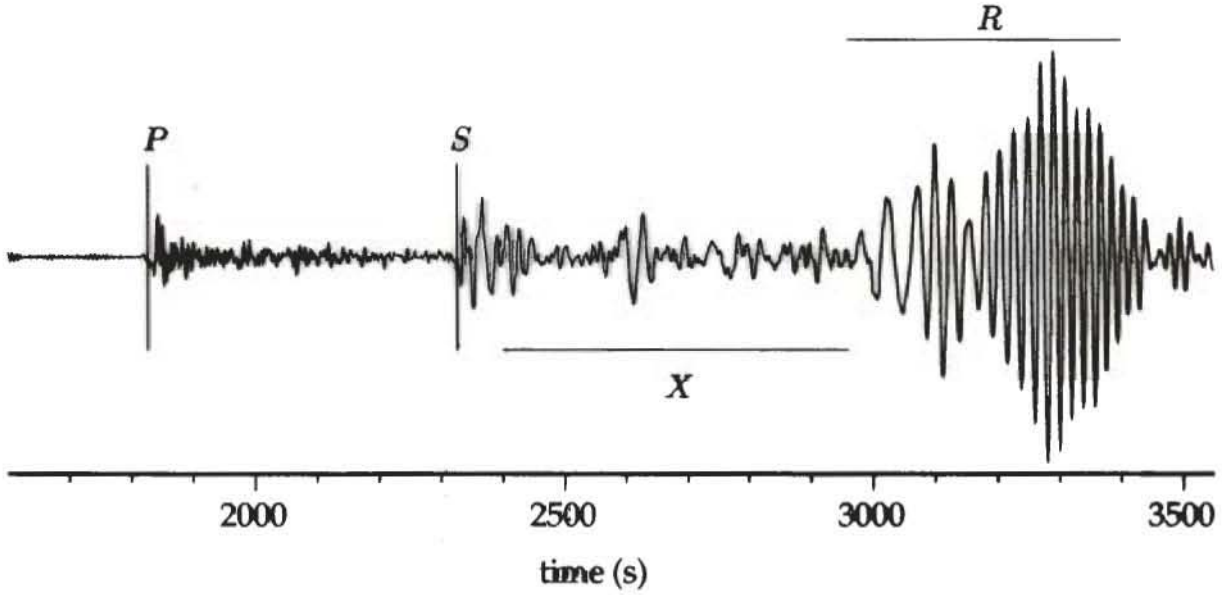

Vertical component of displacement field recorded at DRV station corresponding to the New-Guinea 05/16/1999 earthquake.

F.D.S.N. (Federation of Digital Broadband Seismic Networks)

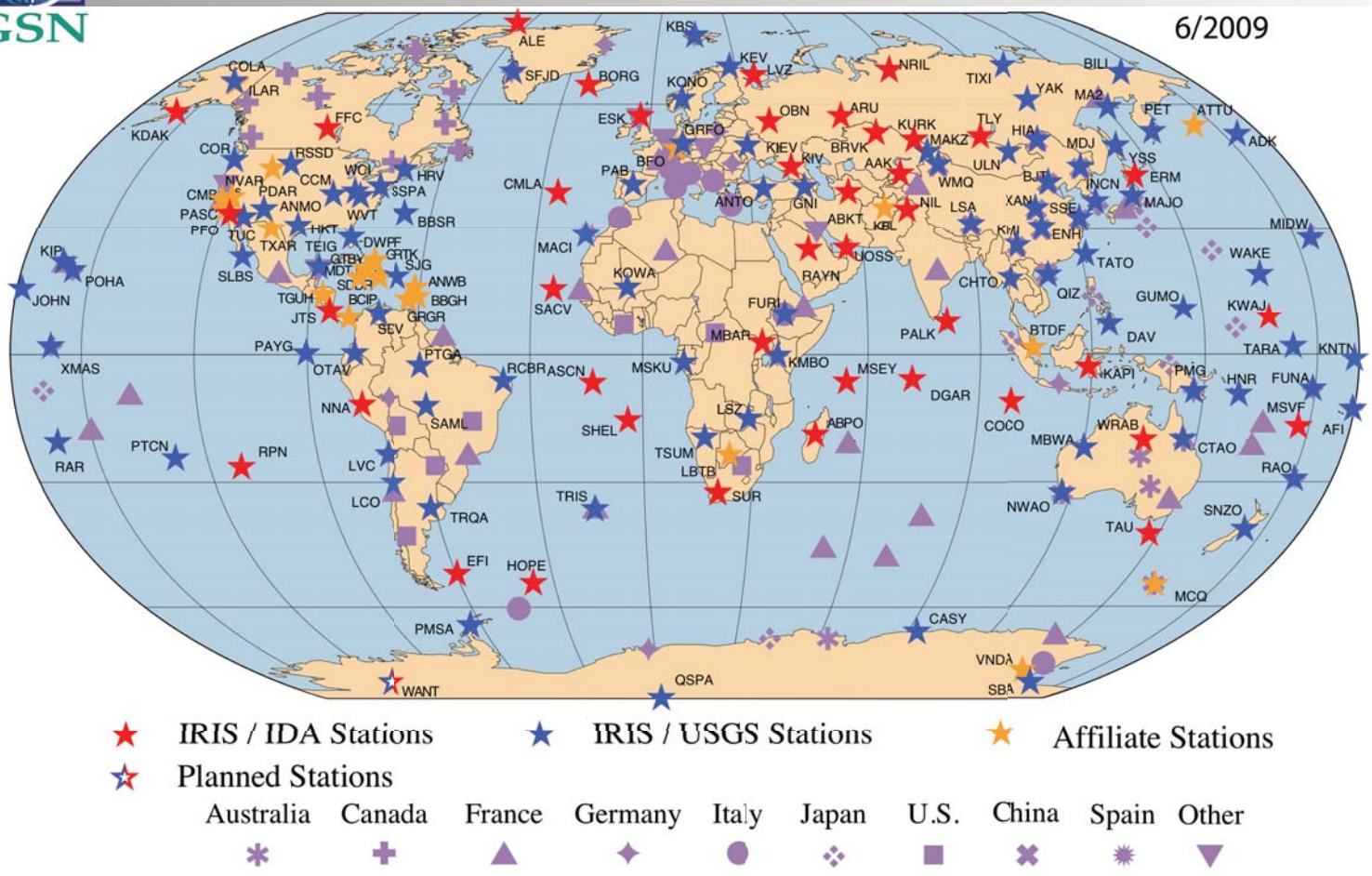

Ocean Bottom Observatories

=> International Ocean network (I.O.N.)

- 2/3 of the Earth are covered by water.
- seafloor seismometers enable:
  - To investigate oceanic regions with a better resolution
  - To fill gaps in the global coverage

I.O.N.

International Ocean Network

ION (International Ocean network) France, Italy, Japan, UK, U.S….

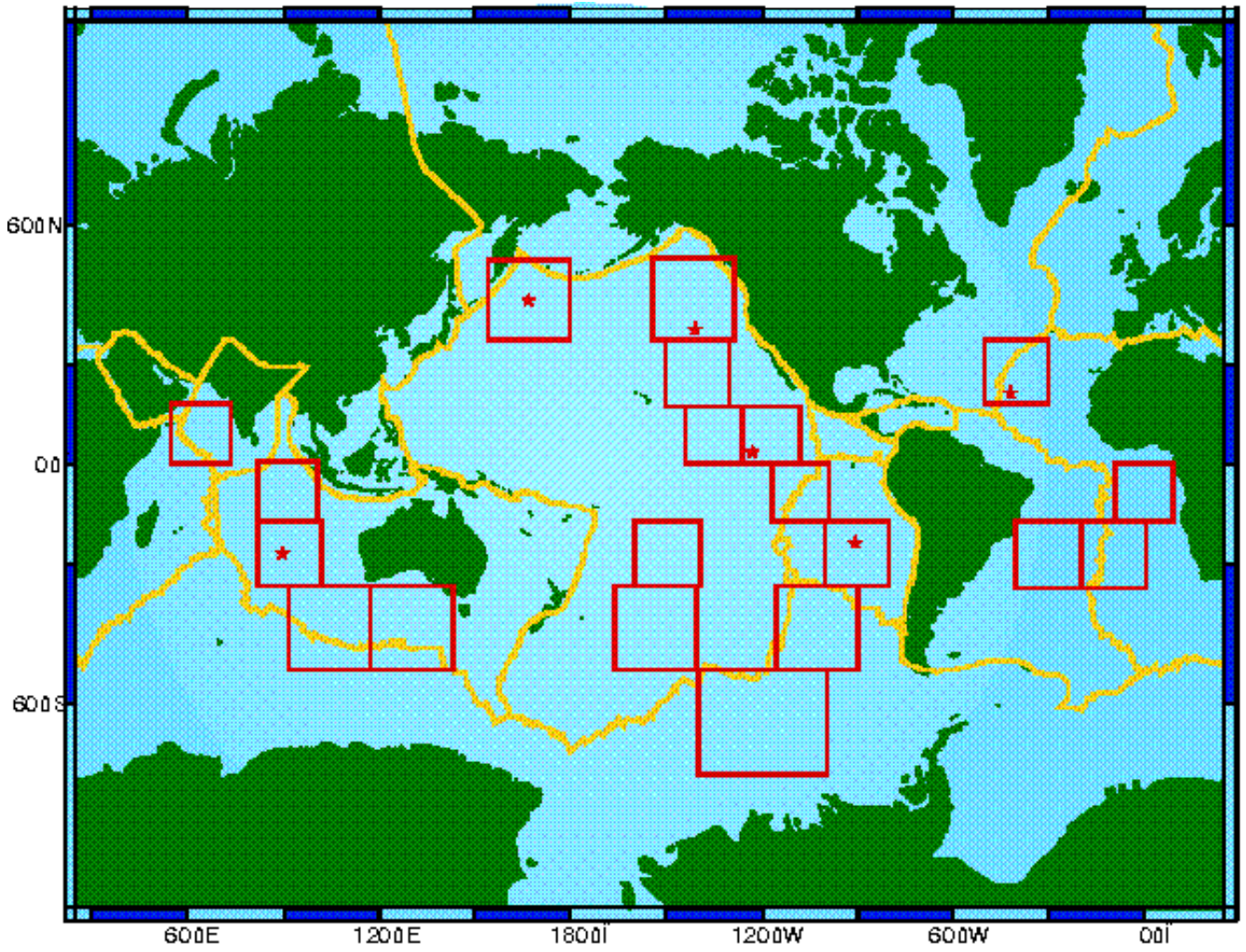

Figure 1: This map shows twenty regions which would require a seafloor seismic

OFM: Ocean bottom station

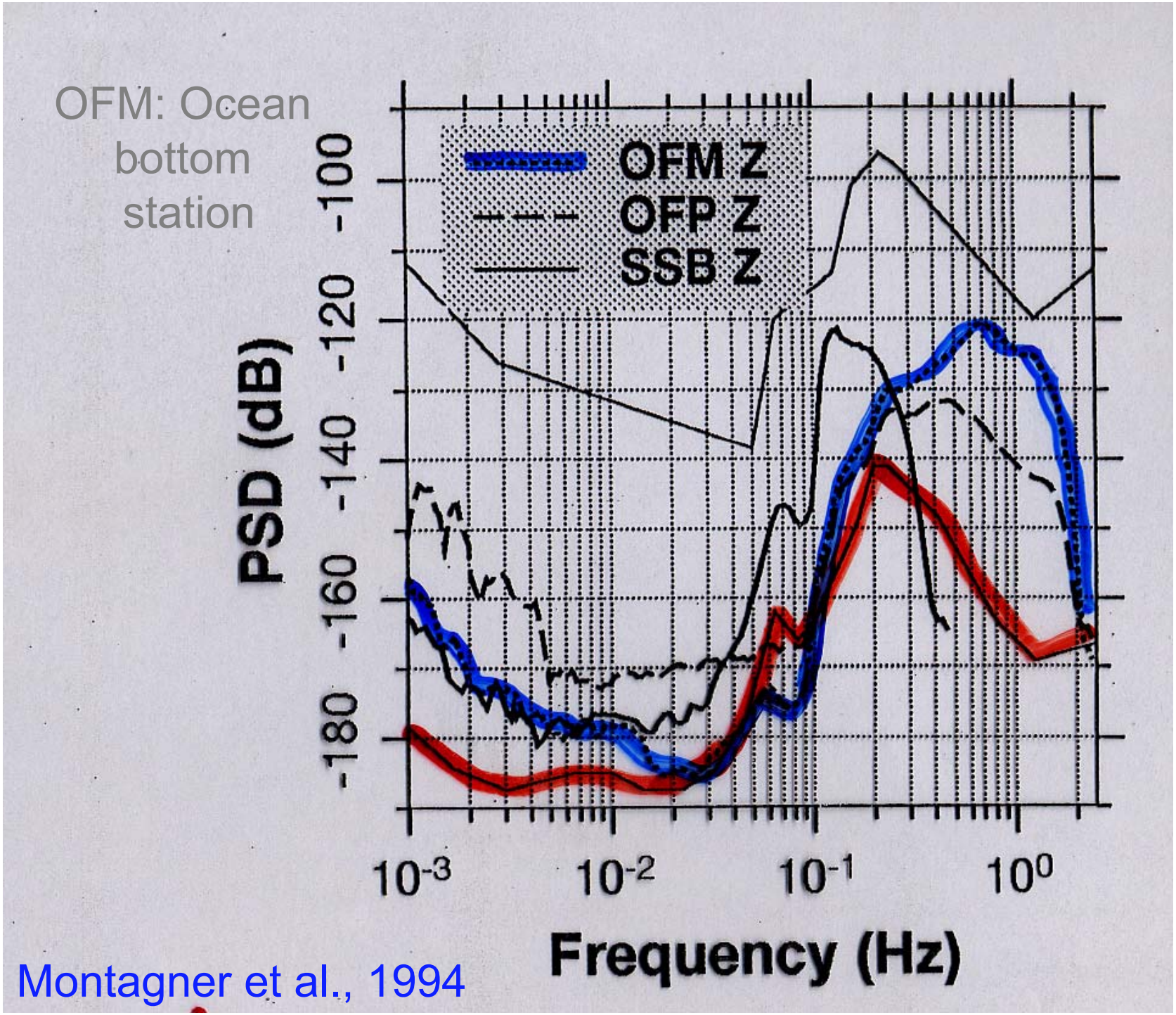

Montagner et al., 1994

M.O.I.S.E (June-Sept. 1997)

(Monterey bay Ocean bottom International Experiment)

MBARI, UC Berkeley, IPG-Paris, UBO-Brest

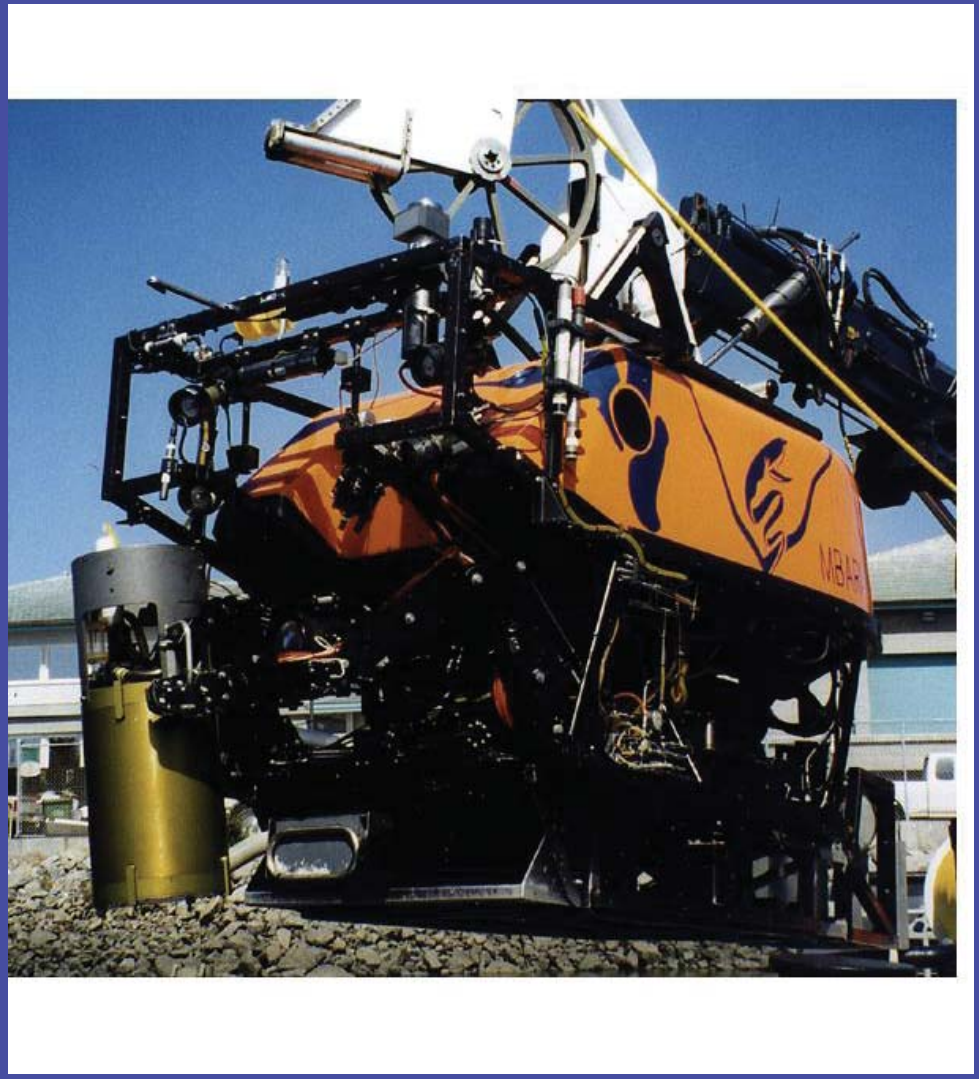

INSTITUT DE PHYSIQUE
DU GLOBE DE PARIS

Multiparameter signals

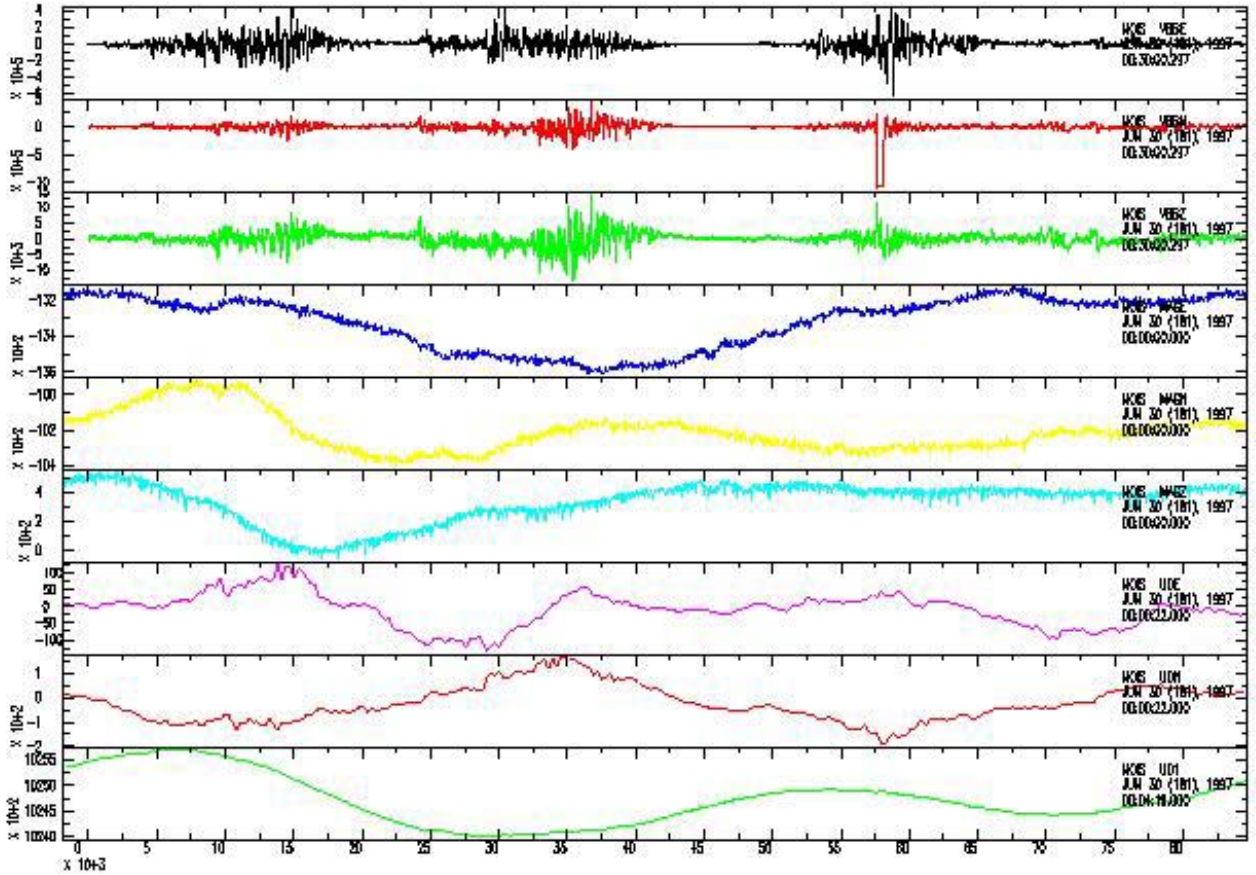

Deconvolution of the seismic signal from the pressure influence

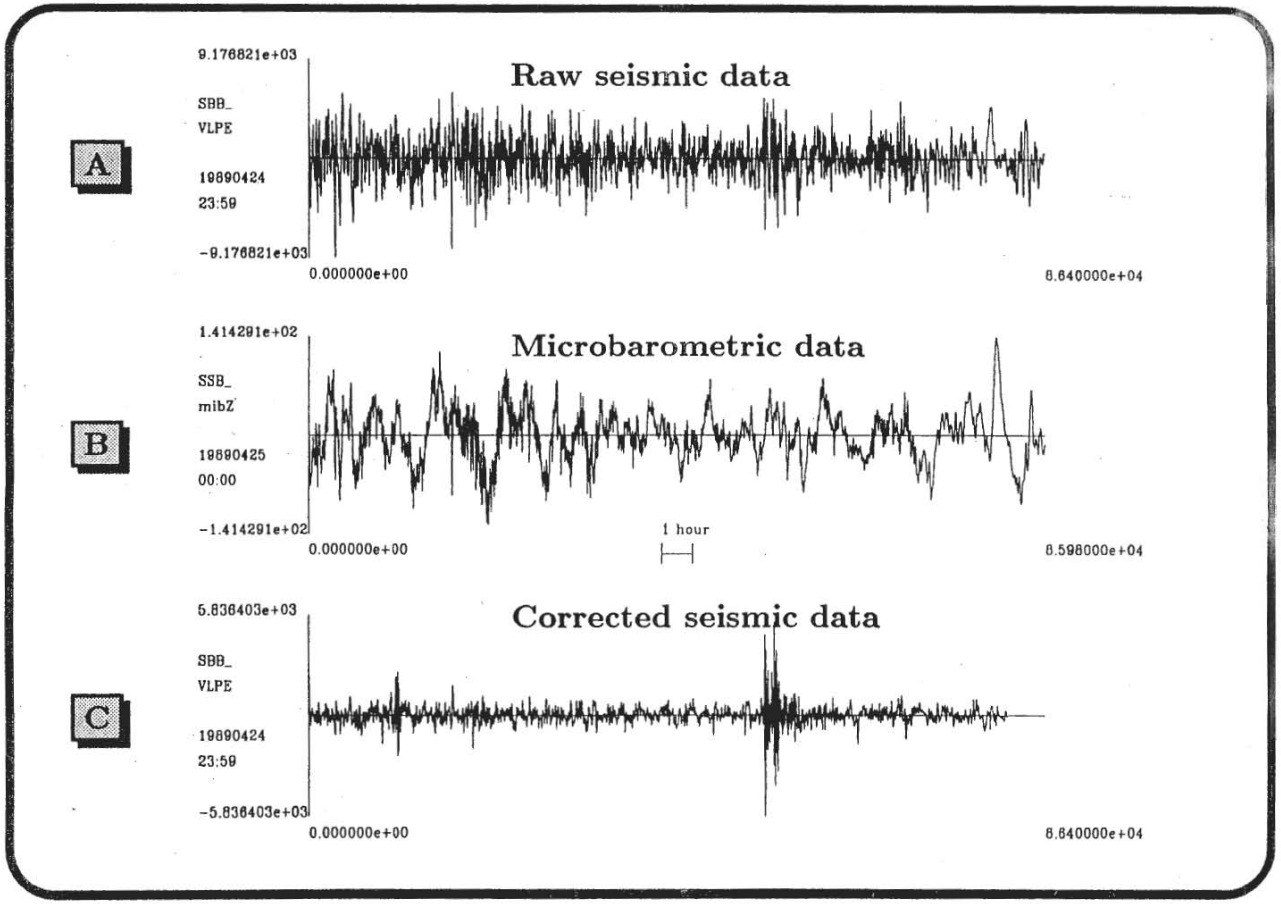

Beauduin et al.,1996

NERO observatory Scientific Interest Global scale

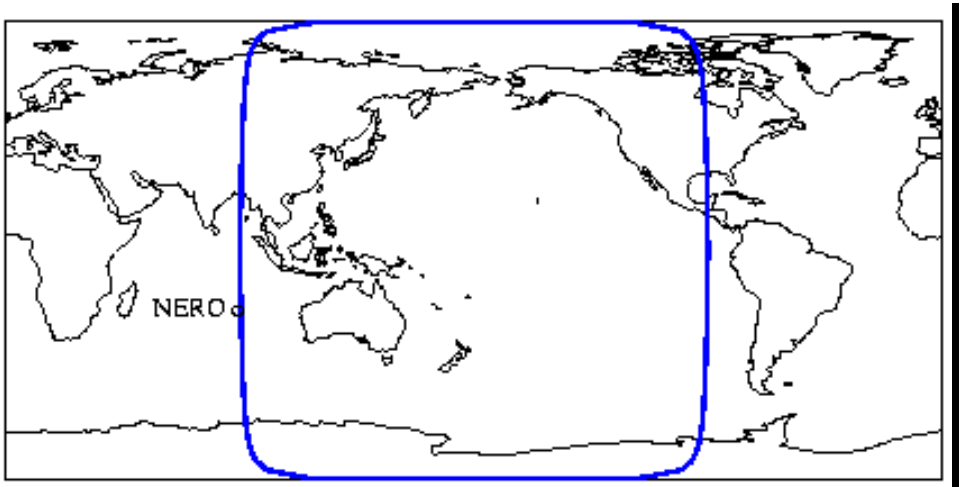

- To fill a gap in global station coverage

-To improve global tomographic model resolution

- To improve azimuthal distribution in determination of large earthquakes focal mechanisms

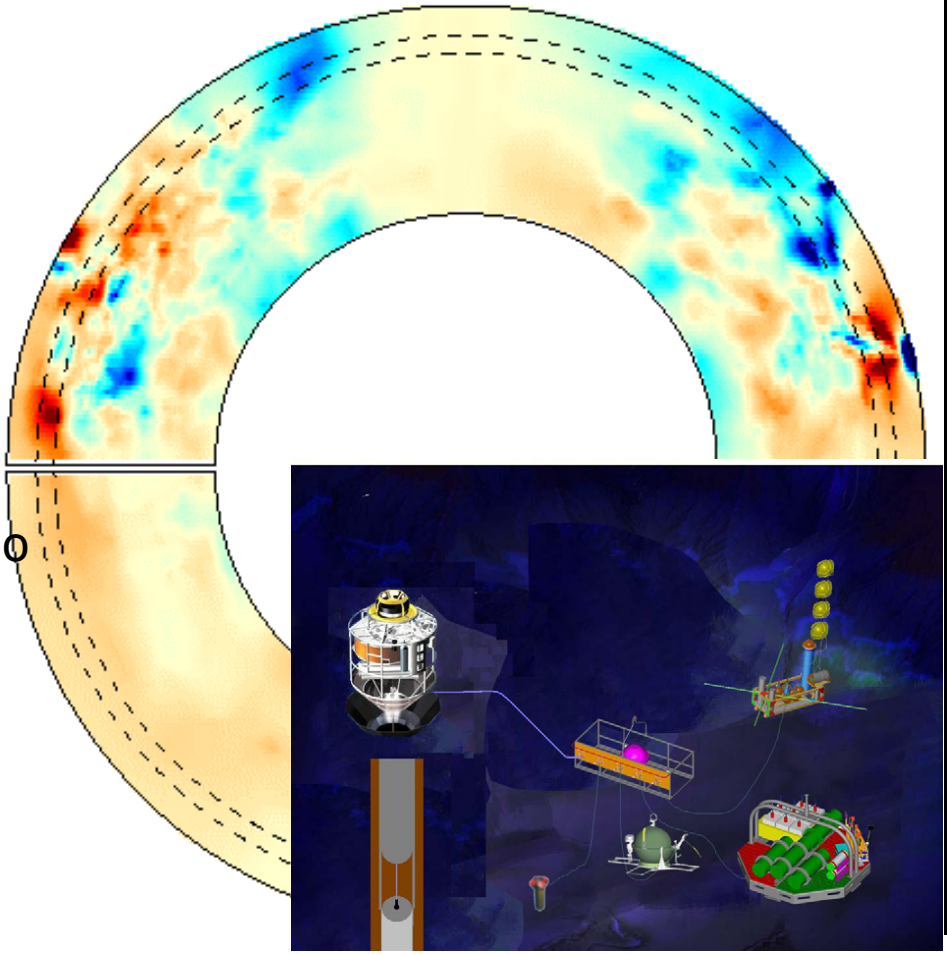

NERO

Karason & van der Hilst, 2003

Project Seafloor Portable Seismometers

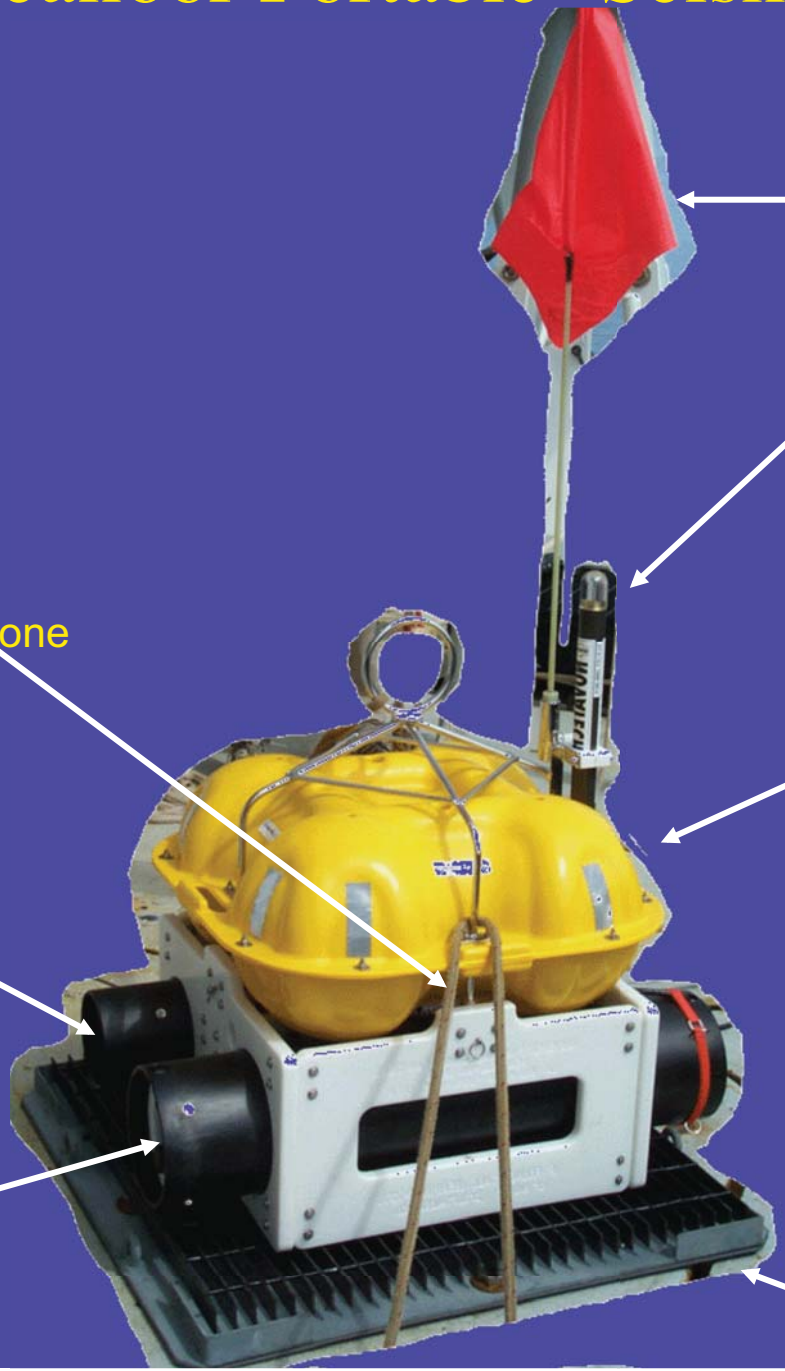

Crawford et al., 2002

Overview
Large scale Seismology: an observational field

- ***Data (Seismic source) + Instrument (Seismometer) -> Observations (seismograms) New instruments***
- Historical evolution: Ray theory, Normal mode theory, Numerical techniques (SEM, NM-SEM)
- Scientific Issues: Earthquakes (Sumatra-Andaman), Anisotropic structure of the Earth
- Tomographic Technique
- Geodynamic Applications

  Seismic Experiment, Plume detection
- Adjoint and time reversal methods

1st QUEST Workshop, Capo Caccia, Sardinia, September 19-26, 2010

Observing and inverting more than translations: rotations and strains

Johana Brokešová[1)] and Heiner Igel[2)], Moritz Bernauer[2)], and Andreas Fichtner[2)]

1) Charles University,
Department of Geophysics
V Holešovičkách 2, 180 00 Prague, Czech Republic

2) Ludwig-Maximilians-University,
Department of Earth Sciences – Geophysics
Theresienstrasse 41, 80333 Munich, Germany

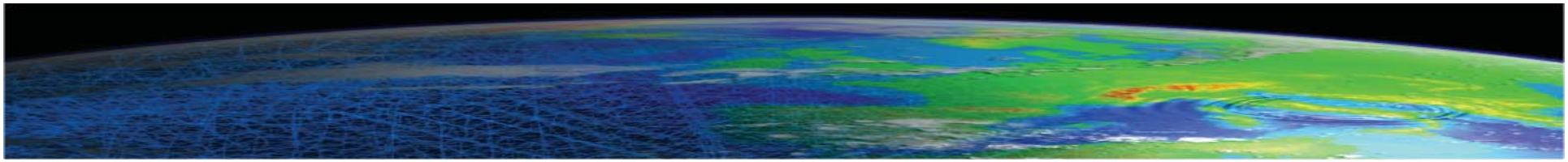

Deformation of a continuum

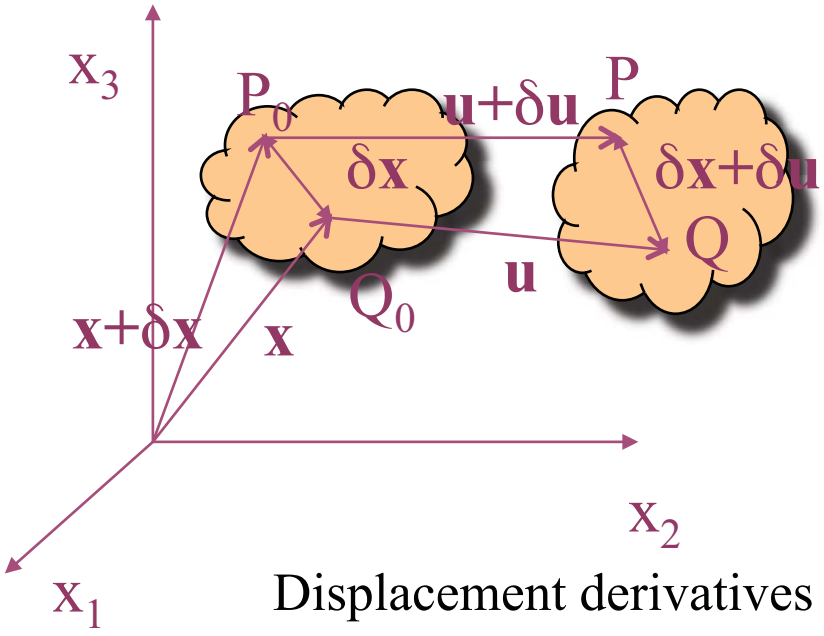

P_0, Q_0 … undeformed medium

P, Q ….. deformed medium

$$u_i(\mathbf{x}+\delta\mathbf{x}) = u_i(\mathbf{x}) + \frac{\partial u_i(\mathbf{x})}{\partial x_j}\delta x_j + O(\frac{\partial \mathbf{u}}{\partial \mathbf{x}})^2$$

Displacement derivatives represent a second-rank tensor which can be resolved into a **symmetric** and **anti-symmetric** parts:

$$\frac{\partial u_i(\mathbf{x})}{\partial x_j}\delta x_j = \frac{1}{2}\left(\frac{\partial u_i}{\partial x_j} + \frac{\partial u_j}{\partial x_i}\right)\delta x_j + \frac{1}{2}\left(\frac{\partial u_i}{\partial x_j} - \frac{\partial u_j}{\partial x_i}\right)\delta x_j = \epsilon_{ij}\delta x_j + \omega_{ij}\delta x_j$$

strain tensor — rotation tensor — $(\text{curl } \mathbf{u} \times \delta\mathbf{x})_i$

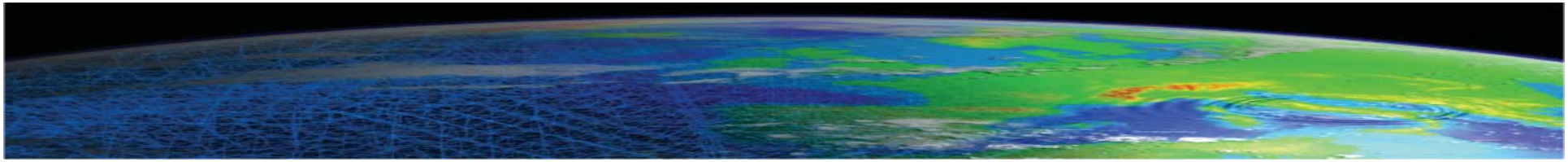

BASIC METHODOLOGIES OF SEISMIC ROTATIONAL MEASUREMENTS

1. **Microarrays** measuring differential motions (finite spatial derivatives)

2. **Ring laser gyrospopes** utilizing the Sagnac effect

3. **Small portable rotational sensors**

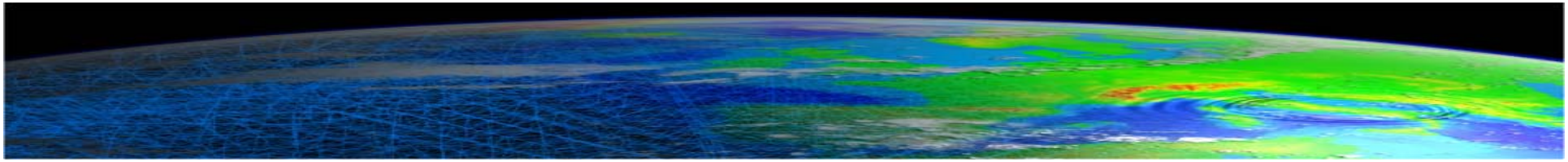

2. Ring lasers

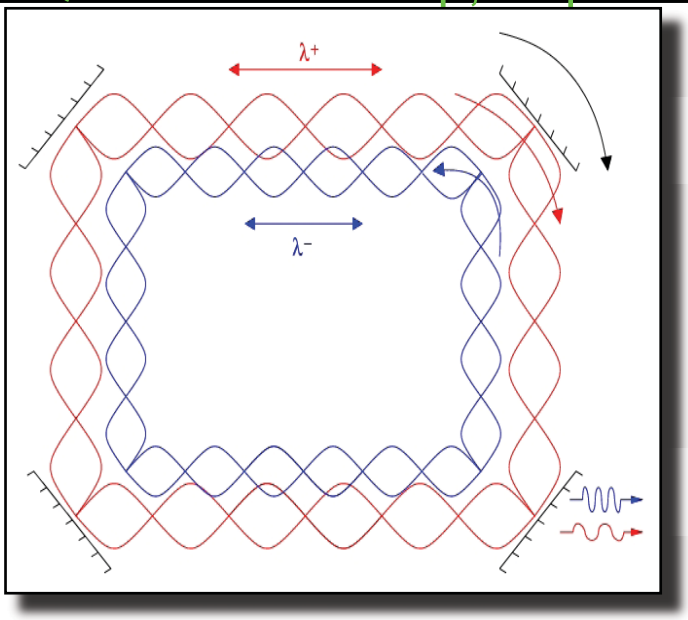

Superposition of co- and counter-rotating laser beams

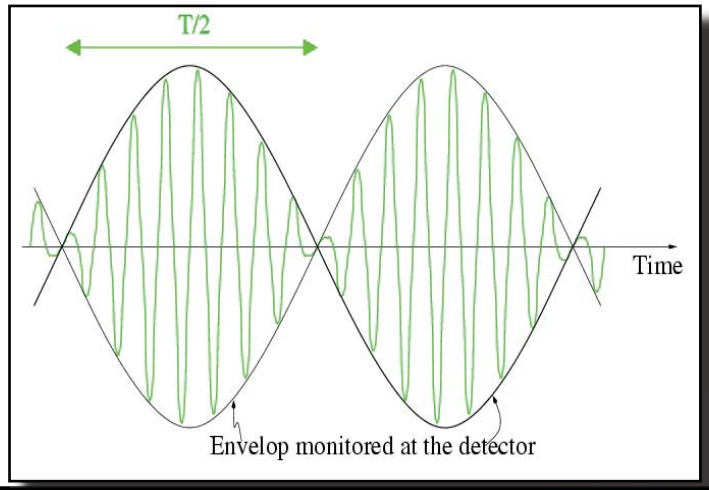

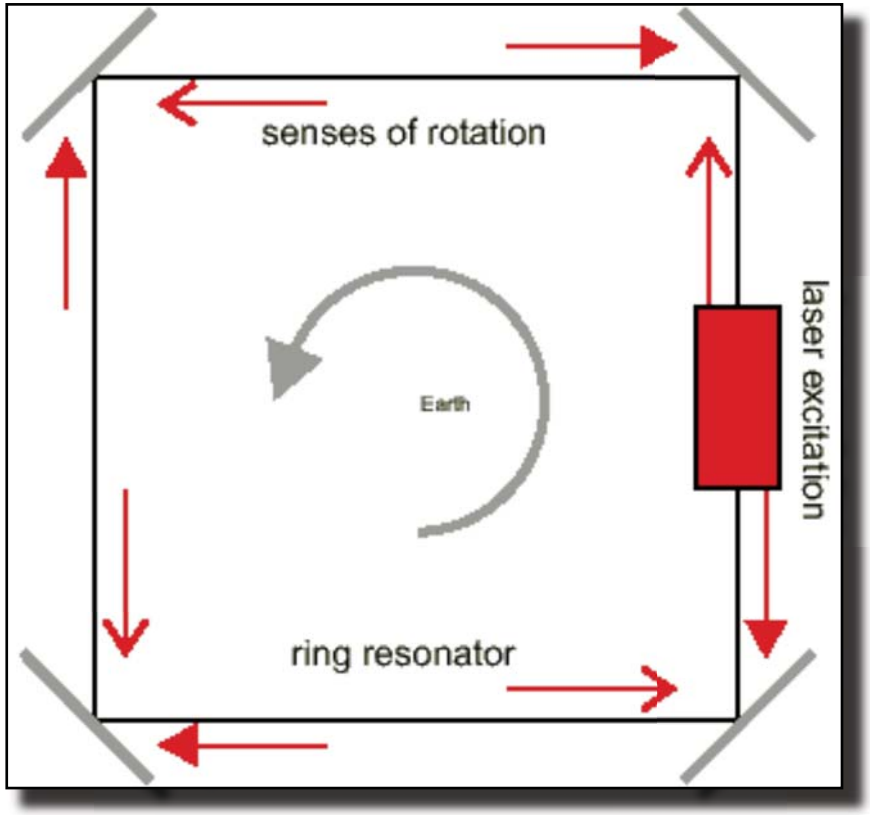

At the output, the frequency difference between the beams carries the information about the rotation rate.

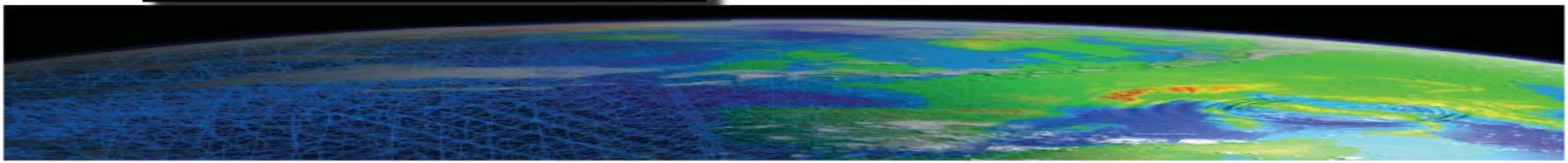

The ring laser at Wettzell

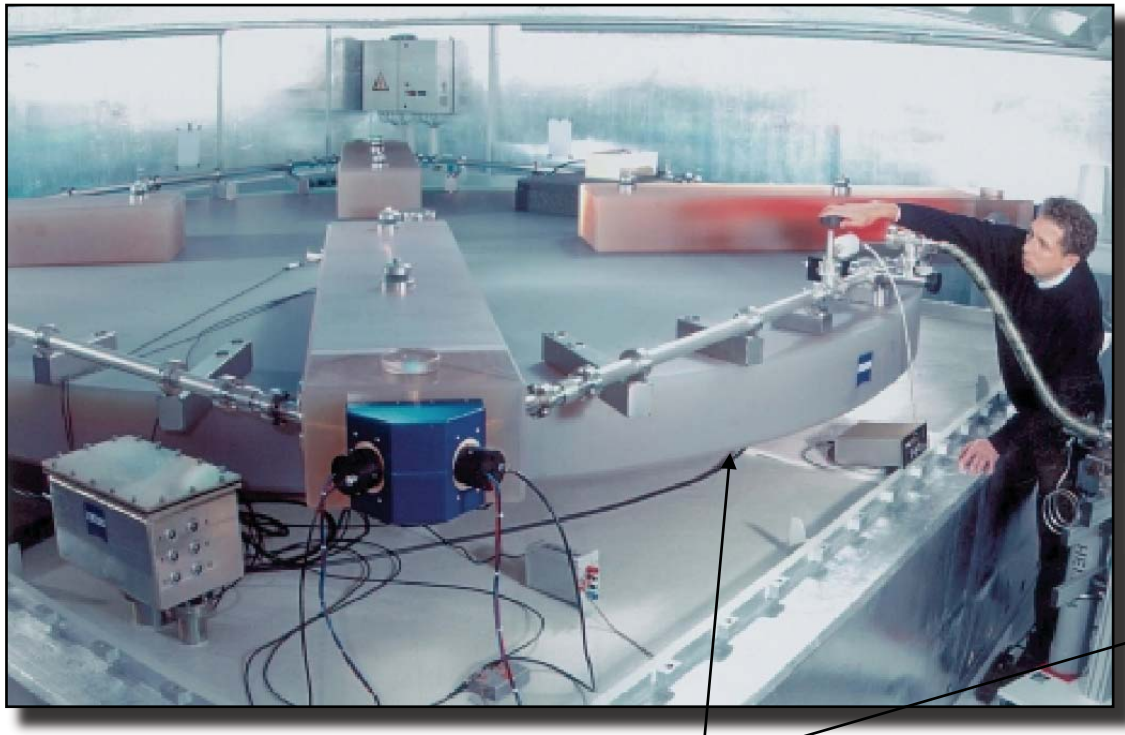

4 x 4 m ring laser

(resolution 10^{-12} rad/s)

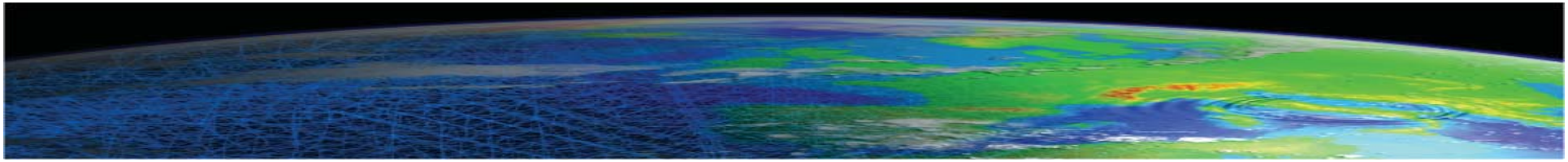

Ring laser installation at Wettzell

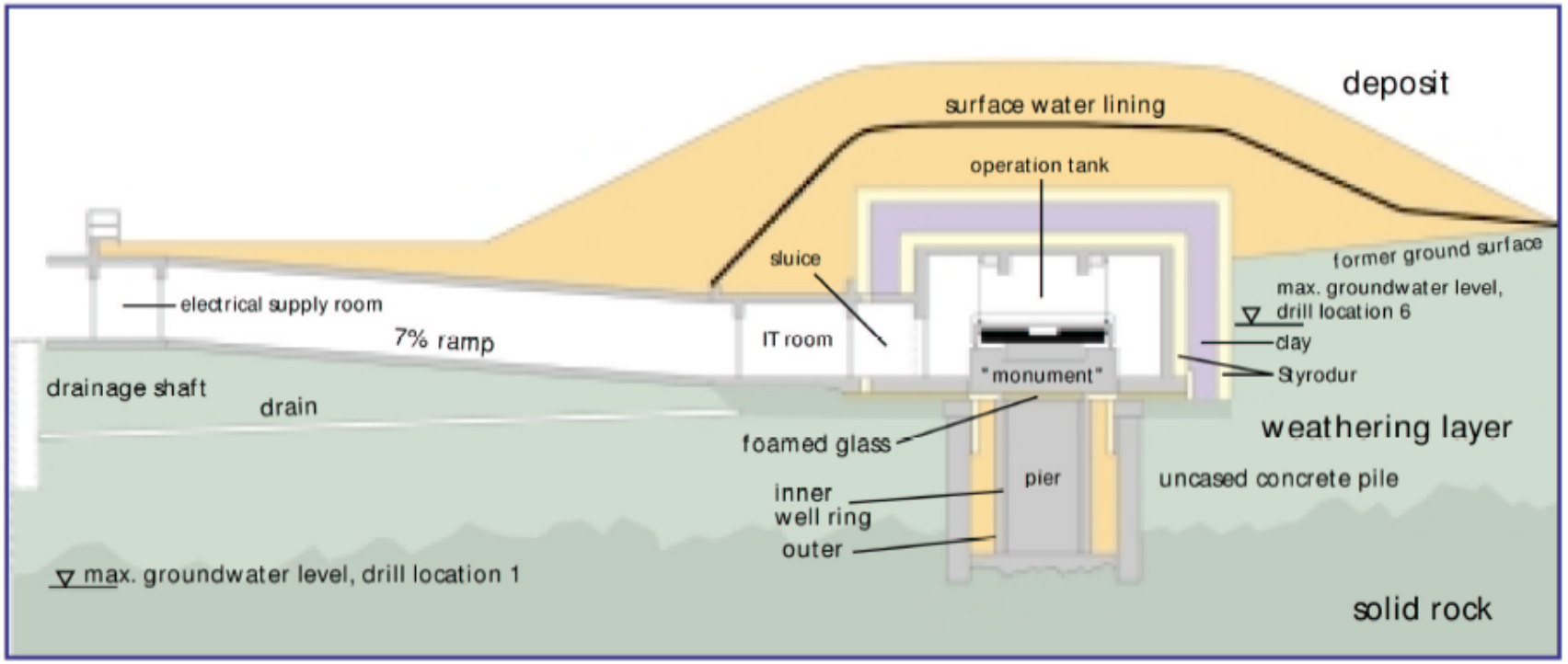

The cavern is located in southern Germany (49.1 N, 12.9 E)

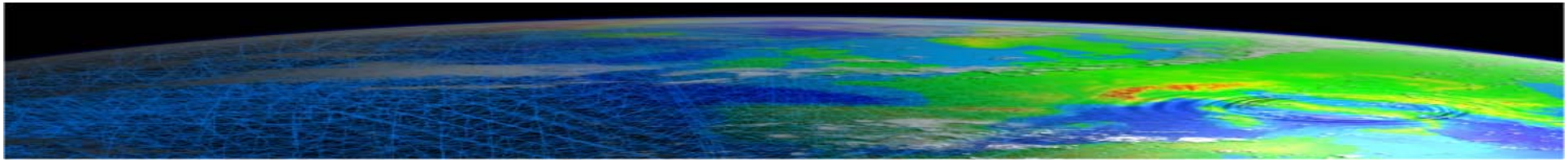

Mw = 8.3 Tokachi-oki 25.09.2003 (Igel et al., GRL, 2005)

transverse acceleration – **rotation rate**

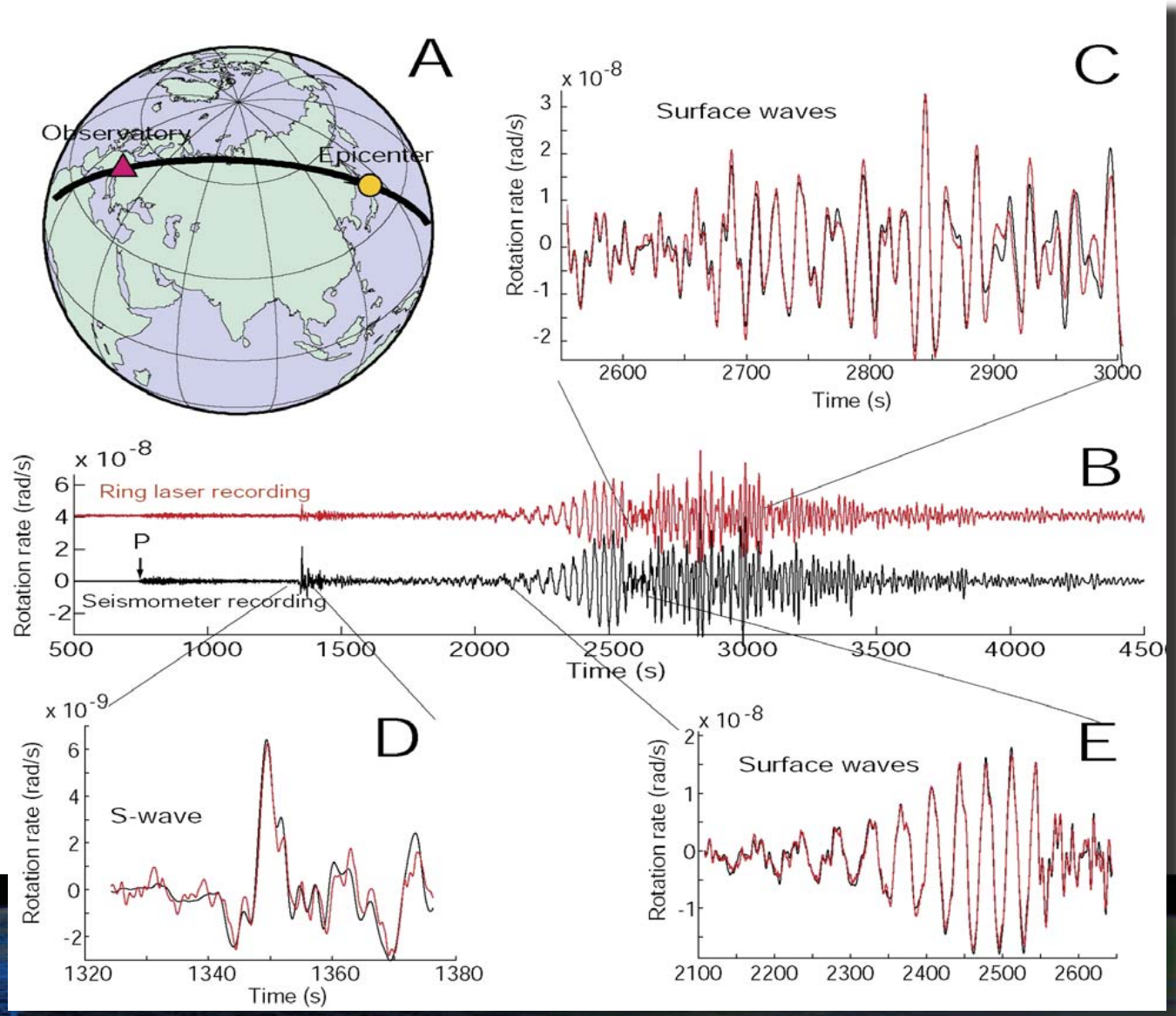

From Space: Terrestrial waves (in ionosphere)…

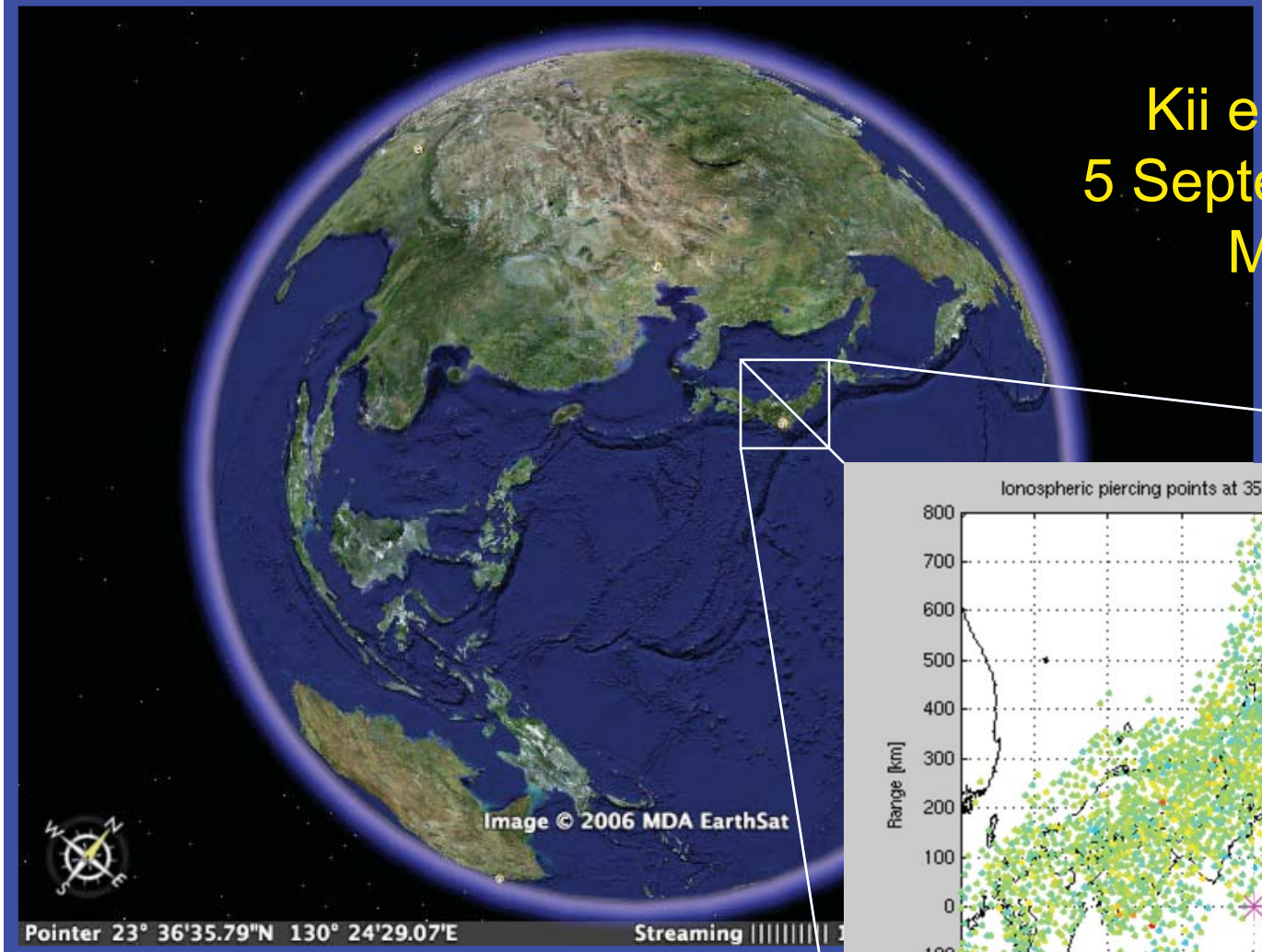

Kii earthquake
5 September 2004
Ms=7.4

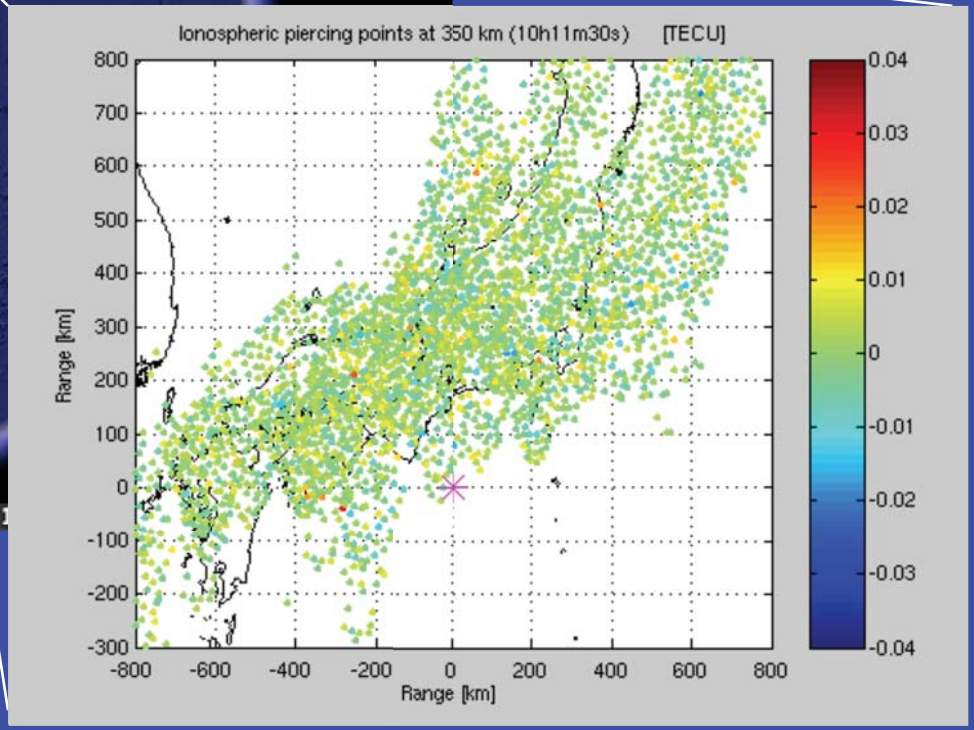

Lognonne, 2006

EXPLORATION OF TERRESTRIAL PLANETS

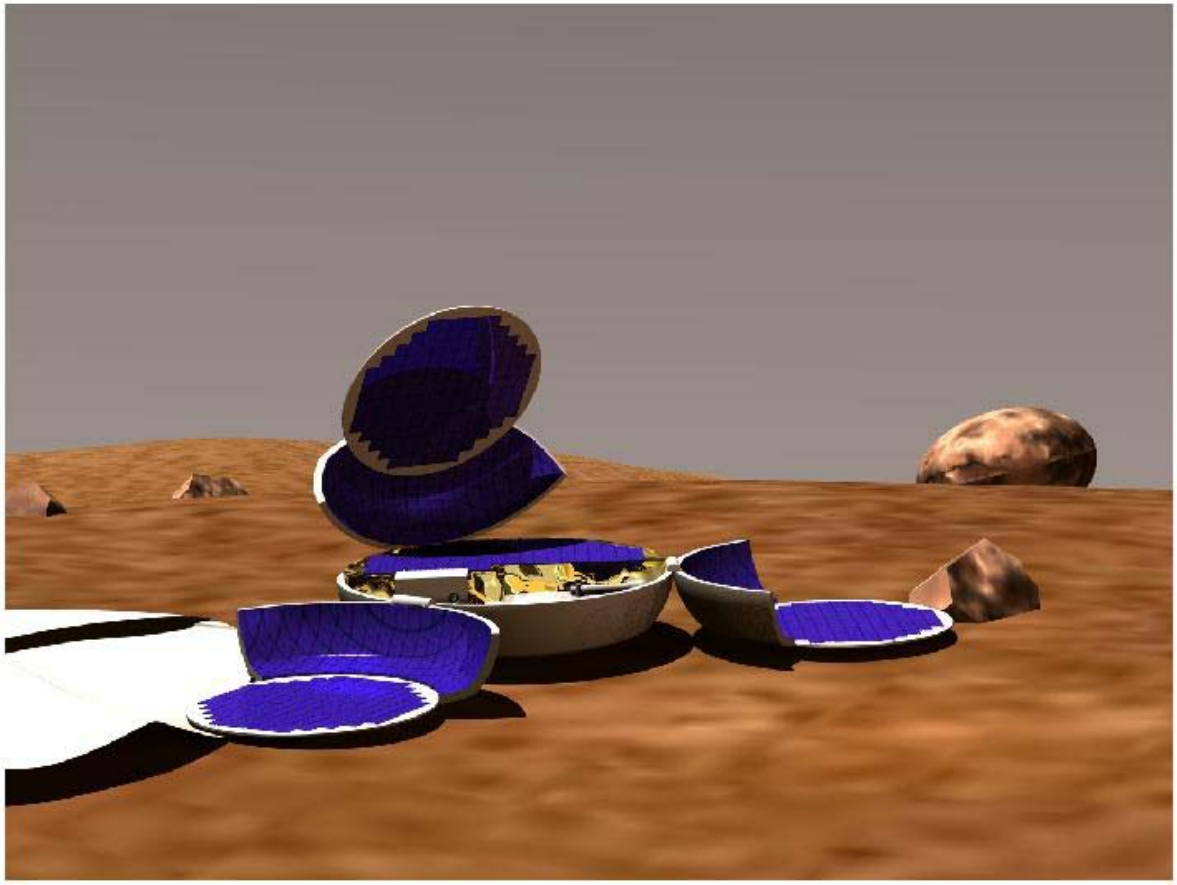

NETLANDER: MARS

(Lognonné et al. 2004)

Overview
Large scale Seismology: an observational field

- Data (Seismic source) + Instrument (Seismometer) -> Observations (seismograms)

- **Historical evolution: Ray theory, Normal mode theory, Numerical techniques (SEM, NM-SEM)**

- Scientific Issues: Earthquakes (Sumatra-Andaman), Anisotropic structure of the Earth
- Tomographic Technique
- Geodynamic Applications

  Seismic Experiment, Plume detection
- Adjoint and time reversal methods

Propagation of seismic waves

Hypothesis: Elastic Medium : $\sigma_{ij} = C_{ijkl}\, \varepsilon_{kl}$

Where ε_{kl} is the strain tensor, σ_{ij} the stress tensor

C_{ijkl} the elastic tensor: 81 elastic moduli

Symmetries of ε_{kl}, σ_{ij} and of the strain energy
$W = 1/2\ \sigma_{ij}\ \varepsilon_{ij}$ => **21** independent elements

Isotropic case => **2** independent elements
$C_{ijkl} = \lambda\, \delta_{ij}\, \delta_{kl} + \mu\, (\delta_{ik}\, \delta_{jl} + \delta_{il}\, \delta_{jk})$

λ , μ are Lamé parameters

Elastodynamic equation of motion

$$\partial_j(C_{ijkl}\,\partial_k u_l) - \rho\,\partial_{tt} u_i = 0$$

In the isotropic case, 2 solutions:

S-wave

P wave

In heterogeneous media, comparison between

Wavelength λ and scale of heterogeneity Λ

2 Two extremes cases $\lambda >> \Lambda$ or $\lambda << \Lambda$

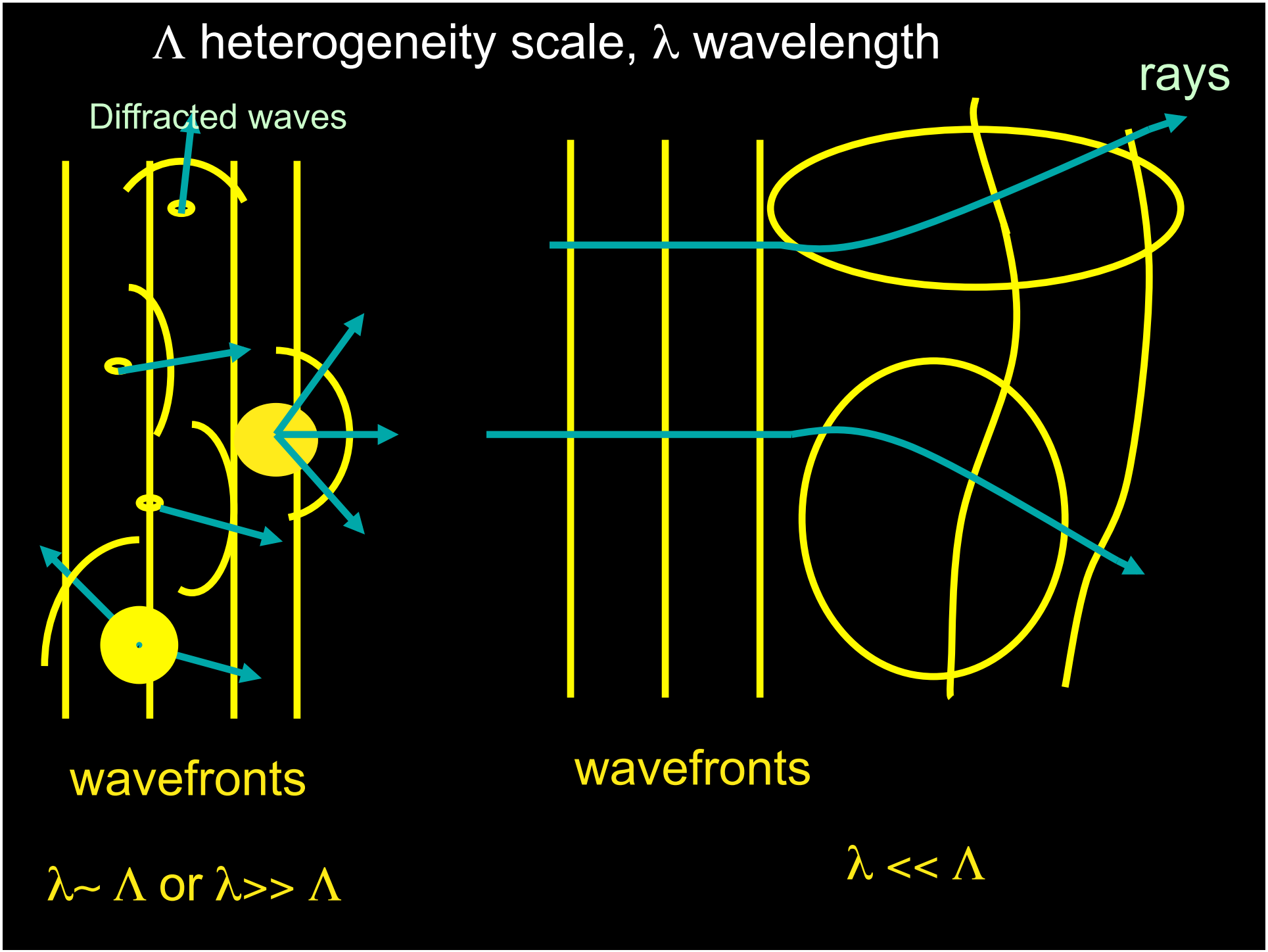
Λ heterogeneity scale, λ wavelength
Diffracted waves
rays
wavefronts
wavefronts
λ~ Λ or λ>> Λ
λ << Λ

Duality wave - particle:

- λ seismic wavelength
- Λ scale heterogeneity

- Particle: Ray theory (XXth century)

$\lambda << \Lambda$

- Wave: Normal mode theory (>1970)
  (Finite frequency effects)

RAY PATHS INSIDE THE EARTH

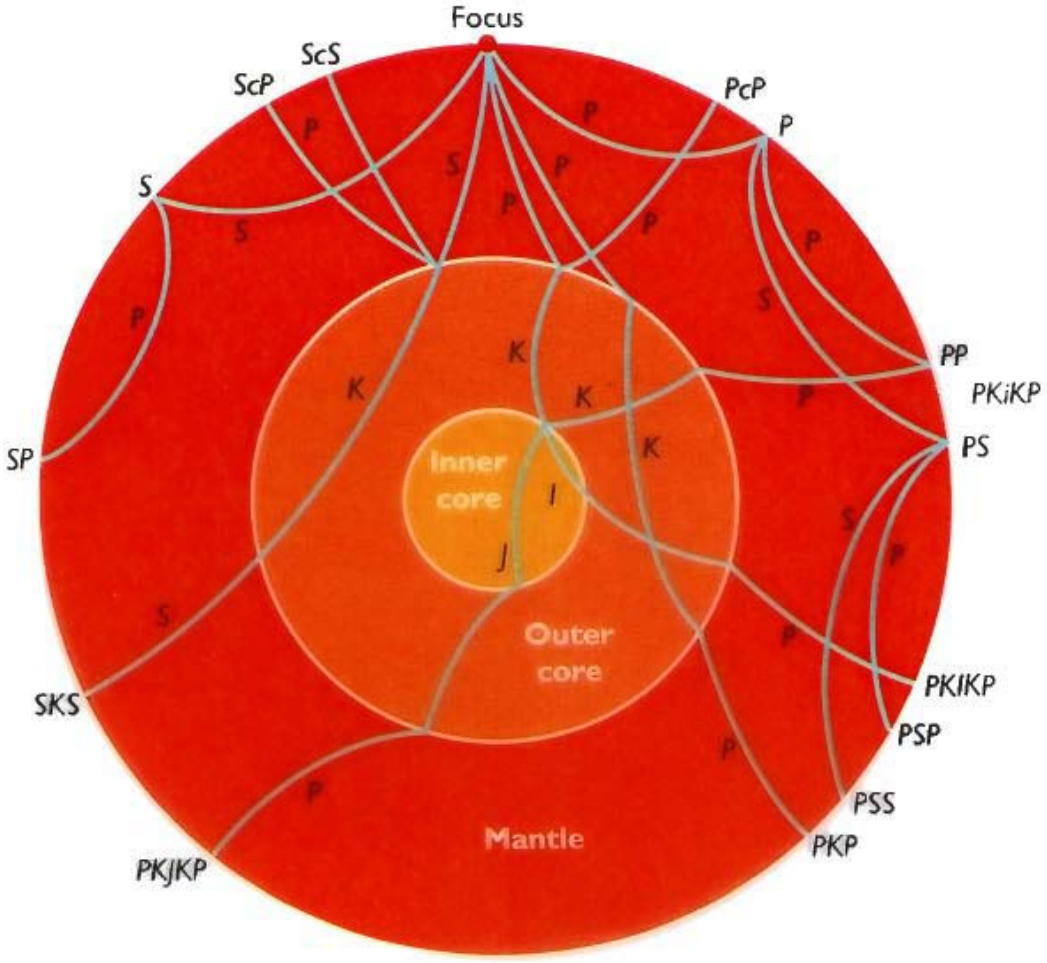

Bolt, 1993

“Travel time” of certain seismic phases vs. epicentral distance

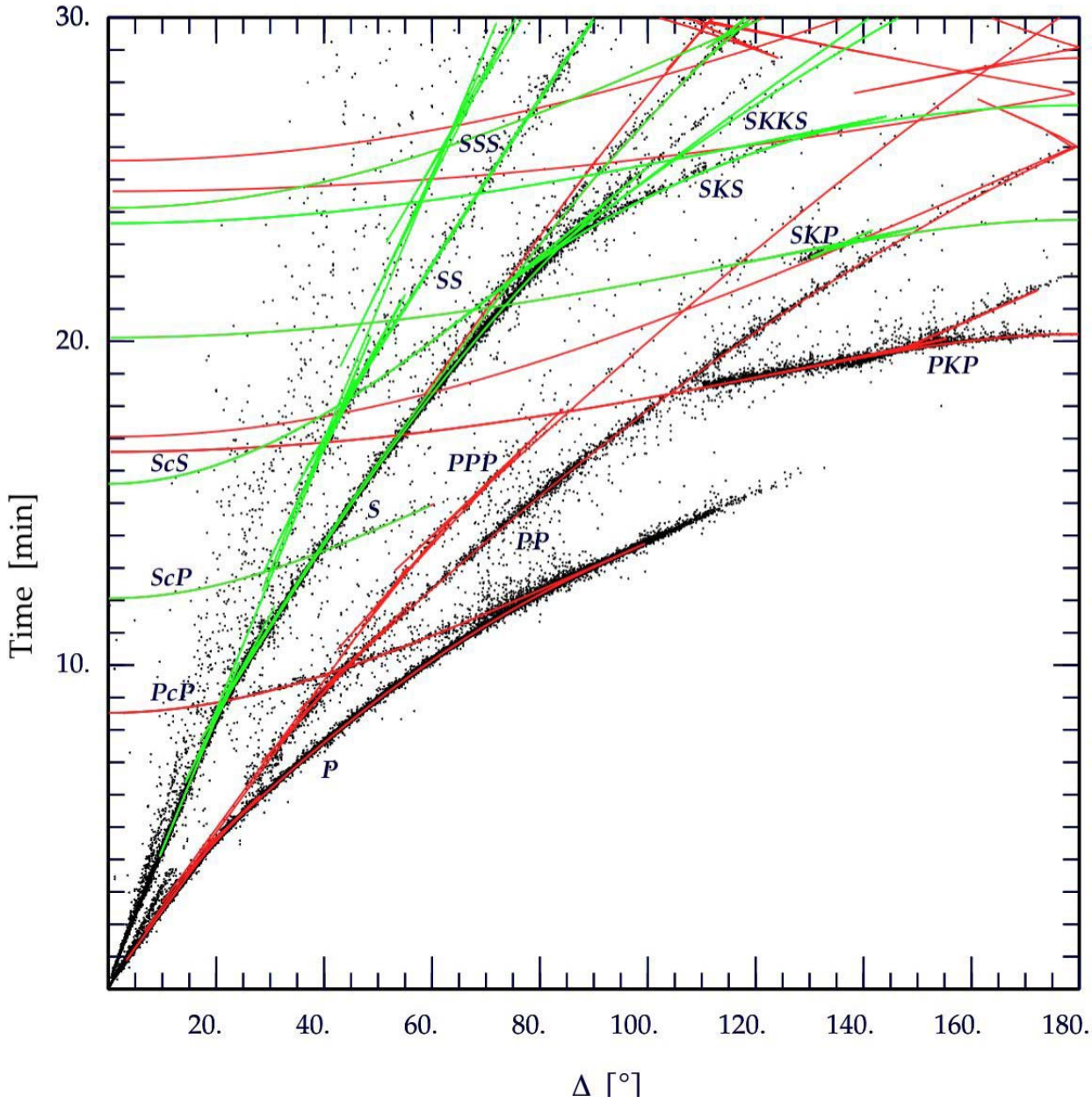

Duality wave - particle:

- λ seismic wavelength
- Λ scale heterogeneity

- Particle: Ray theory (XXth century)

$\lambda << \Lambda$

- Wave: Normal mode theory (>1970)
  (Finite frequency effects) $\lambda >> \Lambda$

Normal modes
Chile Earthquake (22 may 1960) recorded at Paris (IPGP)

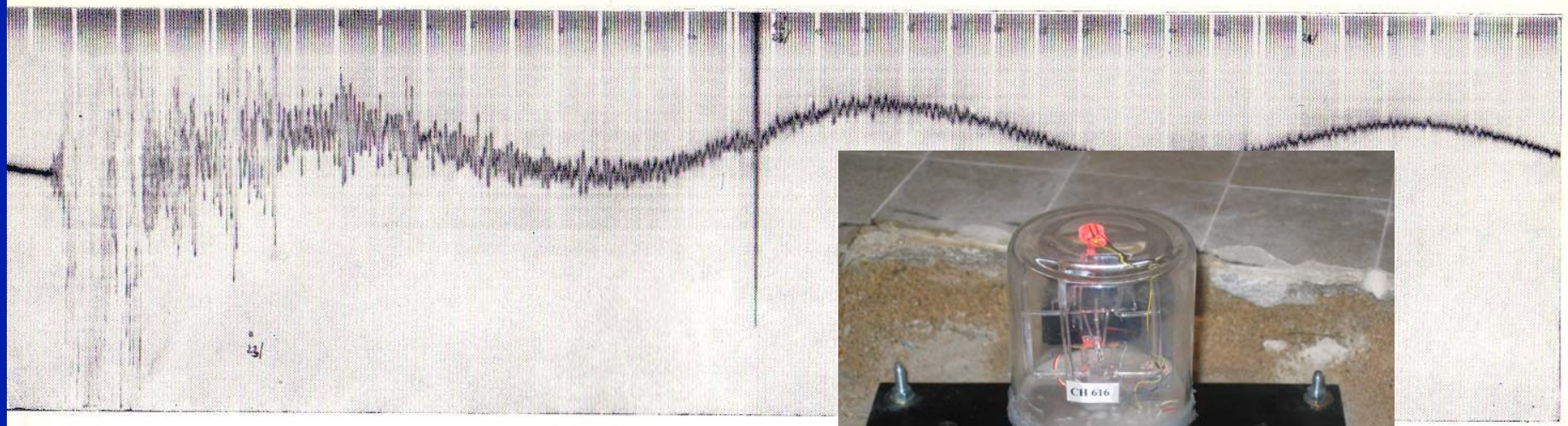

1*a*

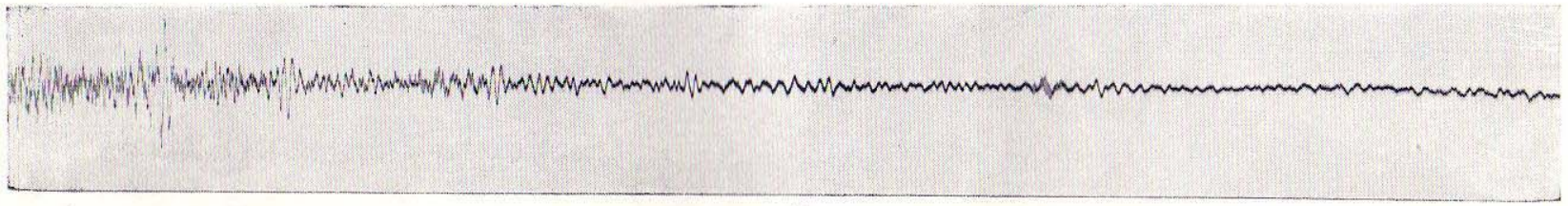

1*b*

FIG. 1. — *a*) Enregistrement du pendule E, nº 1 (voir tableau I).
b) Enregistrement du pendule B, nº 4 (voir tableau I). (Un intervalle de 5 minutes est représenté sur cette figure par 1,45 mm.)

Chile earthquake (may 22 1960) recorded at Paris (IPGP)

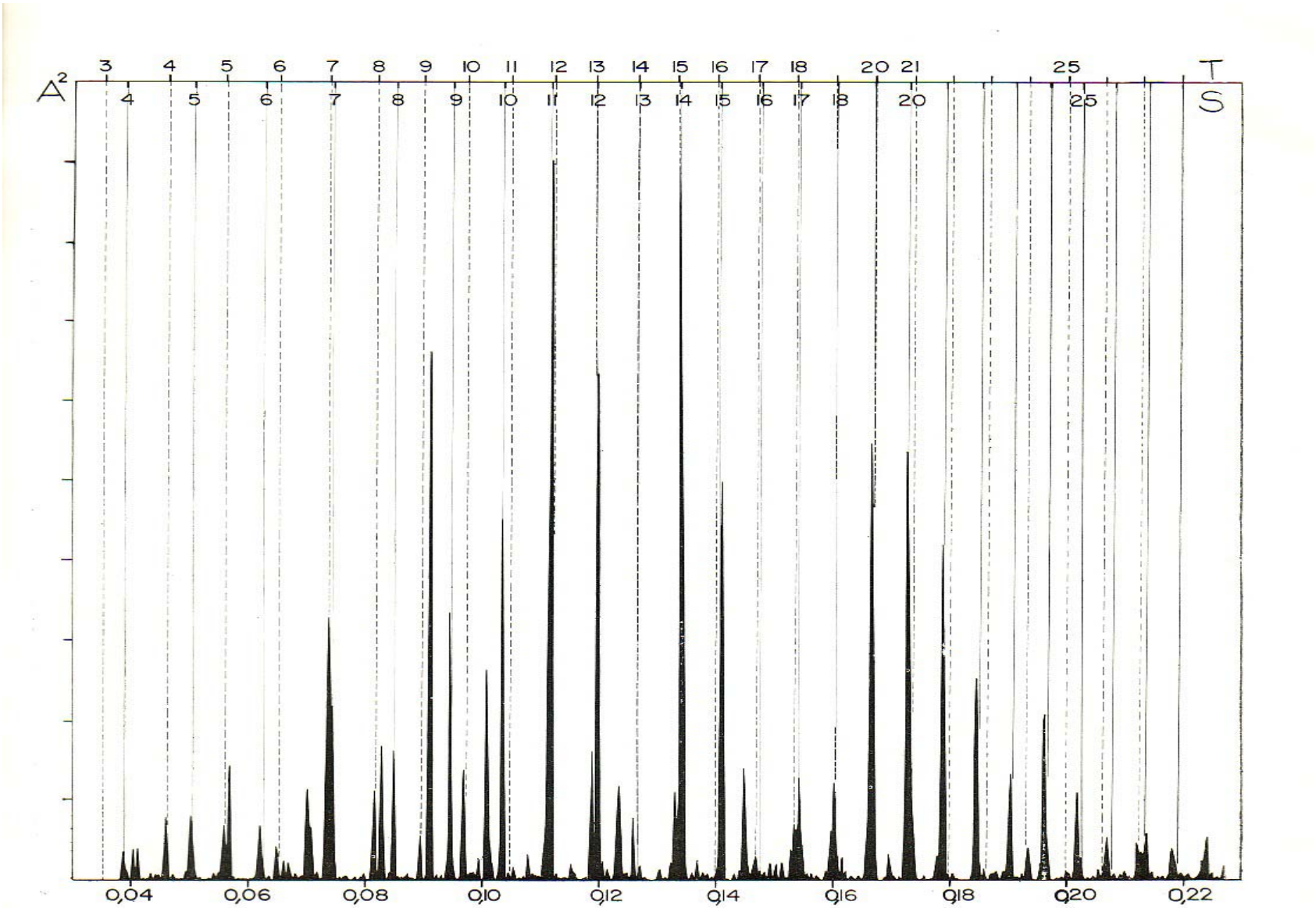

FIG. 3. — Spectre de l'enregistrement du pendule E (n° 1) — En haut : positions des pics théoriques pour les oscillations sphéroïdales S et les oscillations de torsion T du modèle de Gutenberg continental.

First observations of free oscillations of the Earth

1953? -> 1960 (Chile earthquake)

Frequency Peaks were not well understood

Theory was incomplete

Kuril islands 1994-277 Ms=8.3

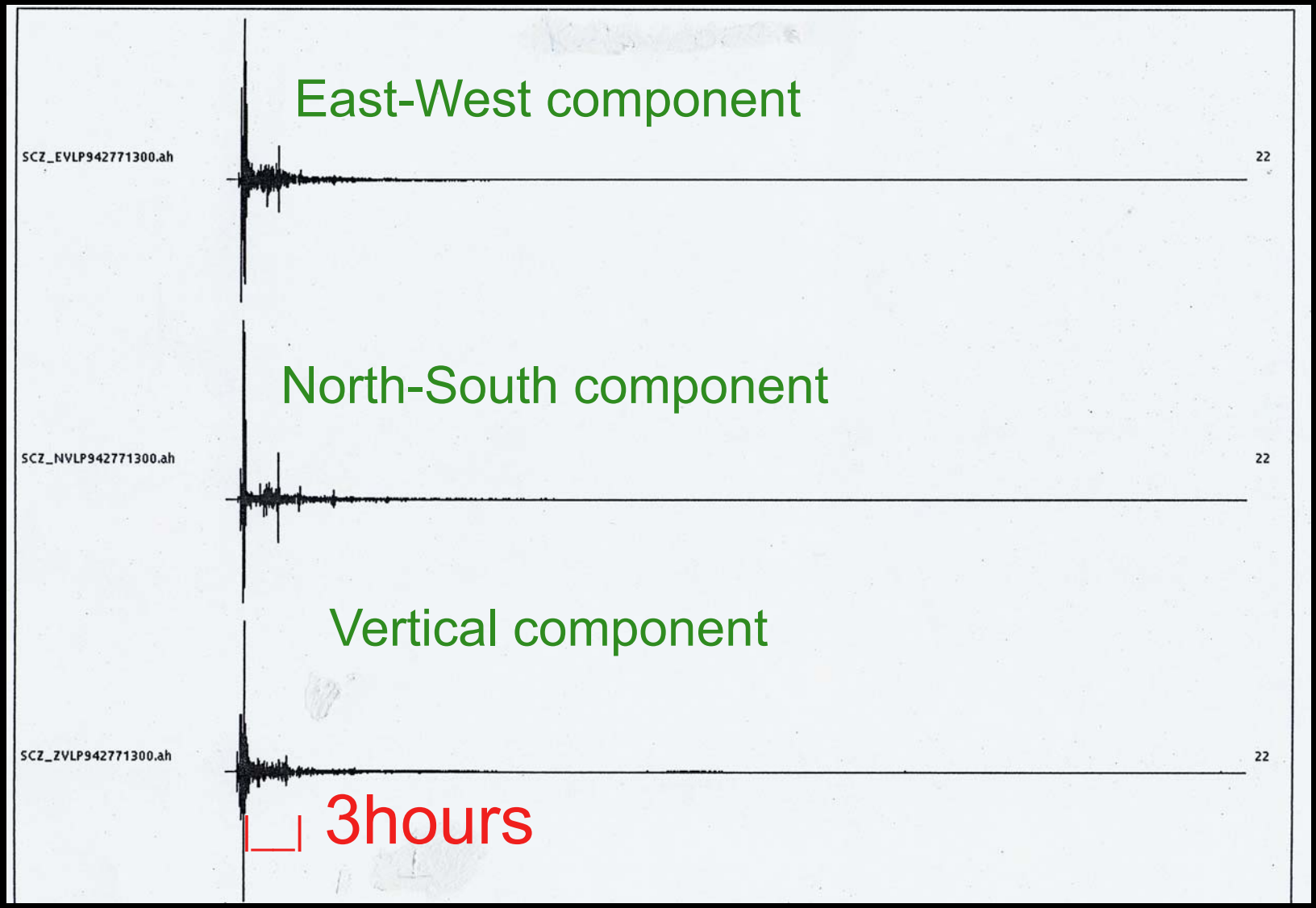

Kuril islands 1994-277 SCZ-VLP
Spectra 3 hours

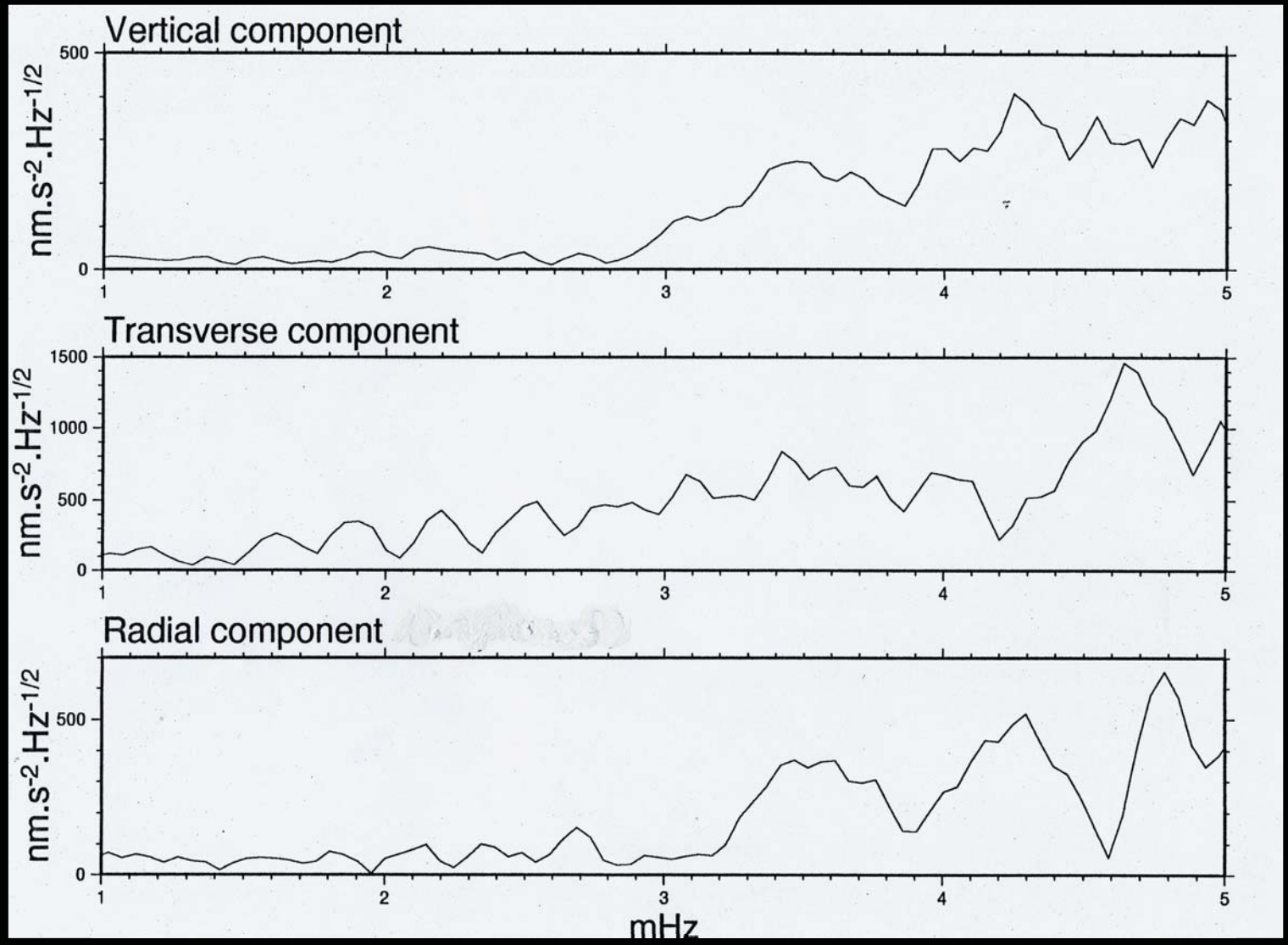

1 **Frequency (mHz)** 5

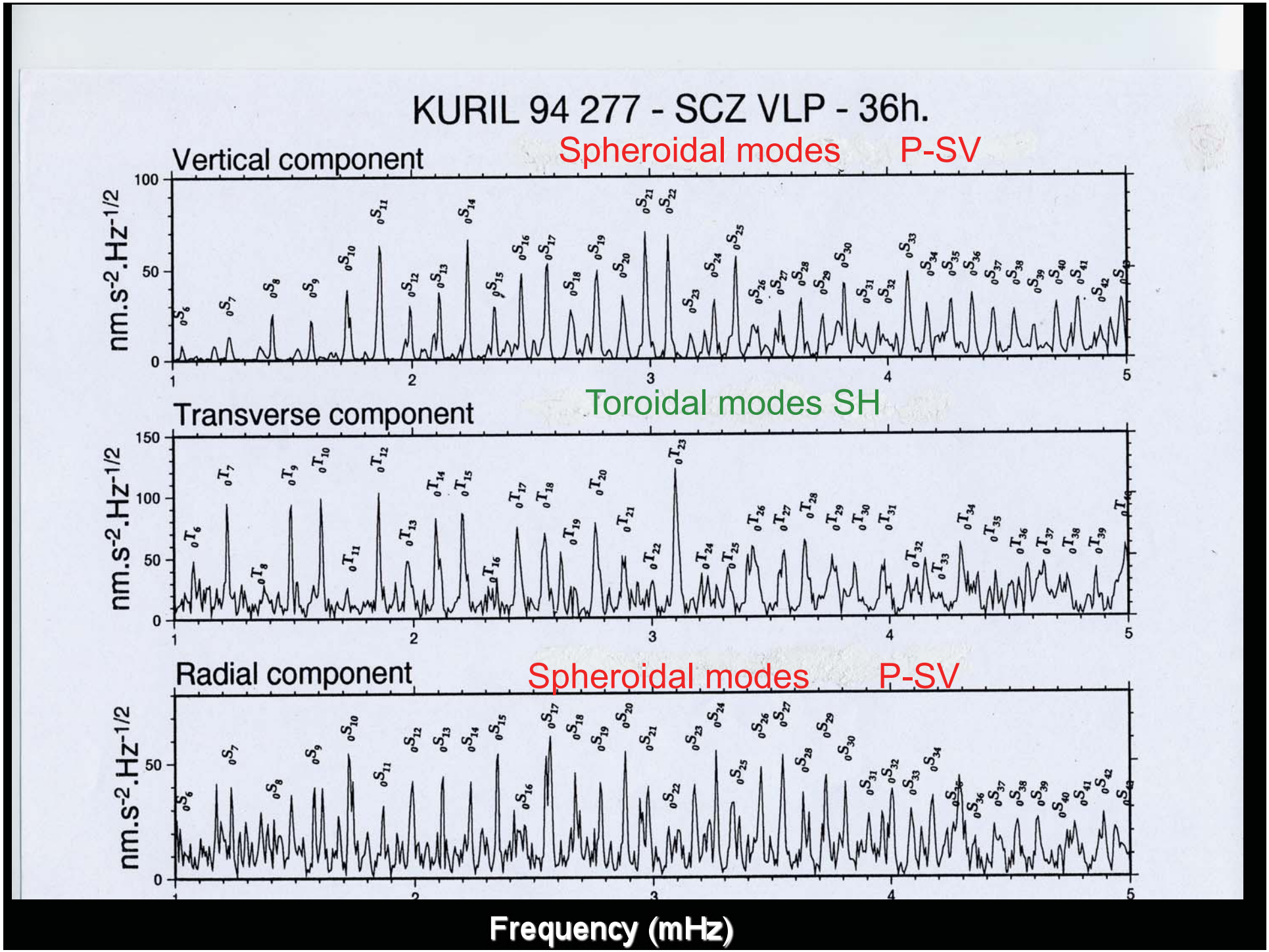
KURIL 94 277 - SCZ VLP - 36h.
Vertical component
Spheroidal modes P-SV
Transverse component
Toroidal modes SH
Radial component
Spheroidal modes P-SV
nm.s-2.Hz-1/2
Frequency (mHz)

Elastodynamic equation

$$\rho \partial_{tt} \mathbf{u}_{0i} = \partial_j \sigma_{ij} + \rho\, \mathbf{g}_i + \mathbf{F}_i \; (+ \mathbf{Fs}_i + \ldots)$$

Which can be rewritten:

$$\rho \partial_{tt} \mathbf{u}_0 = \mathbf{H}_0 \mathbf{u}_0 \;\; (+ \mathbf{Fs})$$

H_0 is an integro-differential operator

1D-Reference Earth Model:

$M_0(r)$, $\rho(r)$, $V_P(r)$, $V_s(r)$

(PREM, Dziewonski and Anderson, 1981
or IASP91, Kennett and Engdahl, 1991)

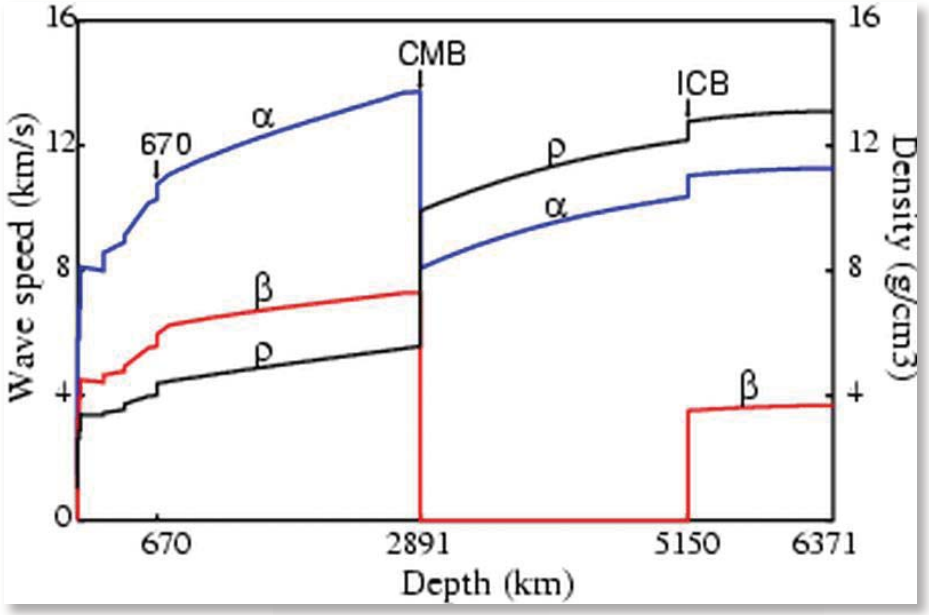

⇨ John Woodhouse lecture

$$\rho \partial_{tt} \mathbf{u}_0 = \mathbf{H_0 u_0} \ \mathbf{(+ Fs)}$$

Eigenfrequencies: ${}_n\omega_l$

Eigenfunctions: ${}_n u_l^m (r,t) = |n,l,m\rangle \exp(-i_n \omega_l t)$

3 quantum numbers ($k=\{n,l,m\}$) => $\mathbf{u}_k(\mathbf{r}) \exp(-i_n \omega_l t)$

$$\int \rho \ \mathbf{u}_k^* \ . \ \mathbf{u}_k \ d^3x = \delta_{ij}$$

$$\mathbf{H_0} \ \mathbf{u}_k = \rho \ {}_n\omega_l^2 \ \mathbf{u}_k$$

Displacement:

$$\mathbf{u}(\mathbf{r},t) = \Sigma_{n,l,m} \ {}_n\mathbf{a}_l^m \ |n,l,m\rangle \exp(-i_n \omega_l t)$$

$$\mathbf{u}_k(\mathbf{r}) = \{U(r)\mathbf{e}_r + V(r)\mathbf{e}_\theta \partial_\theta + V(r)/\sin\theta \ \mathbf{e}_\phi \partial_\phi \} Y_l^m(\theta,\phi)$$
$$+ \{W(r)/\sin\theta \ \mathbf{e}_\theta \partial_\phi - W(r) \ \mathbf{e}_\phi \partial_\theta \} Y_l^m(\theta,\phi)$$

1D-Reference Earth Model:
$M_0(r)$, $\rho(r)$, $V_P(r)$, $V_s(r)$
(PREM, Dziewonski and Anderson, 1981)

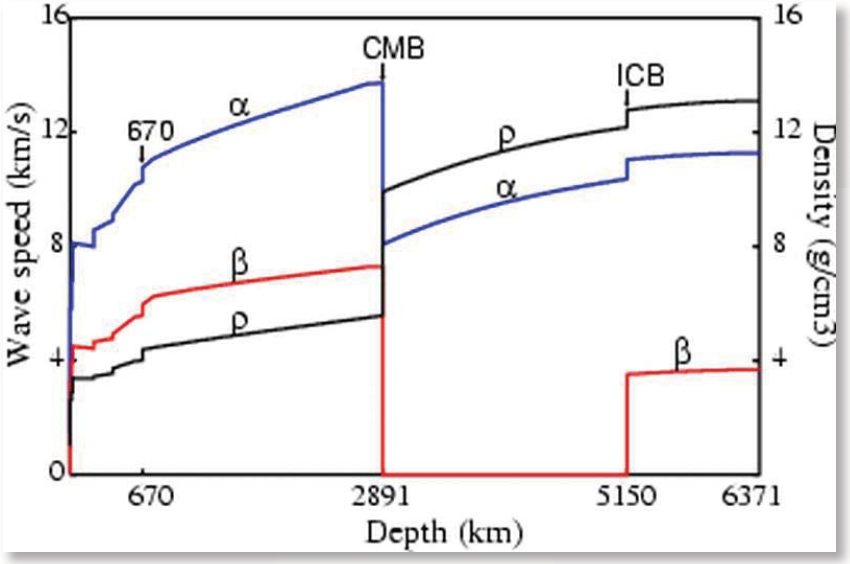

$\rho \partial_{tt} \mathbf{u}_0 + \mathbf{H_0 u_0} = \mathbf{0}$

Eigenfrequencies: ${}_n\omega_l$
Eigenfunctions: ${}_n u_l^m (r,t) = |n,l,m\rangle \exp(-i\,{}_n\omega_l t)$

2 kinds of modes: Toroïdal ${}_nT_l$, Spheroïdal ${}_nS_l$

Degeneracy of eigenfrequencies ${}_n\omega_l$: 2 l +1

Spherical eigenfrequencies

Spheroïdal Modes ${}_nS_l$ (P-SV / Rayleigh)

Toroïdal modes ${}_nT_l$ (SH / Love)

Dispersion Branches

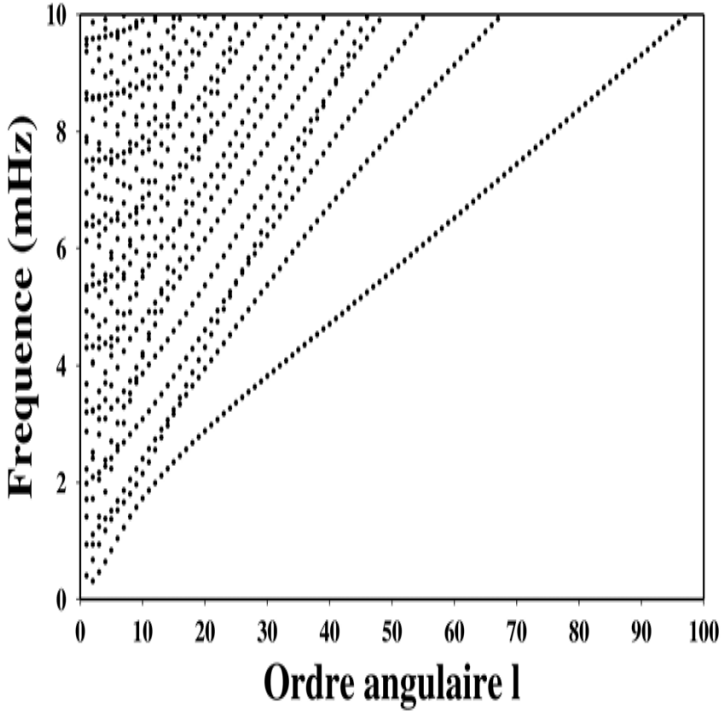

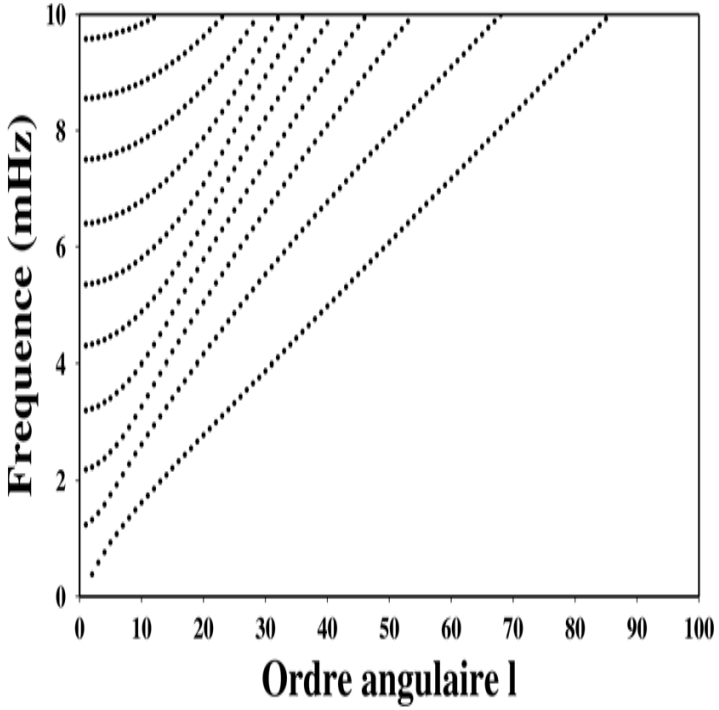

multiplet : (n,l) = 2l+1 singlets
singlet : (n,l,m)

n : radial order
l : angular order
m : azimuthal order

Spheroidal Modes

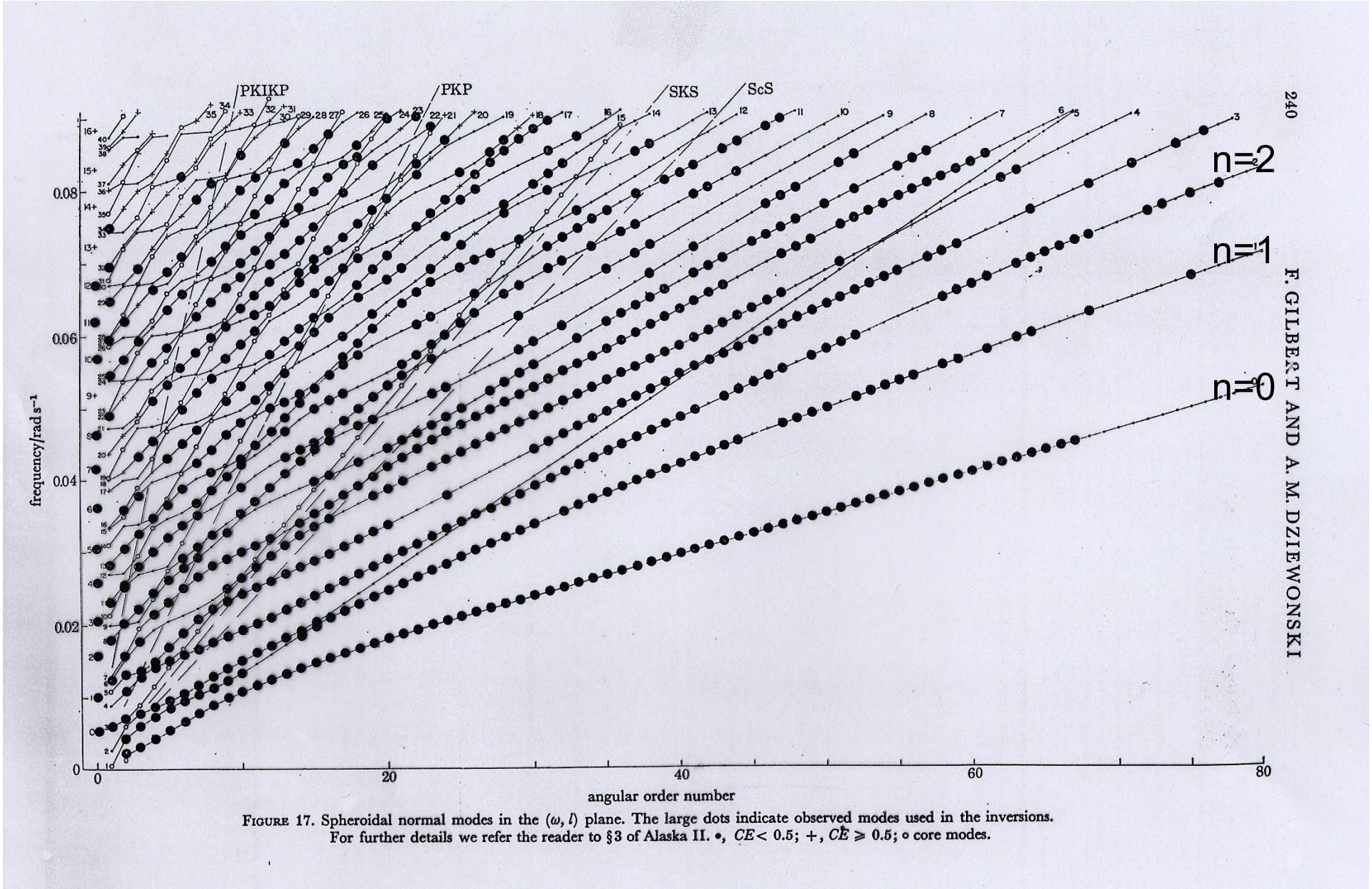

FIGURE 17. Spheroidal normal modes in the (ω, l) plane. The large dots indicate observed modes used in the inversions. For further details we refer the reader to §3 of Alaska II. •, $CE < 0.5$; +, $CE \geq 0.5$; ∘ core modes.

Toroidal modes ${}_0T_2$ (44.2 min), ${}_1T_2$ (12.6 min) and ${}_0T_3$ (28.4 min)

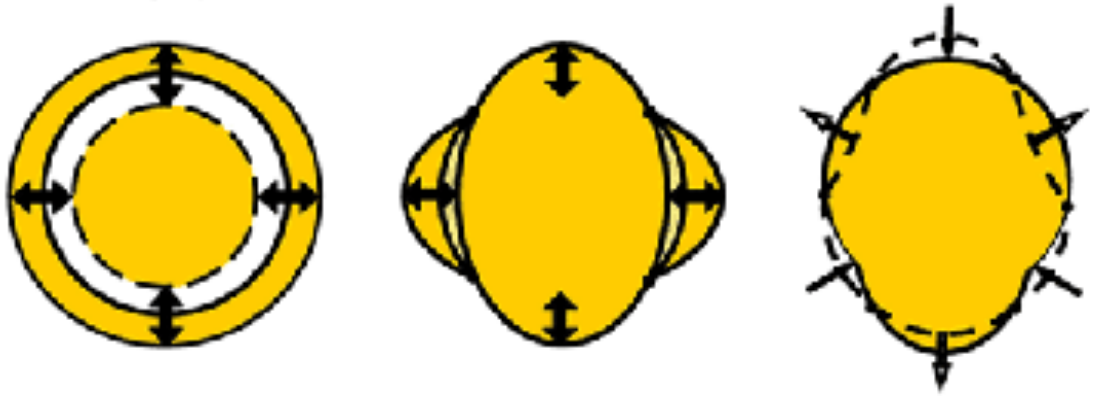

Spheroidal modes ${}_0S_0$ (20.5 min), ${}_0S_2$ (53.9 min) and ${}_0S_3$ ((35.6 min)

Study of Sumatra earthquake (26 december 2004) With GEOSCOPE stations

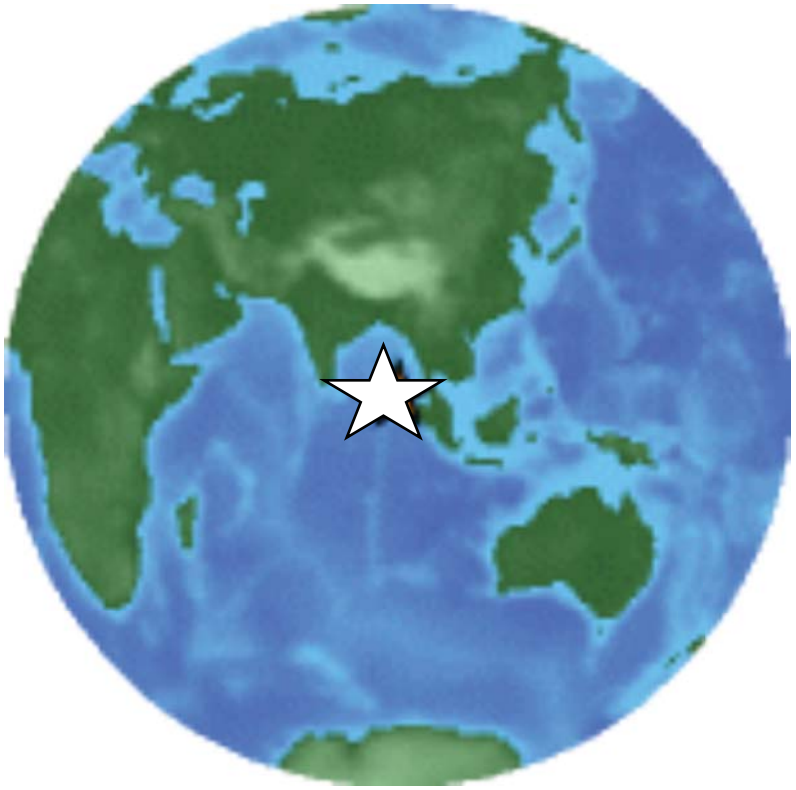

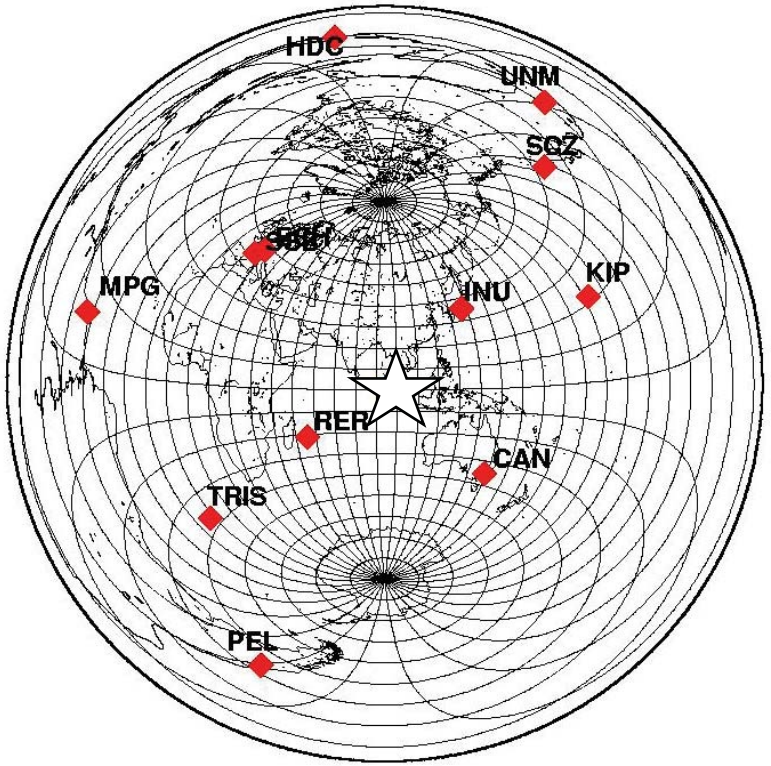

(Roult and Clévédé, 2005 ; Park et al., Science, 2005)

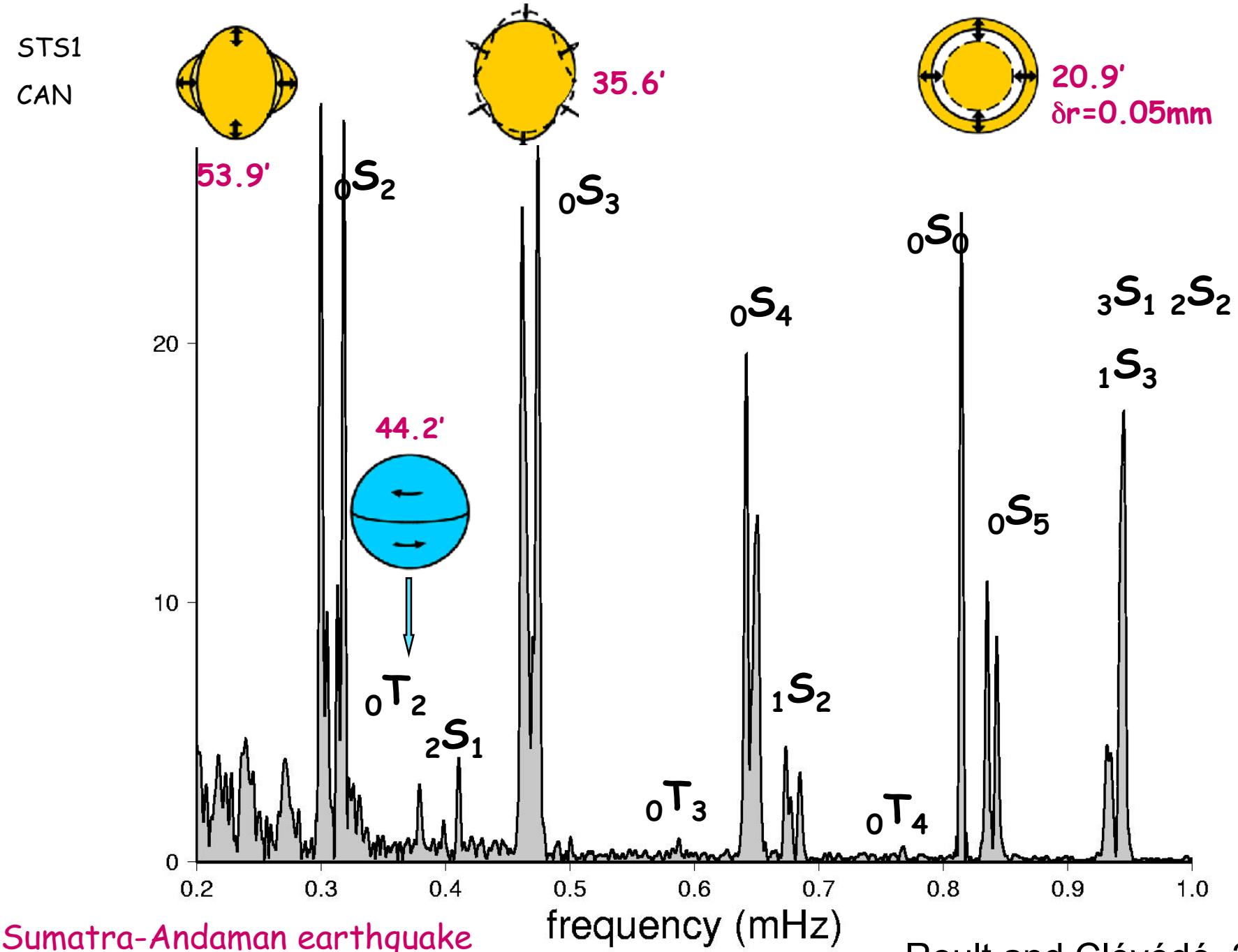

Sumatra-Andaman earthquake
26 December 2004

Roult and Clévédé, 2005

mode ${}_0S_2$ => splitting 5 singlets

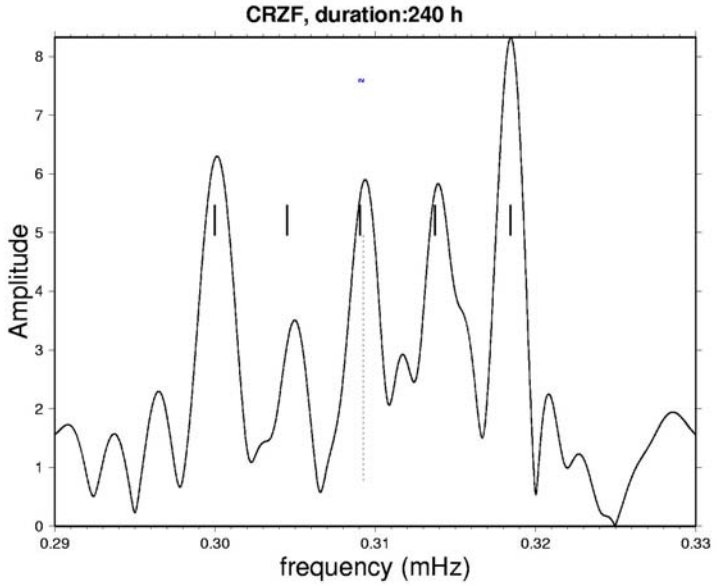

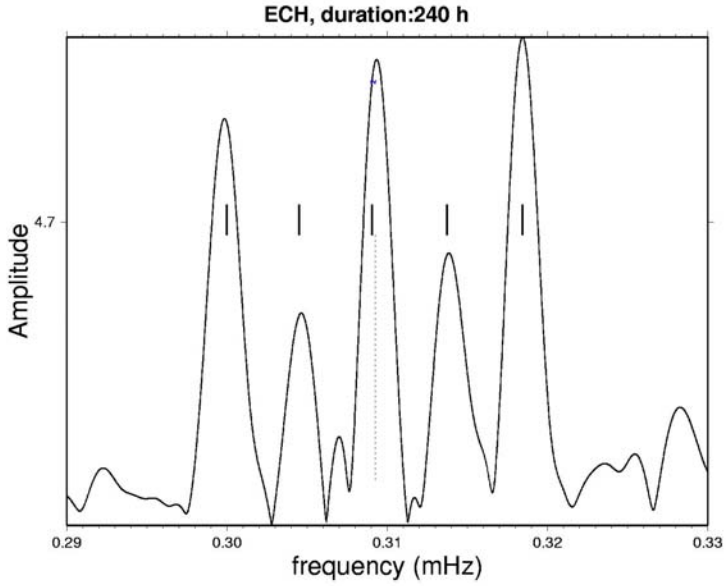

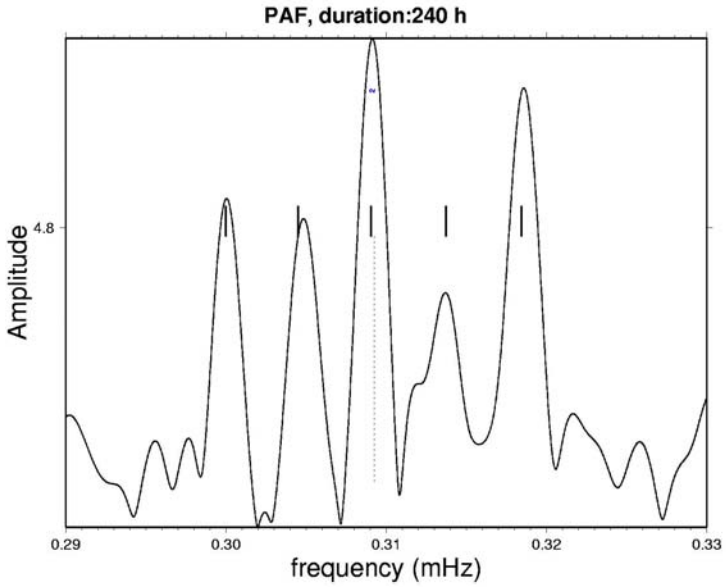

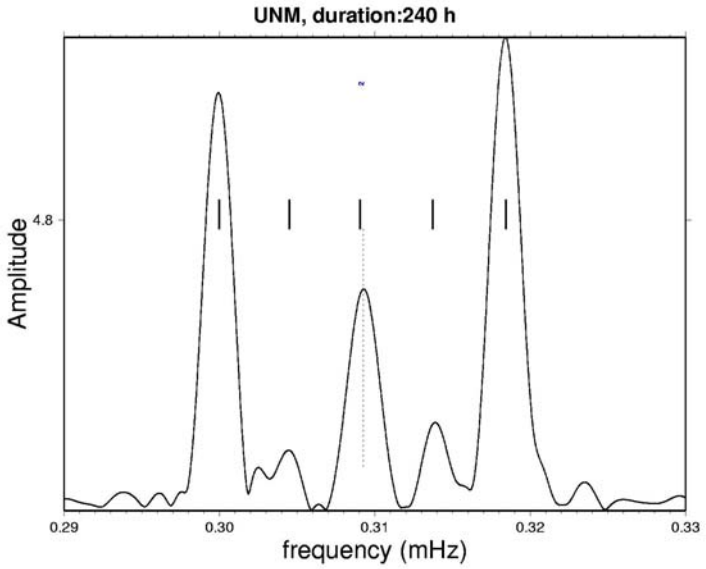

mode $_0S_3$

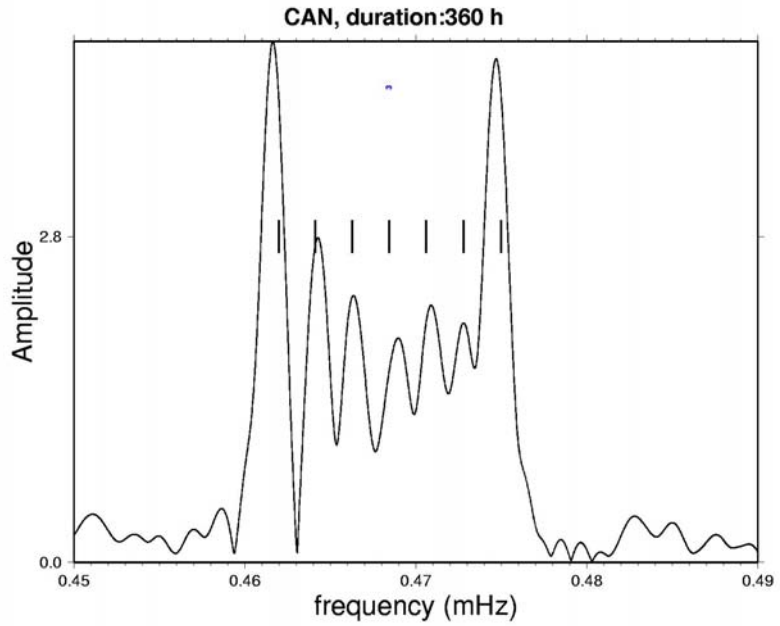
CAN, duration:360 h
Amplitude
2.8
0.0
0.45
0.46
0.47
0.48
0.49
frequency (mHz)

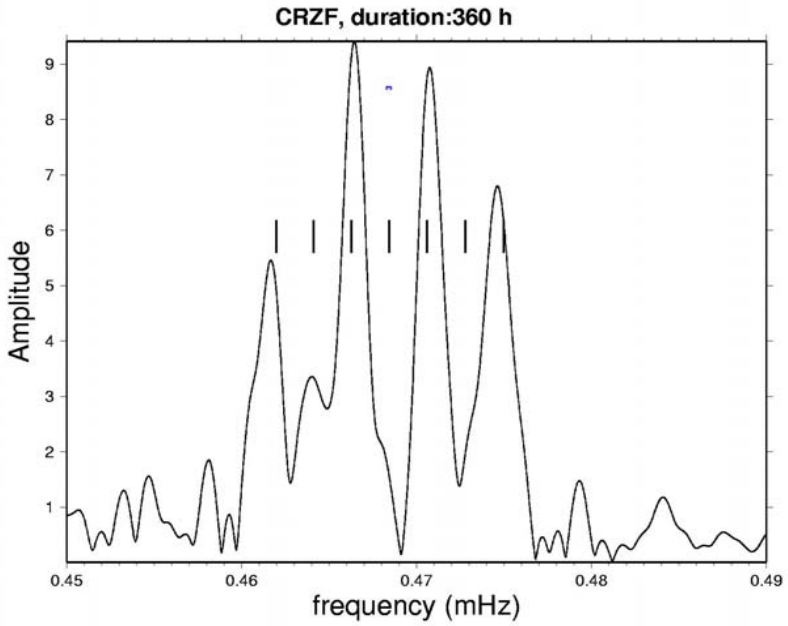
CRZF, duration:360 h
Amplitude
9
8
7
6
5
4
3
2
1
0.45
0.46
0.47
0.48
0.49
frequency (mHz)

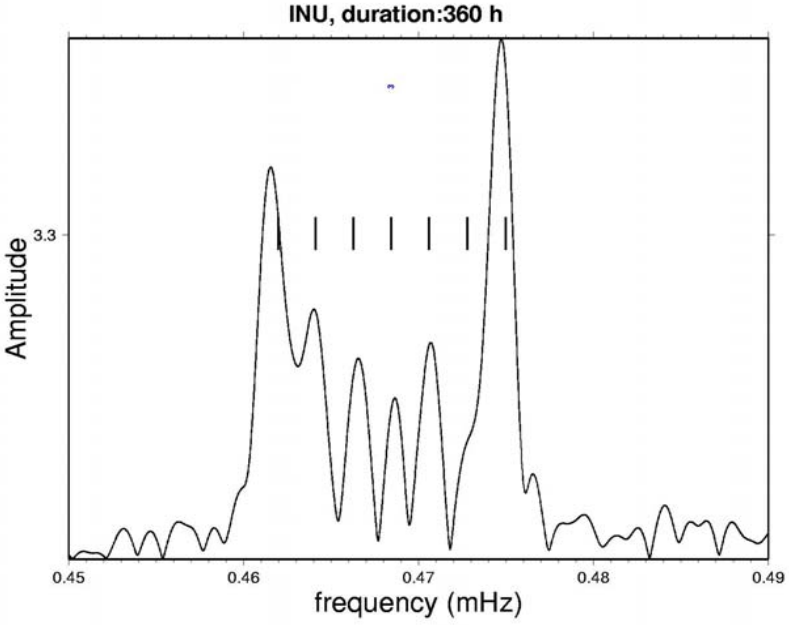
INU, duration:360 h
Amplitude
3.3
0.45
0.46
0.47
0.48
0.49
frequency (mHz)

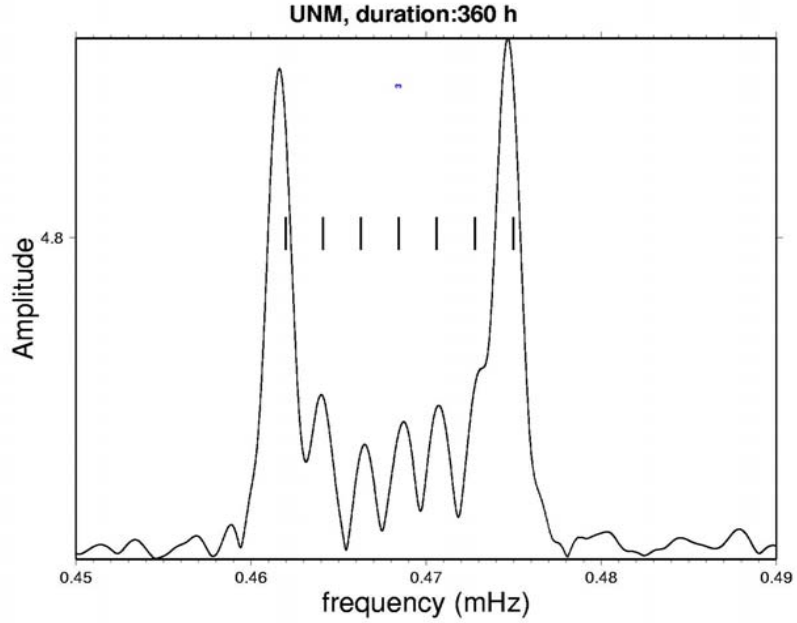
UNM, duration:360 h
Amplitude
4.8
0.45
0.46
0.47
0.48
0.49
frequency (mHz)

Attenuation of some modes

mode $_0S_0$

Q ~ 5300

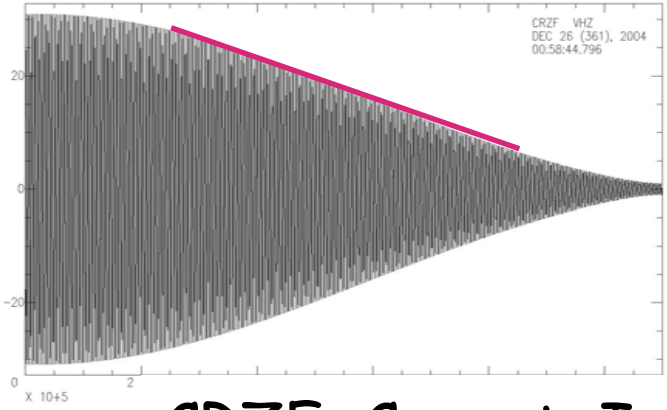

mode $_0S_2$
singlet m=+2

Q ~ 500

CRZF, Crozet, Indian Ocean

Seismic Source

$\rho\partial_{tt}\mathbf{u} + \mathbf{H_0 u} = \mathbf{F_s}$

Displacement at point **r** and time t due to a force system $\mathbf{F_s}$ at point source $\mathbf{r_s}$

eigenfrequencies: ${}_n\omega_l$

eigenfunctions: ${}_nu_l^m(r,t) = |n,l,m\rangle \exp(-i_n\omega_l t)$

$\mathbf{u}(\mathbf{r},t) = \Sigma_{n,l,m}\ {}_n\mathbf{a}_l^m\ |n,l,m\rangle \exp(-i_n\omega_l t)$

Eigenfunction basis is a complete basis => any wave can be modelled by normal mode summation including surface waves and body waves.

1D- Reference Earth Model

- Synthetic Seismograms by normal mode summation $\mathbf{u}_k(k=\{n,l,m\})$.

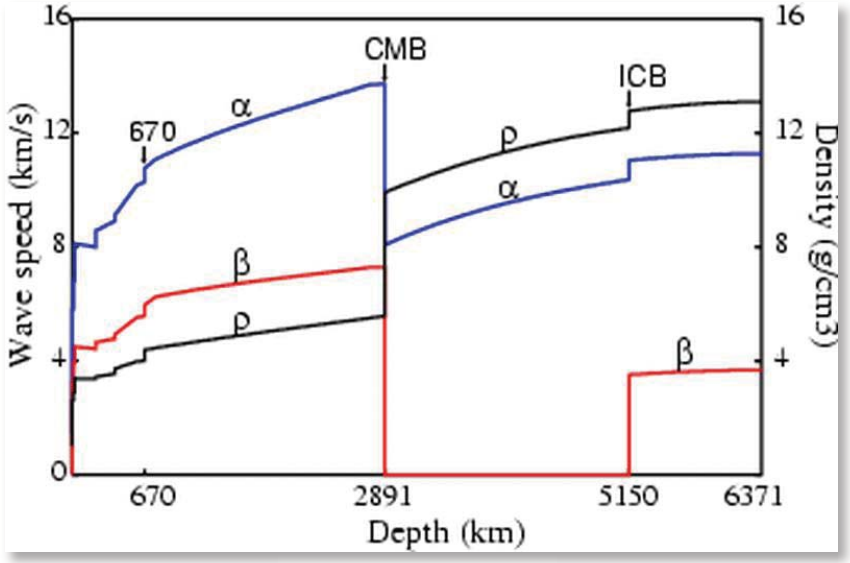

$$\mathbf{u}(\mathbf{r},t) = \Sigma_k\, u_k(r)\cos\omega_k t\,/\omega_k^2 \exp(-\omega_k t/2Q_k)\,(\mathbf{u_k}.\mathbf{F})_S$$

Source Term $(\mathbf{u_k}.\mathbf{F})_S = (\mathbf{M}:\varepsilon)_S$

M Seismic moment tensor, ε deformation tensor

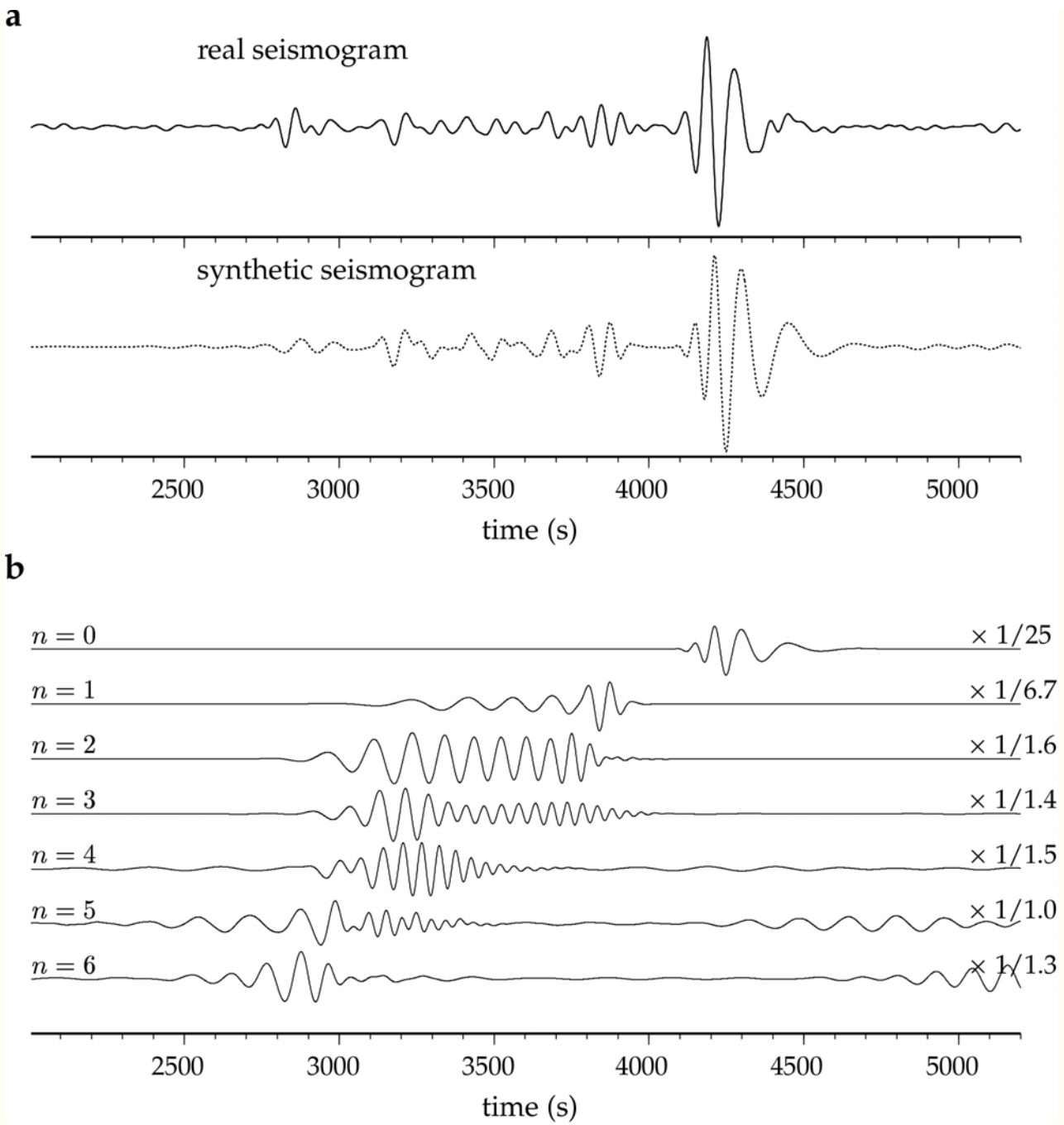

Beucler et al., 2003

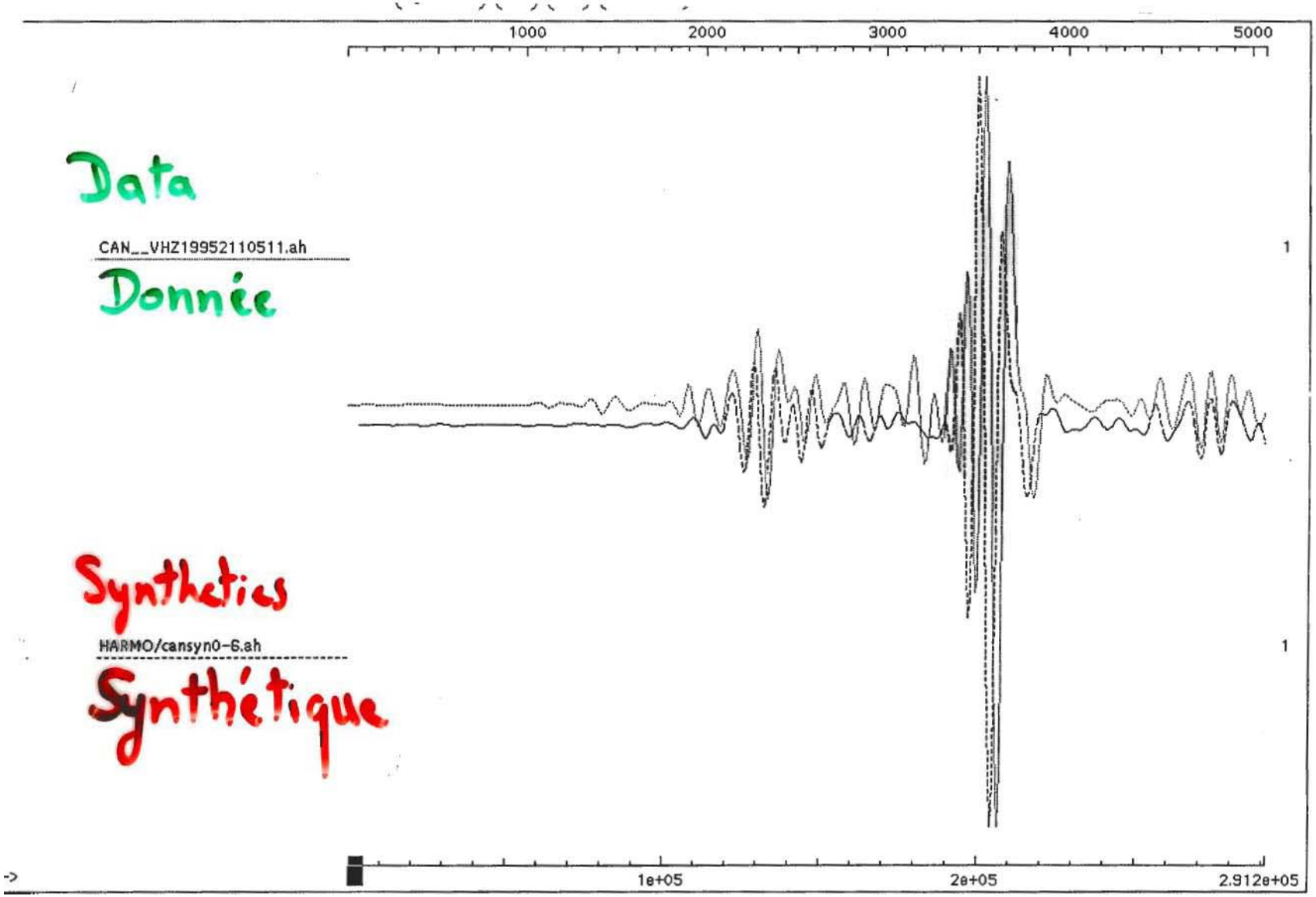
Data
CAN__VHZ19952110511.ah
Donnée
Synthetics
HARMO/cansyn0-6.ah
Synthétique
1000
2000
3000
4000
5000
1
1
->
1e+05
2e+05
2.912e+05

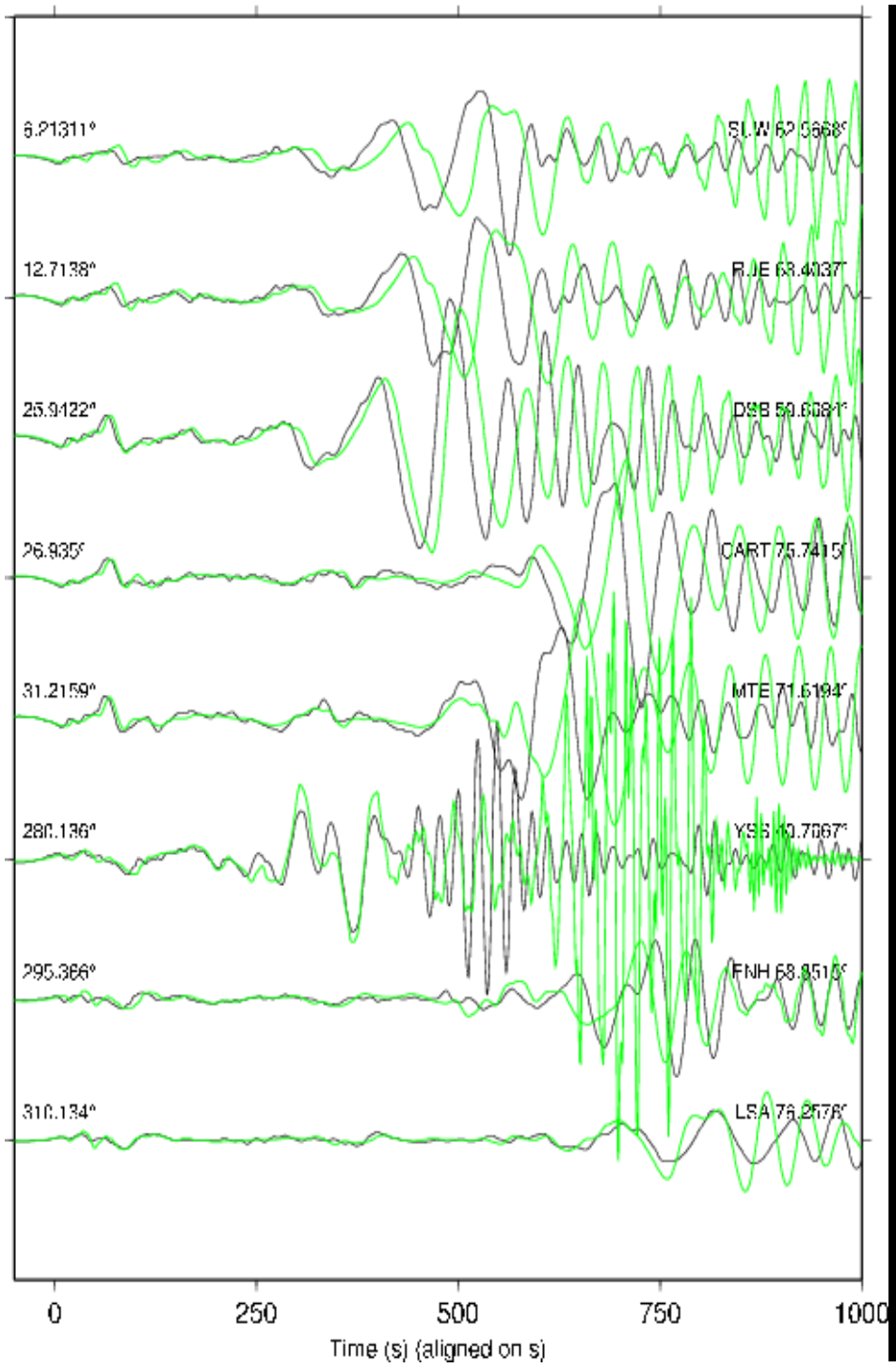

Synthetic seismograms
By normal mode
summation

Denali-Alaska
earthquake (Nov. 2002)

Komatitsch and Tromp, 2003

Duality wave - particle:
λ seismic wavelength
Λ scale heterogeneity

Particle: **Ray** theory $\lambda << \Lambda$
(Finite frequency effects)
Wave: Normal **Mode** theory (NM) + Perturbation theories (small amplitude of 3D- heterogeneities)=> **John Woodhouse**

Numerical modelling of wave equation
Strong or weak forms: $\lambda \approx \Lambda$
-Spectral Element Method (SEM)

(Dimitri Komatitsch)
-Coupled SEM-NM method

Spectral Element Method: D. Komatitsch (1999)

Coupled method of Spectral Elements and Modal Solution

Principle:

- Ω^+: Spectral Element area: 3D model
- Ω^-: Modal Solution area: 1D model

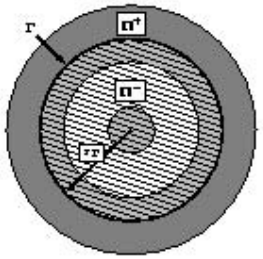

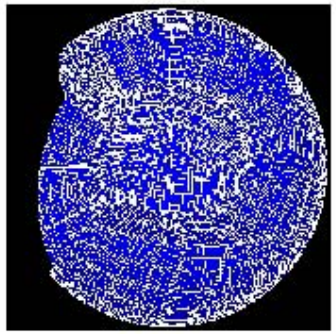

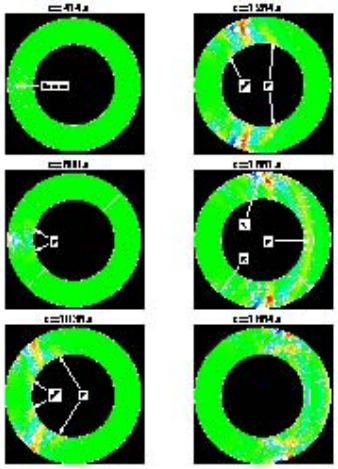

Capdeville et al., 2002

Overview
Large scale Seismology: an observational field

- Data (Seismic source) + Instrument (Seismometer)

-> Observations (seismograms)

- Historical evolution: Ray theory, Normal mode theory, Numerical techniques (SEM, NM-SEM)
- **Scientific Issues: Earthquakes (Sumatra), Anisotropic structure of the Earth**
- Tomographic Technique
- Geodynamic Applications.

  Seismic Experiment Plume detection
- NM-SEM and time reversal

Seismic Source Studies

$$\mathbf{u}(\mathbf{r},t) = \Sigma_k \, u_k(r) \cos \omega_k t / \omega_k^2 \exp(-\omega_k t/2Q) \, (\mathbf{u_k}.\mathbf{F})_s$$

Source Term $(\mathbf{u_k}.\mathbf{F})_s = (\mathbf{M}: \varepsilon)_S$

M Seismic moment tensor, ε deformation tensor

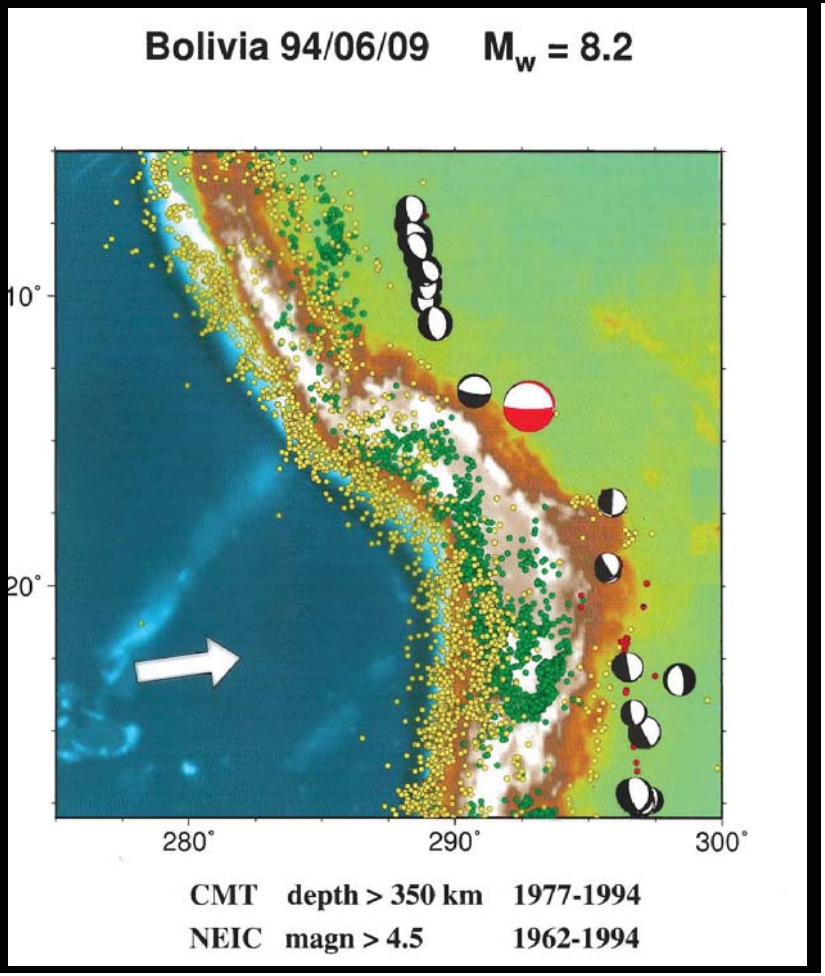

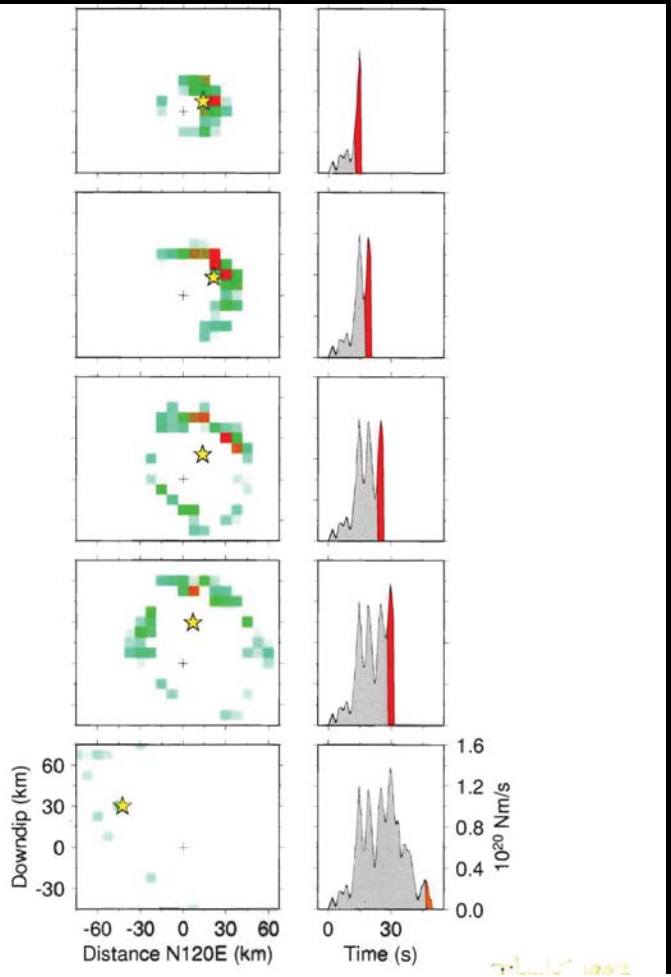

Structure of the Earth

Plate tectonics

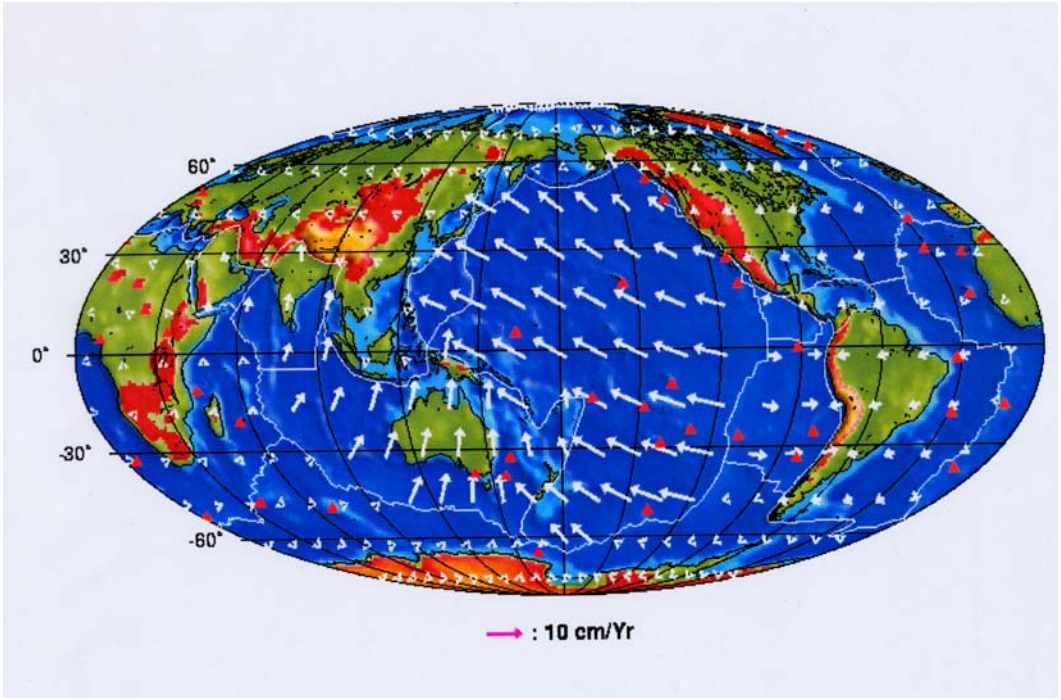

Mantle Convection

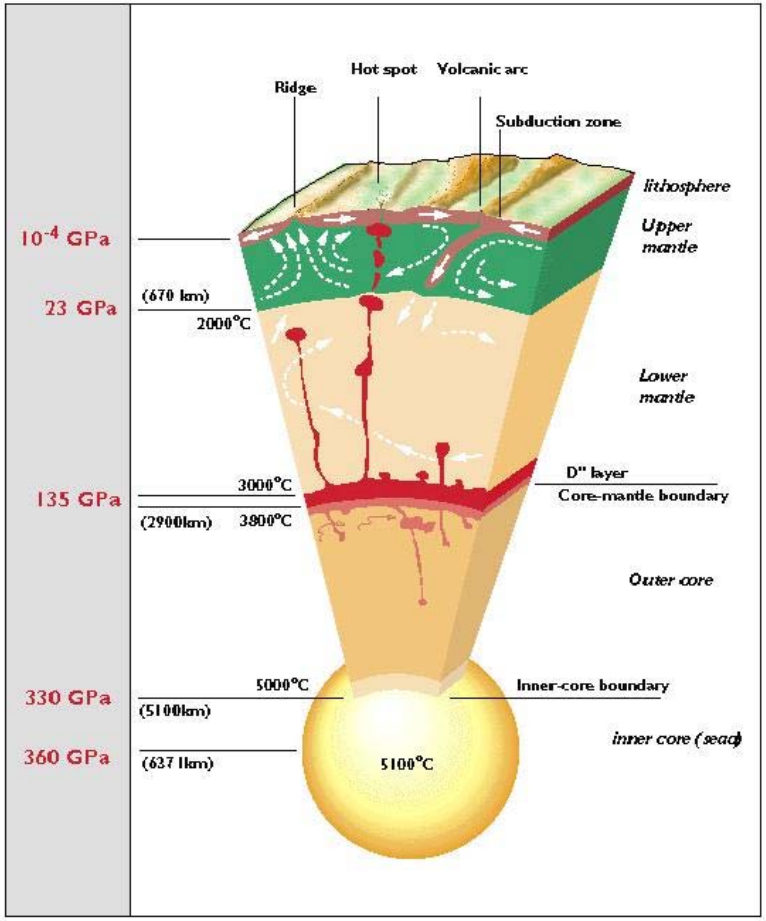

Tomographic Technique

- ***Forward Problem***: Theory $\mathbf{d}=\mathbf{g}(\mathbf{p})$

d data space, **p** parameter space

- Reference Earth model p_0:

$d_0 = g(p_0)$

- Kernels $\partial g/\partial p$
- Cd function (or matrix) of covariance of data

- ***Inverse Problem***: $p-p_0 = g^{-1}(d-d_0)$

- C_{p0} a priori Covariance function of parameters
- C_{pf} a posteriori Covariance function of parameters
- R Resolution

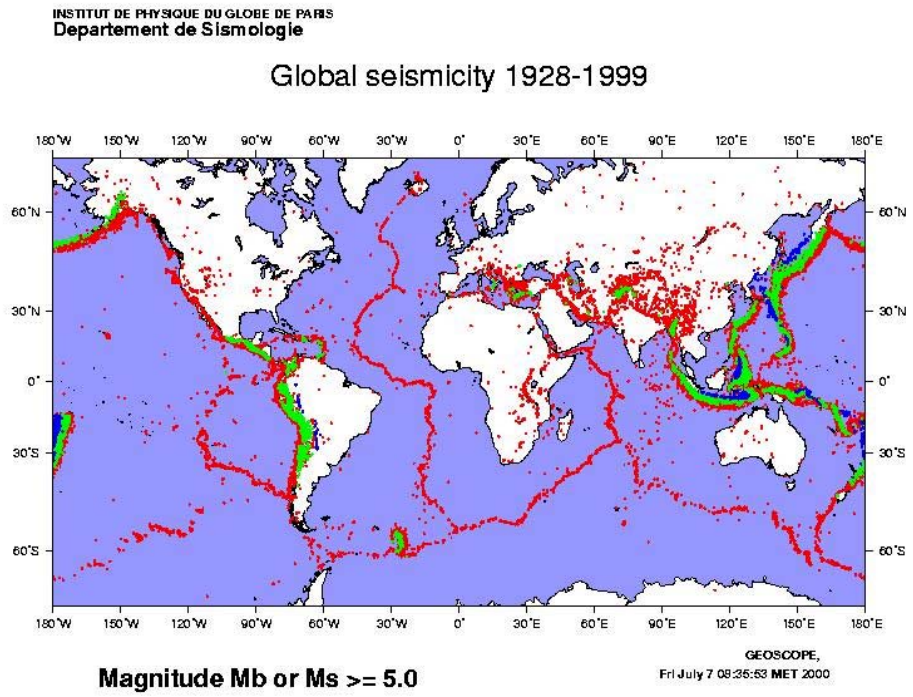

DATA

Receivers

Seismic sources:

- earthquakes
- noise

(1-20s microseismic)

(100-400s seismic Hum)

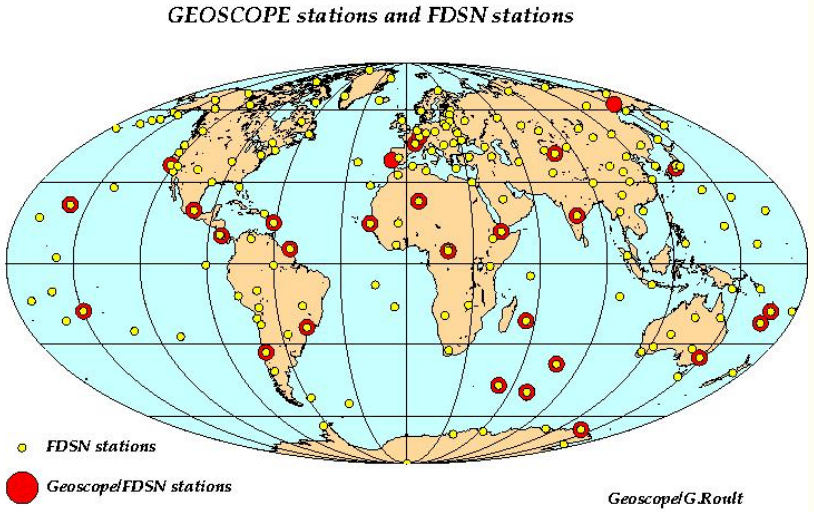

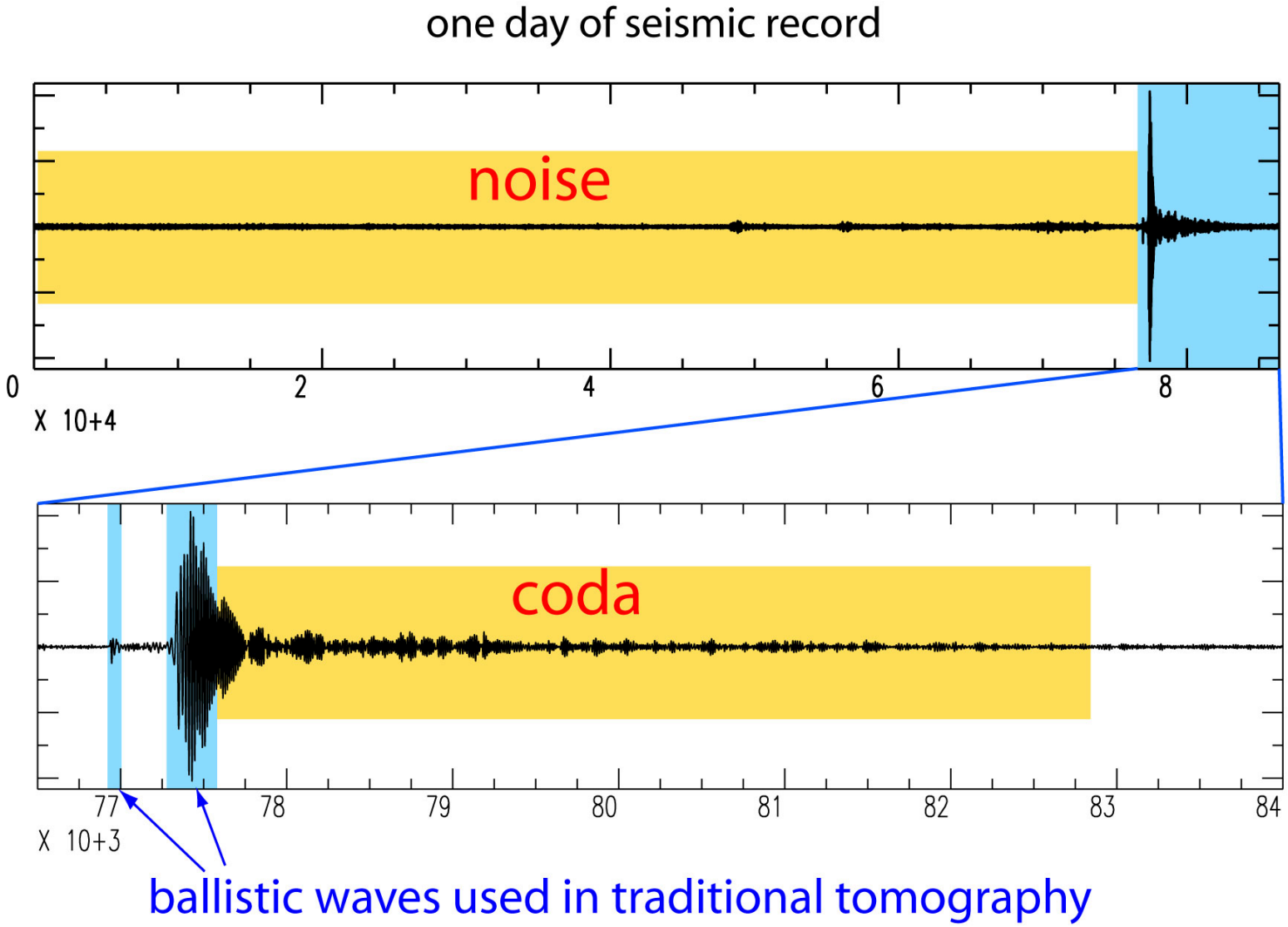
one day of seismic record
noise
0
2
4
6
8
X 10+4
coda
77
78
79
80
81
82
83
84
X 10+3
ballistic waves used in traditional tomography

GEOSCOPE and Noise

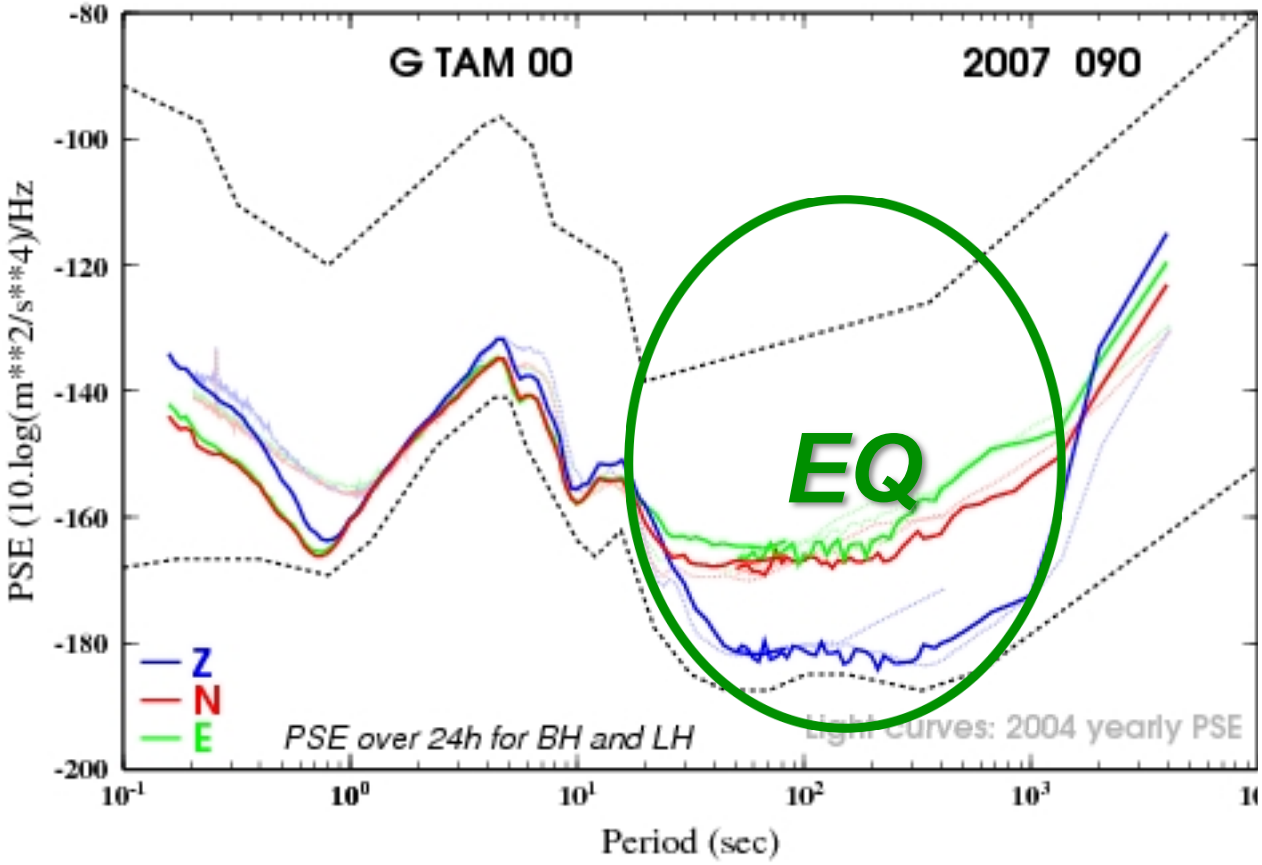

TAM (Tamanrasset, Algeria)

http://geoscope.ipgp.fr

GEOSCOPE and Noise

Microseismic Noise

Shapiro, Campillo, Roux, Brenguier,…

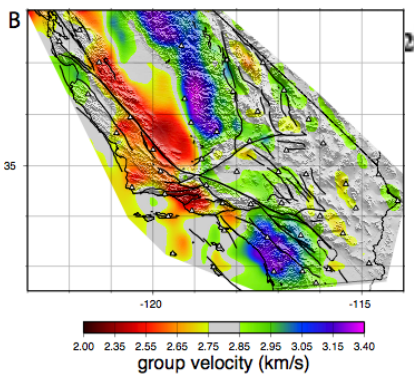

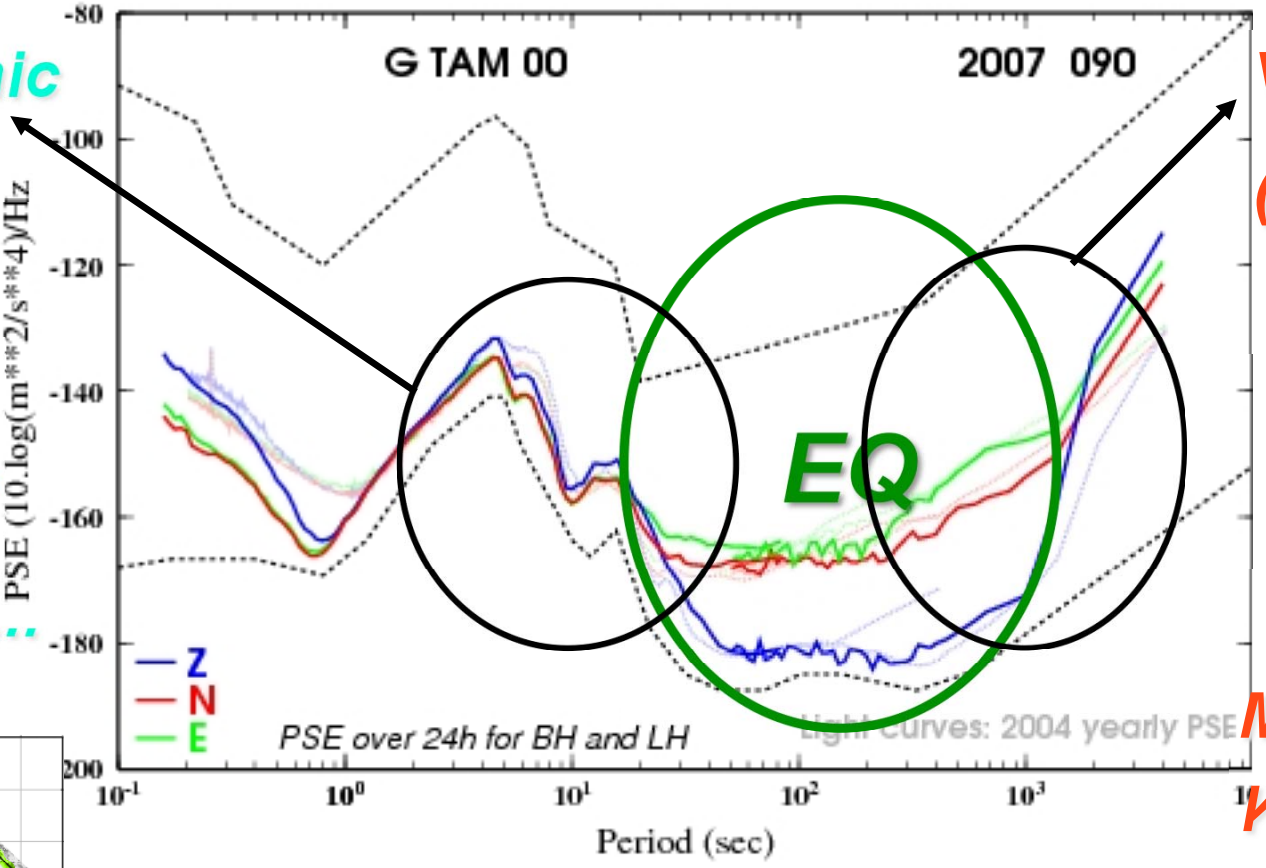

VLP Noise (transient, Hum, …)

Nishida, Montagner, Kawakatsu (2009)

TAM (Tamanrasset, Algeria)

Importance of seismic anisotropy

ANISOTROPY is the Rule not the Exception

Seismic Anisotropy is present at all scales

Importance of seismic anisotropy
ANISOTROPY is the Rule not the Exception

Anisotropy is present at all scales

-From microscopic scale up to macroscopic scale

-Efficient mechanisms of alignment in the upper mantle:
(L.P.O.: lattice preferred orientation;
S.P.O.: shape preferred orientation;
FINE LAYERING)

NON UNIQUE INTERPRETATION

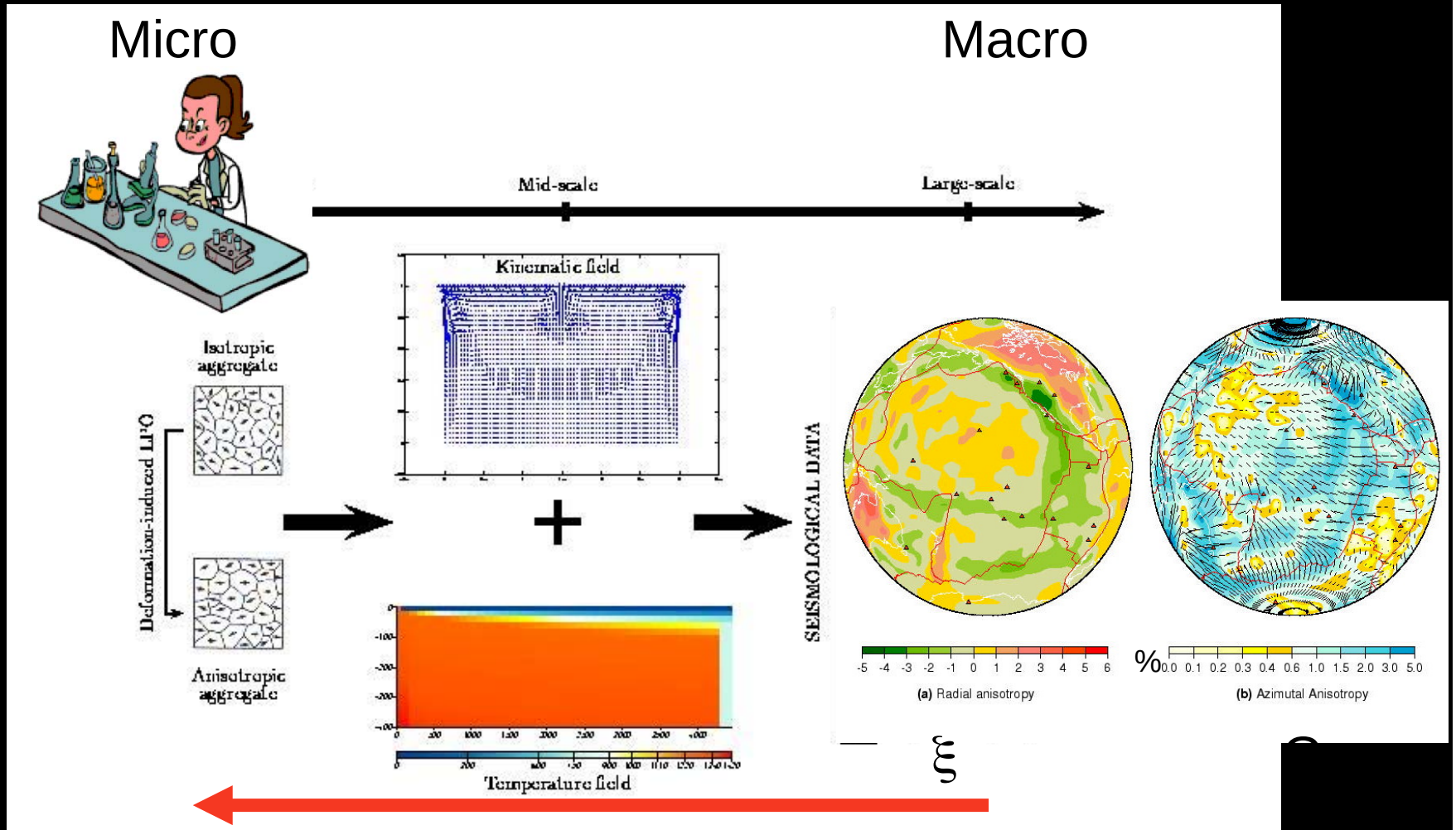

(Montagner and Guillot, 2001)

L.P.O. : Lattice Preferred Orientation (strain field)

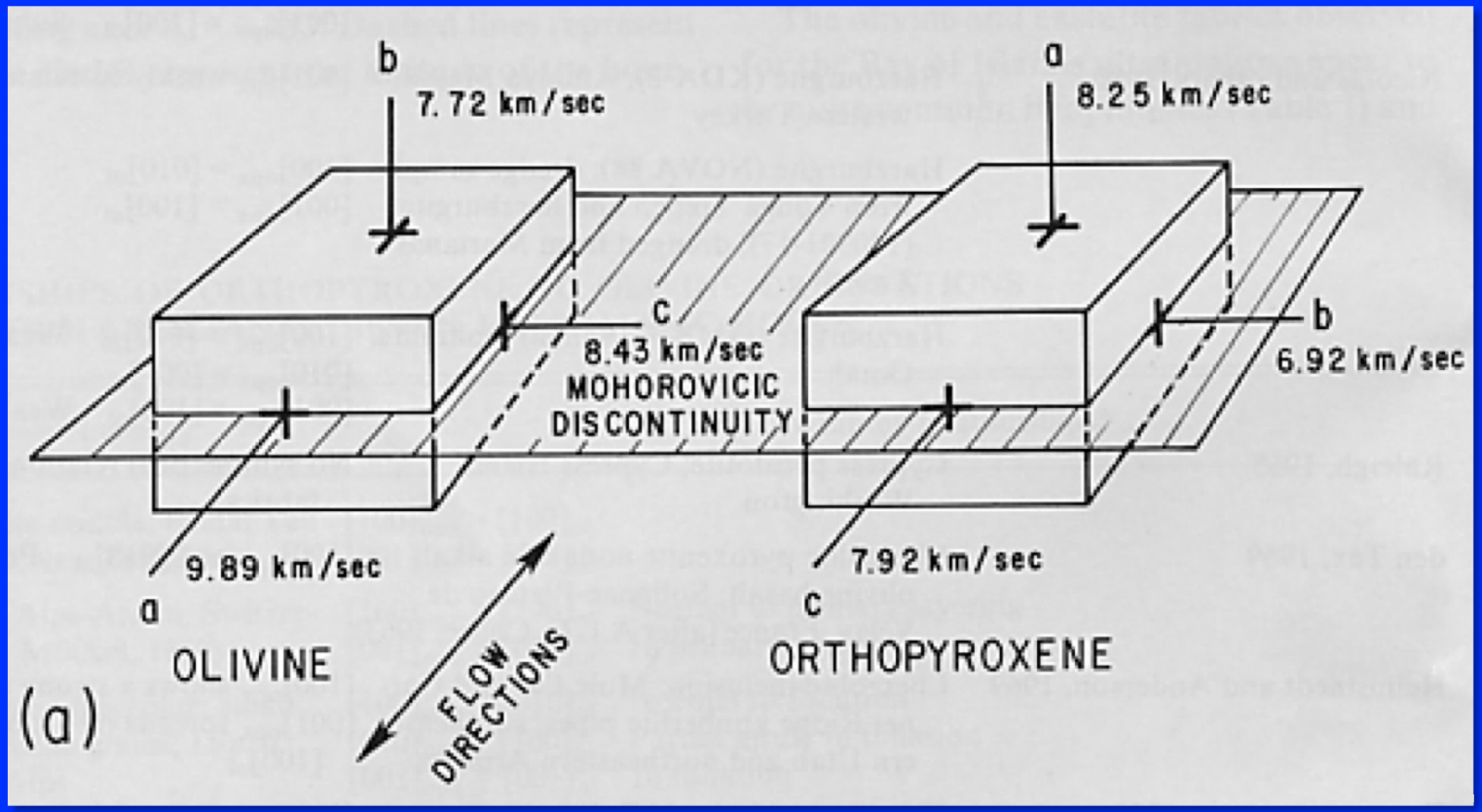

Christensen and Lundquist, 1982

→ ***Mapping of convection***

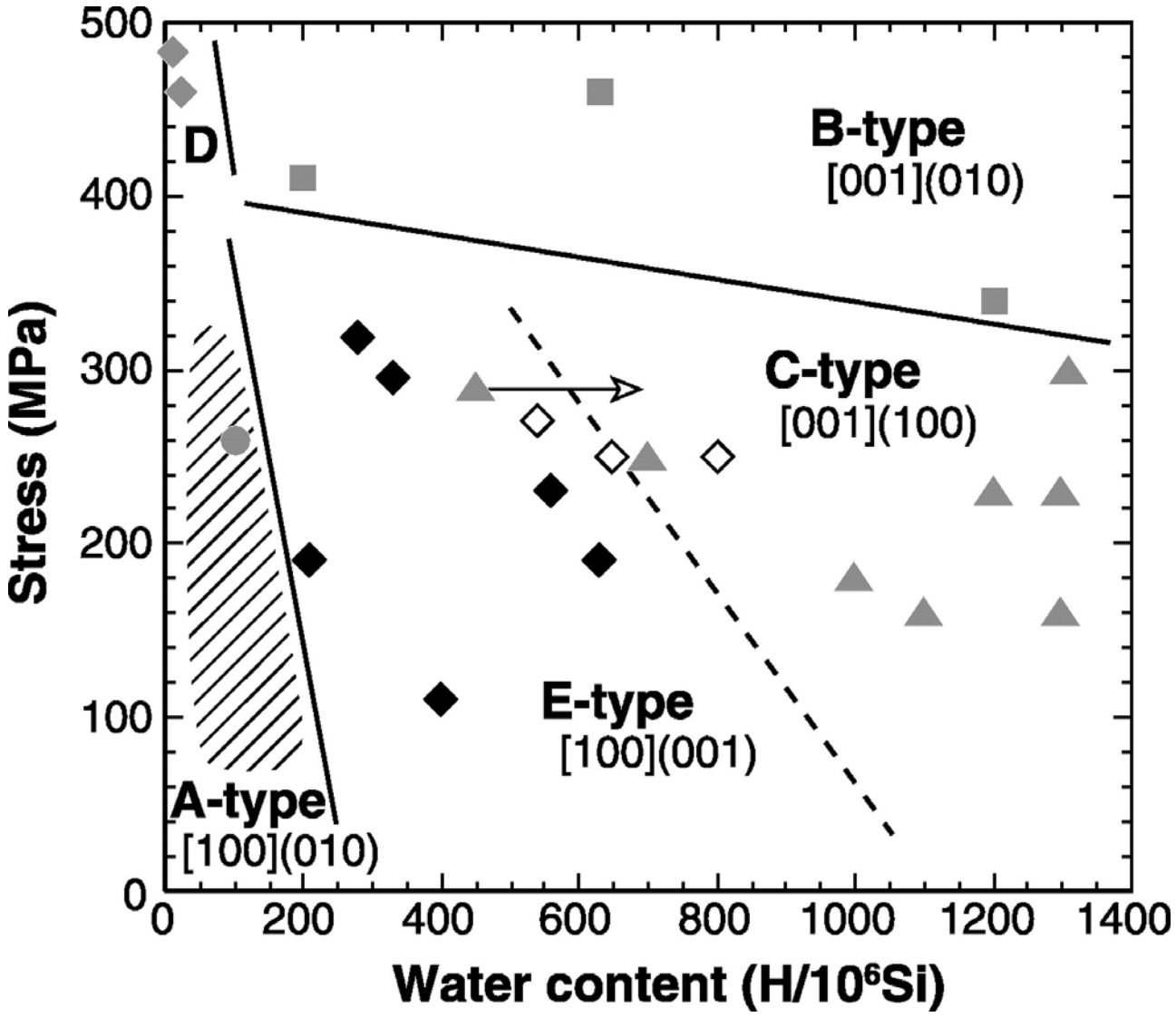

New Types of Olivine Fabric

Katayama et al., 2004

S.P.O.: Cracks, fluid inclusions, … (stress field)

Crust (+lithosphere)

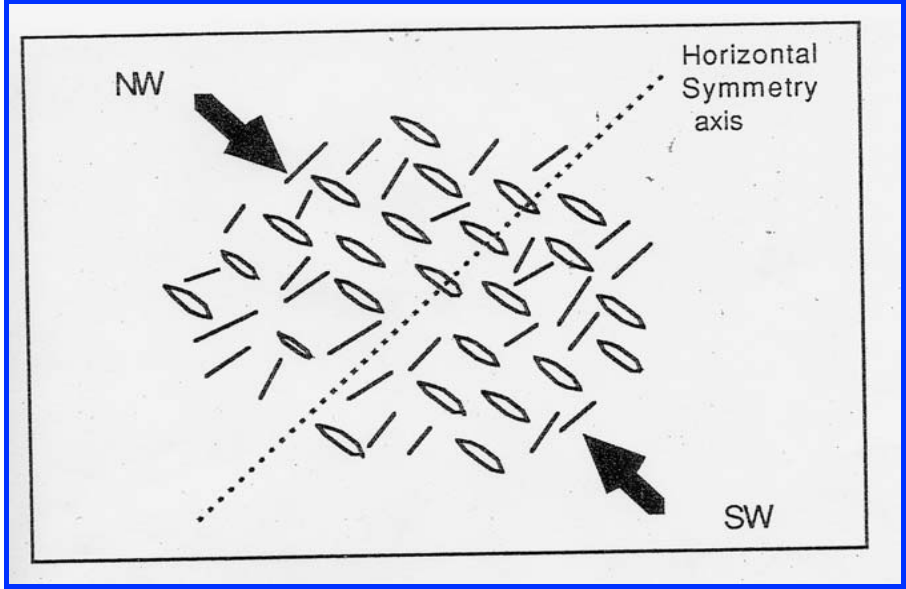

(Babuska and Cara, 1991)

Inner core

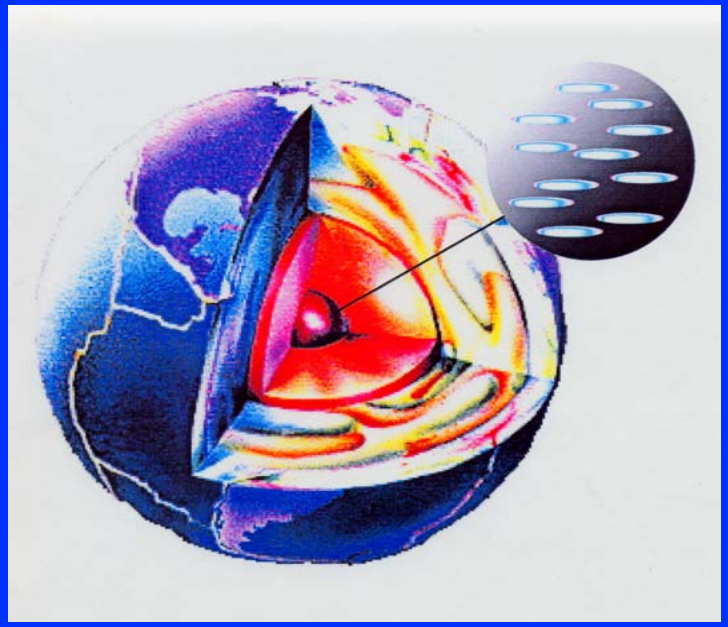

(Singh et al., 2001)

Temporal variations of anisotropy?

Monitoring of seismogenic zones (Durand et al. 2010)

Importance of seismic anisotropy
ANISOTROPY is the Rule not the Exception

Anisotropy is present at all scales

-From microscopic scale up to macroscopic scale
-Efficient mechanisms of alignment (L.P.O.: lattice preferred orientation; S.P.O.: shape preferred orientation; Fine layering)

NON UNIQUE INTERPRETATION

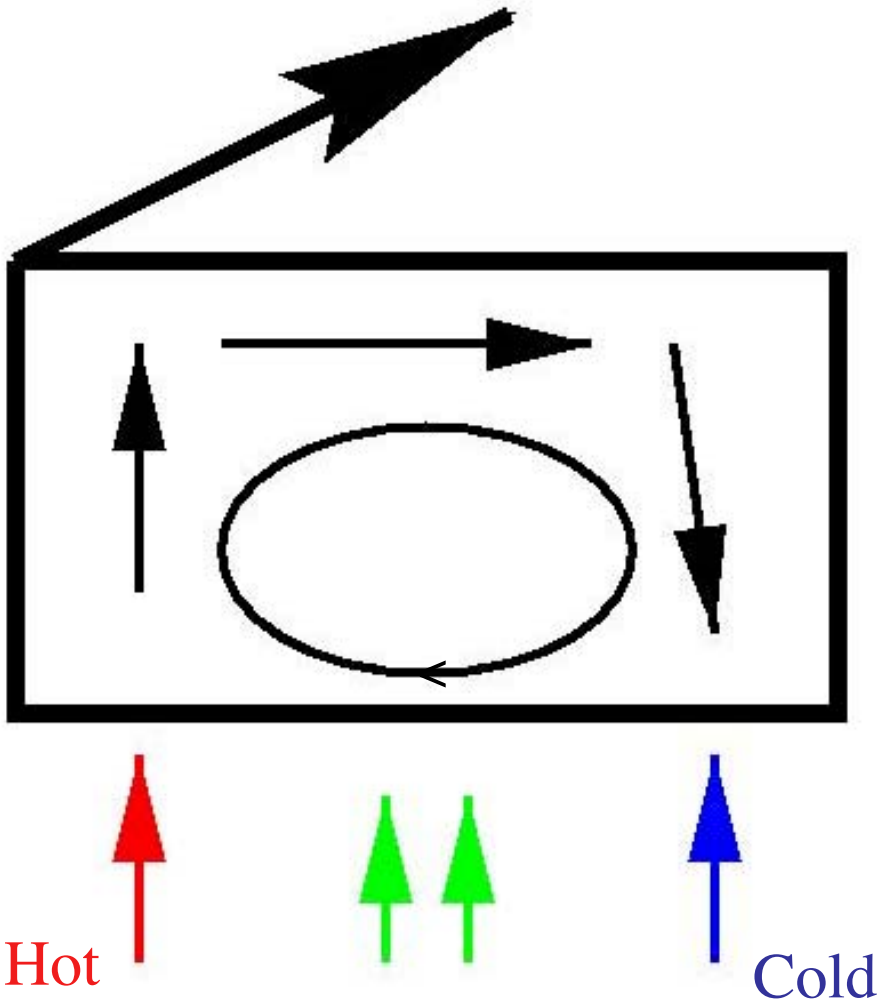

Montagner & Guillot, 2002

$\Delta\alpha$: Anisotropy Effect

ΔT: Temperature Effect

$$\Delta\alpha \approx \Delta T$$

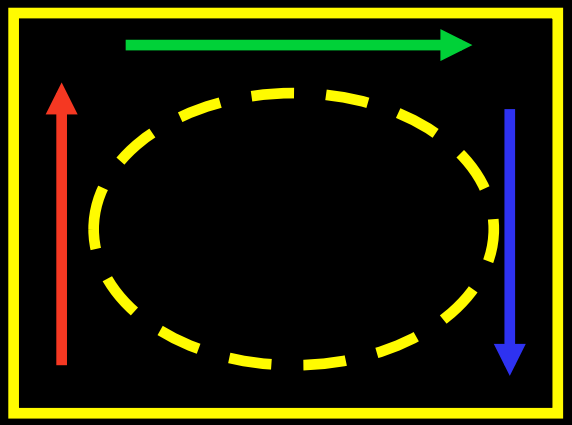

Olivine (60%) +Opx (40%)

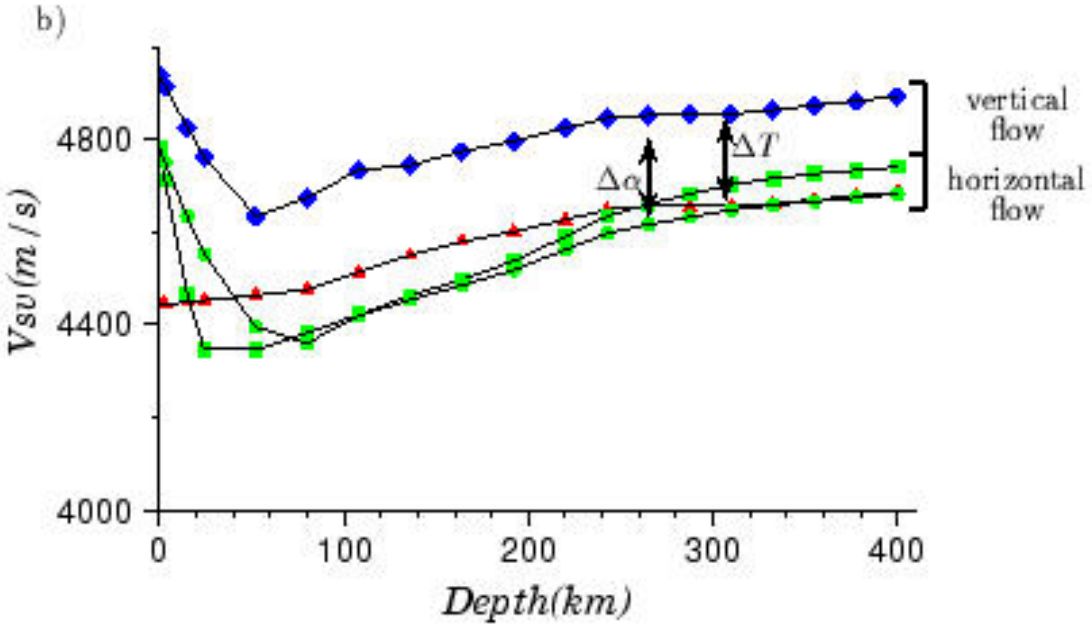

Montagner & Guillot, 2002

Different processes in different layers

-S.P.O.

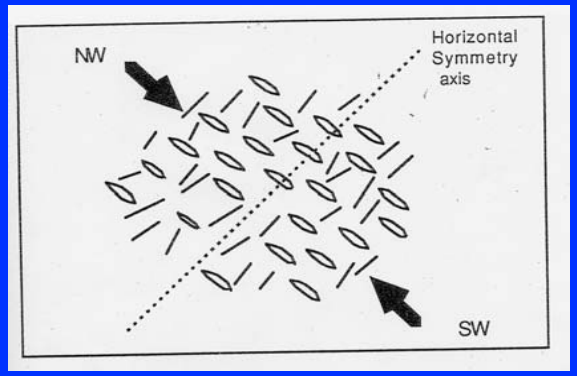

-L.P.O.

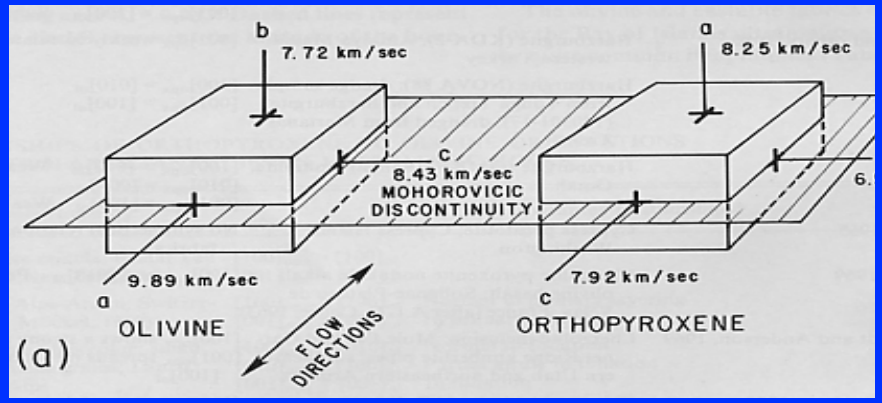

- *Water content*
- *Fine Layering*

- *Present day tectonic, geodynamic processes*
- *Past processes (frozen anisotropy)*

Stratification of anisotropy in the upper mantle

Importance of seismic anisotropy
ANISOTROPY is the Rule not the Exception

Anisotropy is present at all scales

- from microscopic scale to macroscopic scale
-Efficient mechanisms of alignment
(L.P.O.: lattice preferred orientation
S.P.O.: shape preferred orientation; Fine layering)

Anisotropy is observed on different kinds of seismic waves
-Body waves (Pn; S-wave splitting)
-Surface waves (Rayleigh-Love discrepancy, azimuthal anisotropy)

Different kinds of data

Body waves:
P-wave azimuthal variations
SKS, S-wave splitting

Surface waves:
-discrepancy Rayleigh Love (polarization anisotropy)
-Azimuthal variations of phase (or group) velocities
- Effects on amplitudes

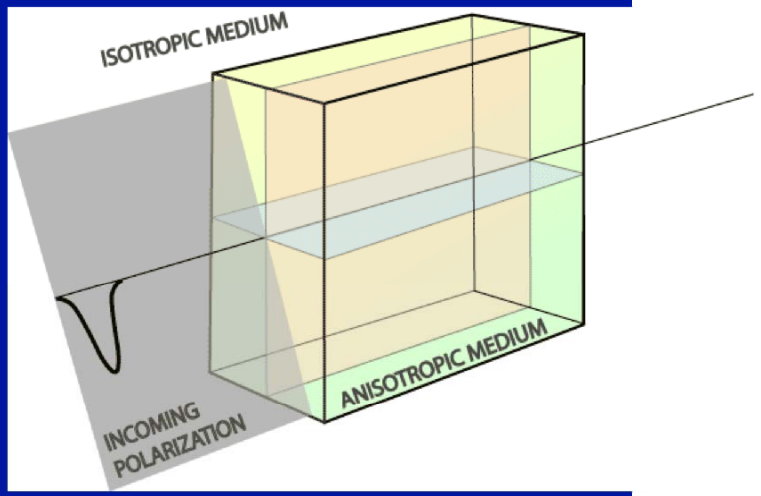

Animation courtesy of Ed Garnero

Pn- velocities

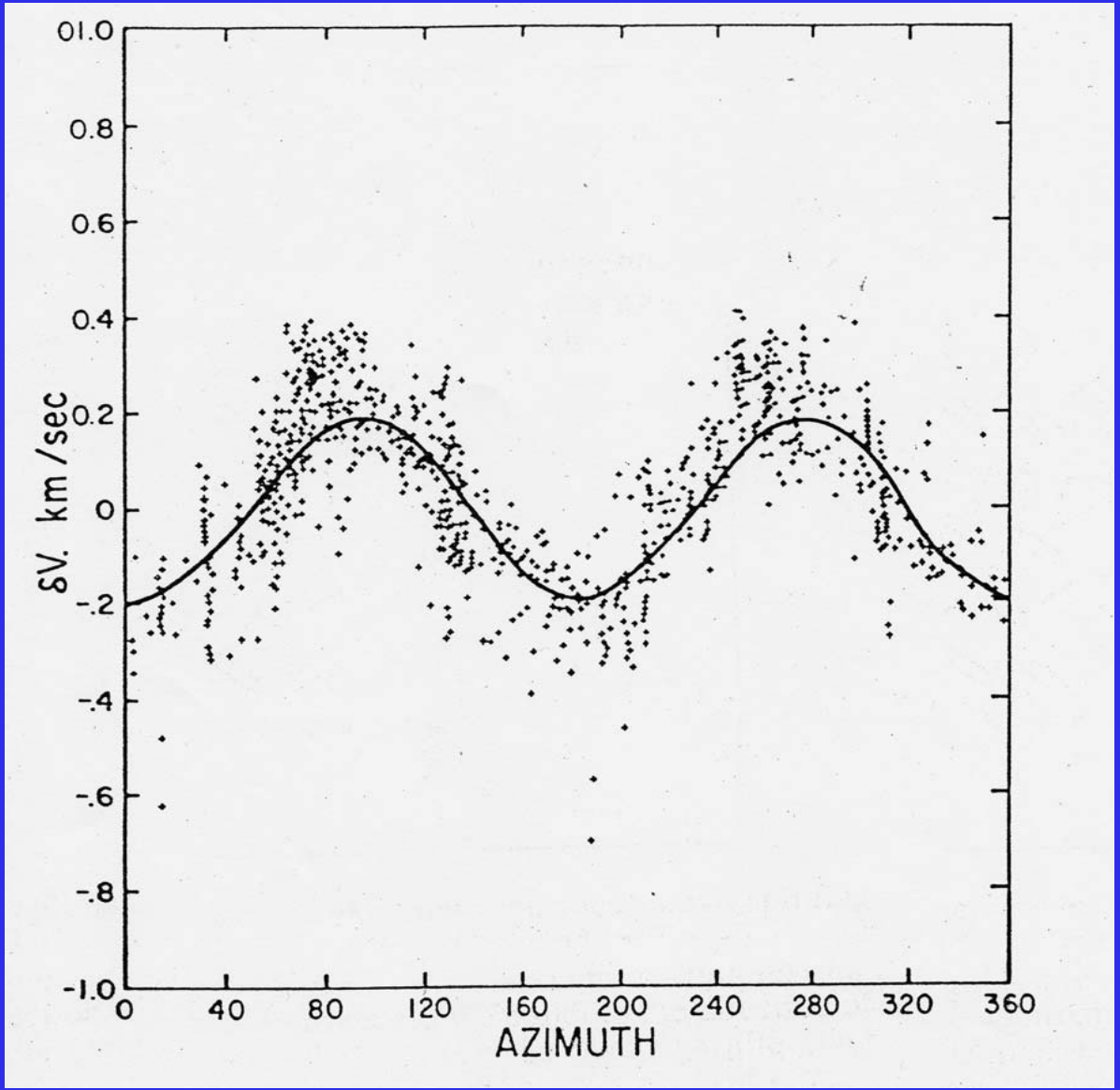

(Raitt et al., 1969)

Shear Wave Splitting (Birefringence)

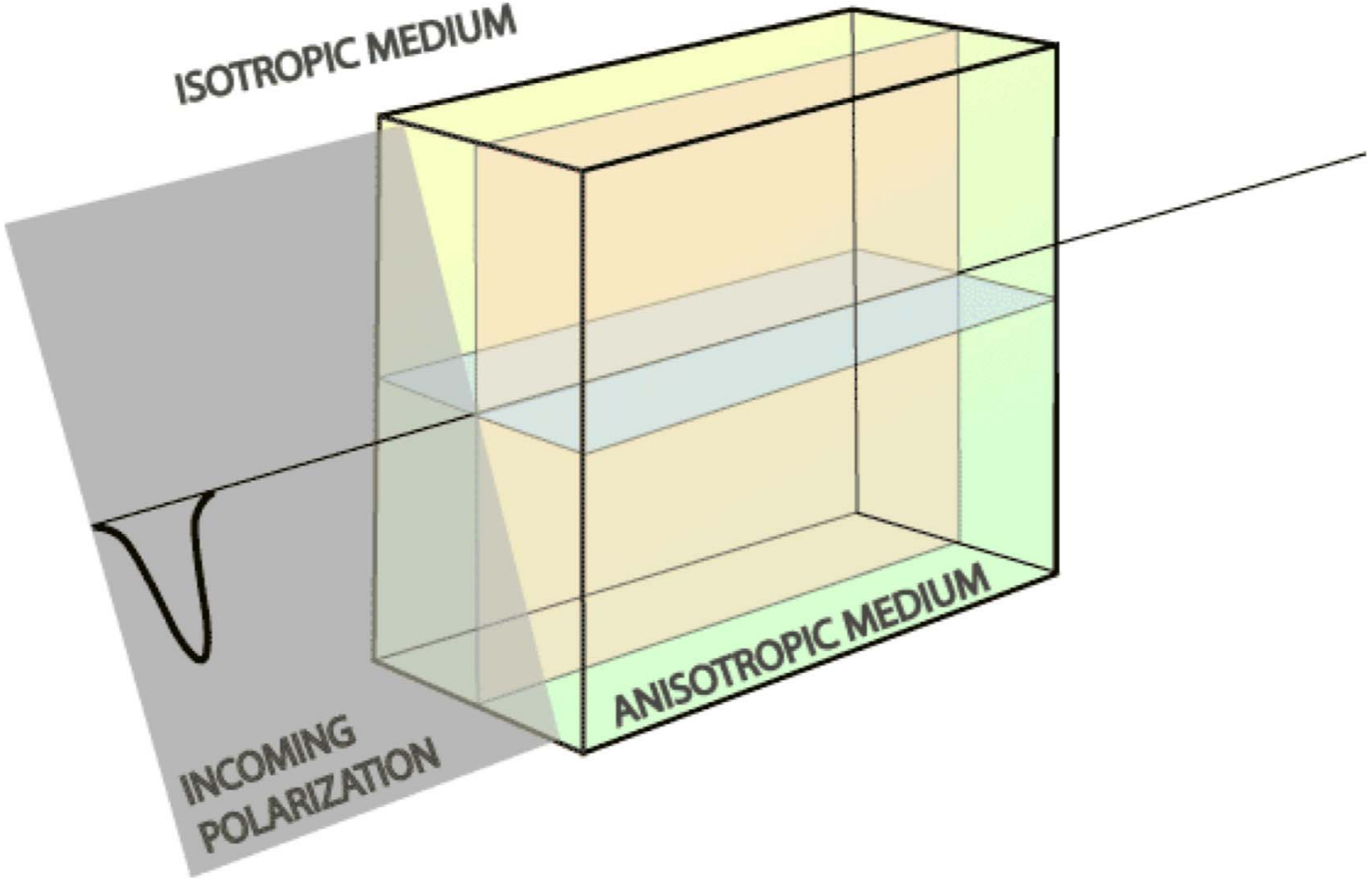

Animation courtesy of Ed Garnero

SKS- Splitting

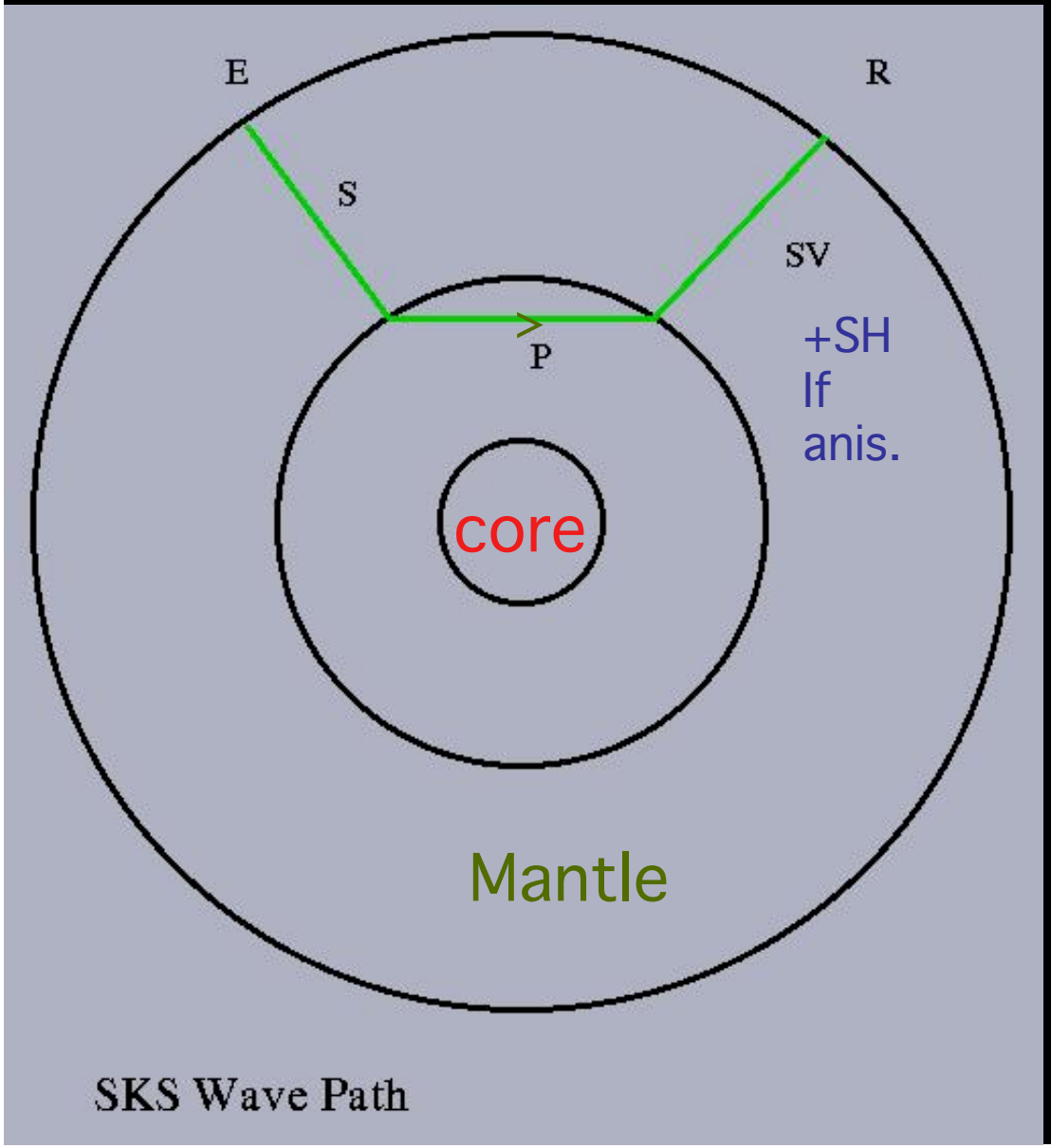

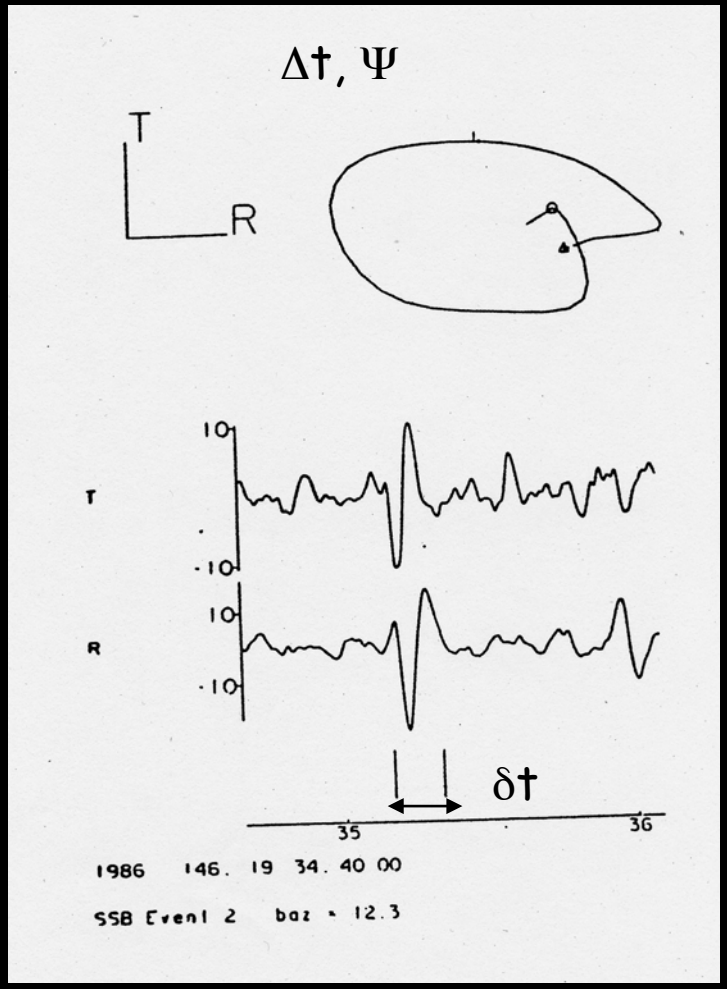

T

R

Vinnik et al., 1989

Compilation of S-wave splitting measurements

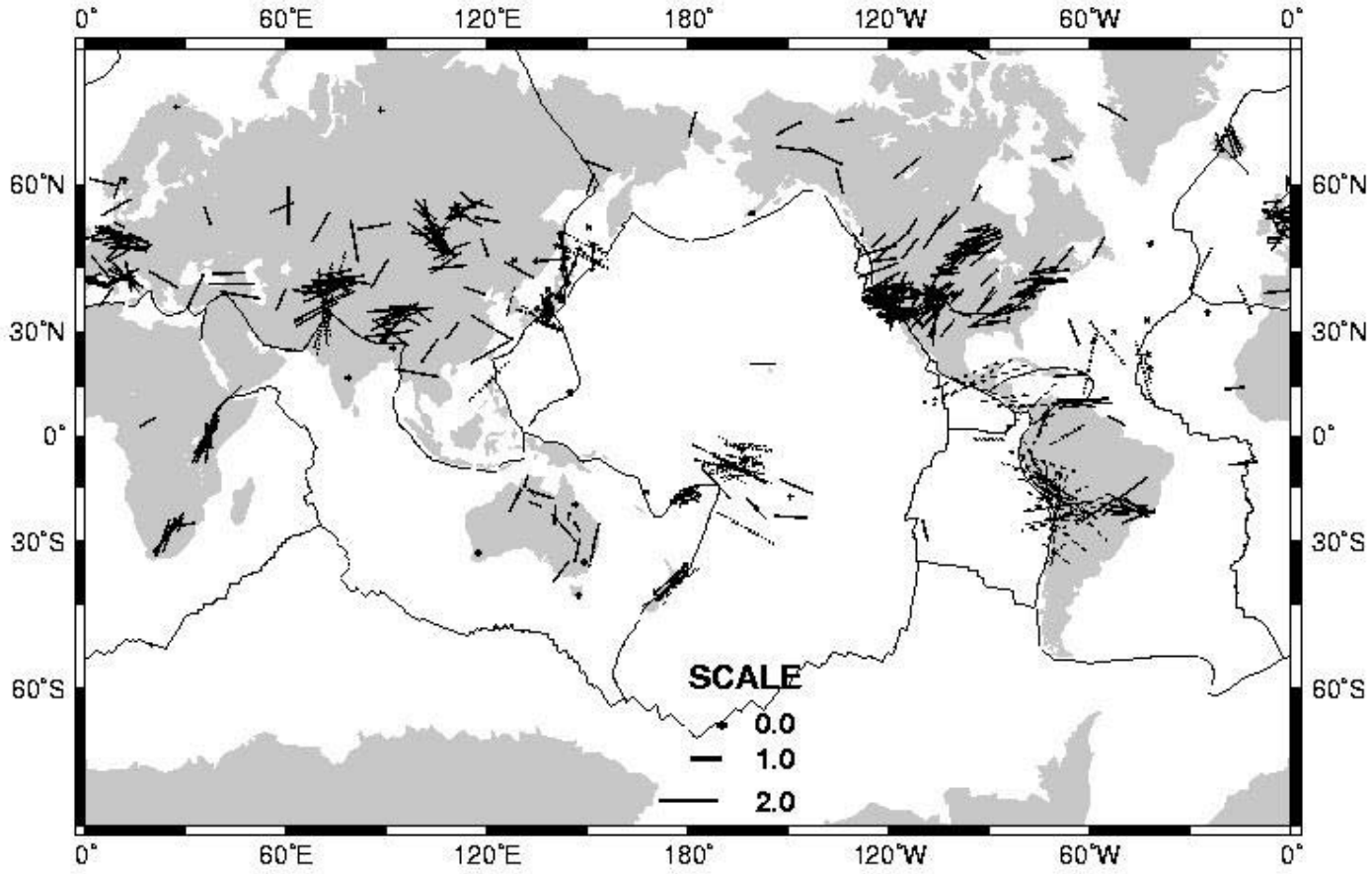

Savage, Rev. Geophys., 1999

SURFACE WAVES

Importance of seismic anisotropy
ANISOTROPY is the Rule not the Exception

Anisotropy is present at all scales

- from microscopic scale to macroscopic scale
-Efficient mechanisms of alignment
(L.P.O.: lattice preferred orientation
S.P.O.: shape preferred orientation; fine layering)

Anisotropy is observed on different kinds of seismic waves
-Body waves (Pn; S-wave splitting)
-Surface waves (Rayleigh-Love discrepancy, azimuthal anisotropy)

ANISOTROPY REFLECTS AN INNER ORGANIZATION

ANISOTROPY IS NOT A SECOND ORDER EFFECT

BUT NON UNIQUE INTERPRETATION

Anisotropic Tomographic Technique

- ***Forward Problem***: Theory **d=g(p)** =>**1st order perturbation theory**

d data space (seismograms)

p parameter space (anisotropy)

- Reference Earth model p_0:

$d_0 = g(p_0)$

- Kernels $\partial g/\partial p$
- Cd function (or matrix) of covariance of data

- ***Inverse Problem***: $p-p_0 = \underline{g}^{-1} (d-d_0)$

- C_{p0} a priori Covariance function of parameters
- C_{pf} a posteriori Covariance function of parameters
- R Resolution

Effect of anisotropy on surface waves

Effect on eigenfrequency ω_k for multiplet k={n,l,m} and phase velocity V

$$\frac{\delta\omega_k}{\omega_k} = \frac{\int_\Omega \varepsilon_{ij}^* \, \delta C_{ijkl} \, \varepsilon_{kl} \, d\Omega}{\int_\Omega \rho_0^* \, u_r^* \, u_r \, d\Omega} = \frac{\delta V}{V}\Big|_k$$

ε strain tensor, u displacement, δC_{ijkl} elastic tensor perturbation

Phase velocity pertubation V (T,θ,ϕ,Ψ) at point r (θ,ϕ) (Smith & Dahlen, 1973)

$$\delta V(T,\theta,\phi,\Psi)/_V = \alpha_0(T,\theta,\phi) + \alpha_1(T,\theta,\phi)\cos 2\Psi + \alpha_2(T,\theta,\phi)\sin 2\Psi + \alpha_3(T,\theta,\phi)\cos 4\Psi + \alpha_4(T,\theta,\phi)\sin 4\Psi$$

Ψ Azimuth (angle between North and wave vector)

Table 1: Calculation of the various $c_{ij}\epsilon_i\epsilon_j$ for Love waves
$\alpha = cos\Psi$; $\beta = sin\Psi$

n	ij	$c_{ij}\epsilon_i\epsilon_j$
1	11	$c_{11}\alpha^2\beta^2.k^2W^2$
1	22	$c_{22}\alpha^2\beta^2.k^2W^2$
1	33	0
2	12	$-c_{12}\alpha^2\beta^2.k^2W^2$
2	13	0
2	23	0
2	24	
4	14	$c_{14}(-i\alpha^2\beta).\frac{kWW'}{2}$
4	15	$c_{15}(i\alpha^2\beta).\frac{kWW'}{2}$
4	16	$c_{16}(-\alpha\beta)(\alpha^2-\beta^2).\frac{k^2W^2}{2}$
4	24	$c_{24}(-i\alpha^2\beta).\frac{kWW'}{2}$
4	25	$c_{25}(-\imath\alpha\beta^2).\frac{kWW'}{2}$
4	26	$c_{26}(\alpha\beta)(\alpha^2-\beta^2).\frac{k^2W^2}{2}$
4	34	0
4	35	0
4	36	0
4	44	$c_{44}\alpha^2.\frac{W'^2}{4}$
8	45	$c_{45}(-\alpha\beta).\frac{W'^2}{4}$
8	46	$c_{46}(-i\alpha)(\alpha^2-\beta^2).\frac{kWW'}{2}$
4	55	$c_{55}\beta^2.\frac{W'^2}{4}$
8	56	$c_{56}(i\beta)(\alpha^2-\beta^2).\frac{kWW'}{2}$
4	66	$c_{66}(\alpha^2-\beta^2).\frac{k^2W^2}{4}$

$C_{mnpq} \longrightarrow c_{ij}$

Indices:

i= 9-m-n

j= 9-p-q

W(r) Love displacement

$W' = (^{dW}/_{dr})$

The first order perturbation in Love wave phase velocity $\delta C_L(k, \Psi)$ can be expressed as:

$$\delta C_L(k,\Psi) = \frac{1}{.2C_{0L}(k)}[L_1(k) + L_2(k)cos2\Psi + L_3(k)sin2\Psi + L_4(k)cos4\Psi + L_5(k)sin4\Psi$$

where

$$L_0(k) = \int_0^\infty \rho W^2 \mathrm{d}z$$

0-Ψ

$$L_1(k) = \frac{1}{L_0}\int_0^\infty \left(W^2\delta N + \frac{W'^2}{k^2}\delta L\right)\mathrm{d}z$$

2-Ψ

$$L_2(k) = \frac{1}{L_0}\int_0^\infty -G_c\left(\frac{W'^2}{k^2}\right)\mathrm{d}z$$

$$L_3(k) = \frac{1}{L_0}\int_0^\infty -G_s\left(\frac{W'^2}{k^2}\right)\mathrm{d}z$$

4-Ψ

$$L_4(k) = \frac{1}{L_0}\int_0^\infty -E_c.W^2\mathrm{d}z$$

$$L_5(k) = \frac{1}{L_0}\int_0^\infty -E_s.W^2\mathrm{d}z$$

The same procedure holds for Rayleigh waves, starting from the displacement given previously.

$$\delta C_R(k,\Psi) = \frac{1}{2C_{0R}(k)}[R_1(k) + R_2(k)cos2\Psi + R_3(k)sin2\Psi + R_4(k)cos4\Psi + R_5(k)sin4\Psi$$

where

$$R_0(k) = \int_0^\infty \rho(U^2+V^2)dz$$

0-Ψ $$R_1(k) = \frac{1}{R_0}\int_0^\infty [V^2 dA + \frac{U'^2}{k^2}.dC + \frac{2U'V}{k}.dF + (\frac{V'}{k} - U)^2 dL]dz$$

2-Ψ $$\begin{cases} R_2(k) = \frac{1}{R_0}\int_0^\infty [V^2.B_c + \frac{2U'V}{k}.H_c + (\frac{V'}{k} - U)^2 G_c]dz \\ R_3(k) = \frac{1}{R_0}\int_0^\infty [V^2.B_s + \frac{2U'V}{k}.H_s + (\frac{V'}{k} - U)^2 G_s]dz \end{cases}$$

4-Ψ $$\begin{cases} R_4(k) = \frac{1}{R_0}\int_0^\infty E_c.V^2 dz \\ R_5(k) = \frac{1}{R_0}\int_0^\infty E_s.V^2 dz \end{cases}$$

The 13 depth-functions $A, C, F, L, N, B_c, B_s, H_c, H_s, G_c, G_s, E_c, E_s$ are linear combinations of the elastic coefficients C_{ij} and are explicitly given as follows:

Love wave partial derivatives

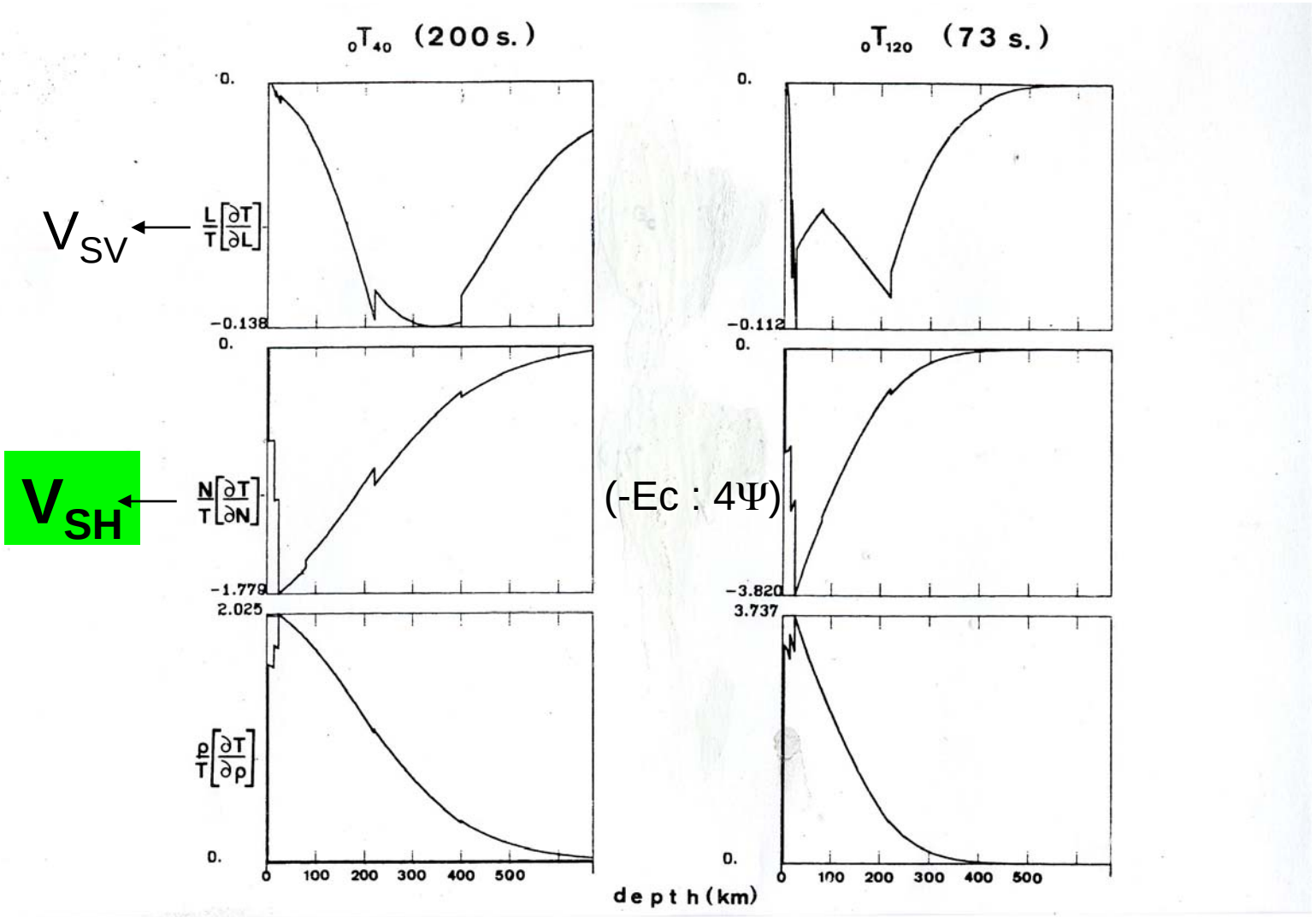

Rayleigh wave partial derivatives

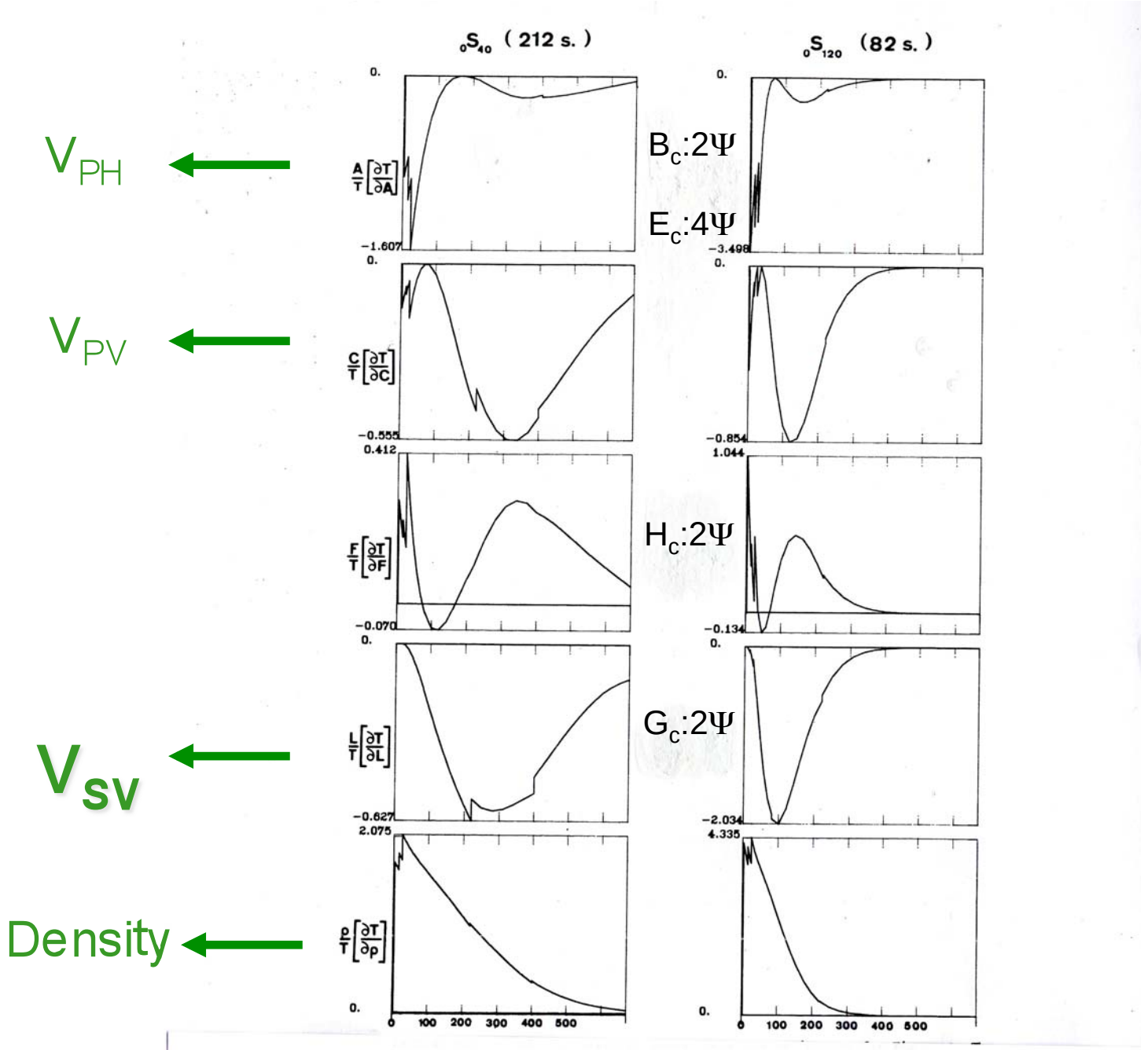

13 parameters

0Ψ term	$A = \frac{3}{8}(C_{11} + C_{22}) + \frac{1}{4}C_{12} + \frac{1}{2}C_{66}$	V_{PH}
	$C = C_{33}$	V_{PV}
	$F = \frac{1}{2}(C_{13} + C_{23})$	
	$L = \frac{1}{2}(C_{44} + C_{55})$	V_{SV}
	$N = \frac{1}{8}(C_{11} + C_{22}) - \frac{1}{4}C_{12} + \frac{1}{2}C_{66}$	V_{SH}
	cos	sin
2Ψ term	$B_c = \frac{1}{2}(C_{11} - C_{22})$	$B_s = C_{16} + c_{26} \rightarrow B$
	$G_c = \frac{1}{2}(C_{55} - C_{44})$	$G_s = C_{54} \rightarrow G$
	$H_c = \frac{1}{2}(C_{13} - C_{23})$	$H_s = C_{36} \rightarrow H$
4Ψ term	$E_c = \frac{1}{8}(C_{11} + C_{22}) - \frac{1}{4}C_{12} - \frac{1}{2}C_{66}$	$E_s = \frac{1}{2}(C_{16} - C_{26}) \rightarrow E$

Physical Meaning

Transversely
Isotropic Medium
With Vertical Symmetry
Axis (VTI)

Azimuthal variation of

V_{PH}

V_{SV}

F

V_{SH} (or V_{PH})

Isotropic medium: 2 parameters

VTI: 5 parameters (A,C,F,L,N)

General + 8 (from surface waves)

- **Best resolved parameters from surface waves** *(among 13 parameters)*

$L = \rho V_{SV}^2$ Isotropic part of V_{SV}

$\xi = N/L = \frac{V_{SH}^2}{V_{SV}^2}$ Radial Anisotropy

G, Ψ_G Azimuthal Anisotropy of V_{SV}, also related to SKS splitting *(when horizontal symmetry axis, vertical propagation, Montagner et al., 2000)*

- **Body waves (Crampin, 1984)**

$$\rho V_{SV}^2 = L + G_c \cos 2\Psi + G_s \sin 2\Psi$$

$$\rho V_{SH}^2 = N - E_c \cos 4\Psi - E_s \sin 4\Psi$$

Synthetic SKS-wave splitting inferred in Pacific Ocean from surface wave anisotropy: **L, G_c, G_s** parameters

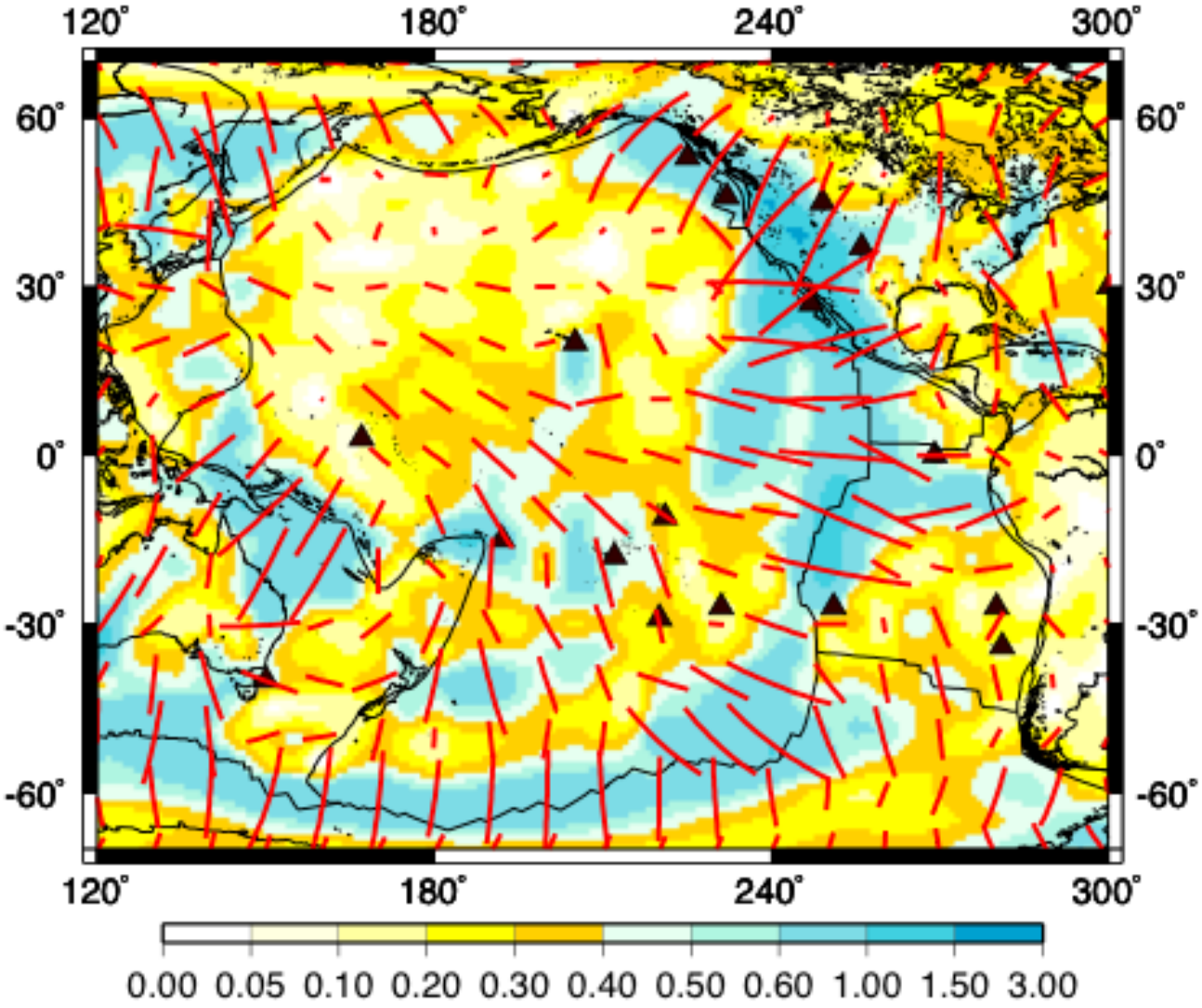

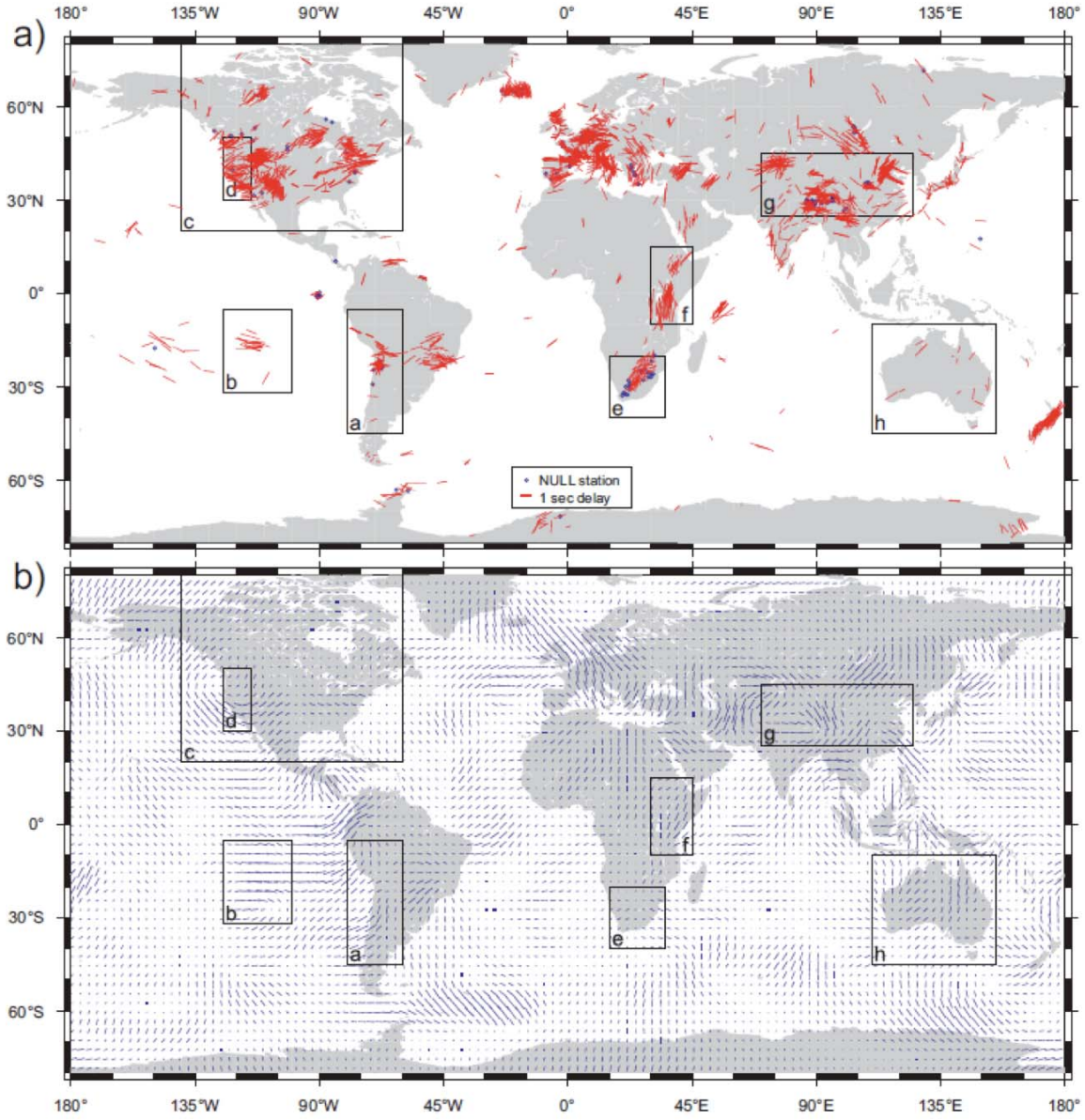

Updated
SKS database

Synthetic SKS from
Surface Wave model
(Debayle et al., 2005)

Wüstefeld et al., 2009

Geodynamic Interpretation: 3 Maps

S- Velocity

Radial Anisotropy

$\xi = (V_{SH}^2 - V_{SV}^2)/V_{SV}^2$

Azimuthal Anisotropy

$V_{SV} \approx V_{SV0} + {}^1/_2 G\cos(2(\Psi - \Psi_G))$

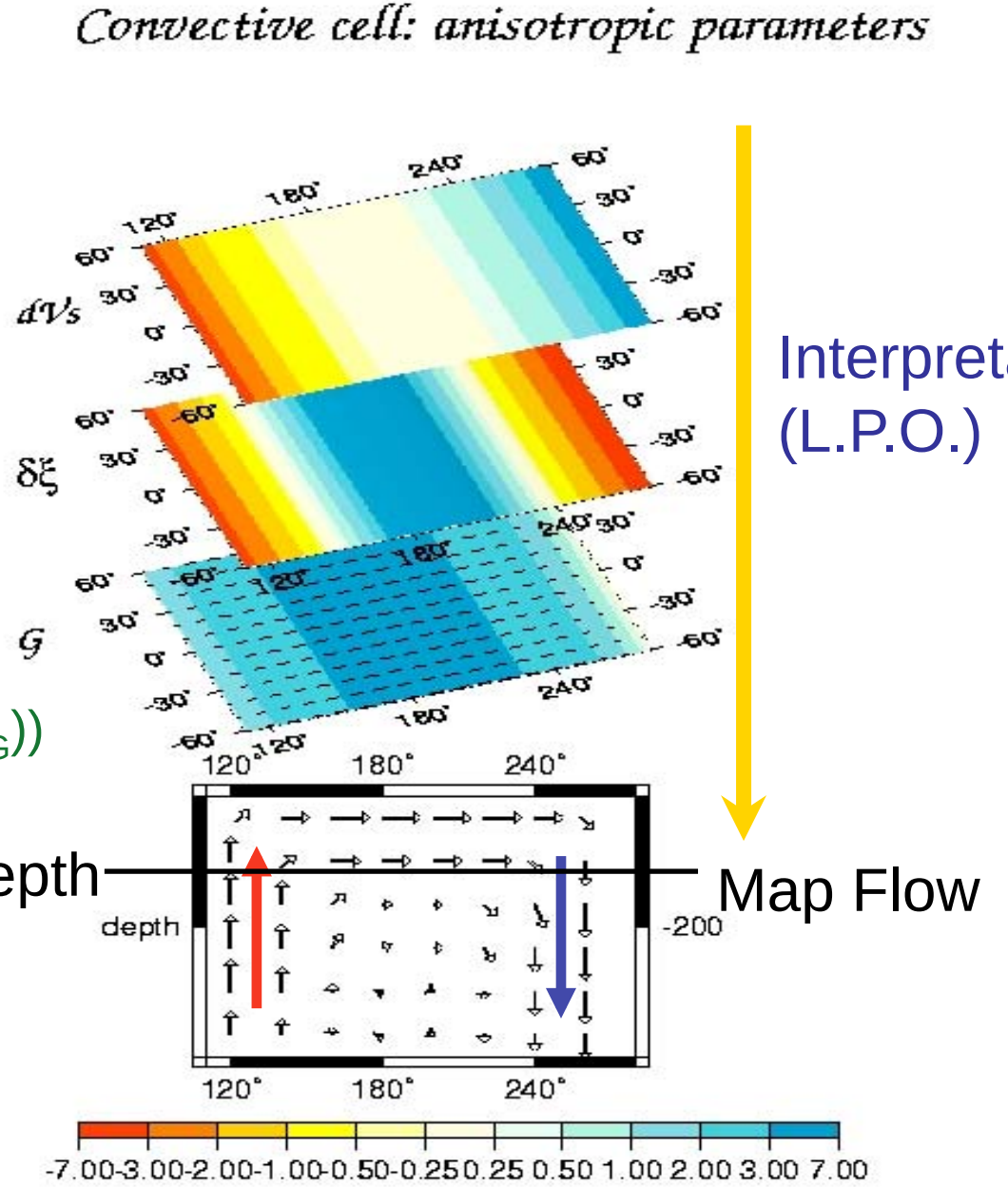

IMAGING OF FAMOUS SCIENTISTS

Anisotropic Imaging

Isotropic Imaging

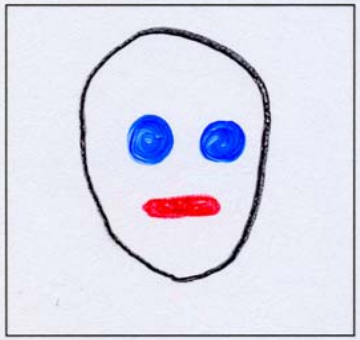

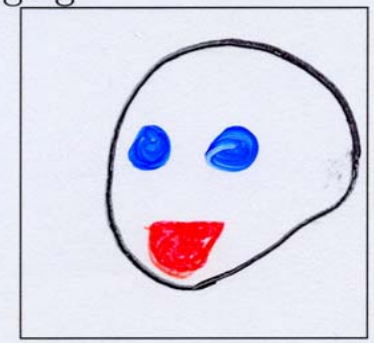

How can we know whether azimuthal anisotropy is significant or not?

Example of 2 D tomography (N cells)

Isotropic Inversion:

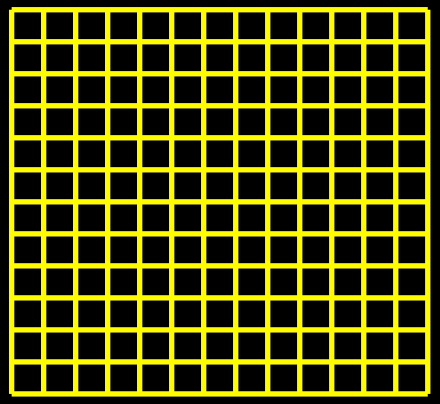

N independent parameters (1/cell)
0-Ψ term
Variance reduction: VR1

Anisotropic inversion

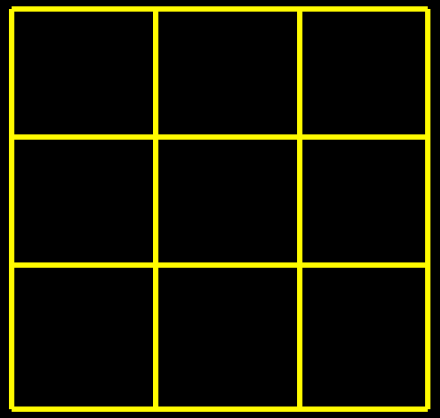

3N’ = N (3/cell)
(N’ cells)
0+2 Ψ terms
Variance reduction: VR2

VR2>VR1 =>the anisotropic model can be simpler than the isotropic model

Parameter Space

Physical parameters: ρ + 13 physical parameters

Geographical parameterization: $\mathbf{p}(r,\theta,\phi)$

- Cells

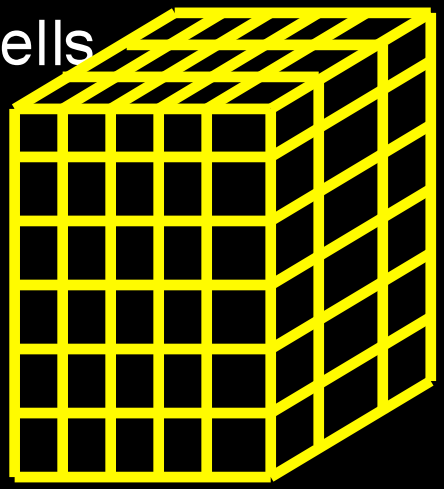

Continuous parameterization

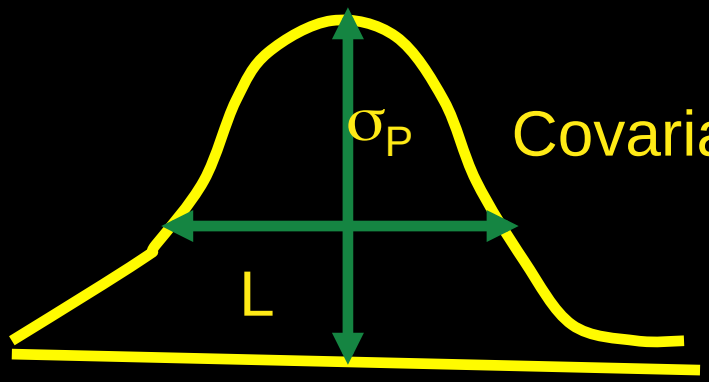

Covariance fonction

- Spherical harmonic expansion → Global scale

- Lateral resolution (global scale):

Hor 1000km, Rad 50km => 500*60*14 ≈ 420,000 parameters

Tomographic Technique

- ***Forward Problem***: Theory **d**=**g**(**p**)

d data space → **Phase or group velocities**

p parameter space

- Reference Earth model p_0:

$d_0 = g(p_0)$

- Kernels $\partial g/\partial p$
- Cd function (or matrix) of covariance of data

- ***Inverse Problem***: $p-p_0 = g^{-1}(d-d_0)$

- C_{p0} a priori Covariance function of parameters
- C_{pf} a posteriori Covariance function of parameters
- R Resolution

Example of seismogram

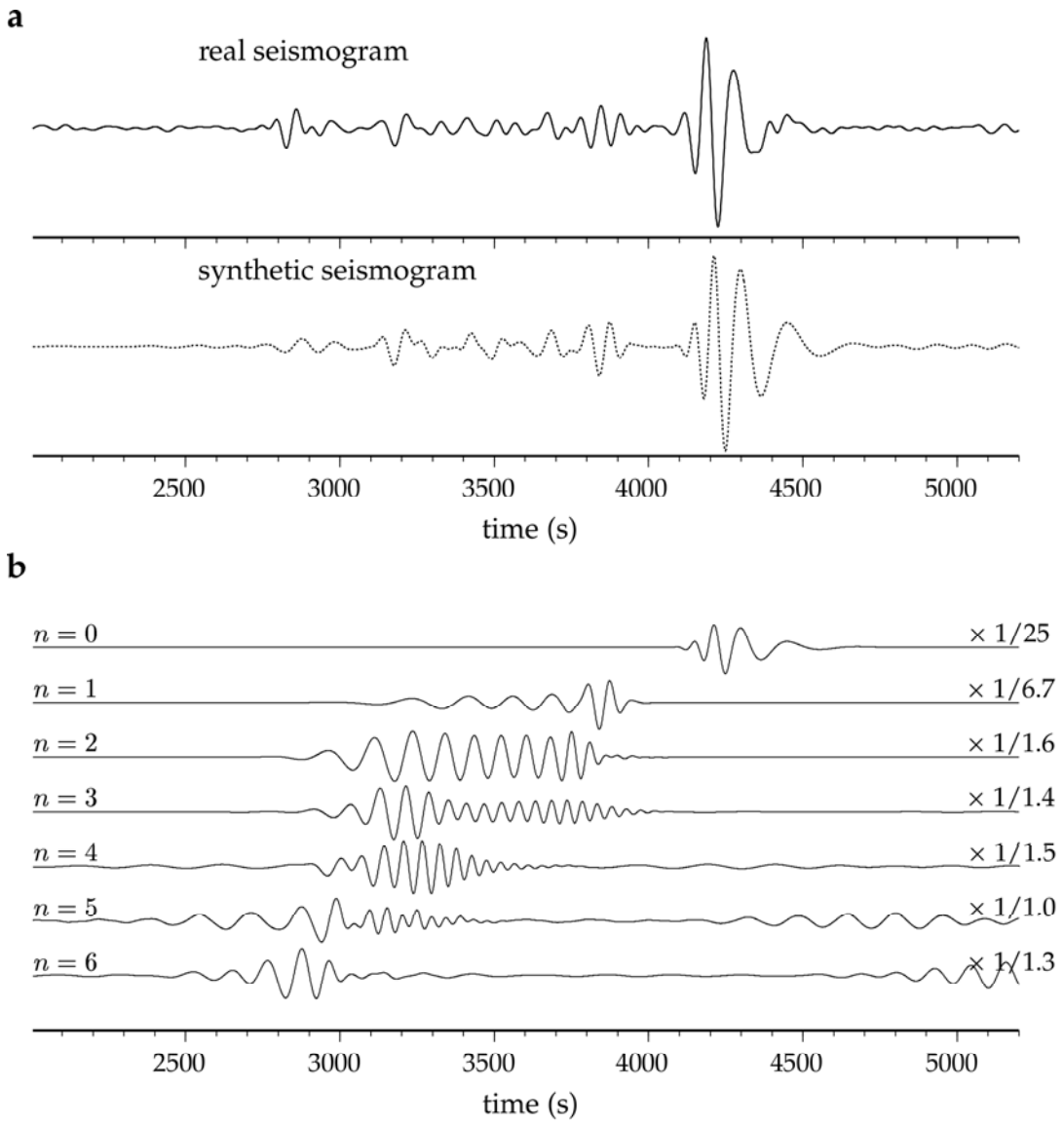

Beucler, 2003

1st step: Calculation of dispersion curves:Fundamental modes and higher modes $c_n^R(T)$, $c_n^L(T)$ (Beucler et al., 2003)

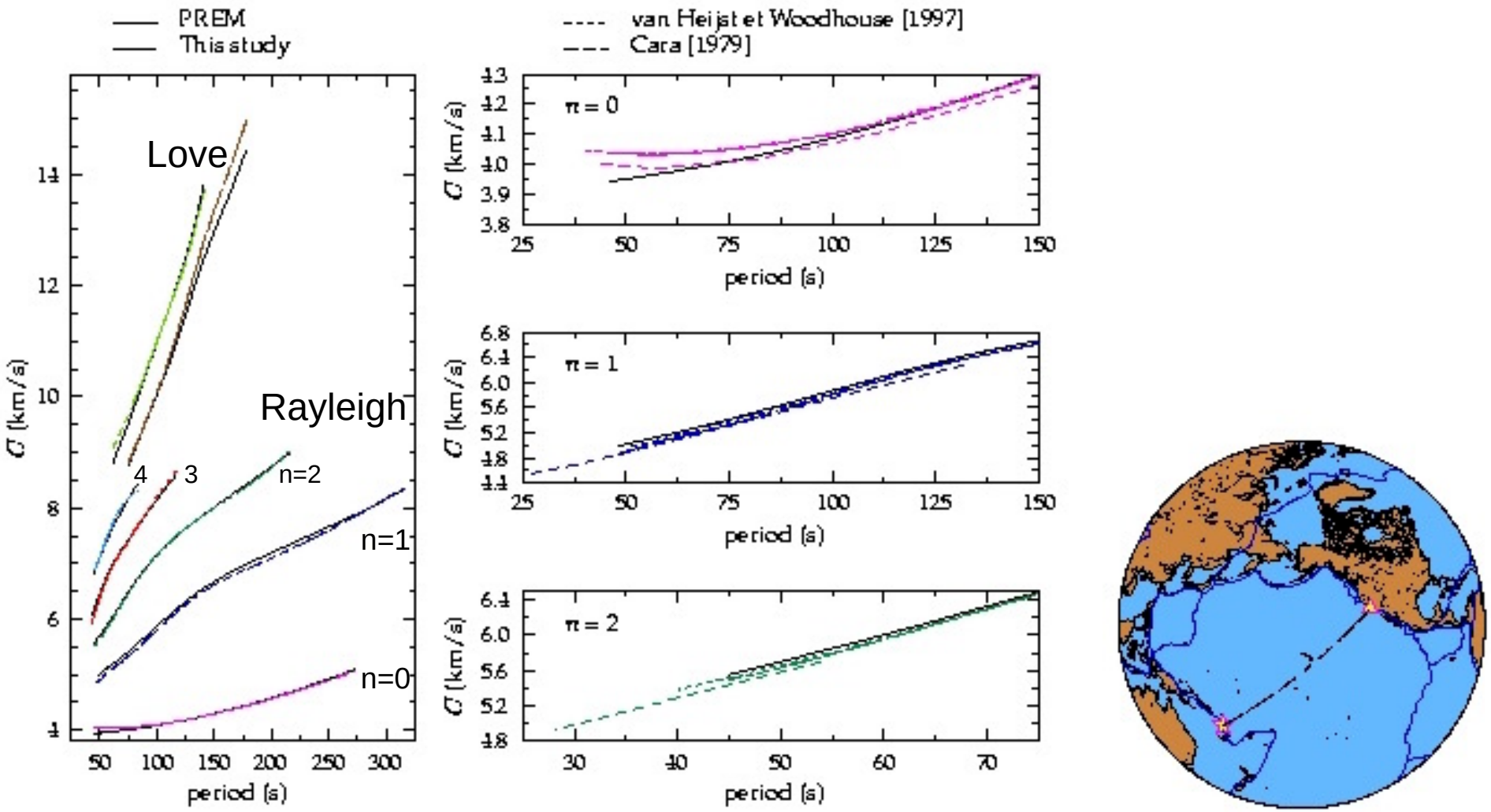

Comparison with previous results along the Vanuatu-California path.

2nd step: Regionalization

Phase velocity maps
At 100s

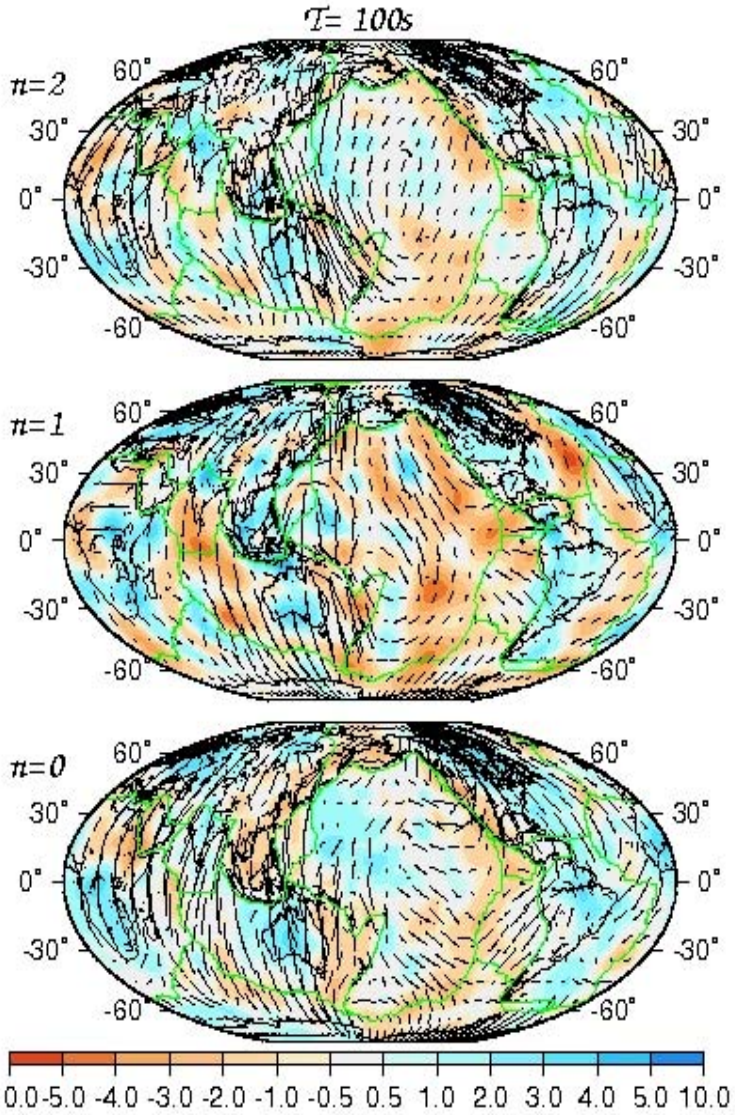

2nd overtone

1st overtone

Fundamental mode

Beucler and Montagner, 2006

Global Tomography

3rd step: inversion at depth

Scale $\Lambda \approx$ 2000km (degree 20)

Seismic wavelength $\lambda \leq$ 500km

⇨ Ray theory applies

Shear wave velocities - depth = 100km

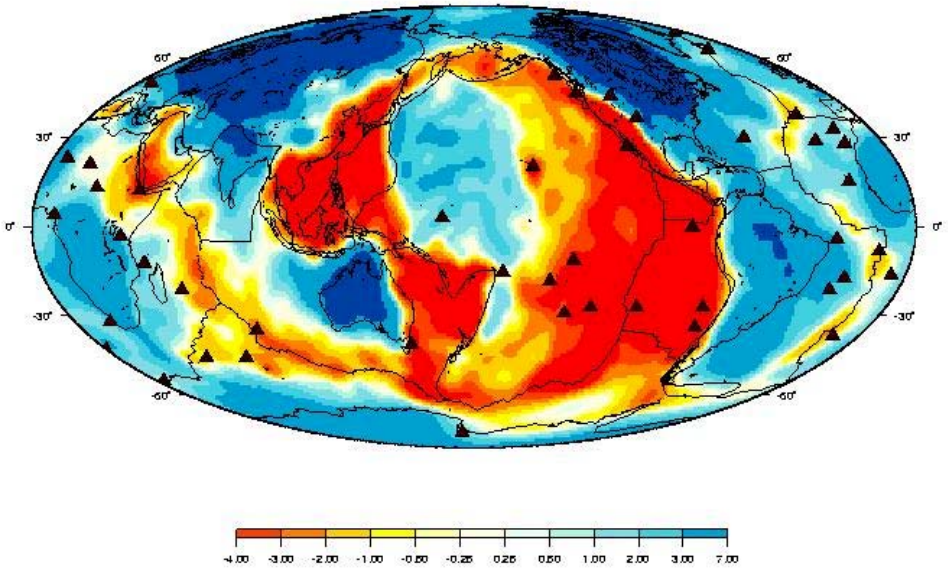

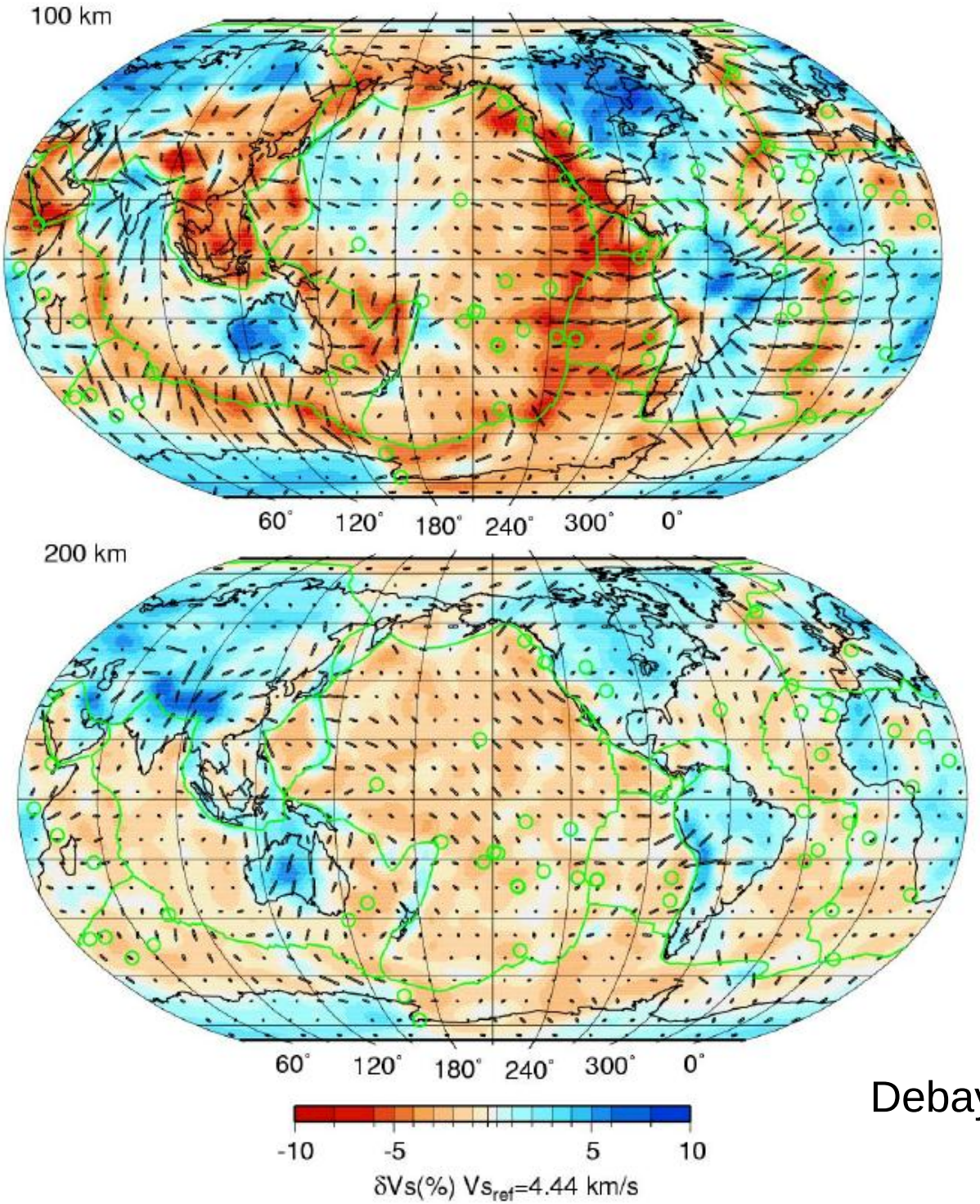

Debayle et al., 2005

CAN WE NEGLECT SMALL-SCALE HETEROGENEITIES?

From Global scale to Regional scale

Scale Λ >1000km $\Lambda \approx$100km

Seismic wavelength 20km $\leq \lambda \leq$ 500km

S-wave velocity -
depth = 100km

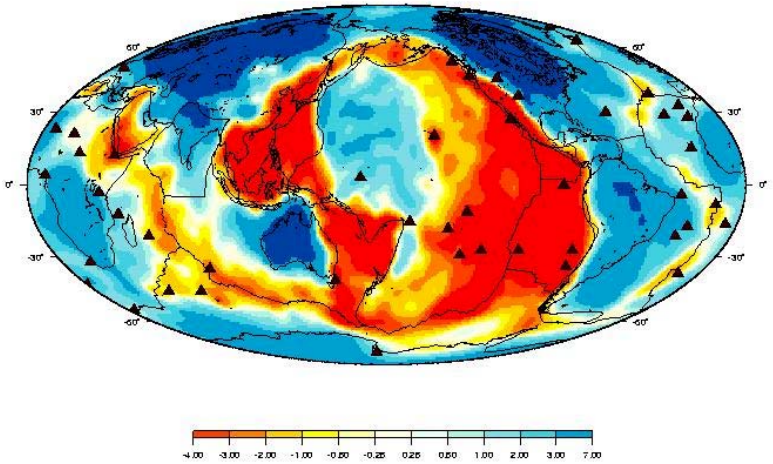

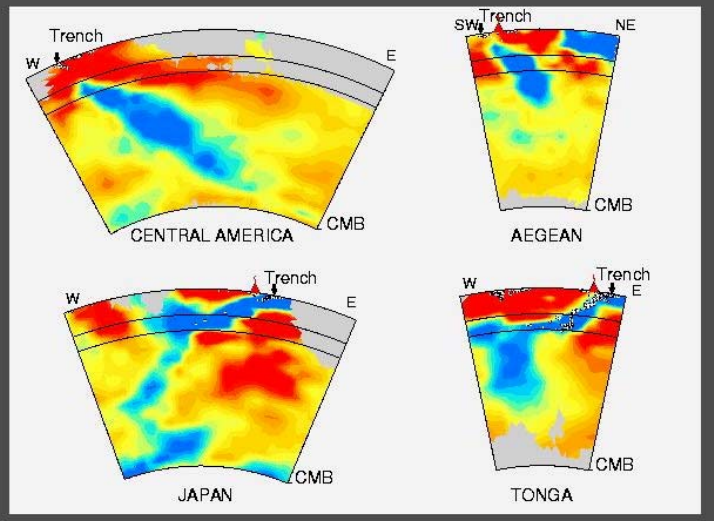

Van der Hilst et al., 1998

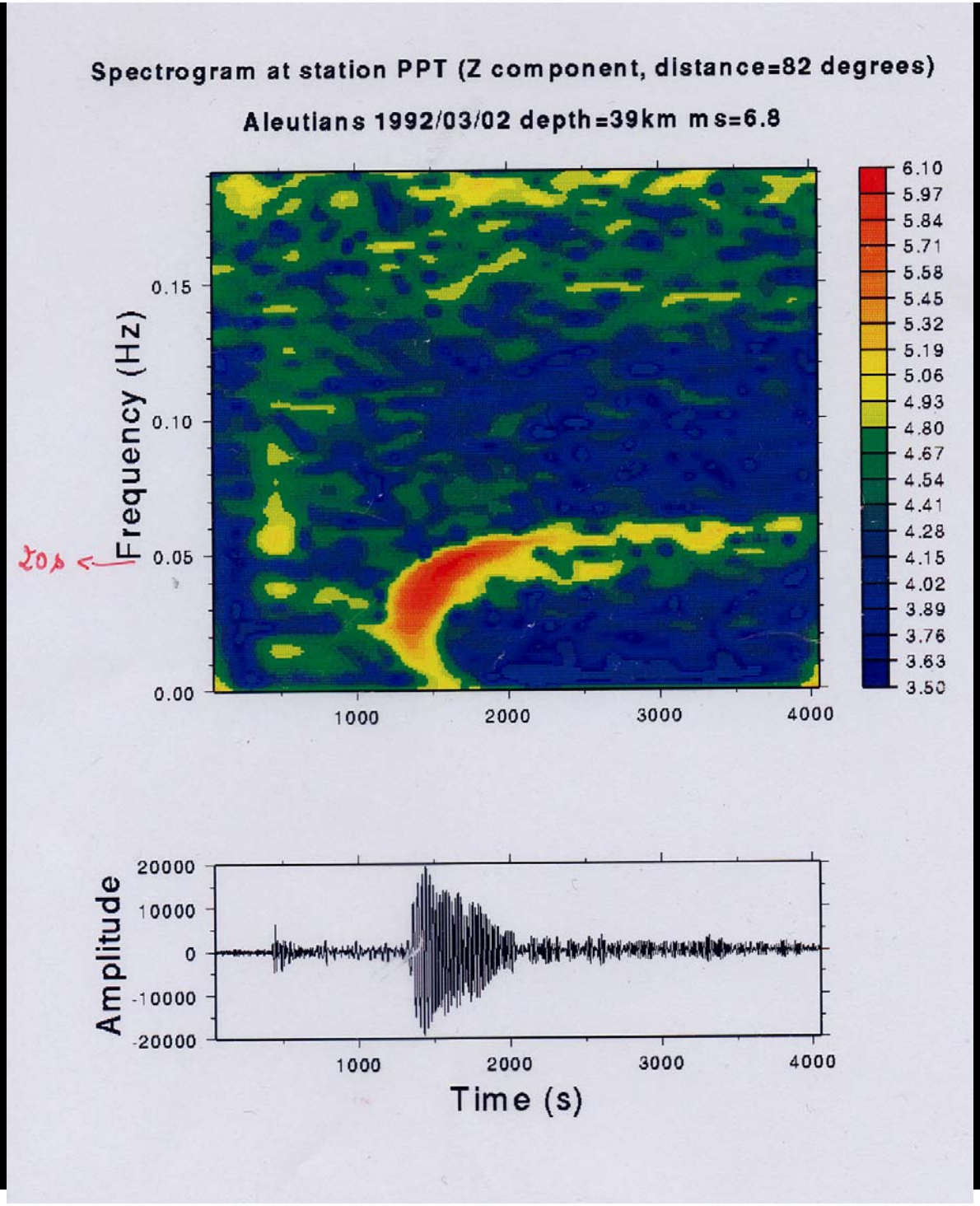

Oceanic
Path

simple
dispersion
Curve
Multiple scattering
For T<30s

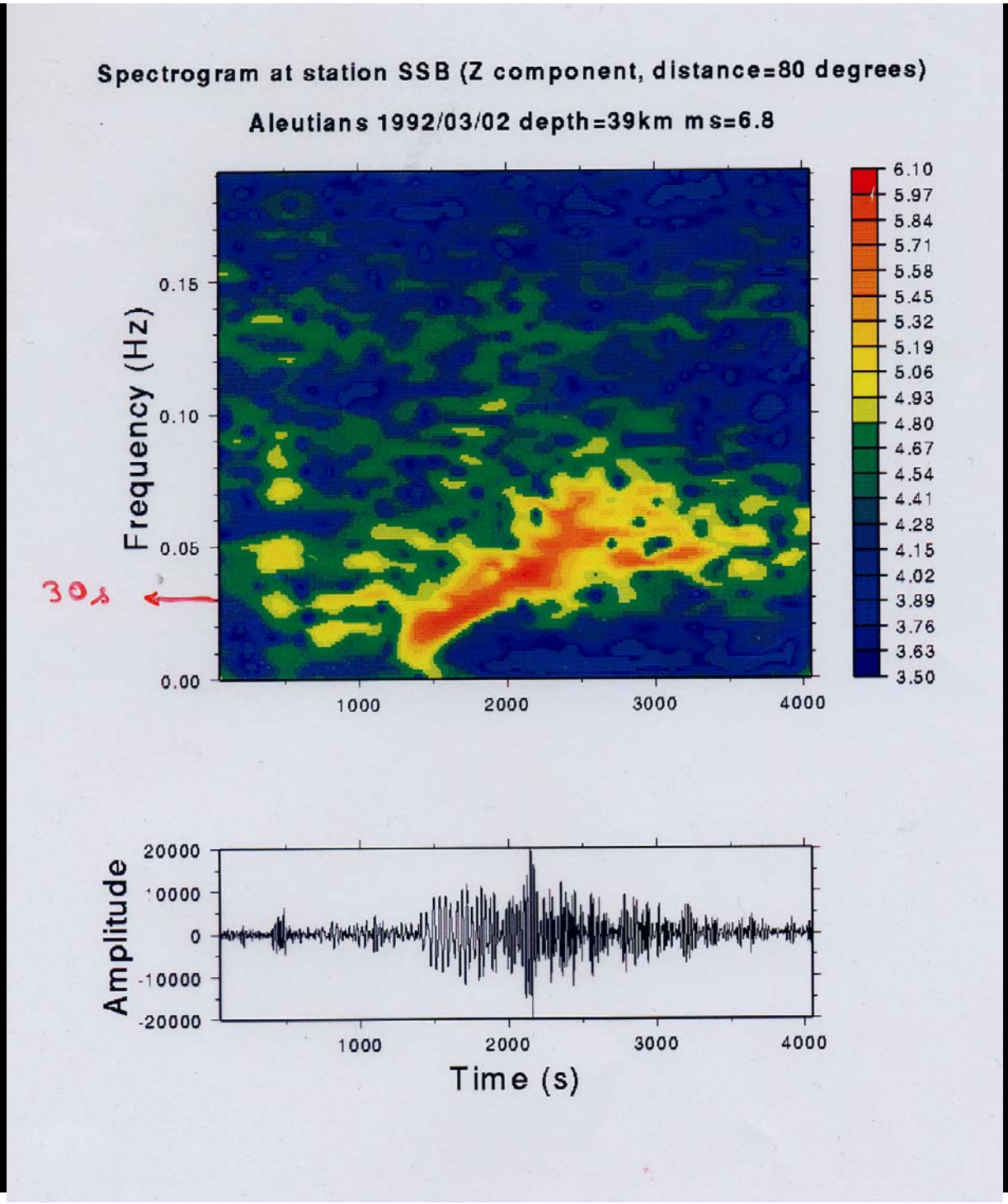

Continental Path

complex dispersion Curve
Multiple scattering
For T<60s

Λ heterogeneity scale, λ wavelength

λ~ Λ or λ>> Λ

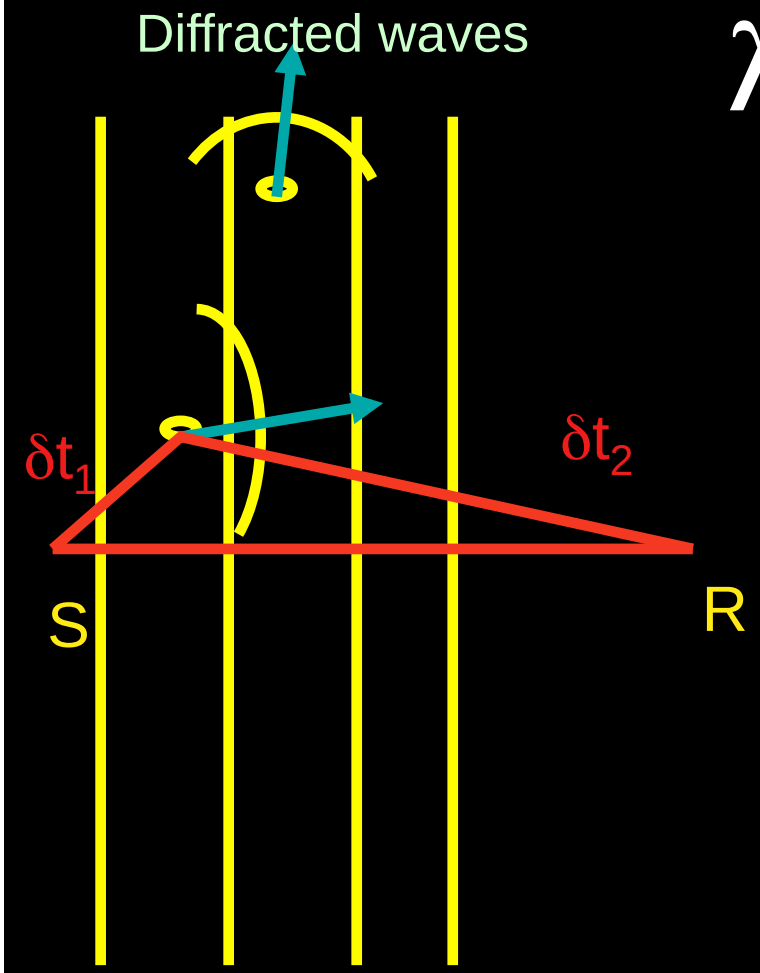

wavefronts

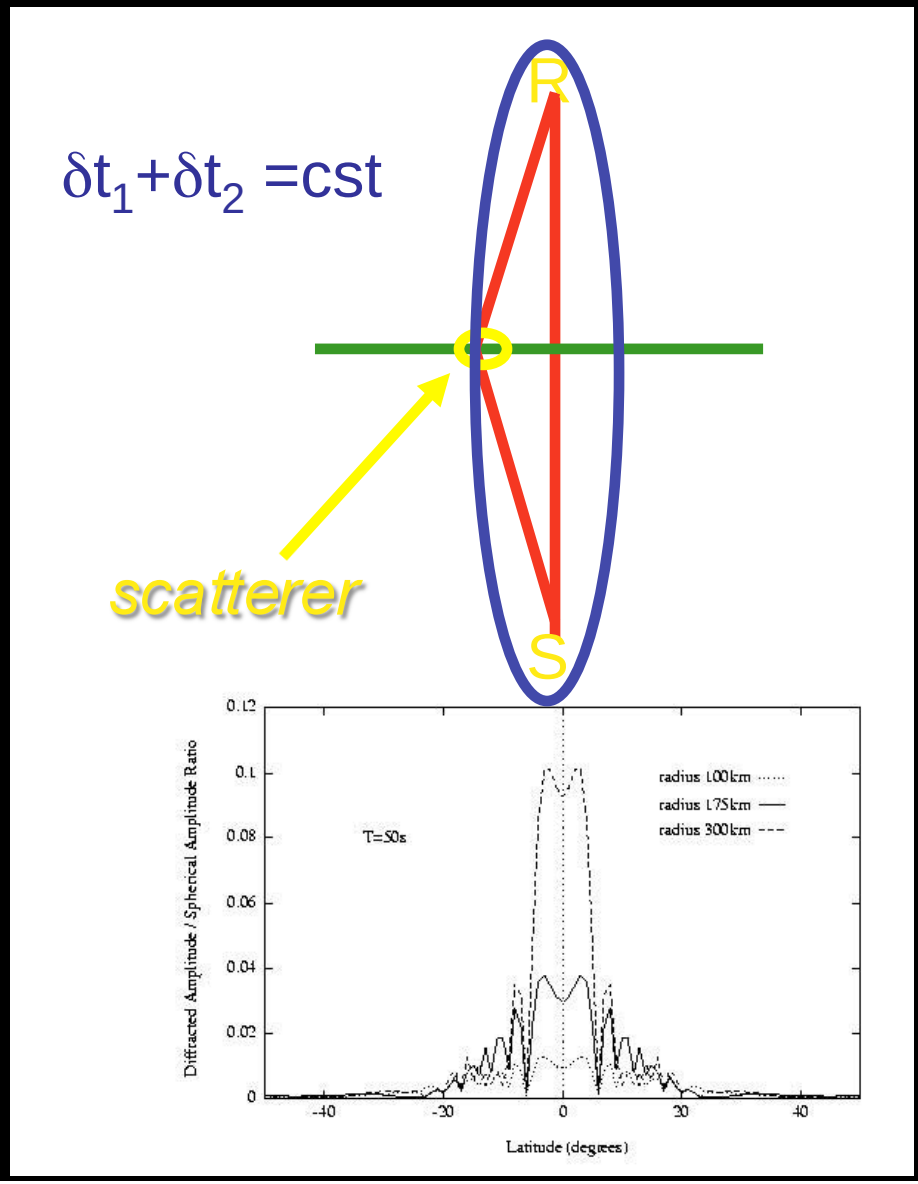

Capdeville et al., 2000

Sensitivity of the delay time to the local seismic velocity

→ Princeton Group (G. Nolet)

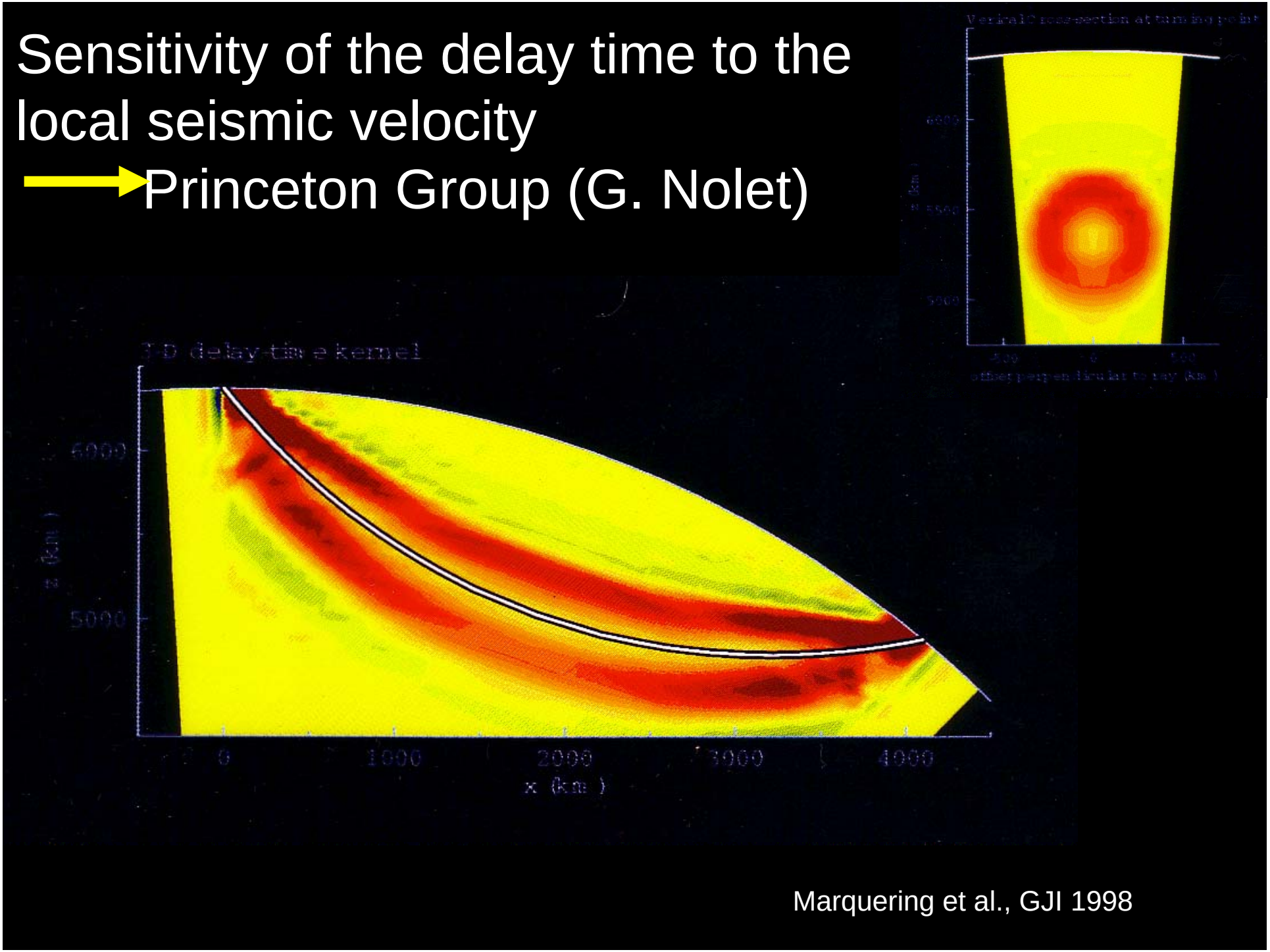

Marquering et al., GJI 1998

Λ heterogeneity scale, λ wavelength

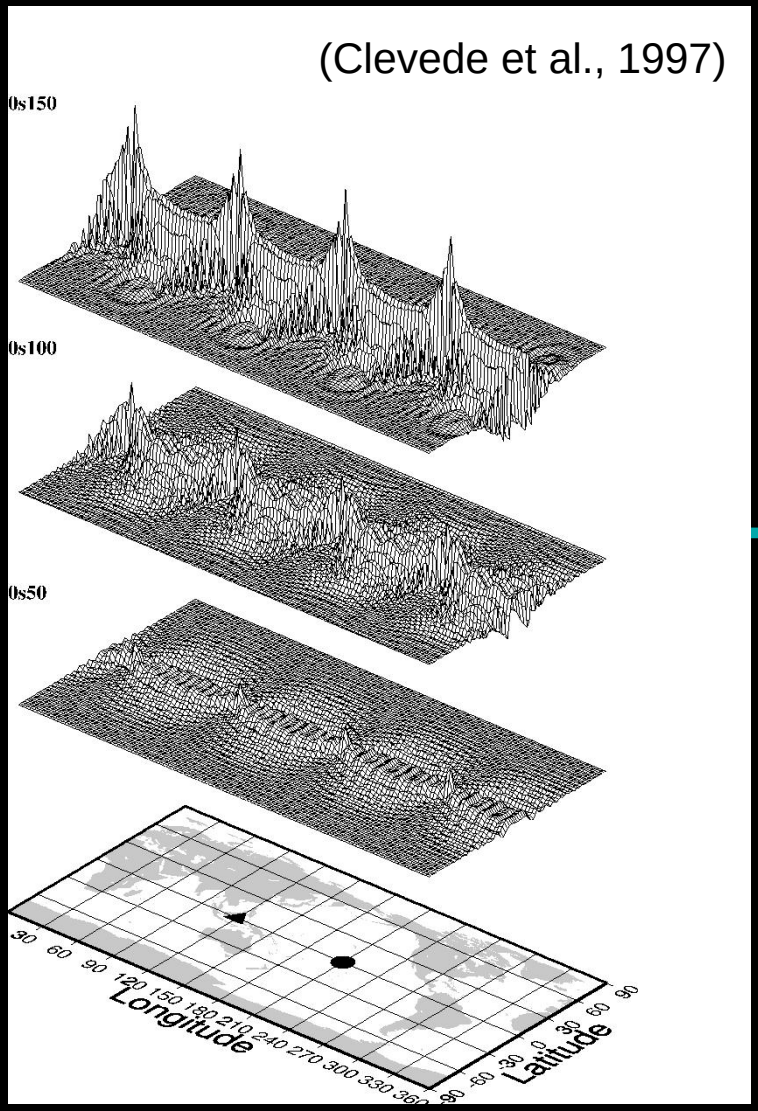

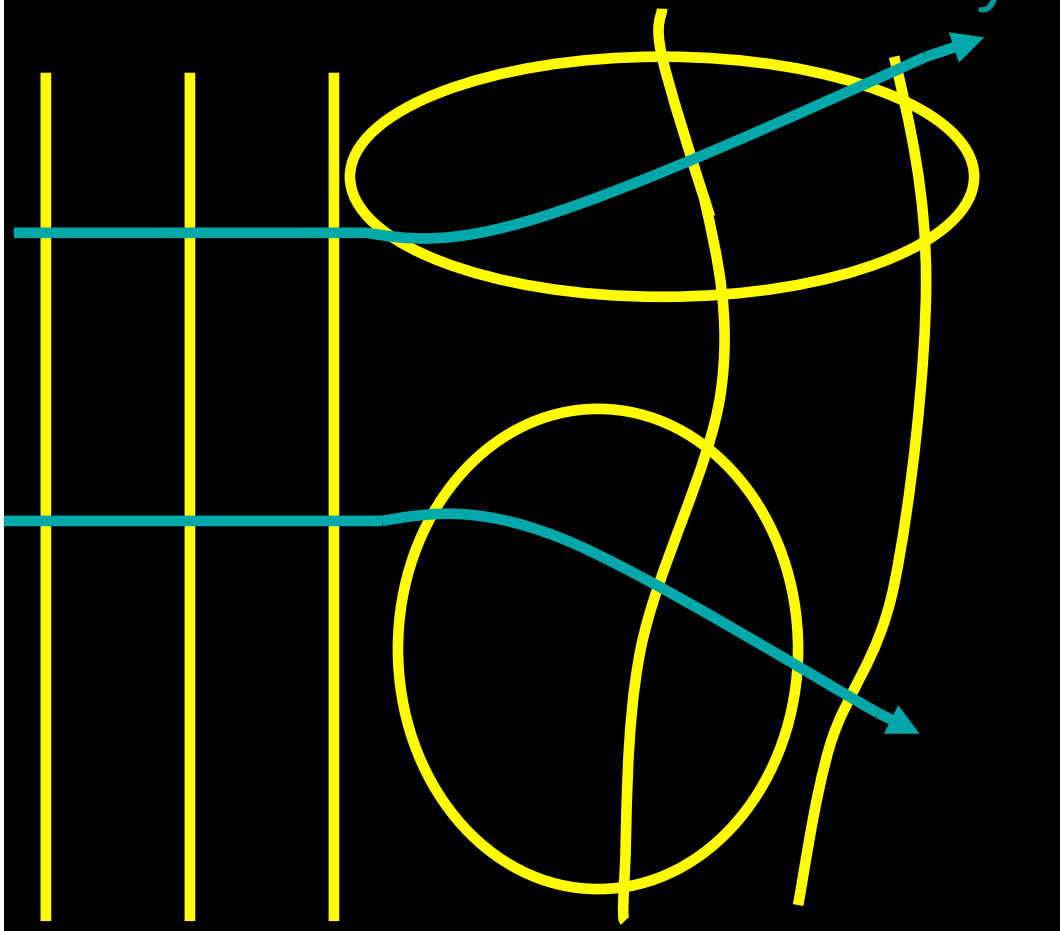

$\lambda << \Lambda$

Typical scales $\Lambda \approx$2,000km, $\lambda \approx$ 500km

Effects on amplitude?

- Surface wave tomography of mantle anisotropy is based on ray theory
- Finite frequency tomography has been tested to improve the imaging of the isotropic mantle
- How do finite frequency surface waves "sense" anisotropy ?
- Computational tool : Adjoint Spectral Element Method (ASEM) (Tromp et al., 2005)

An Example of
Using Quasi-Love waves
to infer anisotropic gradients
(Park, 2006)

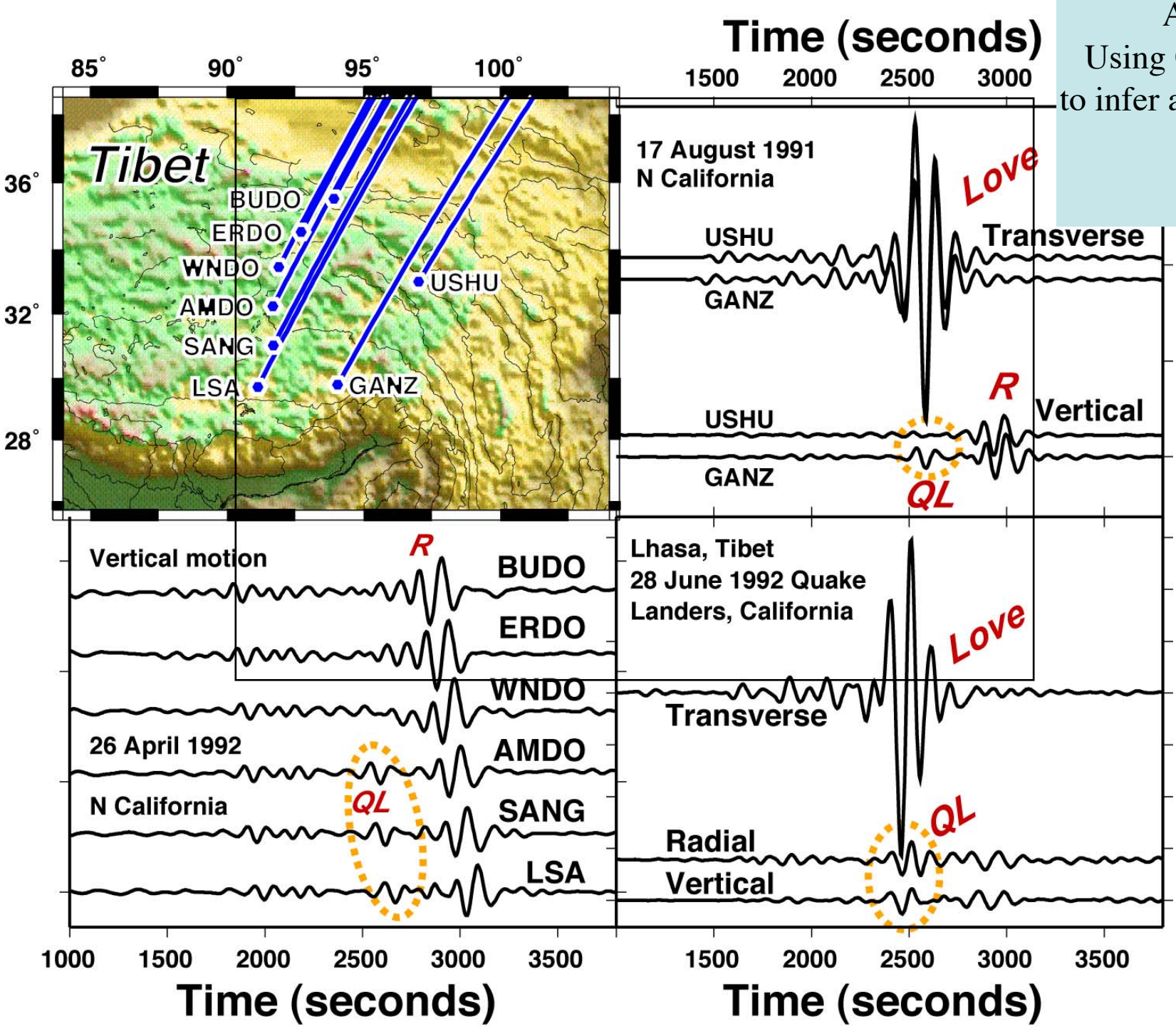

Time Reversal- Adjoint Method

(Tarantola, 1984, Tromp et al., 2005):

Adjoint => Fréchet Derivatives

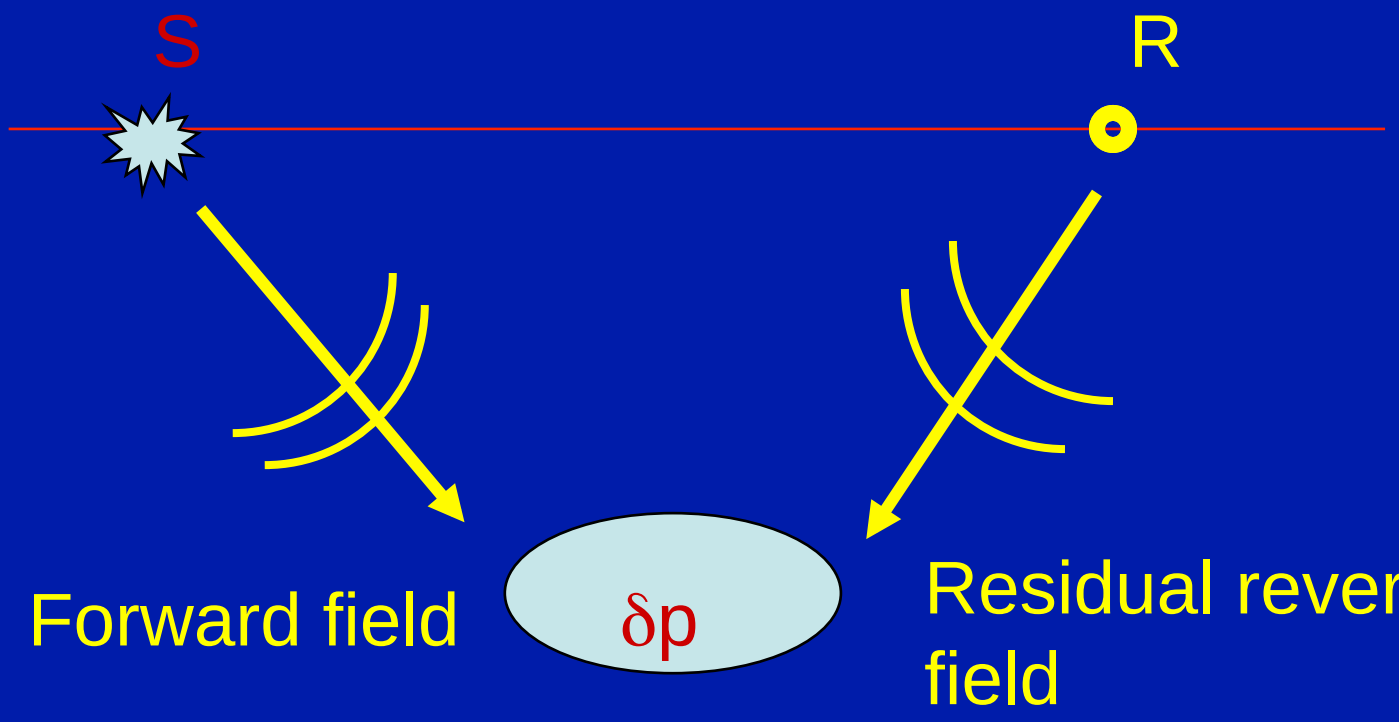

Overview
Large scale Seismology: an observational field

- Data (Seismic source) + Instrument (Seismometer) -> Observations (seismograms)
- Historical evolution: Ray theory, Normal mode theory, Numerical techniques (SEM, NM-SEM)
- Scientific Issues: earthquakes (Sumatra-Andaman earthquake), Anisotropic structure of the Earth
- Tomographic technique
- Geodynamic Applications:

  Continental deformation

  Seismic Experiment: Plume detection

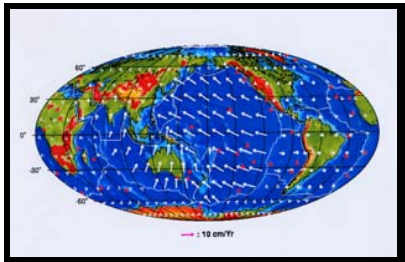

Anisotropy and Geodynamic processes

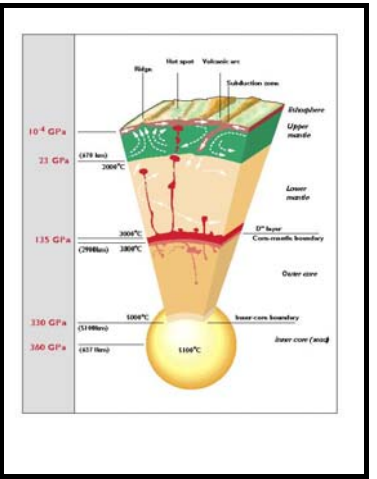

- Mapping of mantle convection (global scale) (Montagner & Tanimoto, 1991; Ekström, 2001; Debayle et al., 2005)
- **Collision India-Asia (Griot et al., 1998; ….)**
- Lithosphere roots (continents- oceans)
- Plume Detection- interaction lithosphere-asthenosphere
- Deformation Processes -> Fluid Mechanics (Gaboret et al., 2003; Becker et al., 2003, 2007…)

Seismic tomography: Instantaneous image
Anisotropy- Geodynamics Relationship

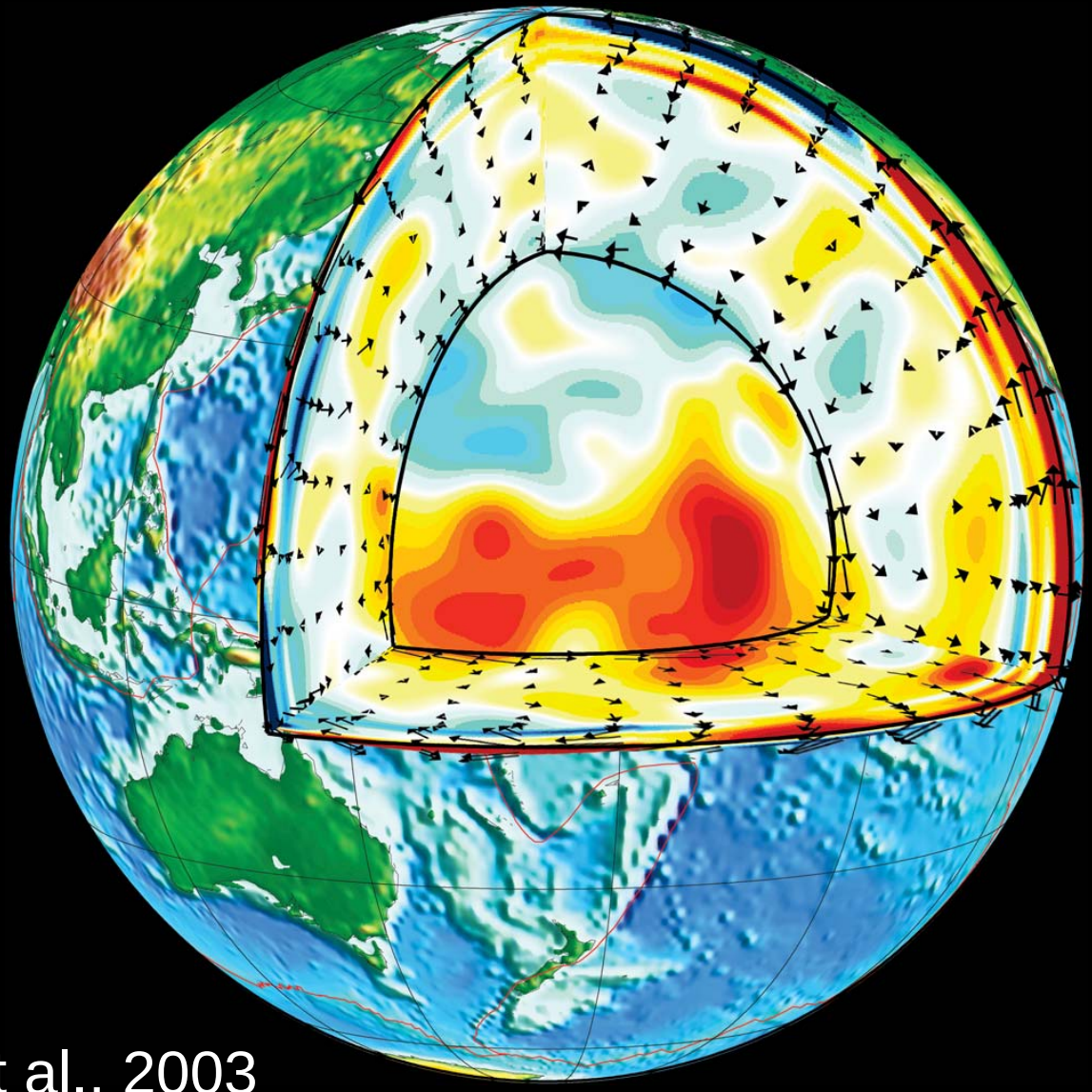

Gaboret et al., 2003

Difference Continent -Ocean

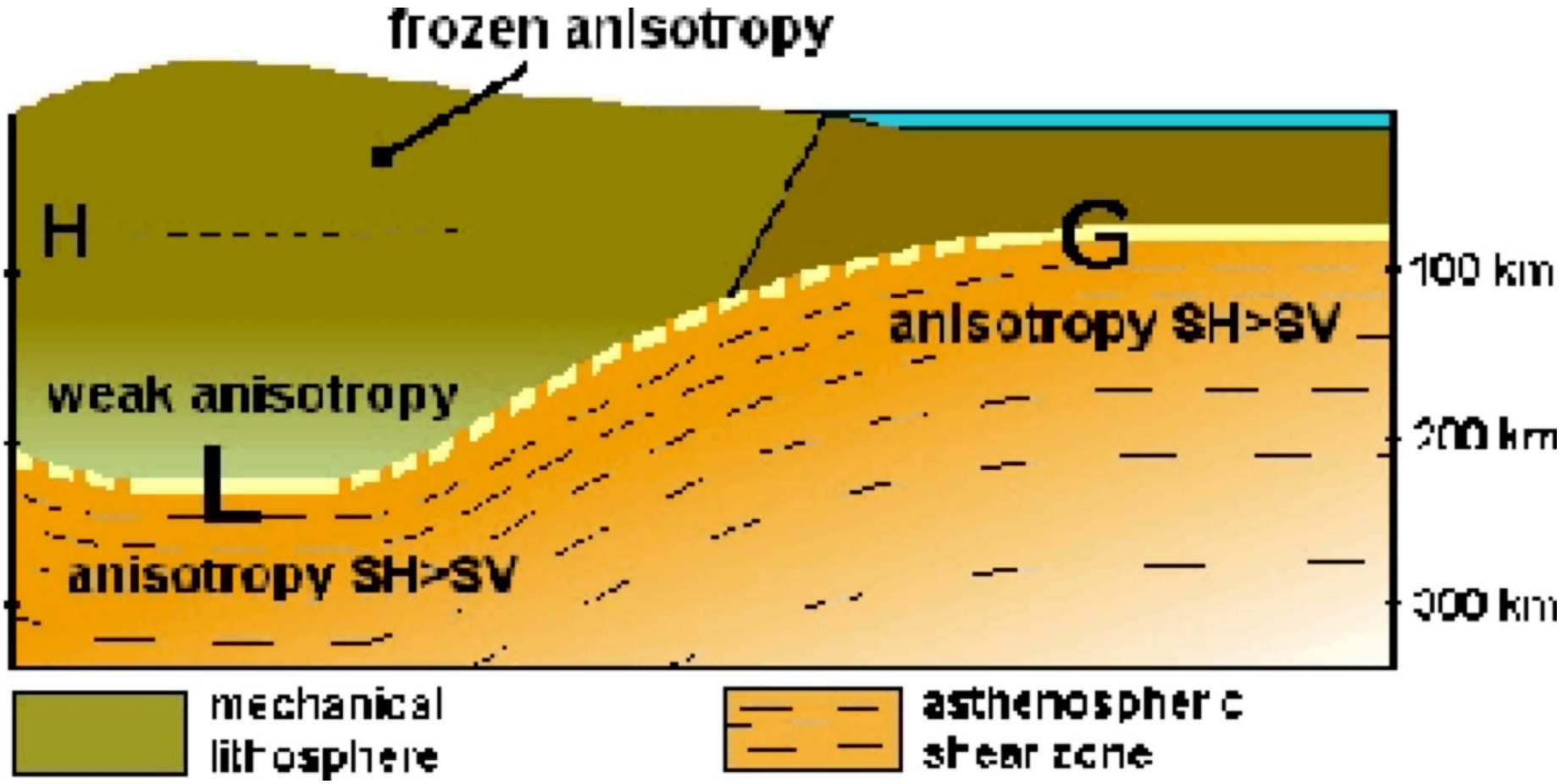

Gung & Romanowicz, (2003)

Central Asia:
Heterogeneous versus homogeneous Deformation

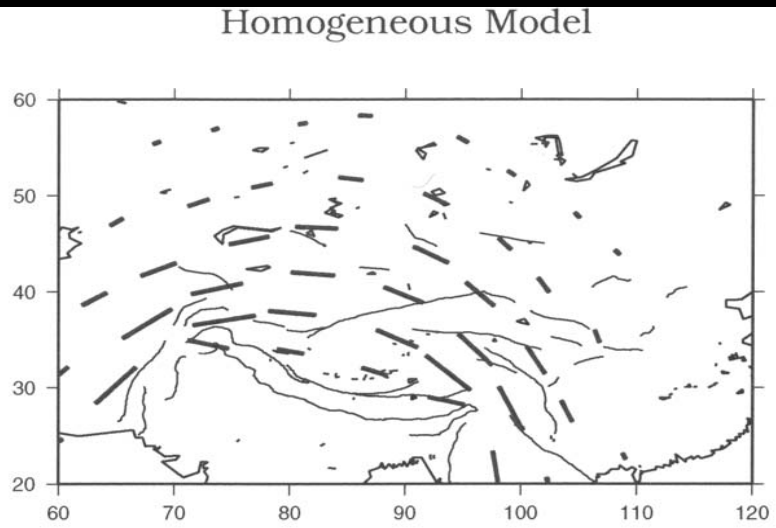

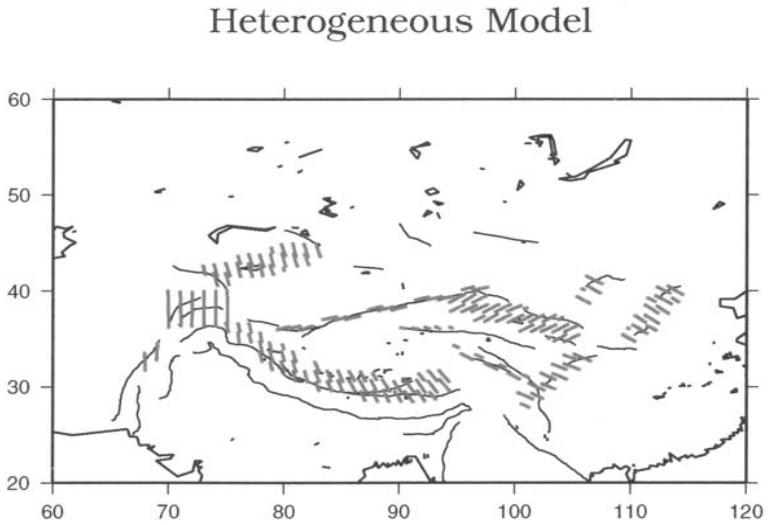

Problems:

-Direction of maximum extension?

- Fossile anisotropy

- Spatial filtering

Griot et al., 1998

Heterogeneous versus Homogeneous Deformation

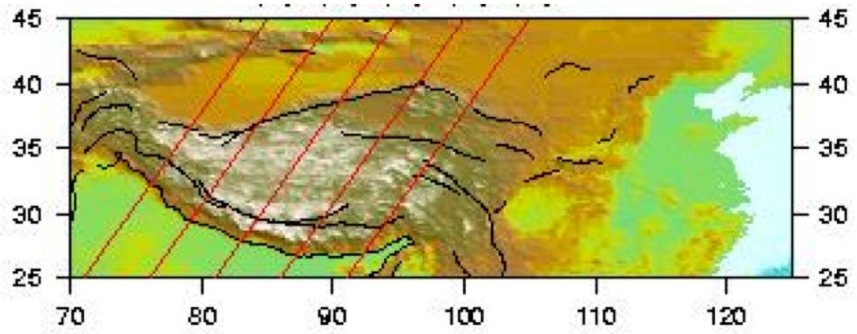

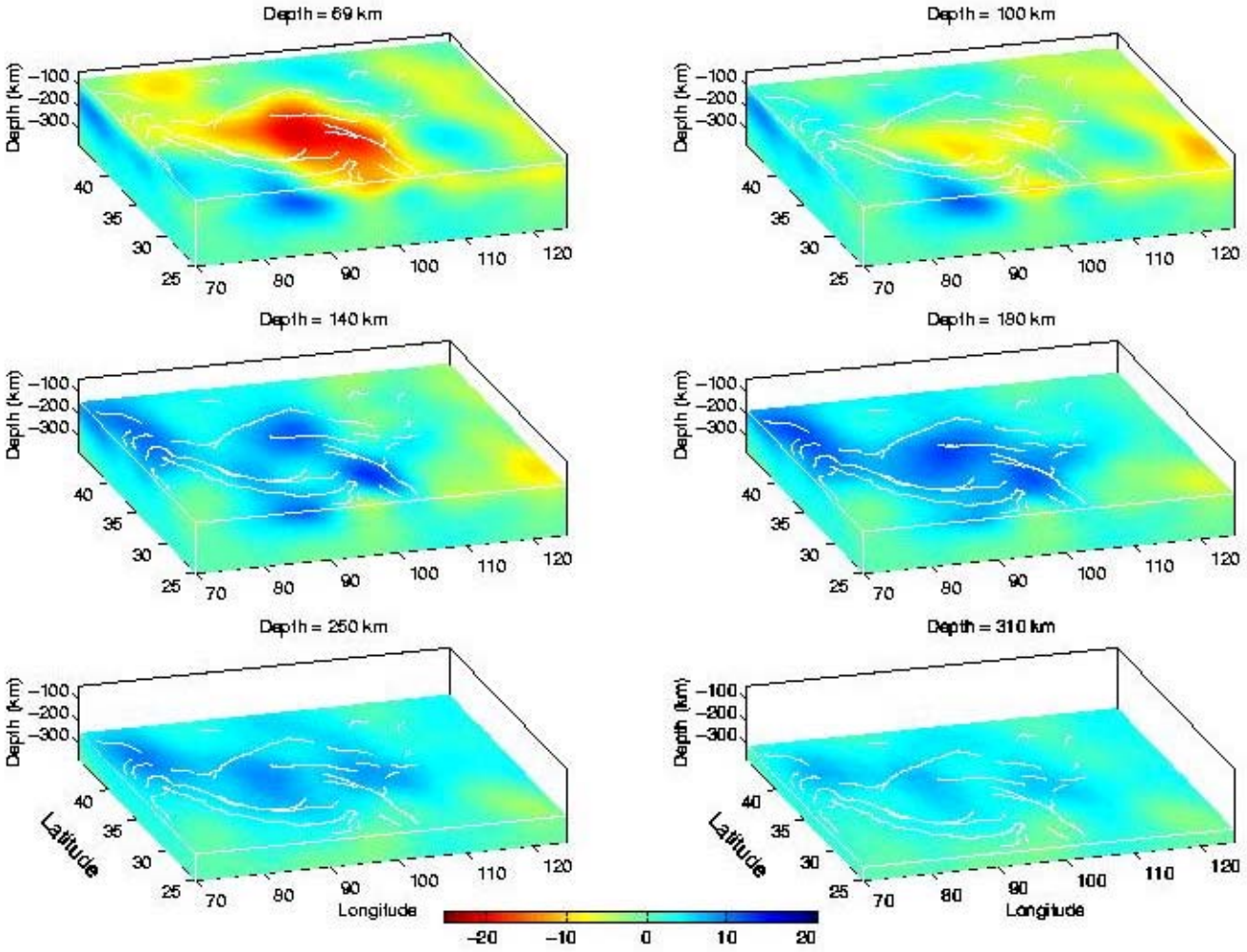

Griot et al., 1998

Heterogeneous vs homogeneous Deformation
2 competing models

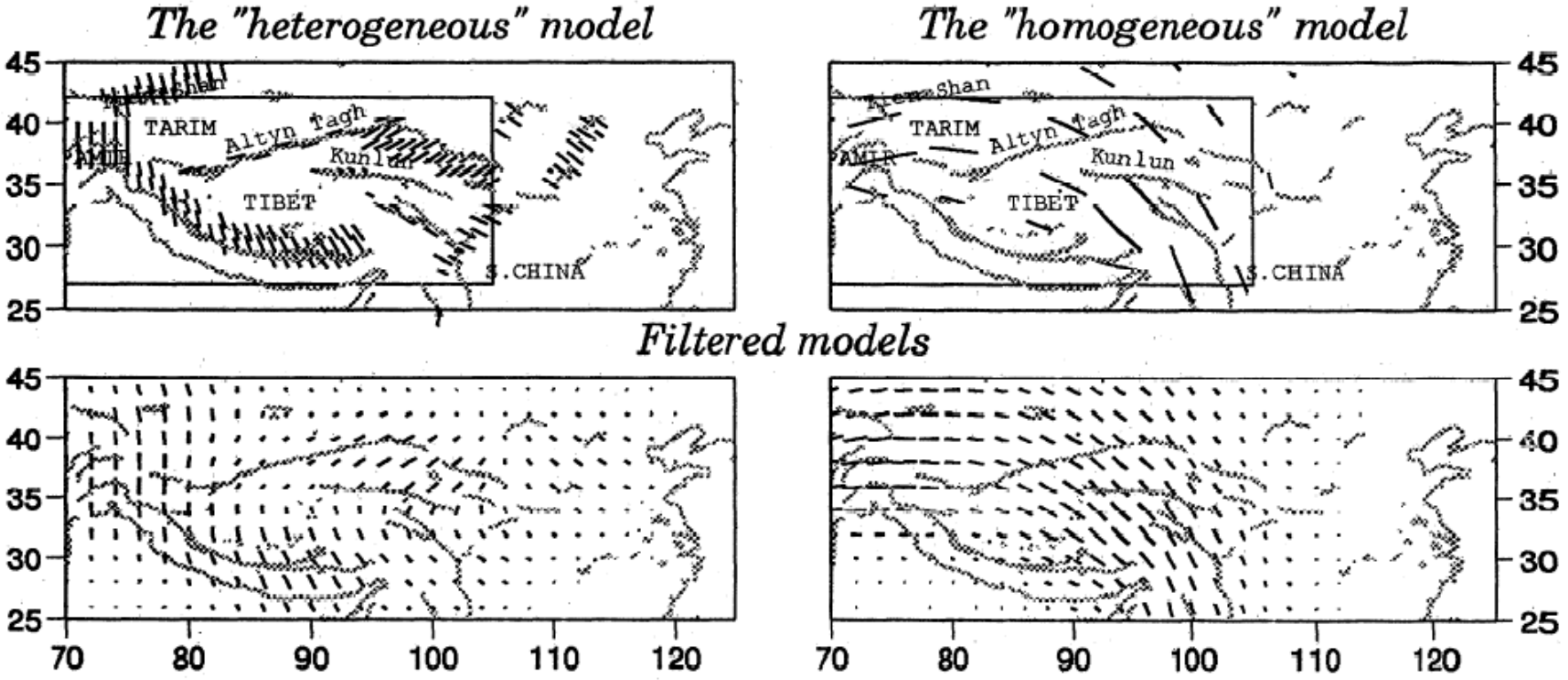

Heterogeneous versus homogeneous Deformation

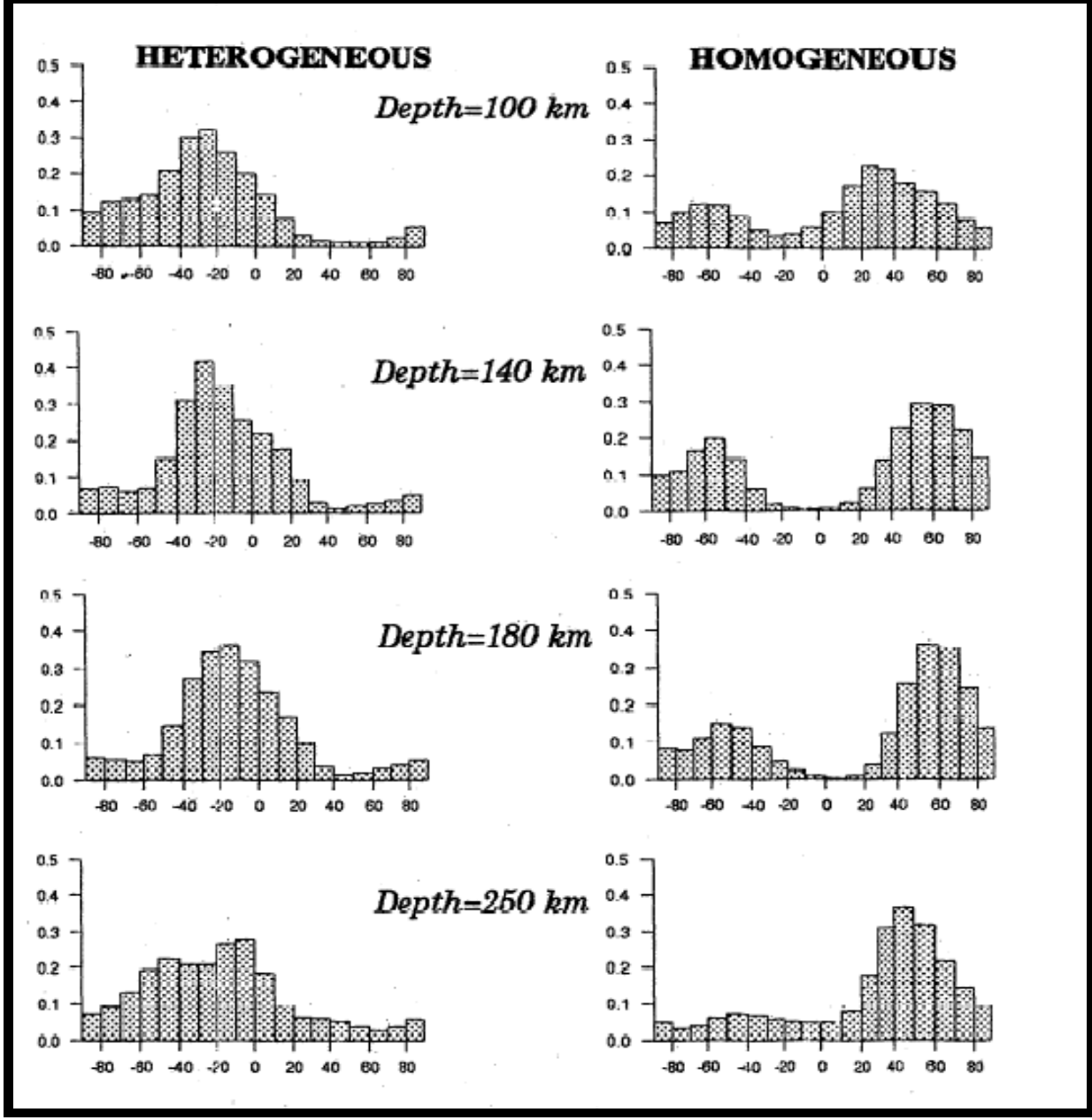

- Continental Root around 200km

- Comparison with SKS

(Montagner et al., 2000)

- Stratification of anisotropy

(Different orientation below 200km)

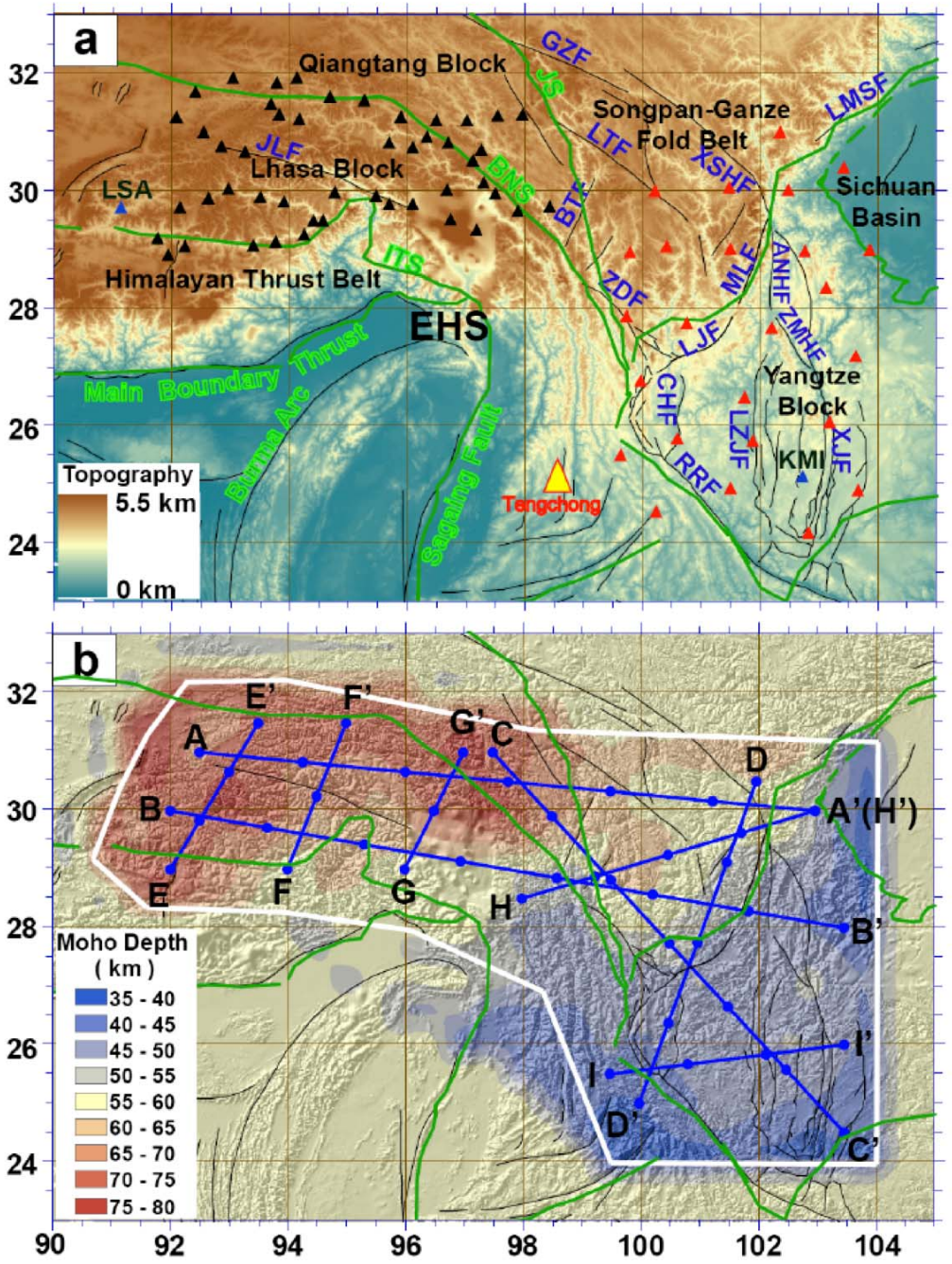

Yao, van der Hilst, Montagner, 2010

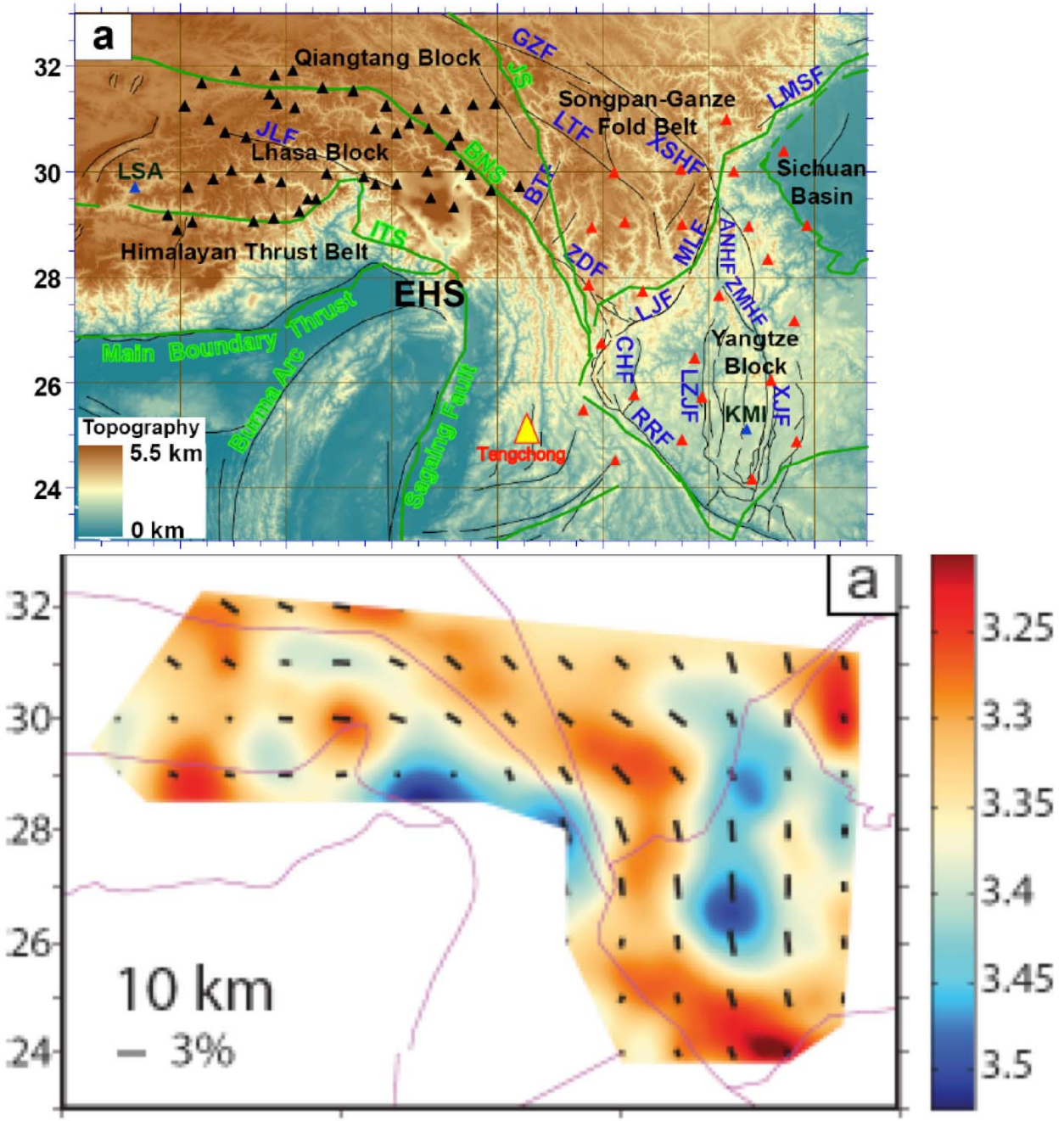

Yao et al., 2010

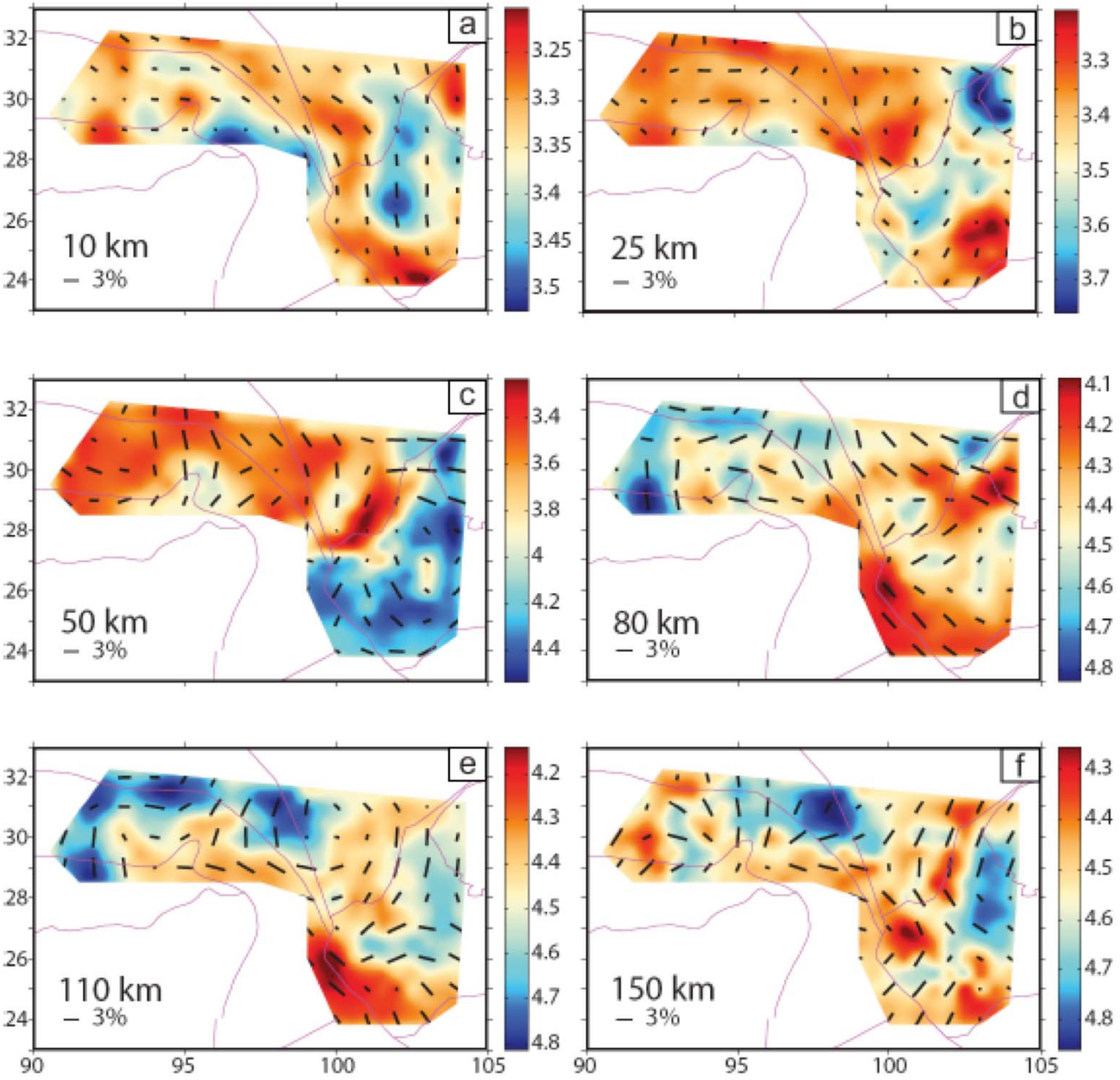

Yao et al., 2010

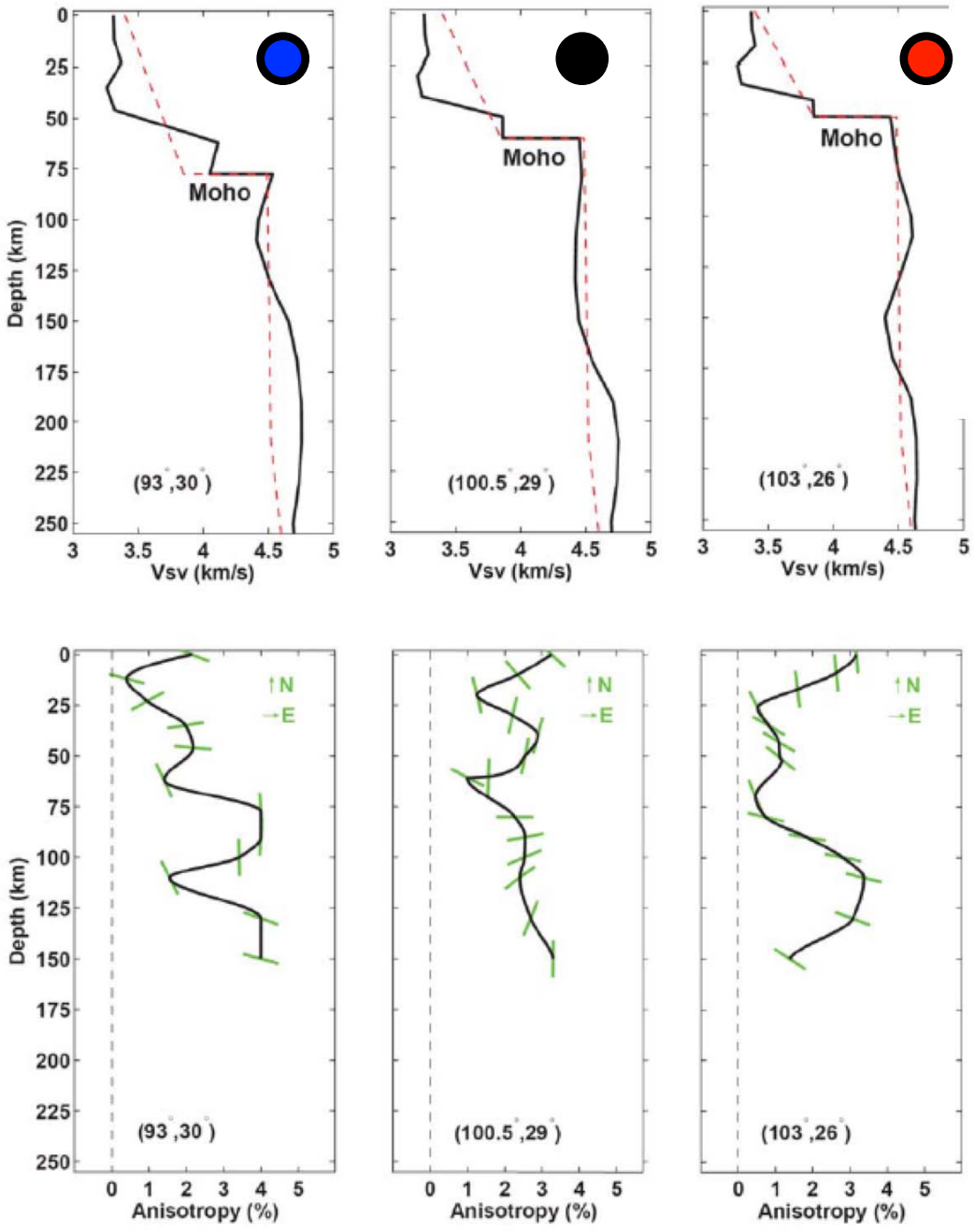

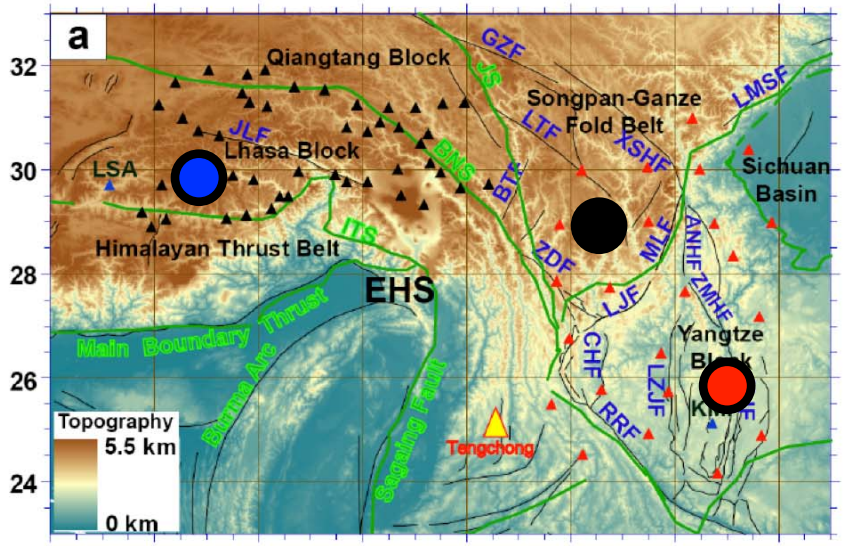

- Several anisotropic layers
- Crustal flow?
- Coupling Crust-Lithosphere?

Yao et al., 2010

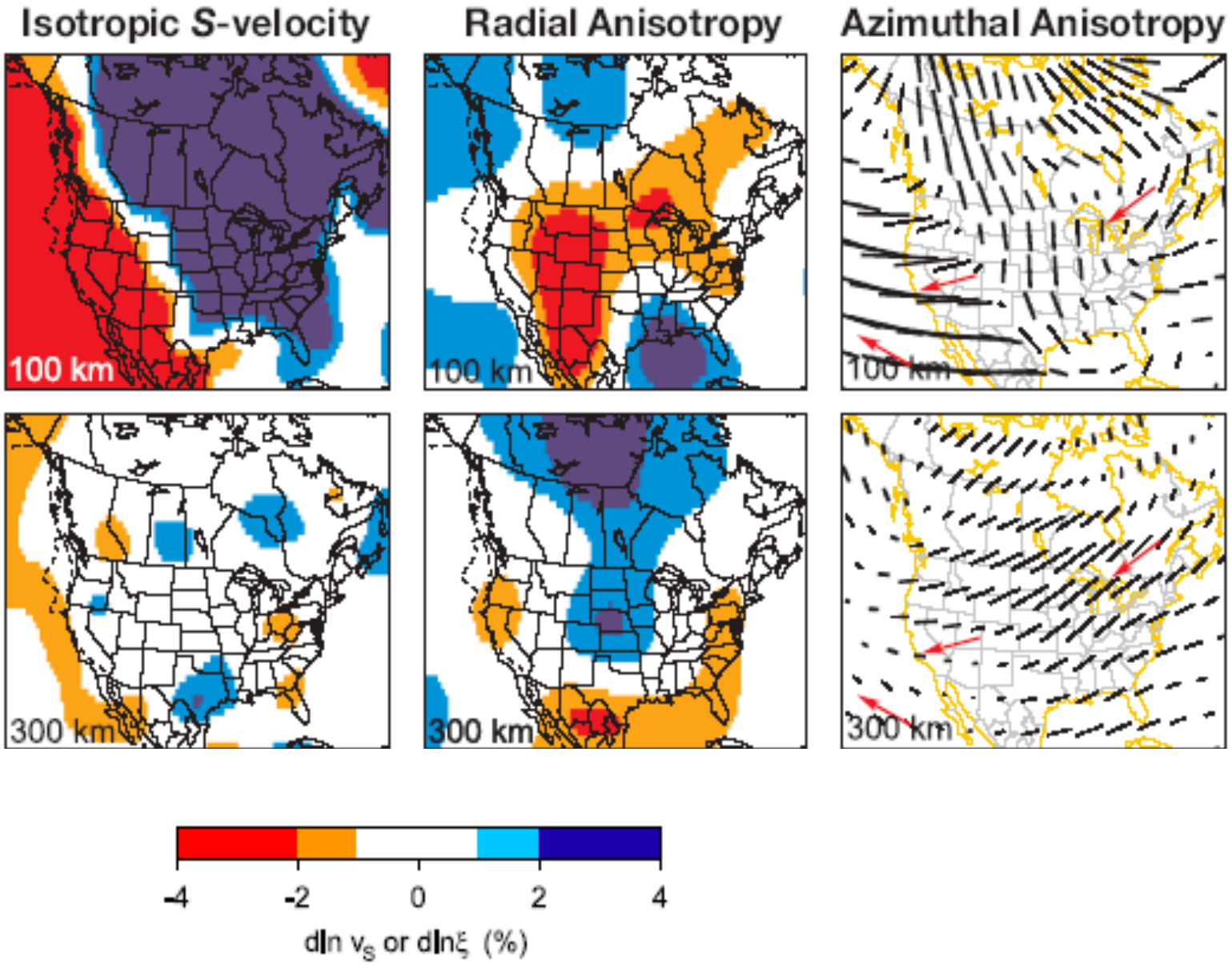

After Marone and Romanowicz (2007)

SKS splitting predictions compared to SKS splitting data

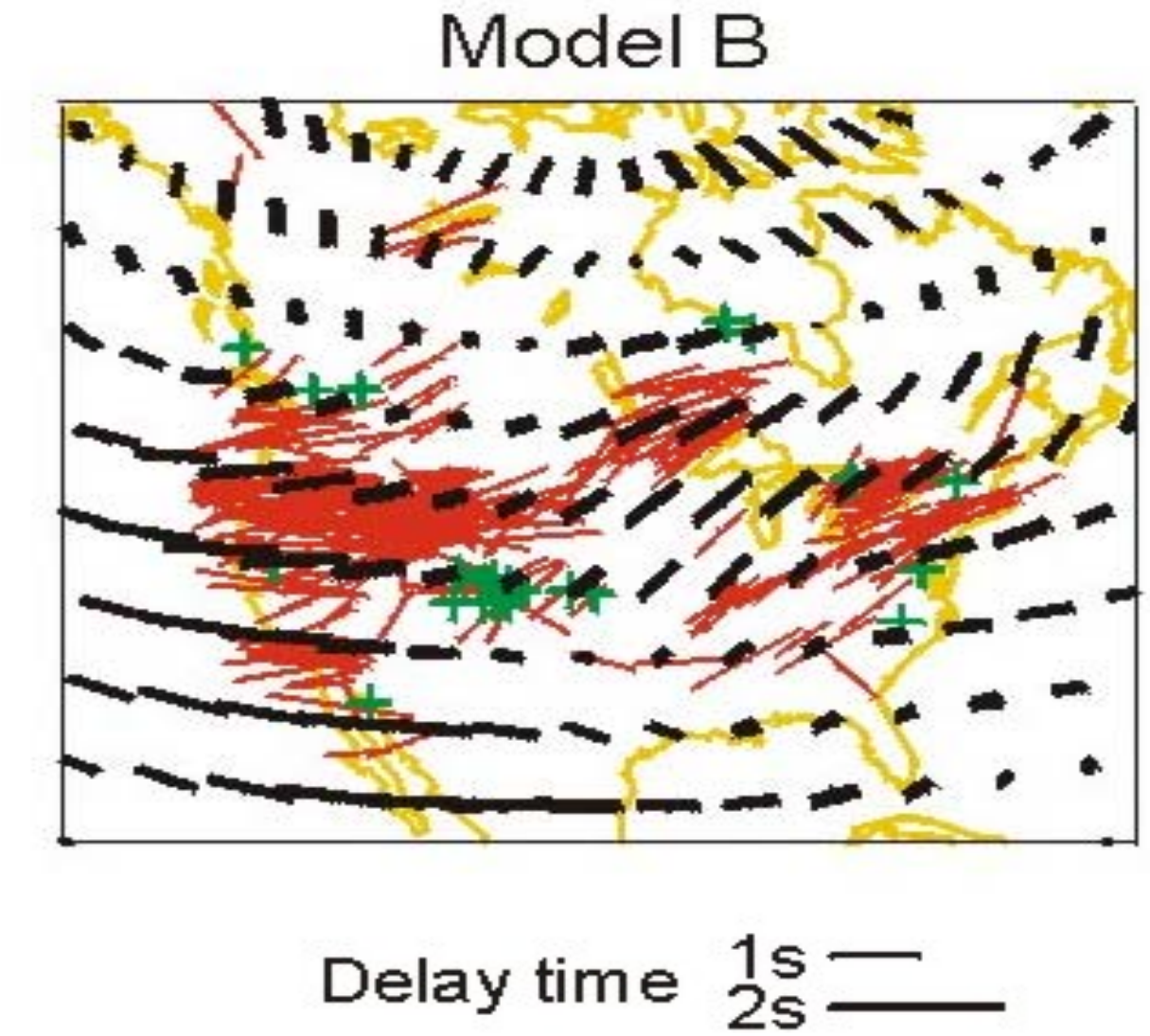

From: Marone and Romanowicz, Nature, 2007

Difference Continent -Ocean

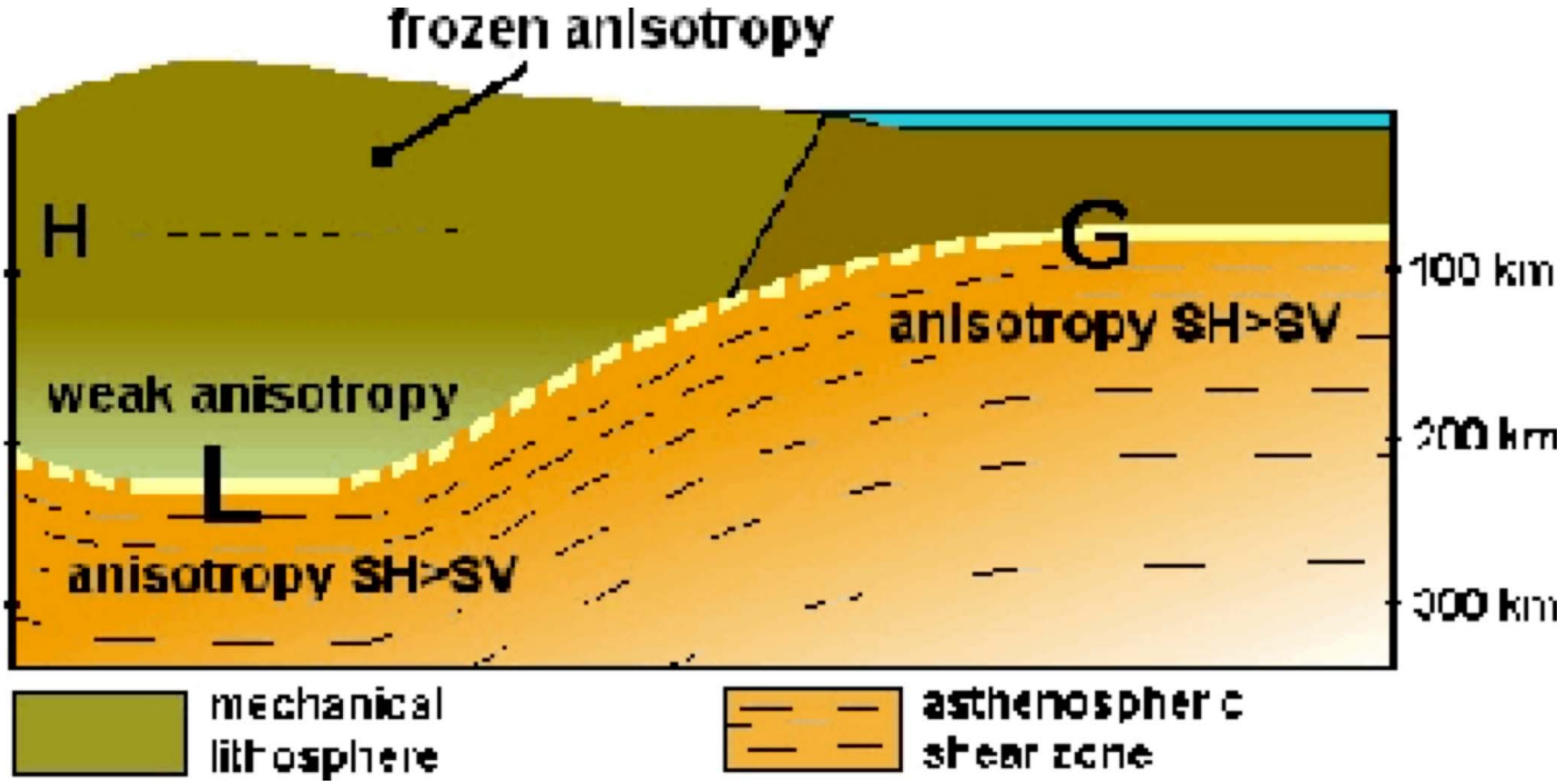

Gung & Romanowicz, (2003)

Hotspots - Plumes

EXPLANATION

- **Divergent plate boundaries—** Where new crust is generated as the plates pull away from each other.
- **Convergent plate boundaries—** Where crust is consumed in the Earth's interior as one plate dives under another.
- **Transform plate boundaries—** Where crust is neither produced nor destroyed as plates slide horizontally past each other.
- **Plate boundary zones—Broad** belts in which deformation is diffuse and boundaries are not well defined.
- **Selected prominent hotspots**

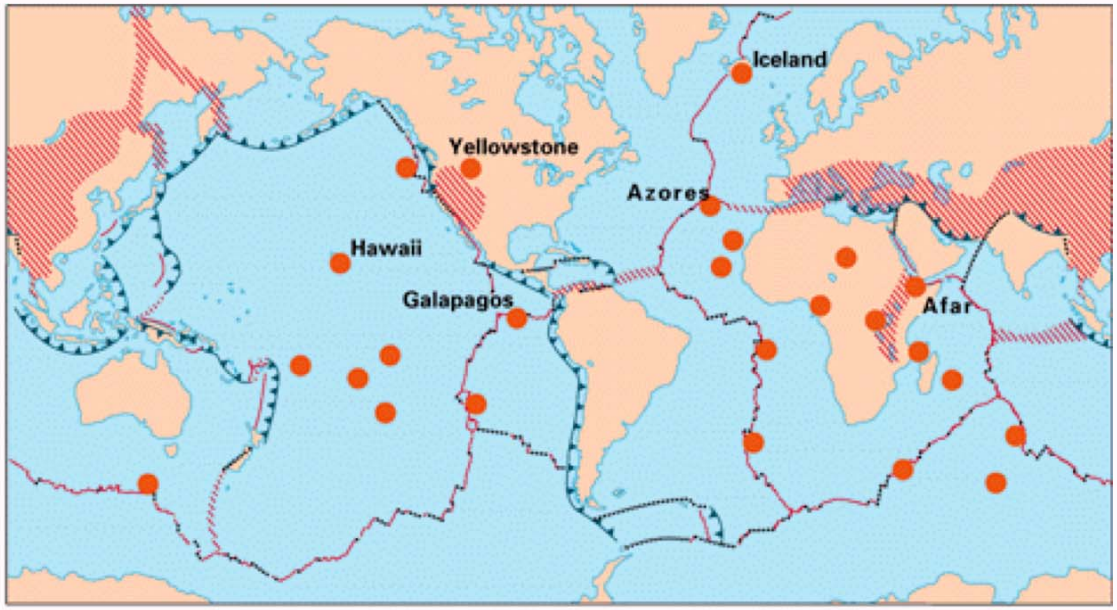

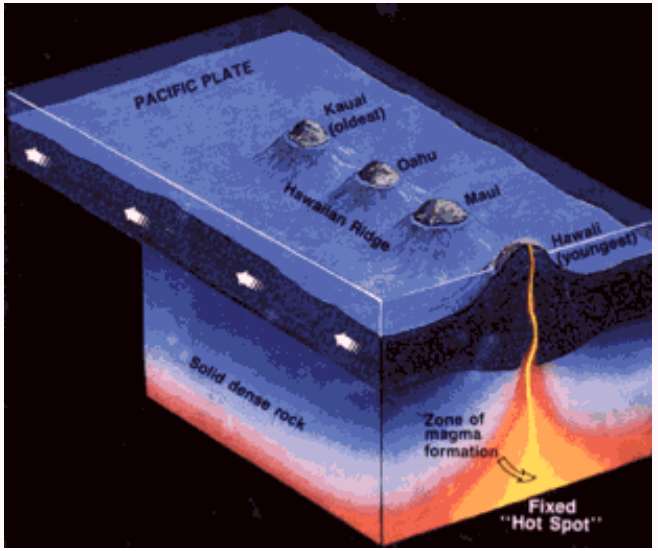

Classical Plume Model from Fluid dynamics(Nataf, 1999)

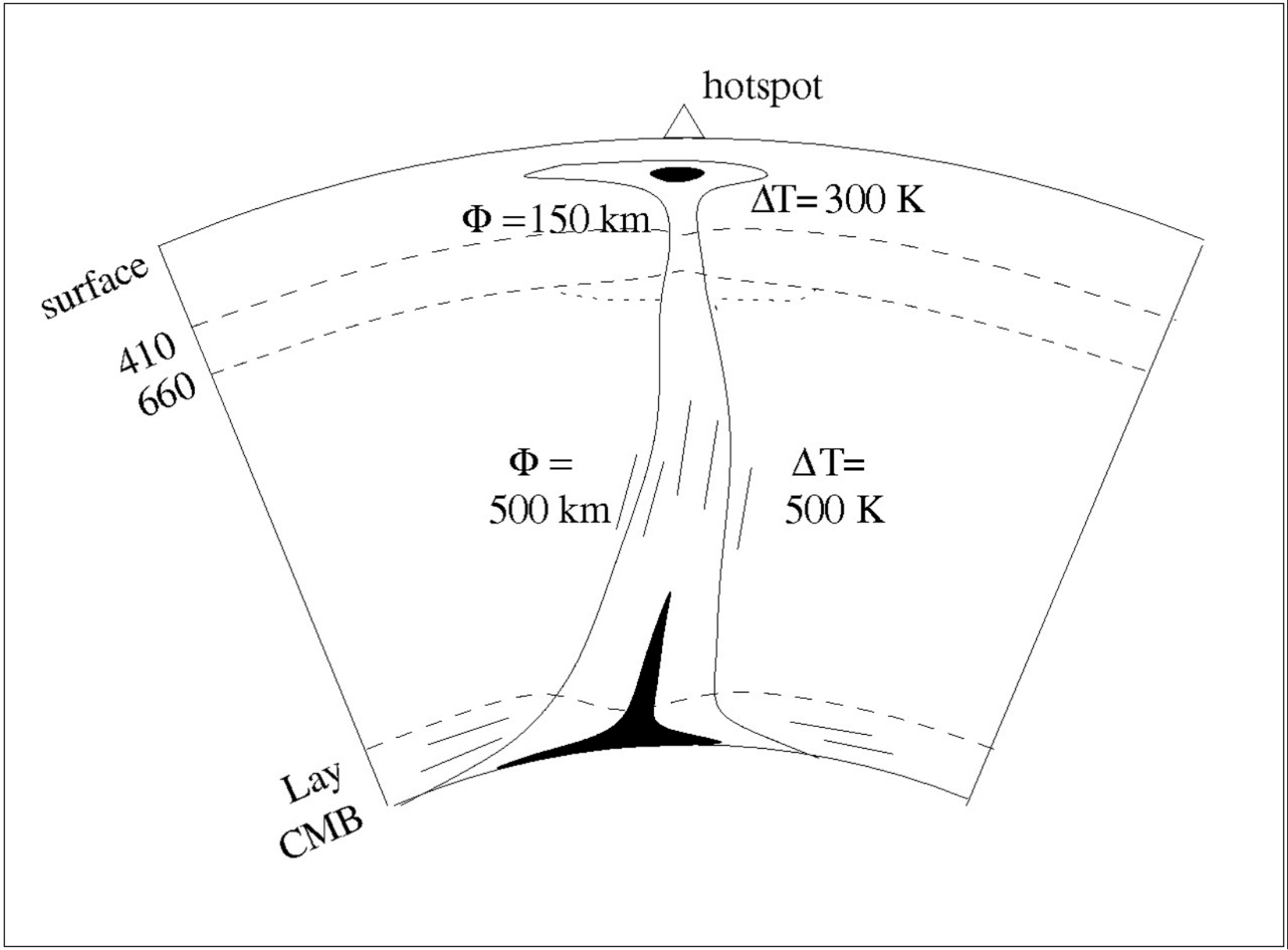

$H/\Phi \approx 20$ => at least 40 stations (2 per λ)

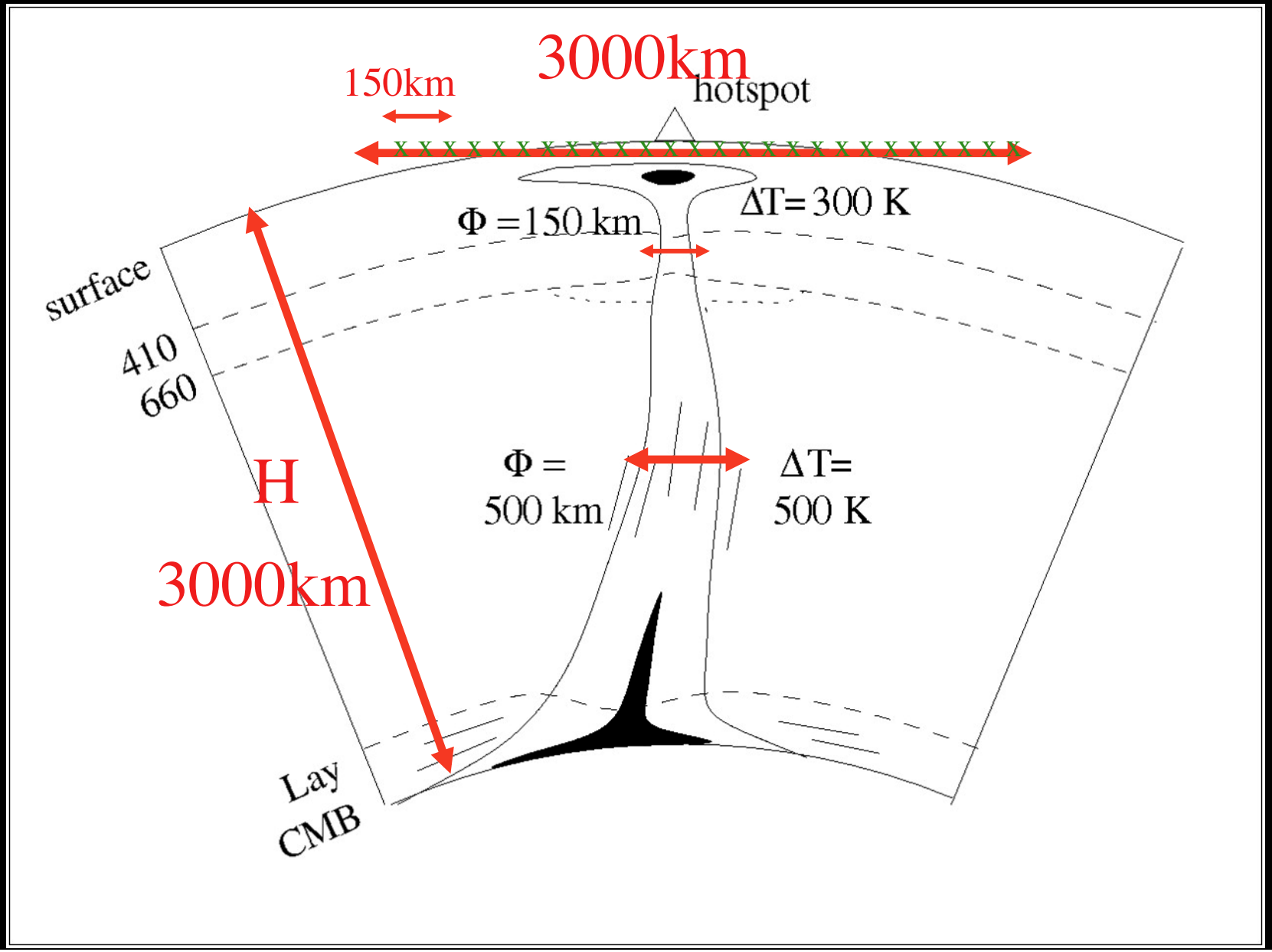

At least, 2 Competing models

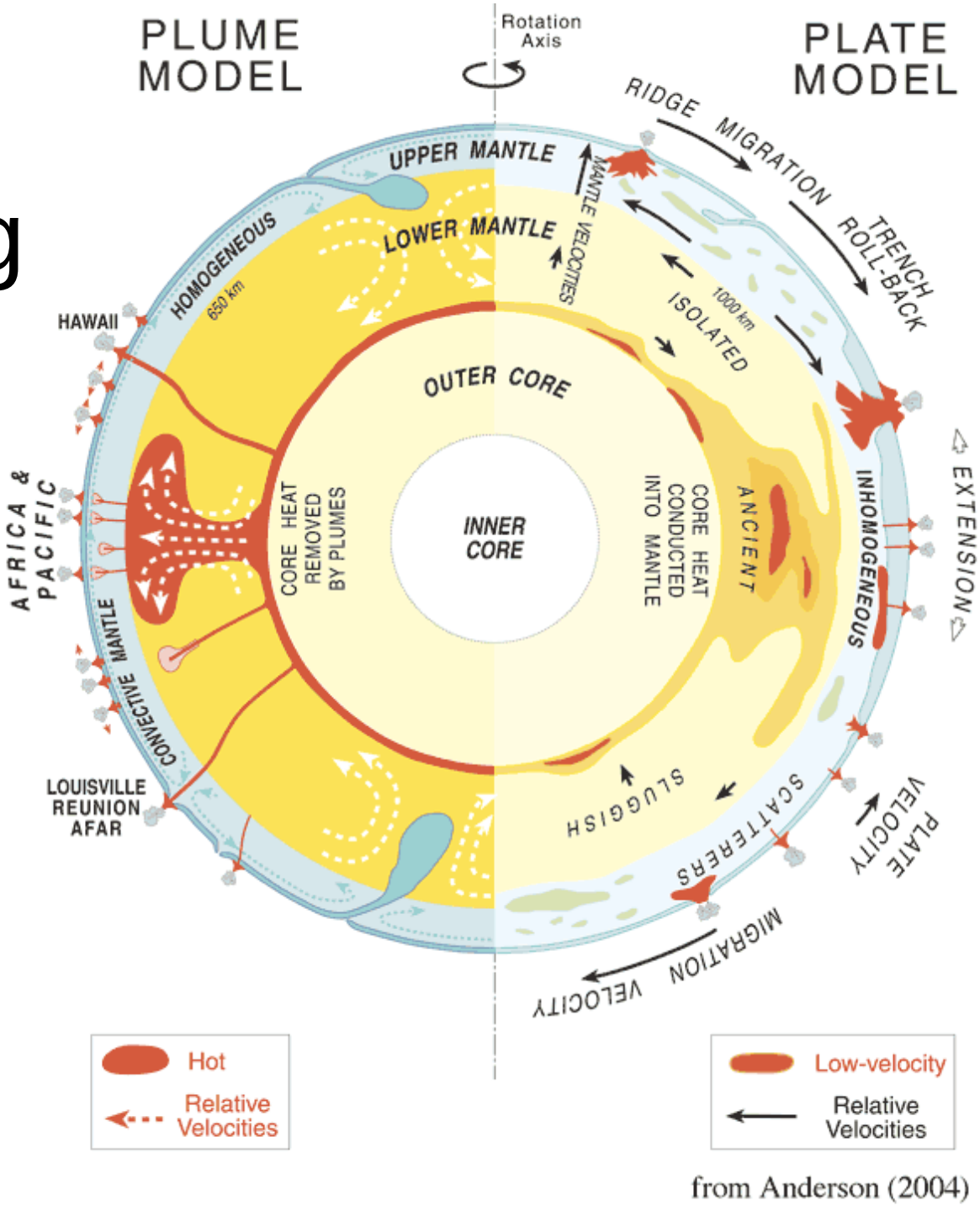

from Anderson (2004)

Definition of plume: thermal instability in a boundary layer:
- Core-mantle boundary
- Transition Zone (400-660- 1000km)?
- Asthenosphere- lithosphere?

But

-Is the plume model correct?
-What is their geodynamical role?
-What is their biological role?

-What is their structure, their origin at depth?

-Are there really several types of plumes?

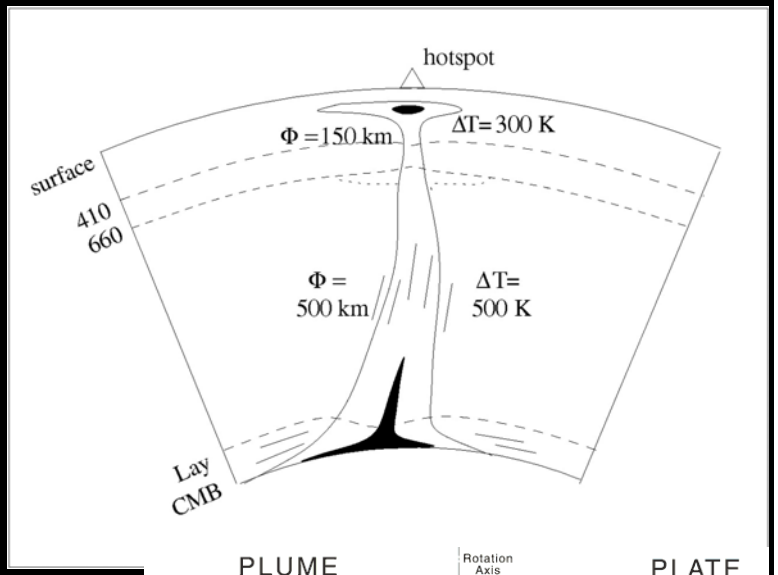

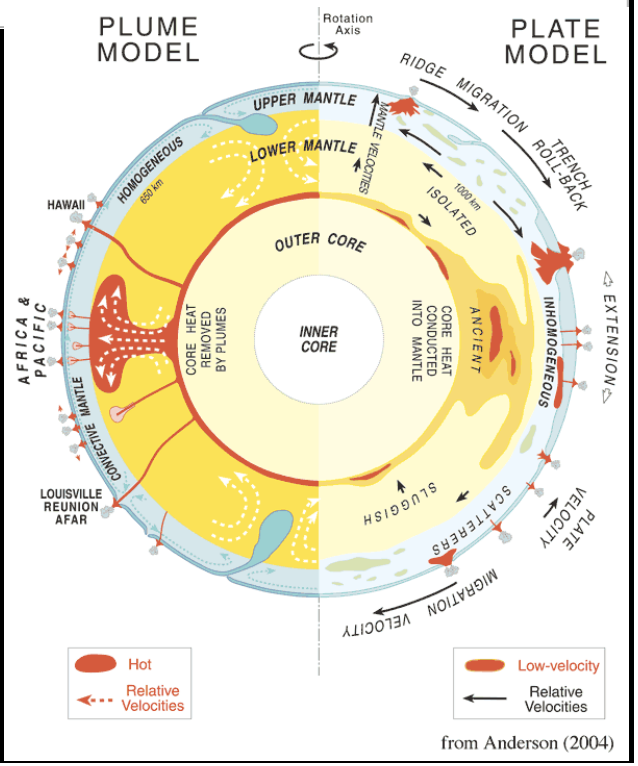

from Anderson (2004)

Detection of a Plume

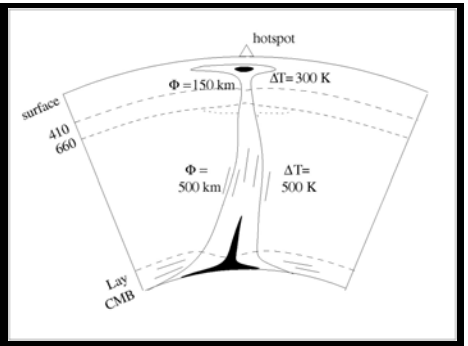

Expected Effects of Plume on seismic data

- Thermal effect: $\Delta T>0 \Rightarrow \delta V_S<0, \delta V_P<0$

- Upwelling flow =>crystal alignment by LPO

Weak azimuthal seismic anisotropy,

$V_{SV}>V_{SH}$ ($\xi<1$: radial seismic anisotropy)

- Large attenuation => low quality factor Q

- Thinning of the Transition zone thickness (410km deflected downward, 660km upward)

Global Scale

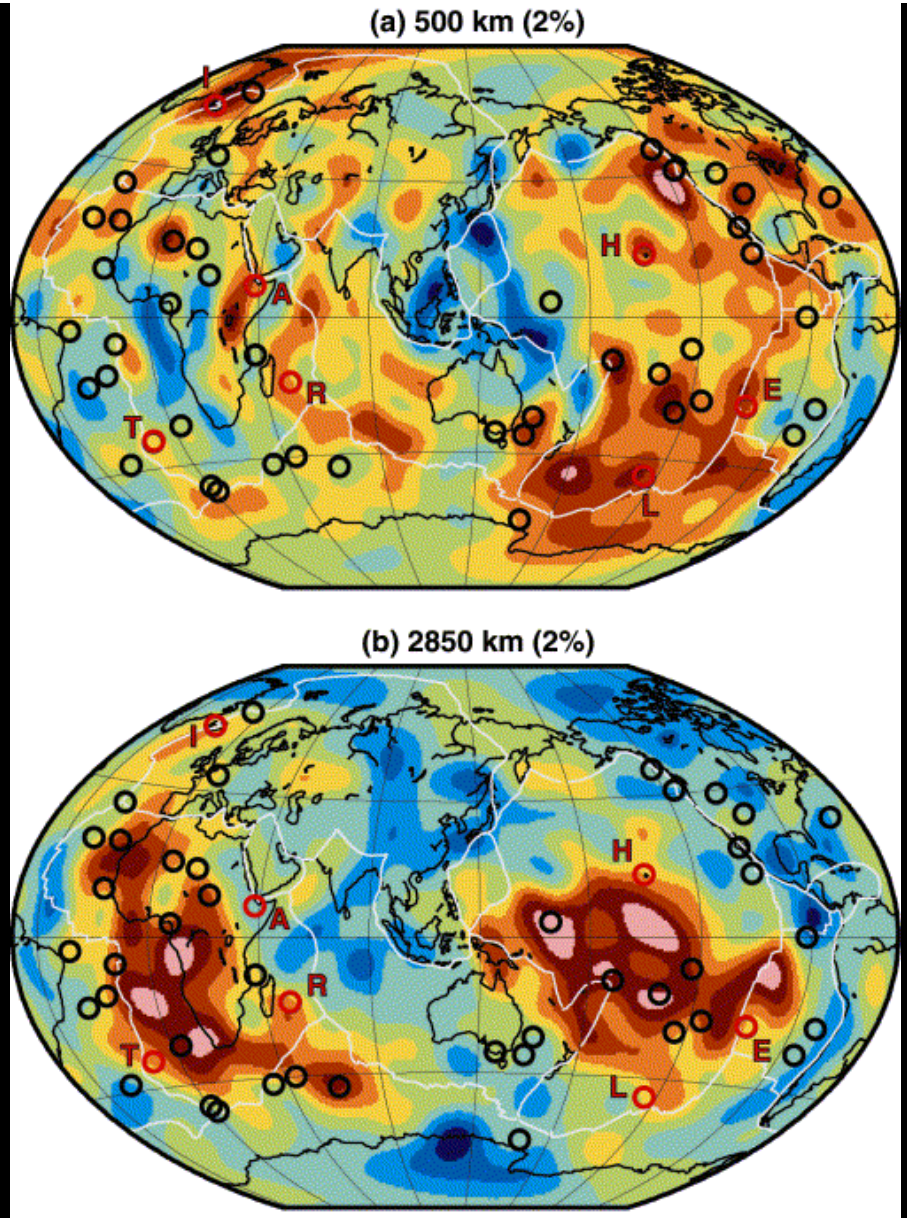

Ritsema et al., 2000

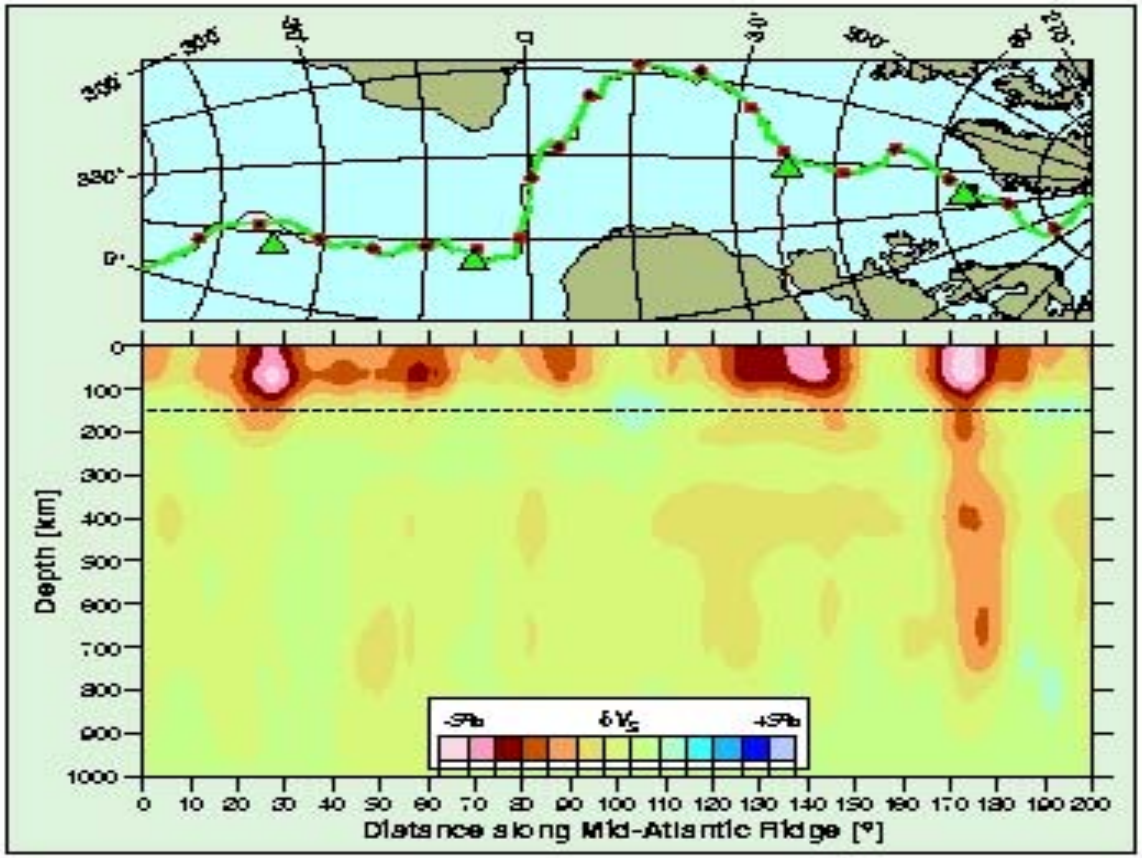

(Montagner and Ritsema, science, 2001)

From Banana-Doughnut Theory (Dahlen et al.)

Application to global tomography (Montelli et al., science, 2004)

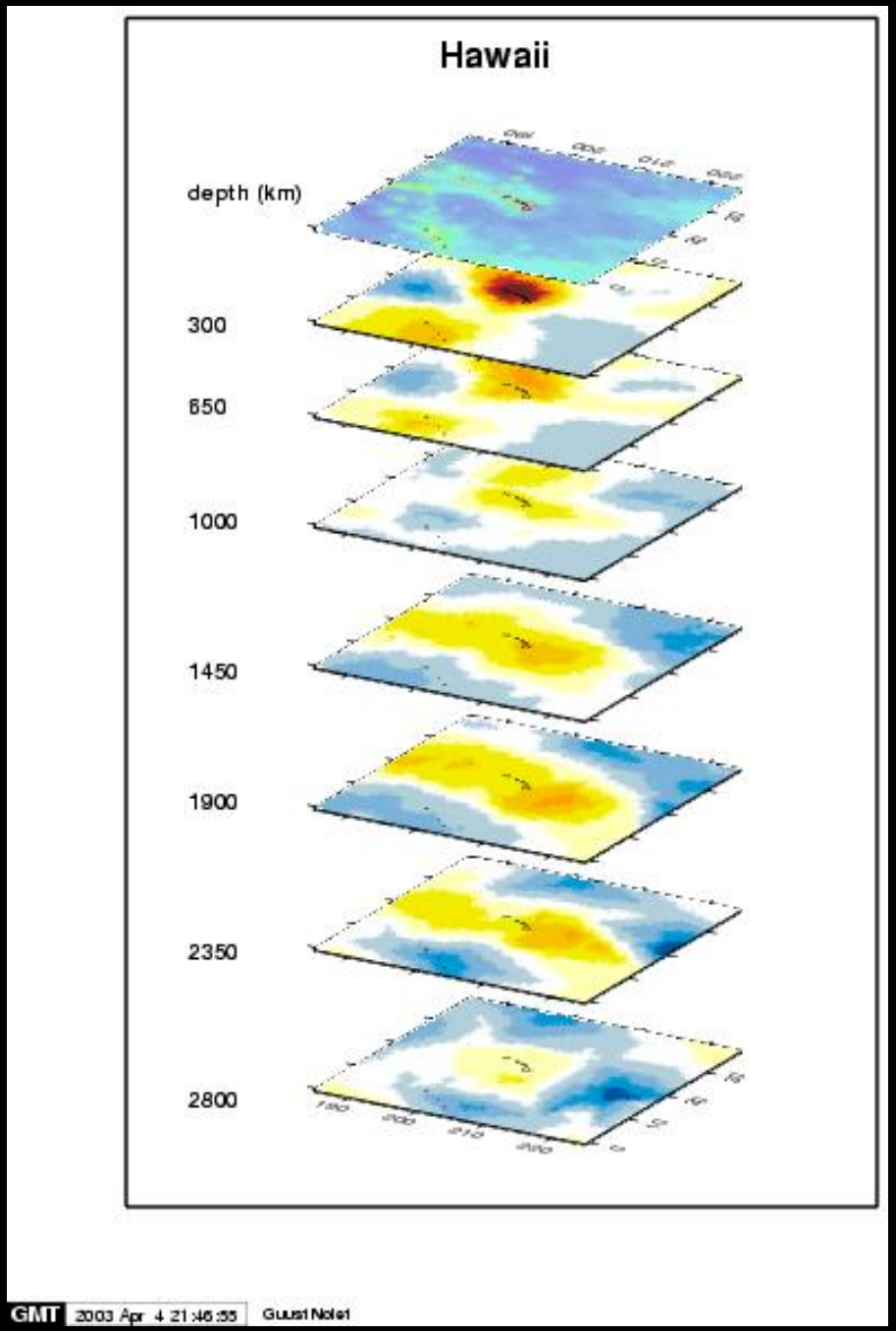

Hawaii plume (Wolfe et al., science, 2009)

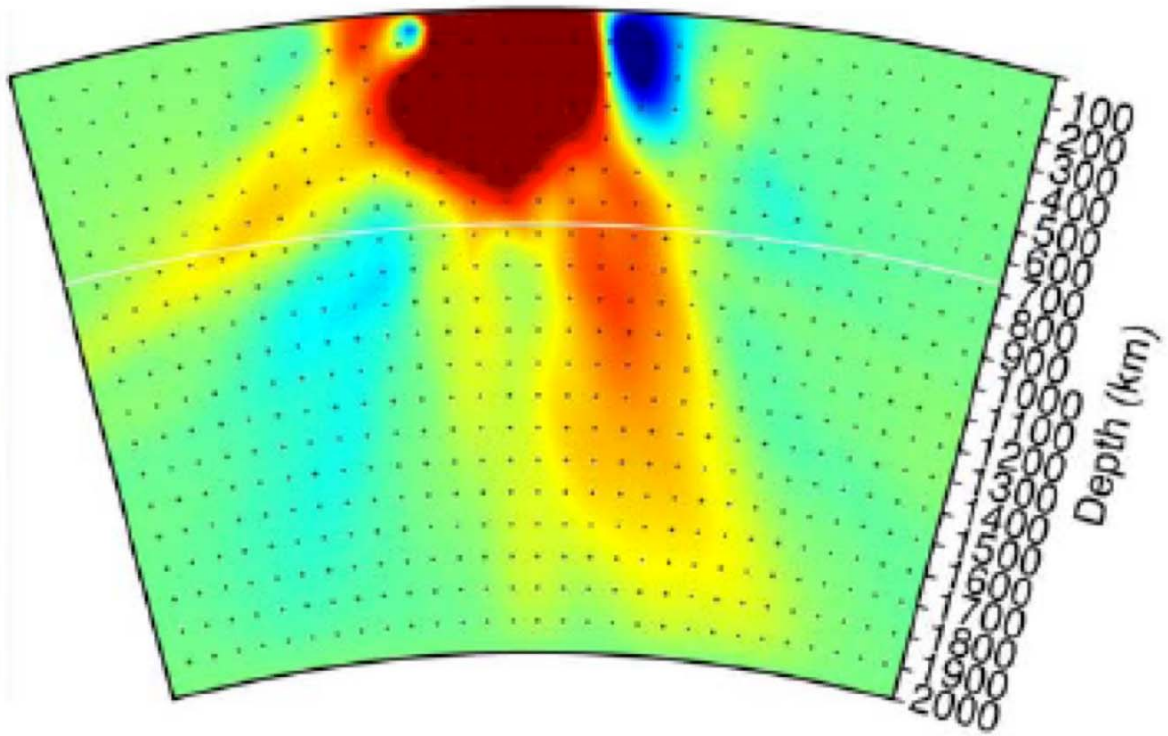

Complex Interaction of lithosphere, Asthenosphere and continents

Plume Detection - interaction with the upper mantle

Regional studies:

Pacific Ocean (Montagner, 2002; Maggi et al., 2006)

Horn of Africa (Debayle et al., 2001; Sebai et al., 2006; Montagner et al., 2007; Sicilia et al., 2008, Obrebski et al., 2010)

Anisotropy and Detection of Plume

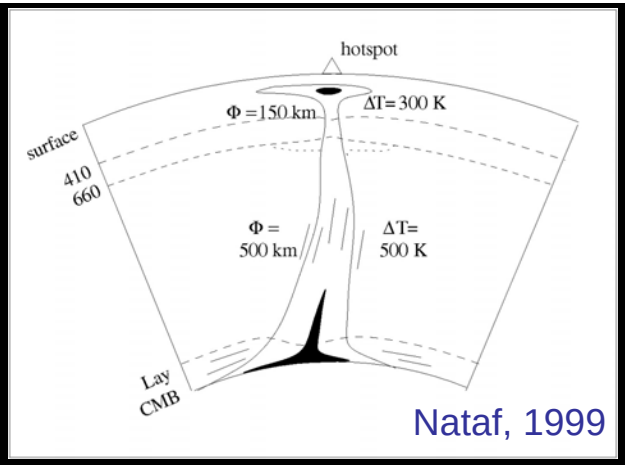

Nataf, 1999

Expected Effects of plume on seismic data in UM

- Thermal effect: $\Delta T>0$ => $\delta V_S<0$, $\delta V_P<0$

- Upwelling flow => crystals alignment by LPO
Weak azimuthal seismic anisotropy,
$V_{SV}>V_{SH}$ ($\xi<1$: radial seismic anisotropy)

- Large attenuation => low quality factor Q

- Thinning of the Transition zone thickness
(410km deflected downward, 660km upward)

Plume affects not only S-wave distribution but also seismic anisotropy

- Head: easy to detect

- Conduit: difficult to detect

$\Delta\alpha$: Anisotropic effect => V_{SV} ↗

ΔT: Température effect => V_{SV} ↘

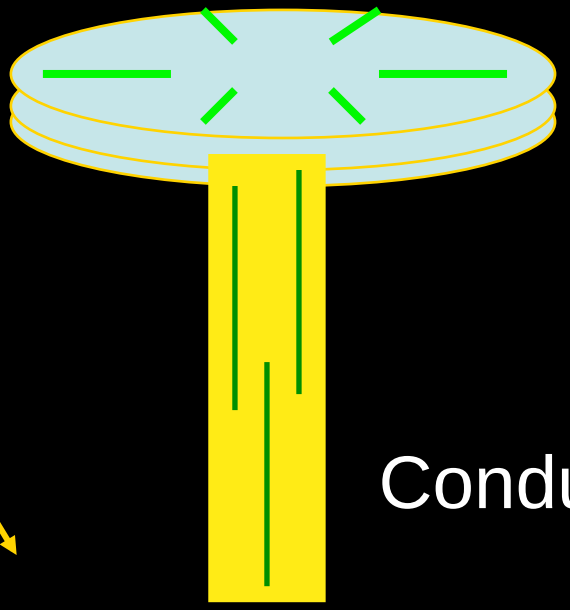

Opposite effects=> difficult to detect below asthenosphere

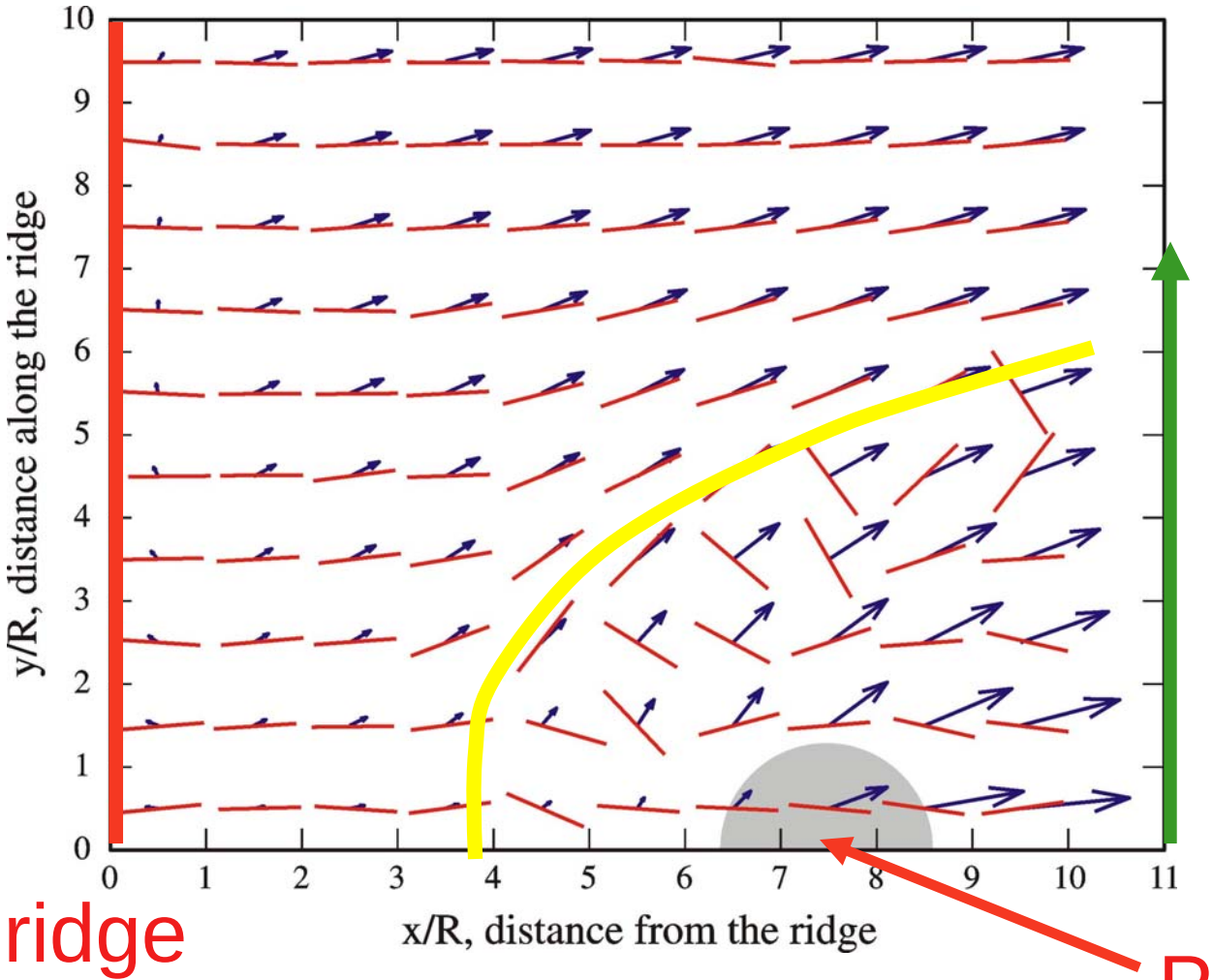

Azimuthal Anisotropy ➡ Indirect detection of plume (parabolic flow)

(Kaminski and Ribe, 2001)

Complex Interaction of upwellings with lithosphere, asthenosphere, or continent will affect the anisotropy distribution

Continents

Horn of Africa

(Debayle et al., 2001;
Sebai et al., 2006;
Montagner et al., 2007
Sicilia et al., 2008
Obrebski et al., 2010)

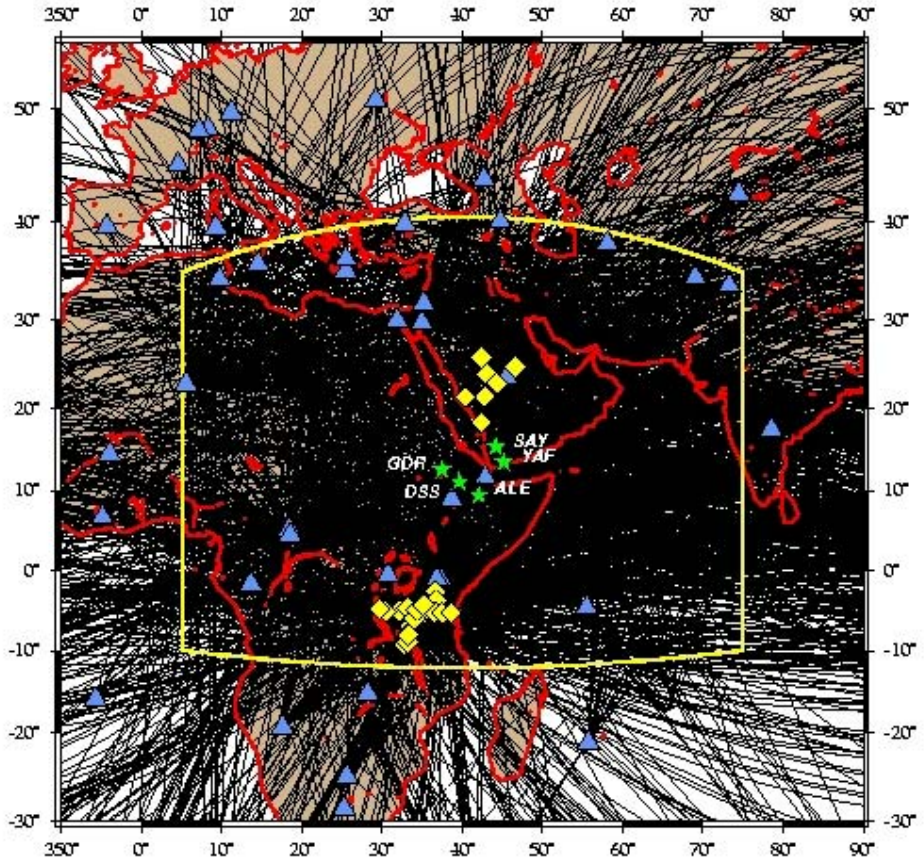

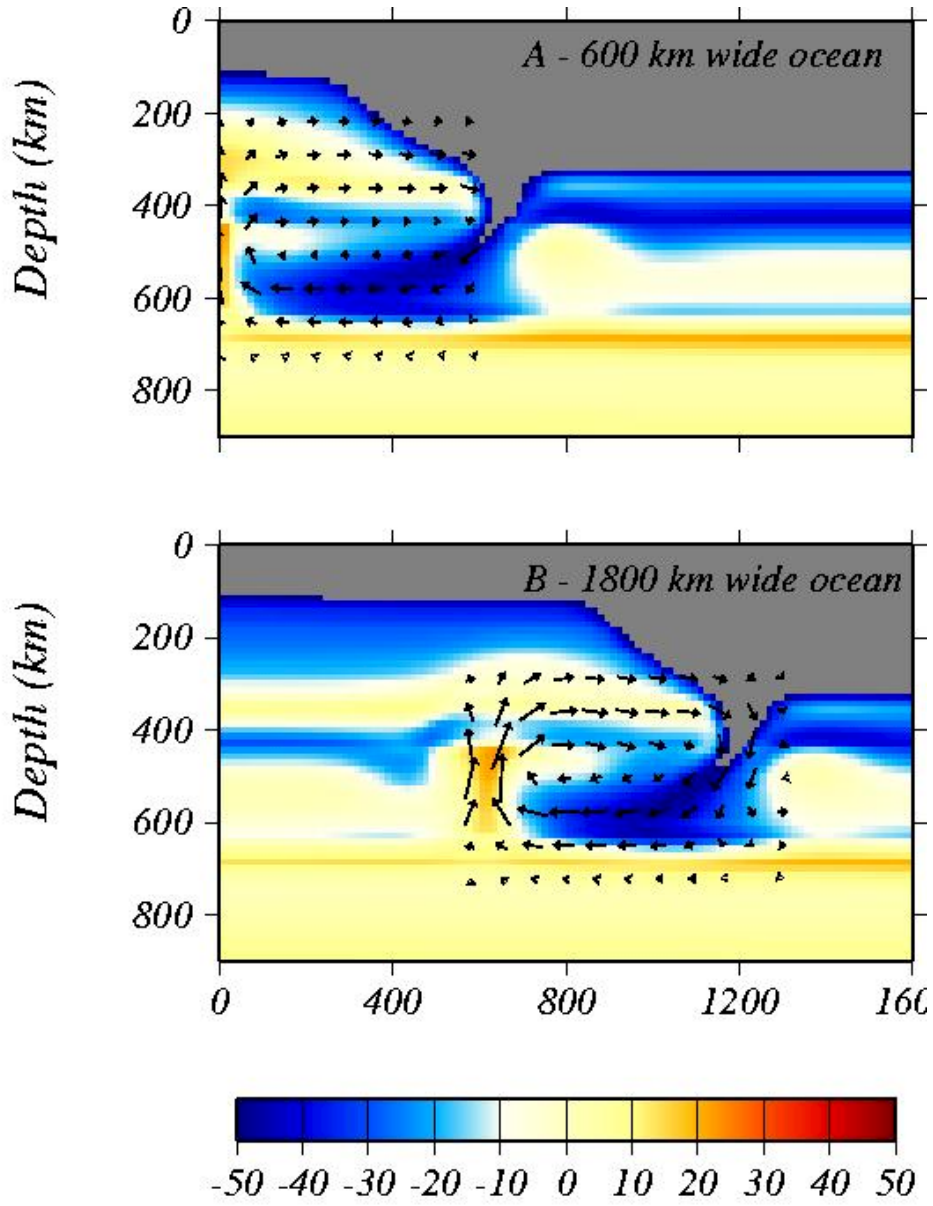

King & Ritsema, 1999

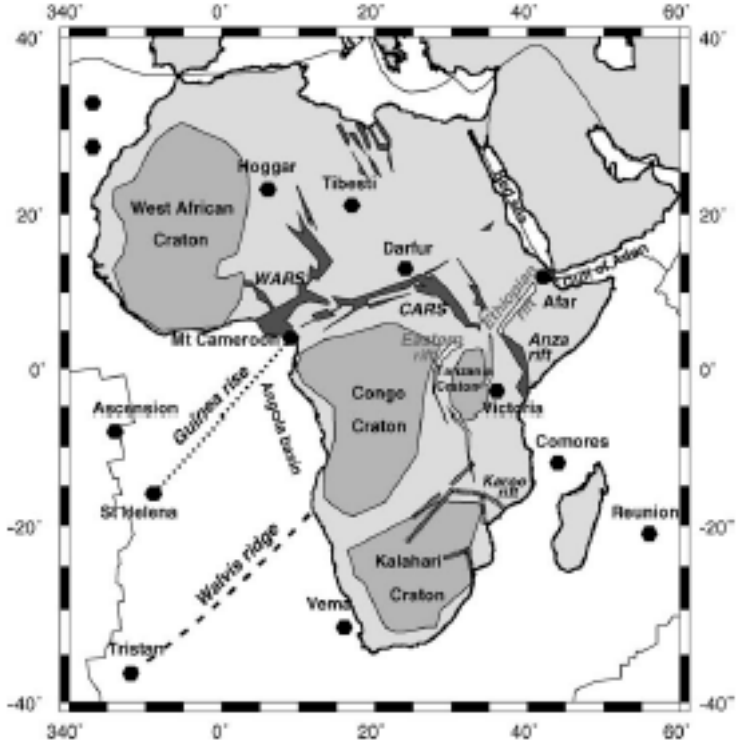

Sebai et al., 2006

(Sebai et al., 2006)

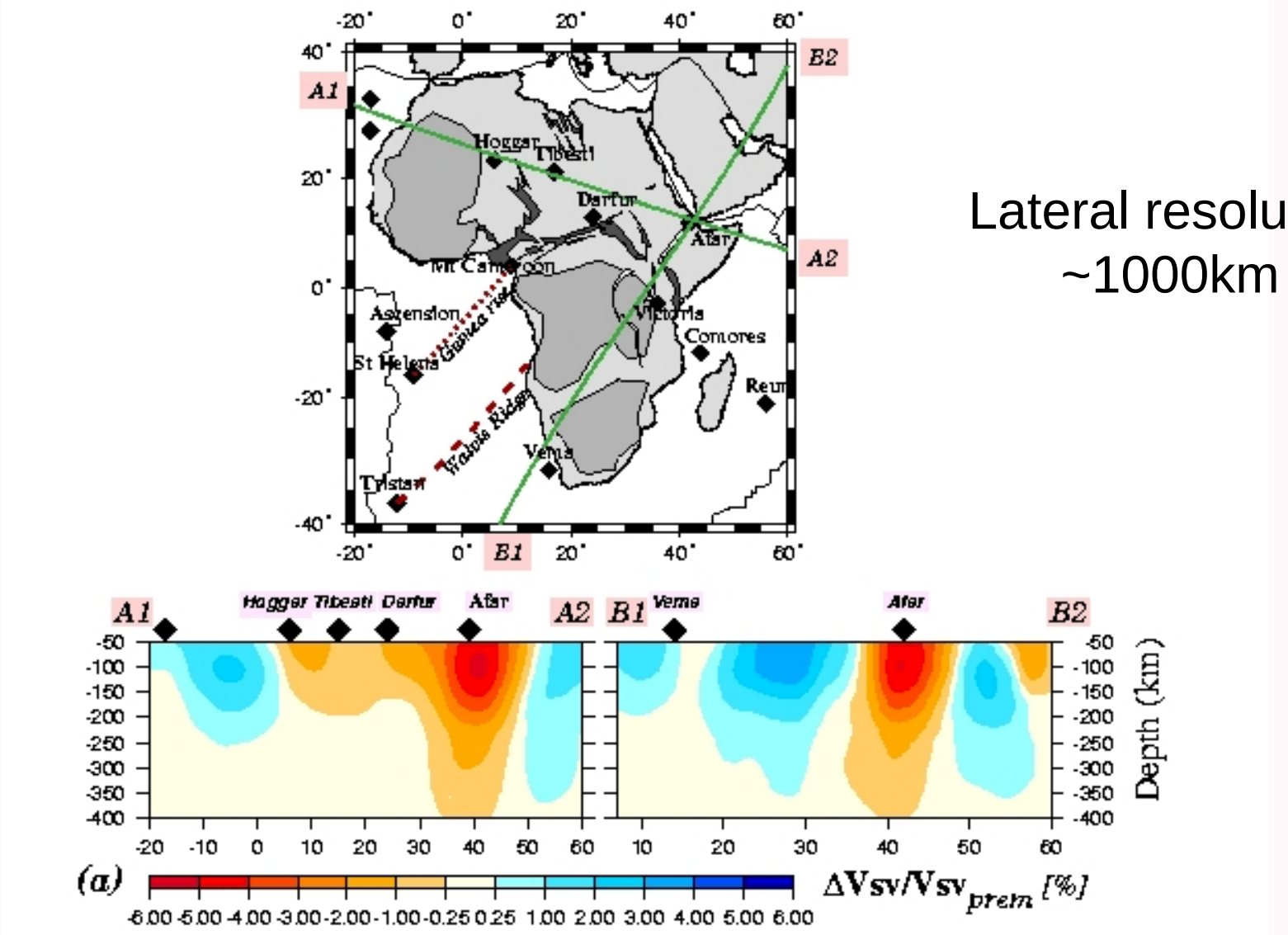

Lateral resolution
~1000km

G azimuthal anisotropy
$\Delta\xi$ radial anisotropy (Sicilia et al., 2008)

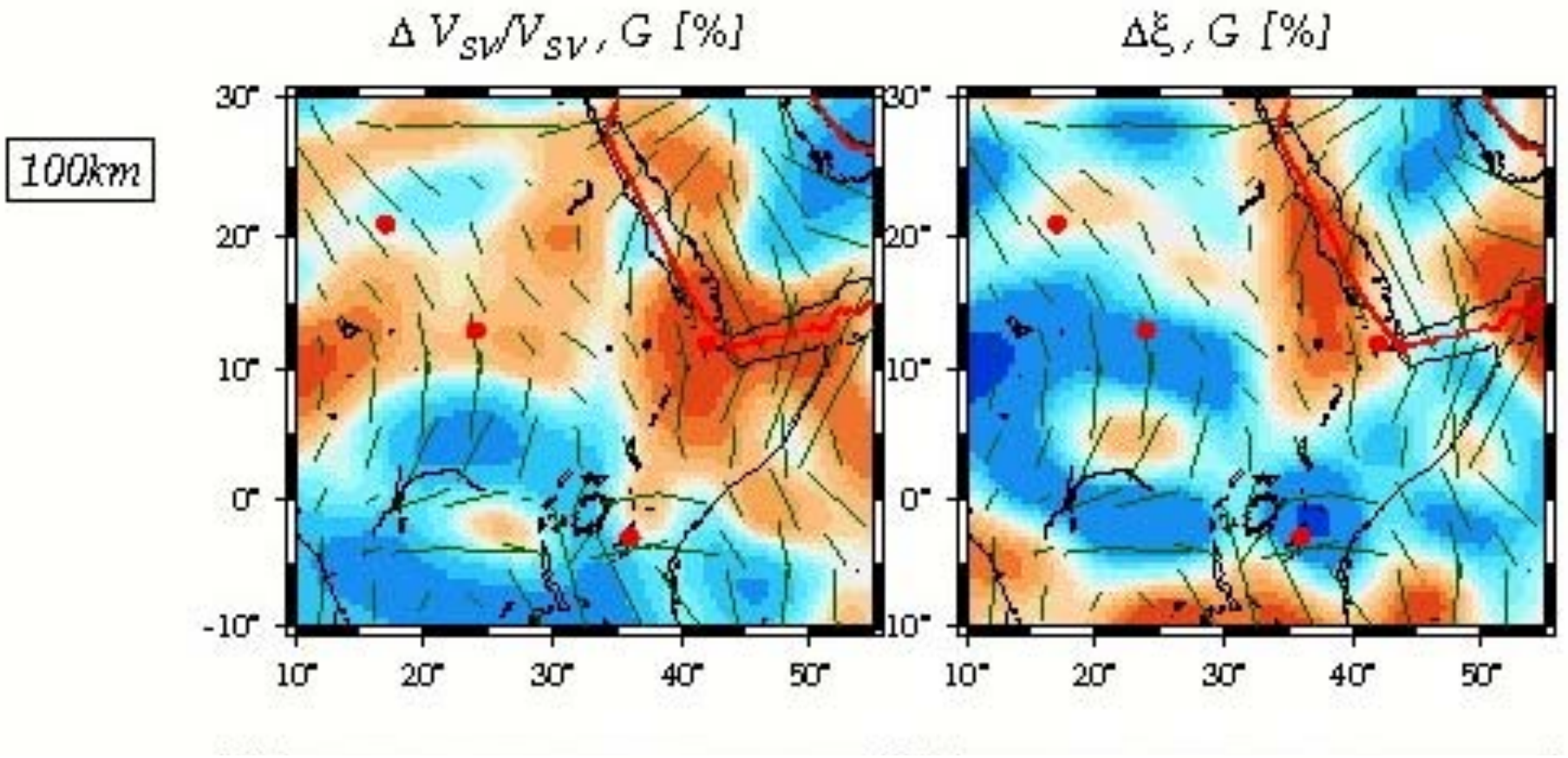

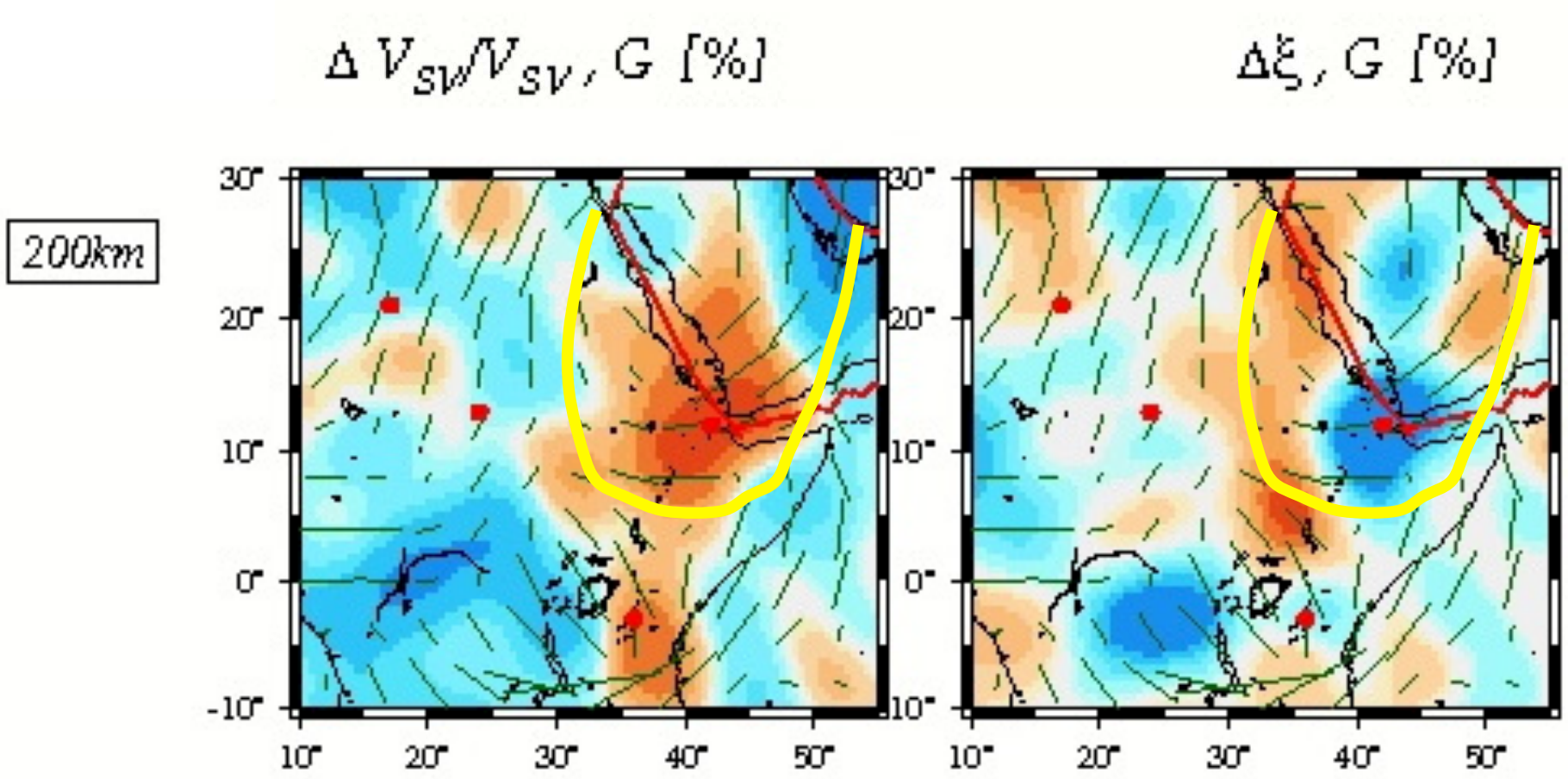
200km
$\Delta V_{SV}/V_{SV}$, G [%]
$\Delta\xi$, G [%]
30°
20°
10°
0°
-10°
10°
20°
30°
40°
50°

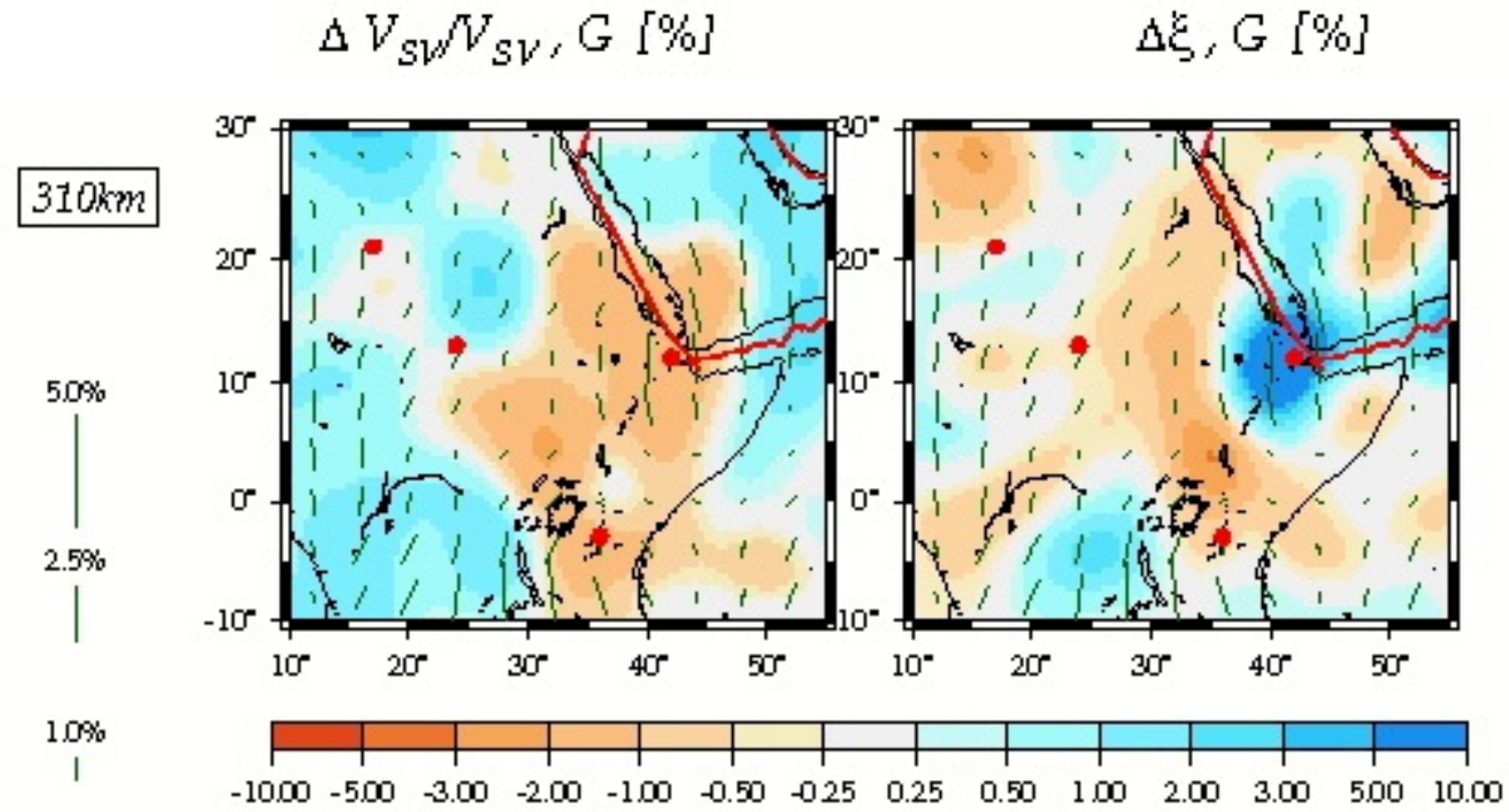
$\Delta V_{SV}/V_{SV}$, G [%]
$\Delta\xi$, G [%]
310km
5.0%
2.5%
1.0%
30°
20°
10°
0°
-10°
10°
20°
30°
40°
50°
-10.00
-5.00
-3.00
-2.00
-1.00
-0.50
-0.25
0.25
0.50
1.00
2.00
3.00
5.00
10.00

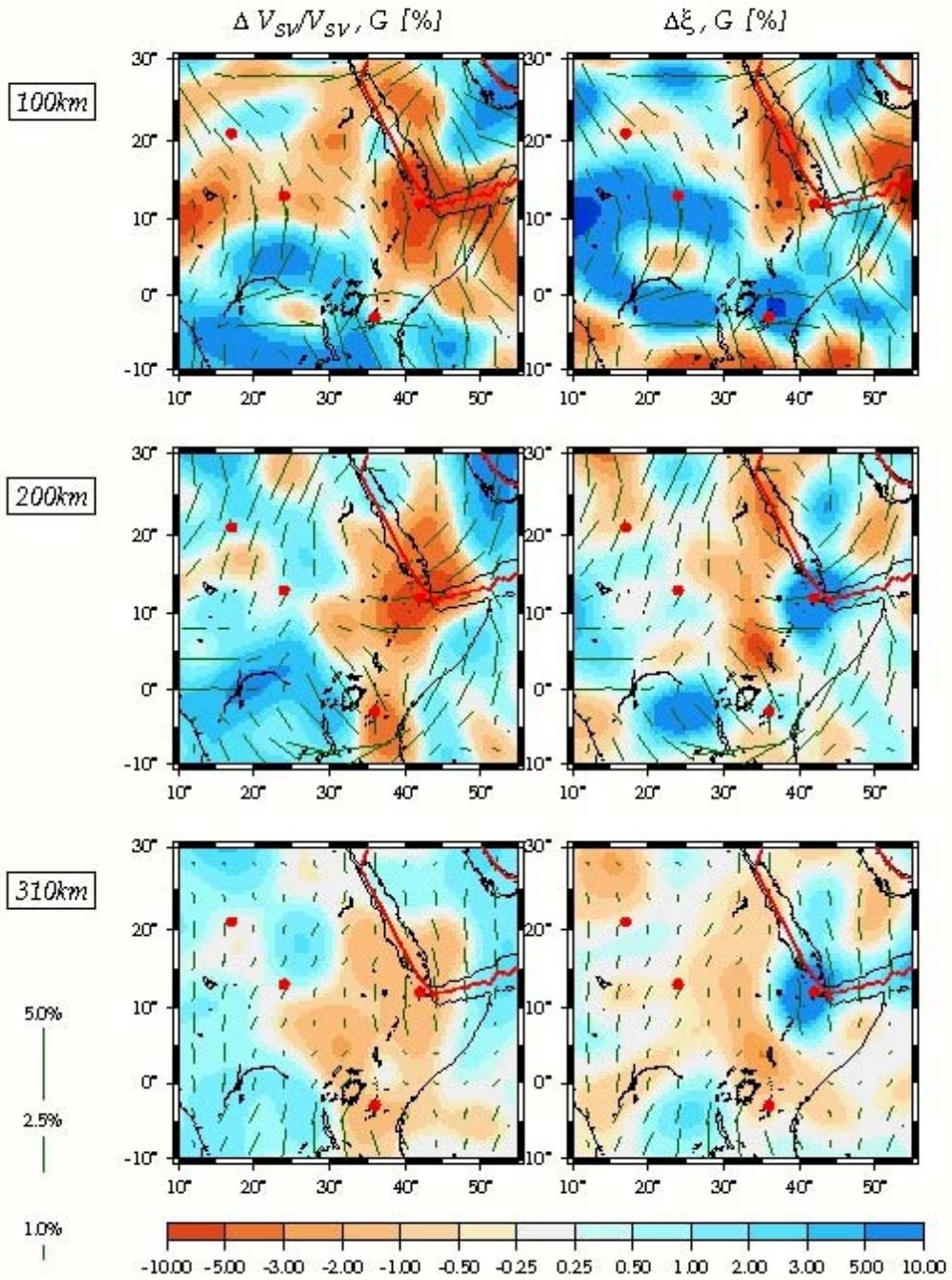

3D- Anisotropy Tomography of Eastern Africa

- Parabolic flow around Afar
- Stratification of Anisotropy: >3 layers in Eastern Africa

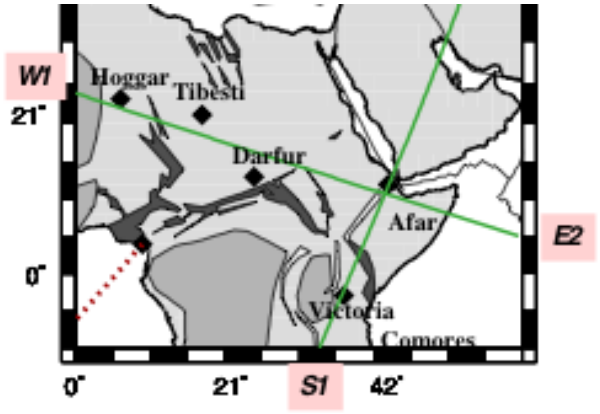

E-W

N-S

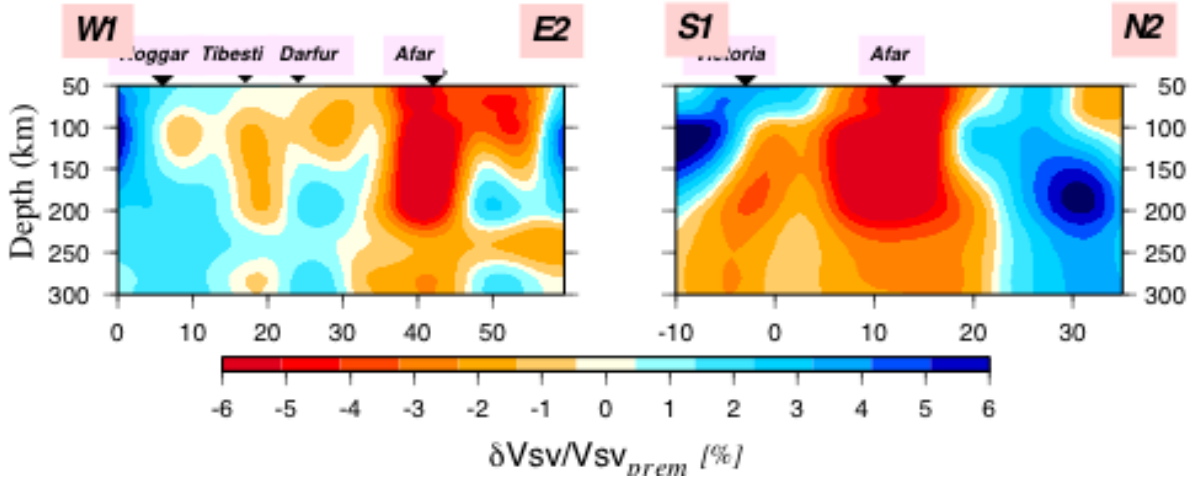

S-Velocity

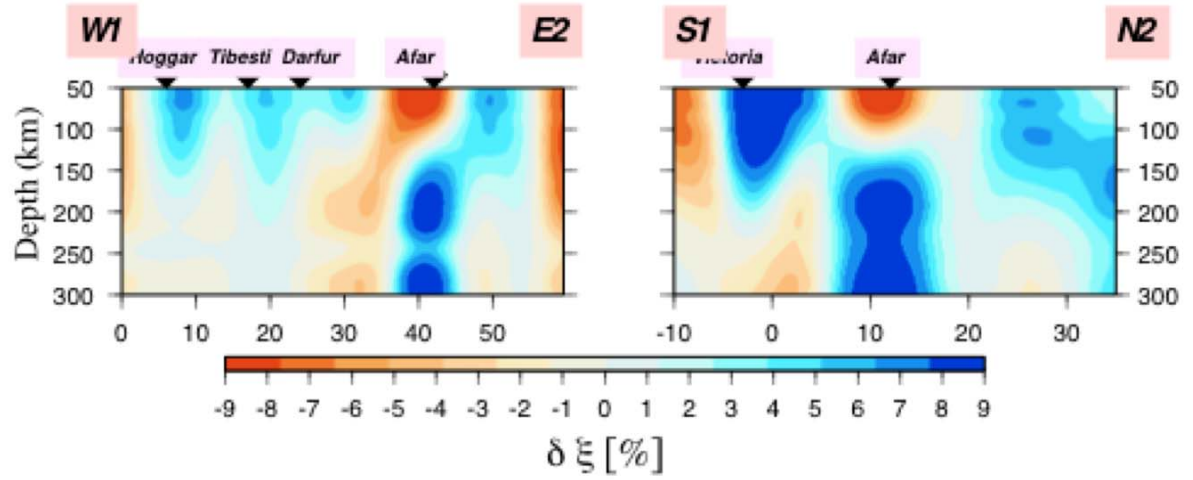

dξ Radial Anisotropy

Geodynamic Interpretation

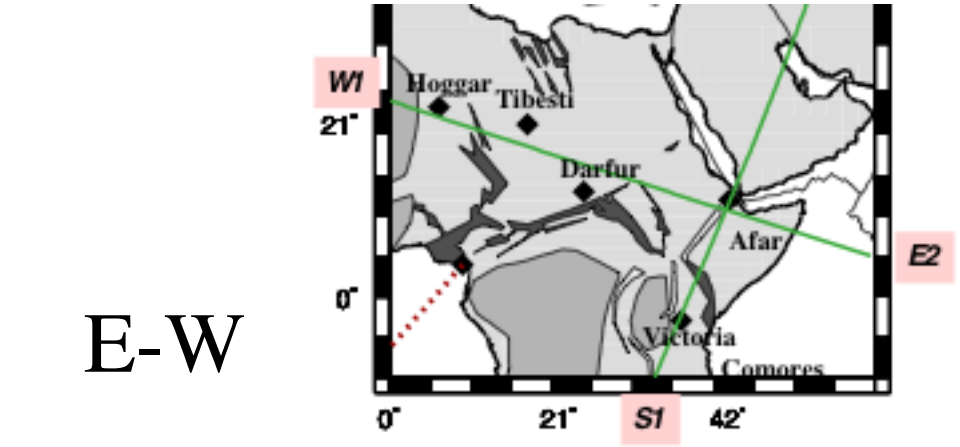

E-W

N-S

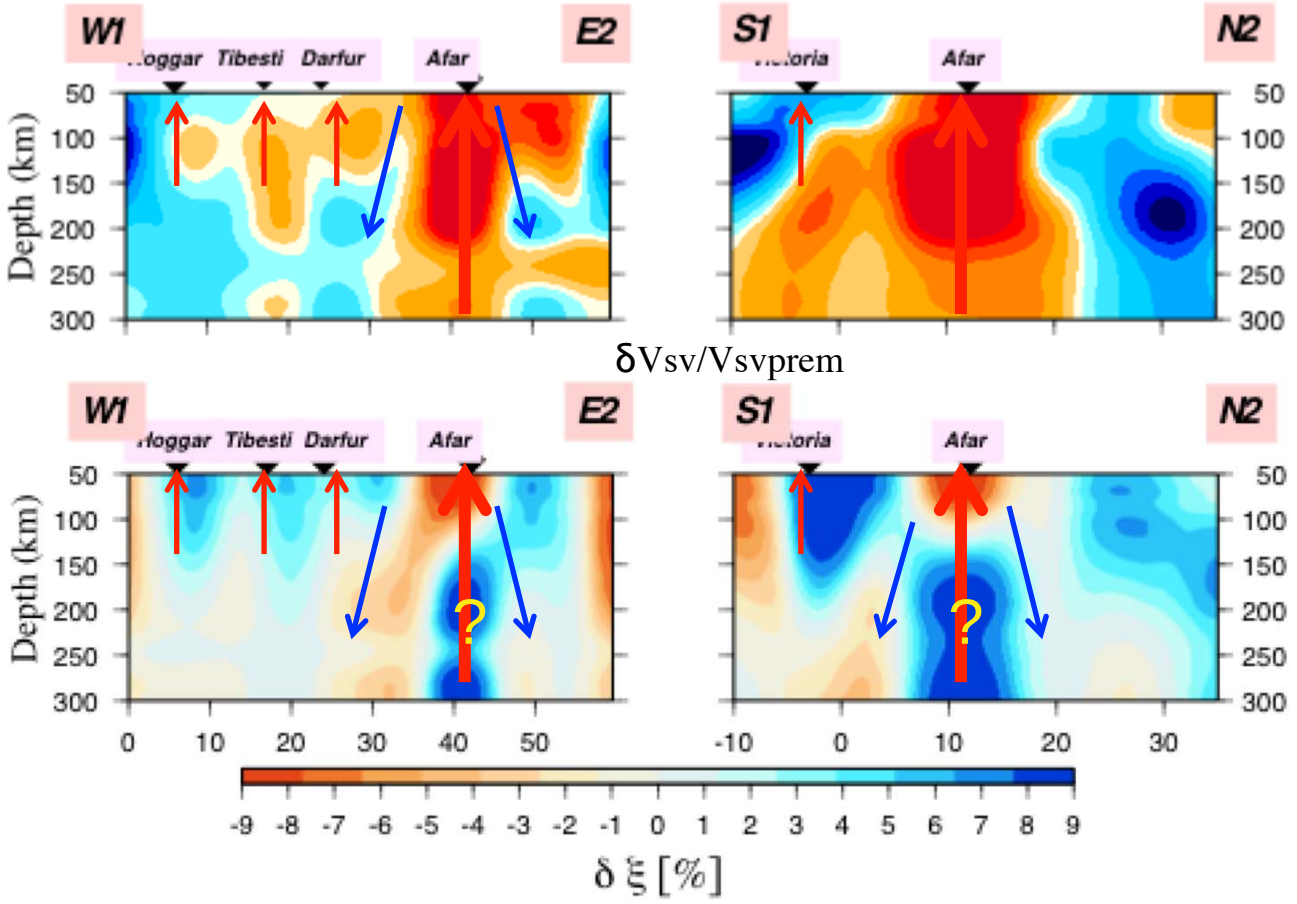

Stratification of anisotropy

Convective Instabilities (~1000km)

Water?

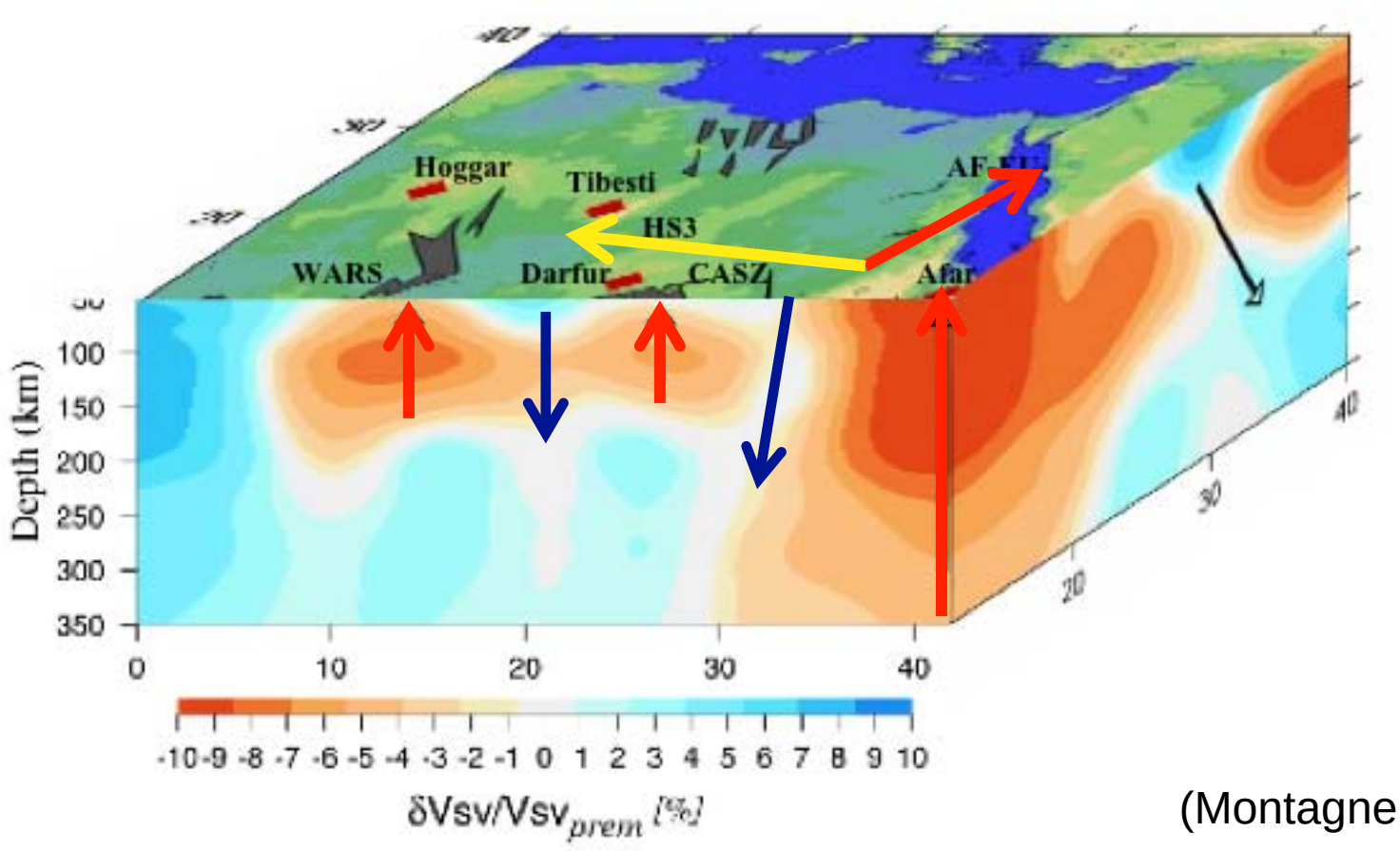

(Montagner et al., 2007)

2 kinds of Plumes

Stratification of anisotropy (>3 layers)

Secondary Convection below lithosphere λ~1000km ?

Geochemical data Helium (B. Marty, R. Pik)

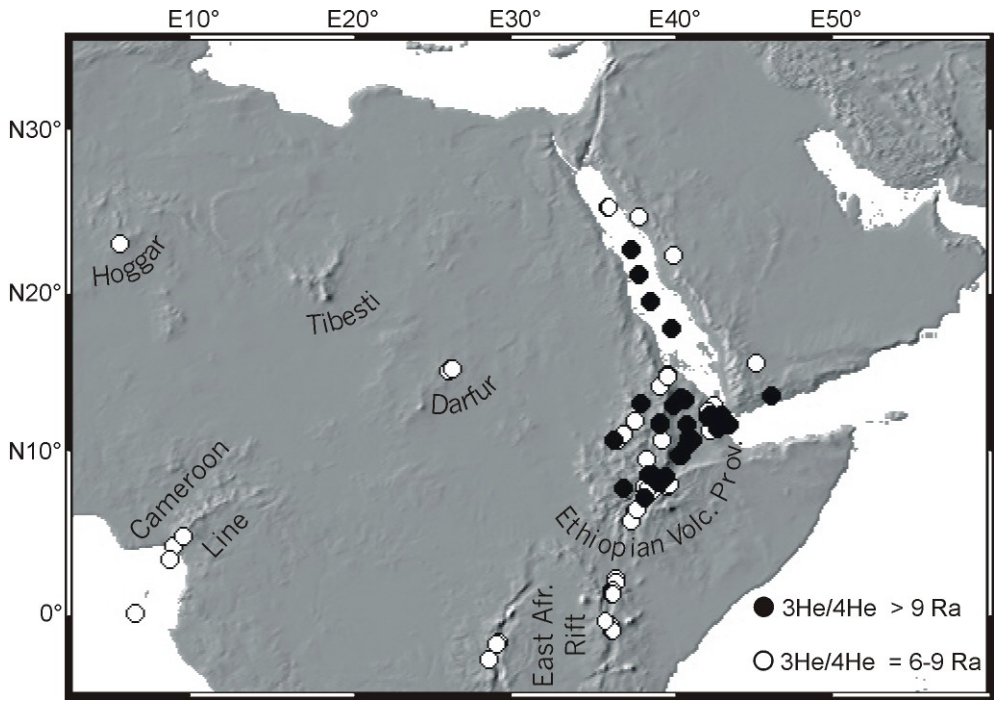

How to retrieve the Stratification of anisotropy in the upper mantle?

-Surface waves

Good vertical resolution, bad lateral resolution

- SKS data

interpretation of SKS splitting data?

1 delay time δt, 1 angle Ψ: bad vertical resolution

Several layers: Silver, Savage, Wolfe, Rumpker…

- Receiver function (R.F.)

Joint inversion of SKS and R.F. data

(Vinnik et al., 2007)

Joint inversion of SKS and receiver functions

(M. Obrebski, S. Kiselev, L. Vinnik, J.P. Montagner)

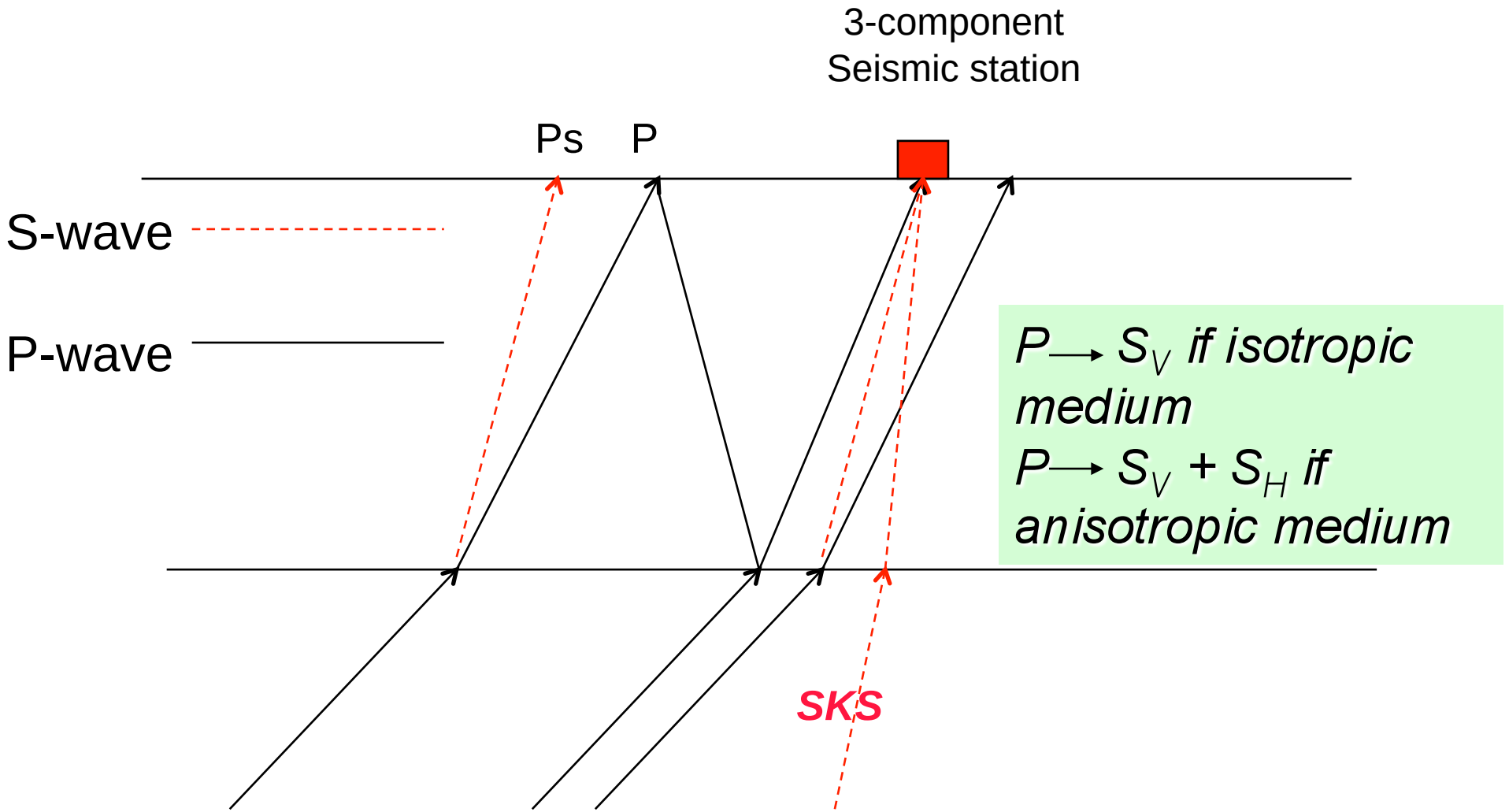

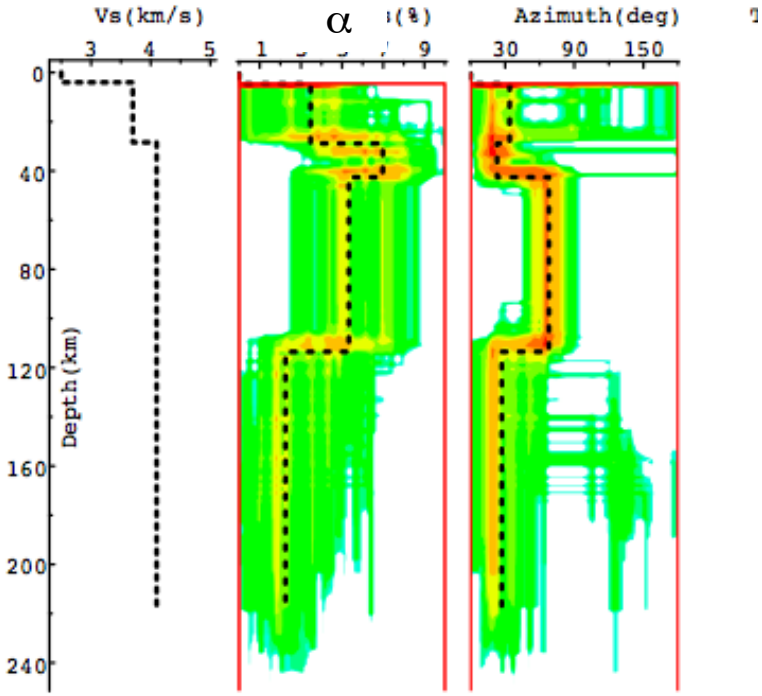

ATD Geoscope Station (Djibouti)

RF

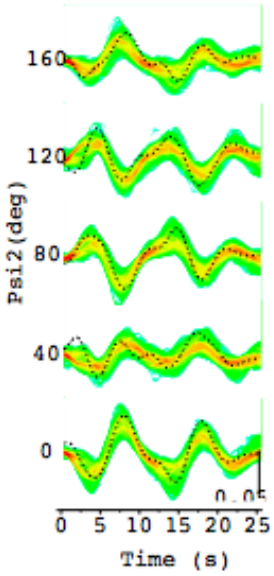

SKS

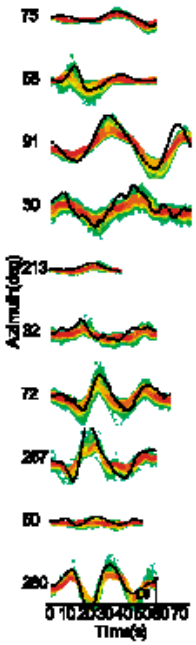

Receiver functions (RF)
+
SKS

Good Azimuthal Coverage

Obrebski et al., JGR 2010

Simultaneous inversion of SKS and receiver functions

ATD Station

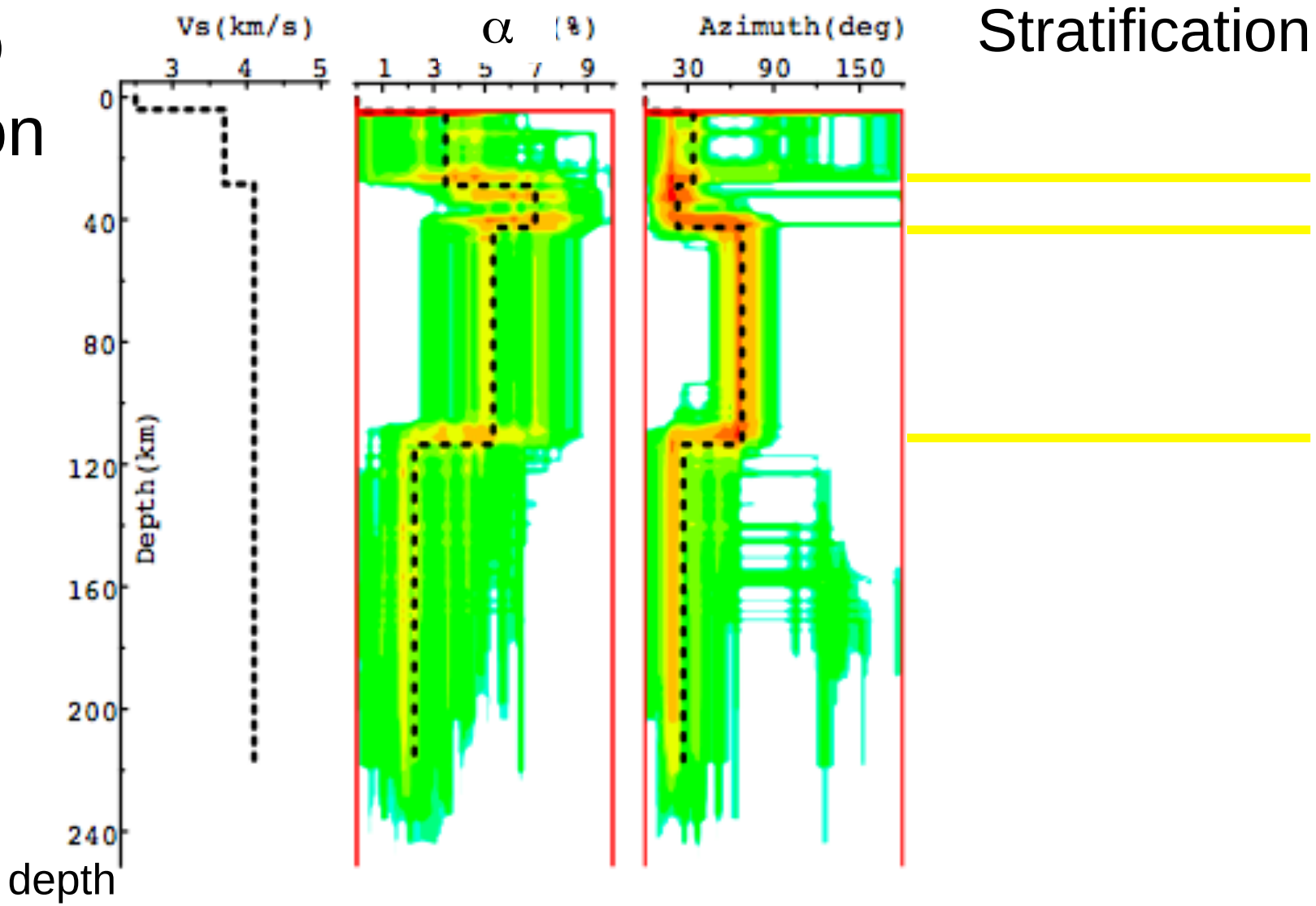

Stratification

Obrebski et al., 2010

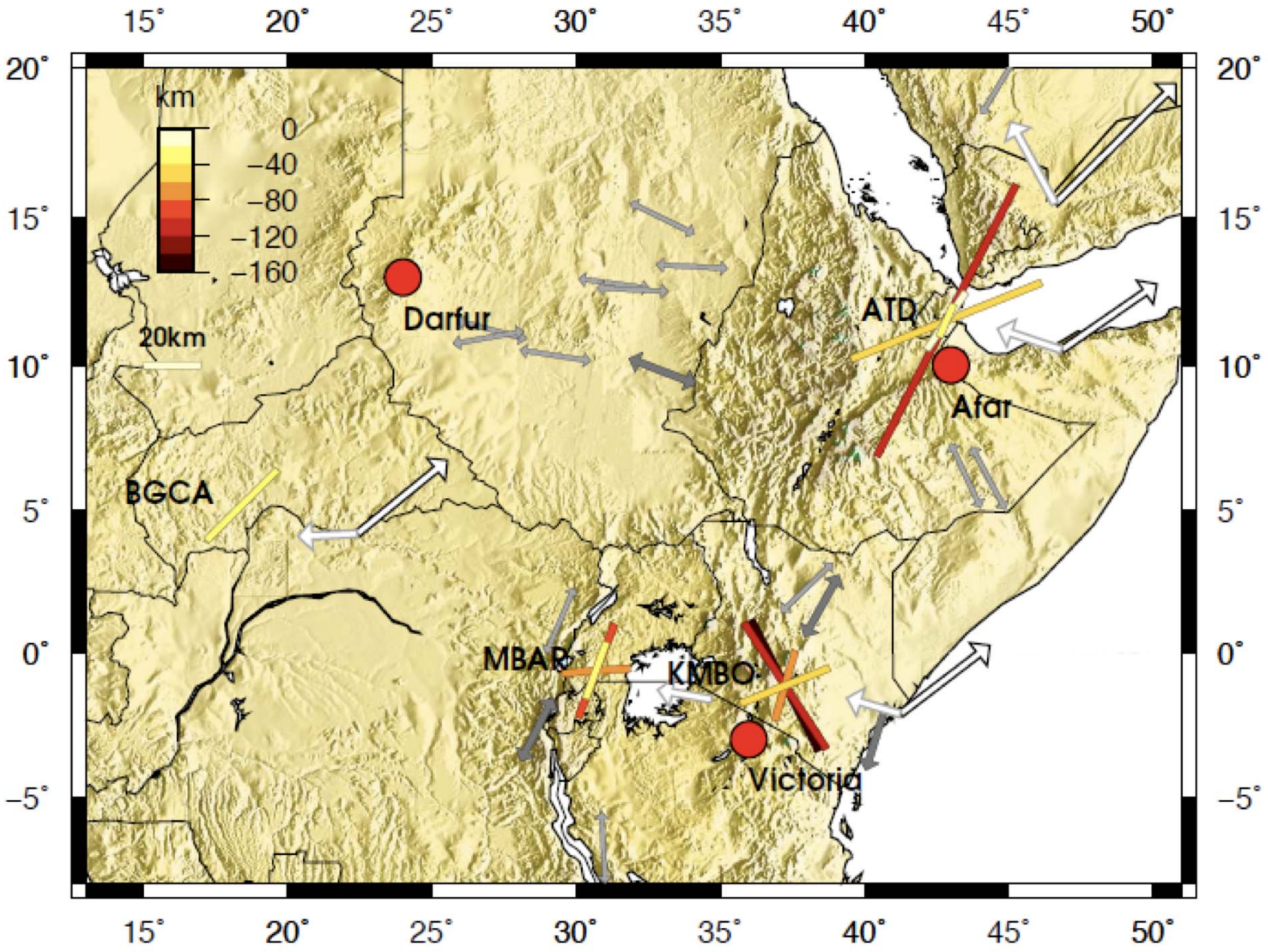
15˚
20˚
25˚
30˚
35˚
40˚
45˚
50˚
20˚
15˚
10˚
5˚
0˚
−5˚
km
0
−40
−80
−120
−160
20km
Darfur
ATD
Afar
BGCA
MBAR
KMBO
Victoria

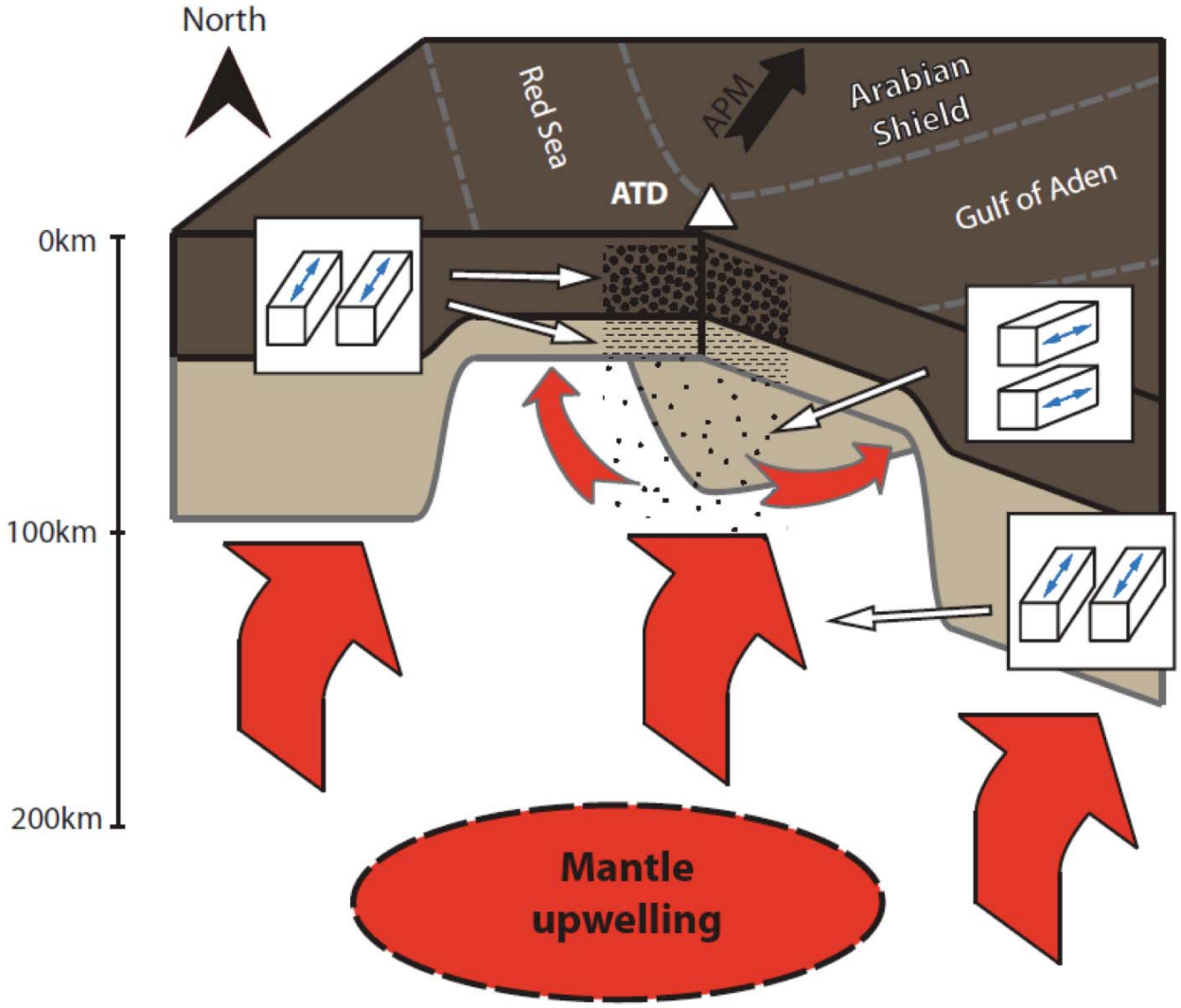

Tentative tectonic model to explain the stratification of anisotropy around Afar.

Obrebski et al., 2010

Stratification of anisotropy in The upper mantle is the rule Not the exception

What is the significance of geodynamic interpretation of SKS splitting data? 1 δt, 1 angle Ψ?

Different processes are playing at the same time

-S.P.O.

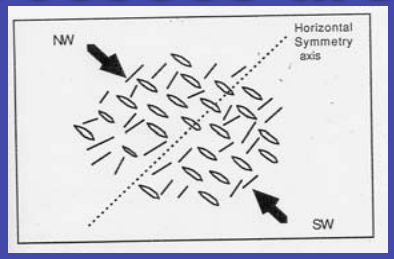

-L.P.O.

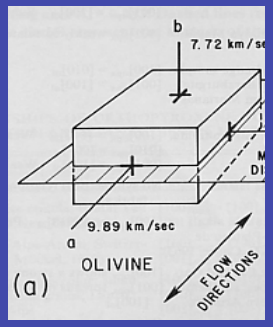

-Water content

-Fine Layering

Conclusions

- Anisotropy: New insight into geodynamic processes.
- Anisotropy maps mantle flow.
- For Horn of Africa, anisotropy displays a complex pattern around AFAR and a complex interaction Plume-lithosphere-asthenosphere: Stratification of anisotropy
- 2 families of plumes have been detected beneath African Continent:
  - Plume from deep in the mantle, transition zone (or lower mantle?): AFAR
  - Babyplumes: consequence of secondary convection (<300km depth): Darfur, Tibesti, Hoggar, Cameroon
- Central Asia: Deformation processes (Mountain Building)
- Crustal anisotropy different from lithospheric anisotropy

General CONCLUSIONS

- *From Seismic Anisotropy to Anisotropic Seismology*

- Anisotropy is not a second order effect (non-unique interpretation, layering of anisotropy)

- Anisotropy provides new insight into geodynamic issues:
- Mapping of mantle convection (detection of boundary layers)
- Plume- lithosphere- asthenosphere interactions
- Indirect detection of upwellings in the upper mantle.
- Deformation processes (Mountain Building)
- Continental and oceanic lithosphere thickness

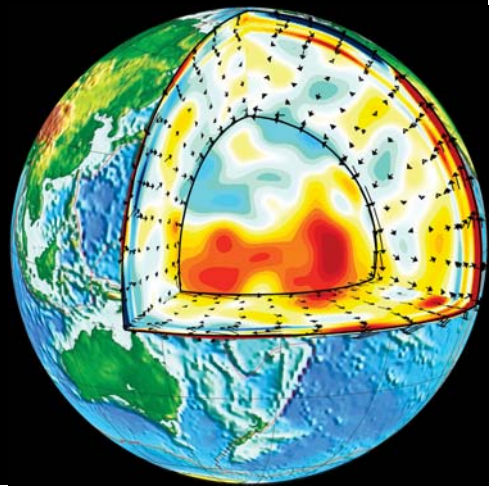

Seismic tomography: Instantaneous image
Anisotropy- Geodynamics Relationship

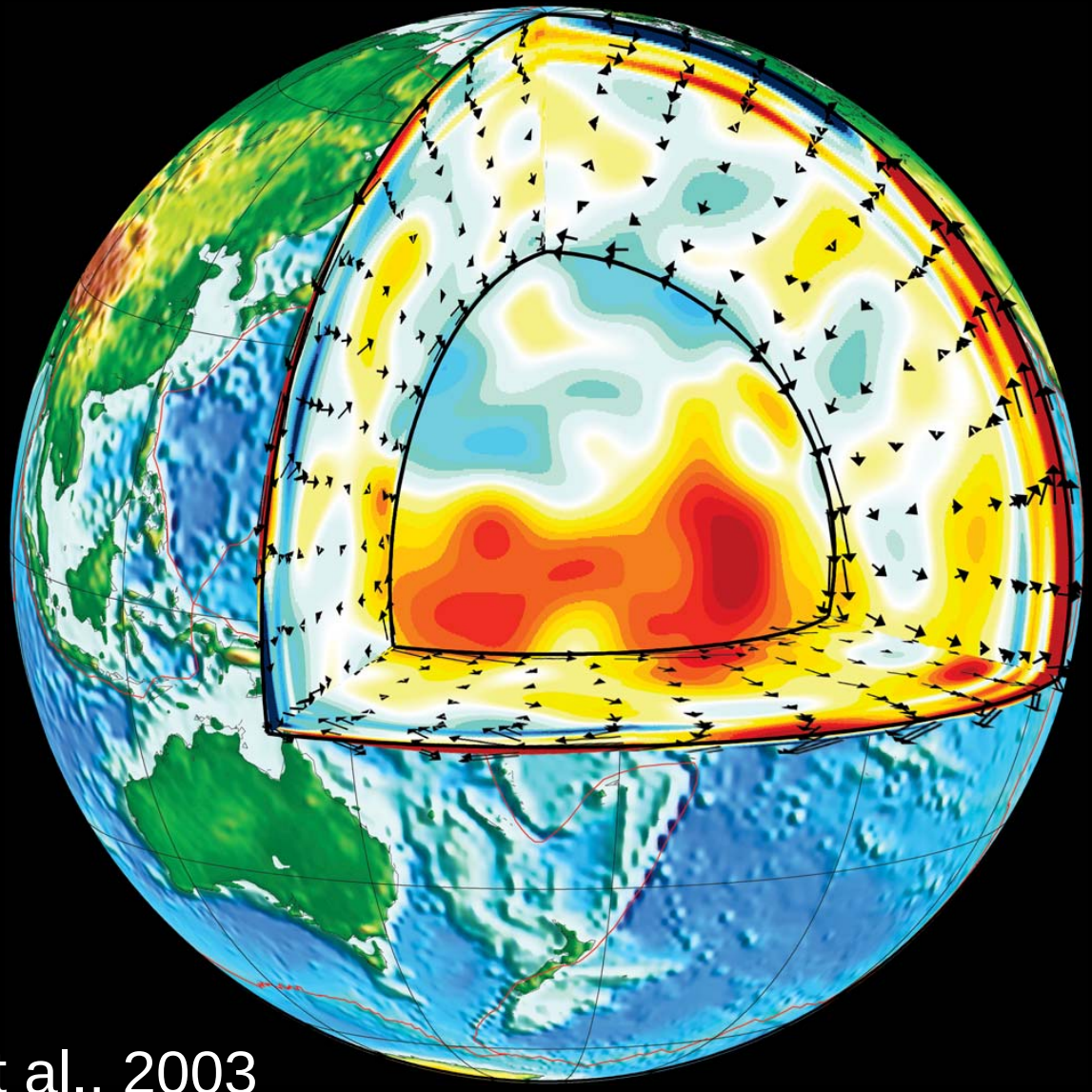

Gaboret et al., 2003

CONCLUSIONS

- Progress in instrumentation (Dense networks, Ocean bottom, Planet Mars; Spatial exploration)
- Ray Theory - Normal Modes -> Numerical Methods more and more powerful and accurate by using more and more powerful computers.
- From Global scale towards regional scale:

  Incorporation of new parameters (anisotropy, anelasticity) in tomography

  Finite-frequency effects
- Systematic Multidisciplinary Approach: Confrontation of seismological results with numerical and laboratory experiments